Breaching of earth embankments and dams

Thesis

Breaching of Earth Embankments and Dams

Mark Morris

PhD 2011

Breaching of Earth Embankments and Dams

Mark William Morris BEng. CEng.

A thesis submitted to the Open University for the degree of

Doctor of Philosophy

December 2011

Sponsoring establishment

HR Wallingford
Working with water

Date of Submission: 16 December 2011
Date of Award: 16 January 2013

NO CD/DVD ATTACHED

PLEASE APPLY TO THE UNIVERSITY

ABSTRACT

Despite 'modern' construction and management techniques, flood embankment and embankment dam failures occur almost routinely around the world. The need to understand, predict and prevent the breaching process remains a high priority for owners and flood risk managers alike. This research provides new understanding and improved methods for predicting breach initiation and growth through earth flood embankments or dams.

The improvement of breach model accuracy has made slow progress over the past 20 years, with confusion around breaching processes arising from a lack of appreciation of soil mechanics interacting with hydraulics and structural behaviour. The prediction of different breach processes requires the integration of techniques from all three disciplines.

This thesis makes advances from earlier work (Mohamed, 2002) to produce a predictive breach model intended for industry application. The research develops improved approaches for flow calculation, sediment erosion and structural response for predicting breach initiation and growth and uses field data, including video footage, from the EU IMPACT project and large scale test and case study data from collaboration with the International Dam Safety Interest Group breach modelling project.

Sediment erosion equations, rather than equilibrium transport equations are used and the significance of the estimated performance of any grass cover and the influence of breach drowning recognised. The relationship between reservoir surface area and the erodibility of the embankment soil for the characteristics of the breach outflow hydrograph is also highlighted.

Building from these developments, a new method to simulate breach through embankments comprised of different zones of material type and state has been developed which provides a significant step forward in our ability to simulate breach through real rather than idealised structures. This thesis demonstrates how this modelling approach can predict significantly different breach behaviour, and hence outflow hydrograph, dependent upon the embankment construction and soil state.

ACKNOWLEDGEMENTS

I would like to thank my supervisors, Prof. Paul Samuels and Dr Gurmel Ghataora, for providing support and always offering different perspectives and interesting discussion on the many issues as they arose. Thanks also to Dr Mohamed Hassan for his continued support, model development work and technical discussions regarding the intricacies of breach modelling.

This research has been undertaken in parallel with a series of wider research projects. In particular, core research work has been undertaken as part of the European FLOODsite project (an integrated project under the sixth framework programme - contract number: GOCE-CT-2004-505420). Research has also been partly funded by HR Wallingford and cooperation with the CEATI Dam Safety Interest Group breach modelling project has also been very helpful. Data used within the research includes significant amounts of field data from the earlier European IMPACT project (an RTD project under the fifth framework programme – contract number EVG1-CT2001-00037). Through these various projects I have had the opportunity to spend many hours and sometimes days, discussing breach related issues with experts, colleagues and friends from around the world; their continued support and prompt responses on many issues was very much appreciated. In particular, my thanks to Dr Roger Bettess (HR Wallingford), Dr Greg Hanson (USDA-ARS, HERU, Stillwater), Dr Tony Wahl (USBR, Denver), Dr Paul Visser (TU Delft), and Dr Jean-Robert Courivaud (EDF, France).

And finally, to my kids, Sébastien, Phoebe and Oscar, each of whom kept me sanely distracted throughout the research!

Contents

Tables

Figures

ABBREVIATIONS

BSI	British Standards Institution
ASTM	American Society for Testing and Materials
CADAM	Concerted Action on Dambreak Modelling (European R&D Concerted Action, FP4)
CEATI	Centre for Energy Advancement through Technological Innovation
CIRIA	Construction Industry Research and Information Association
Defra	Department for Environment, Food and Rural Affairs
DoE	Department of the Environment
DSIG	Dam Safety Interest Group
EDF	Electricité de France
EST	Equilibrium Sediment Transport (equations)
EU	European Union
FLOODsite	FLOODsite: Integrated flood risk analysis and management methodologies (European R&D Integrated Project, FP6)
FloodProBE	FloodProBE: Technologies for the cost effective flood protection of the built environment (European R&D RTD Project, FP7)
FOS	Factor of Safety
FWMA	Flood and Water Management Act (2010)
HET	Hole Erosion Test
HMSO	Her Majesty's Stationary Office
HRW	HR Wallingford
ICOLD	International Commission on Large Dams
IJKDIJK	IJKDIJK: Dutch research project investigating the performance of flood embankments
IMPACT	IMPACT: Investigation of Extreme Flood Processes and Uncertainty (European R&D RTD Project, FP5)
IPET	Inter-agency Performance Evaluation Task Force (USA investigation into New Orleans flooding)
JET	Jet Erosion Test
NWS	National Weather Service (USA)
PCA	Principal Component Analysis
SPR	Source-Pathway-Receptor
UrbanFlood	UrbanFlood: The use of sensors within flood embankments to support online early warning, real time emergency management and routine asset management. (European R&D RTD Project, FP7)
USACE	United States Army Corp of Engineers
USBR	United States Bureau of Reclamation
USCS	Unified Soil Classification System
USDA – ARS - HERU	United States Department of Agriculture, Agricultural Research Service – Hydraulic Engineering Research Unit

NOTATION

Parameter	Description	Dimensions	Units	
			SI	Imperial
A	Modular limit (HR Wallingford, 1989)	1	-	-
A_s	Reservoir surface area	L^2	m^2	ft^2
b	Breach bottom width; weir crest width	L	m	ft
B_b	Section averaged breach width	L	m	ft
c	Soil cohesion	M/LT^2	N/m^2	lb/ft^2
c%	Degree of compaction	1	-	-
C	Headcut migration rate	L/T	m/s	ft/s
C_t	Sediment load concentration (ppm by weight)	1	–	–
C_b	Base weir discharge coefficient (Ackers et al., 1978, Crabbe, 1974, Singer, 1964)			
C_d	General weir discharge coefficient	1	–	–
C_e	V notch weir discharge coefficient	1	–	–
C_p	Weir discharge coefficient depending upon weir geometry (Ackers et al., 1978, Crabbe, 1974, Singer, 1964)	1	–	–
C%	Percentage of clay	1	-	-
D	Pipe diameter	L	m	ft
D_{50}	Median particle size	L	m	inch
e	Force eccentricity	L	m	ft
e, E	Erosion rate	L/T	$m^3/s/m^2$	$ft^3/s/ft^2$
E	Energy head	L	m	ft
f	Drowned flow reduction factor	1	-	-
f	Friction coefficient determined as a function of D_{50}	1	-	-
F	Coefficient adjustment factor (depending upon head and geometry) (Ackers et al., 1978, Crabbe, 1974, Singer, 1964)	1	-	-
g	Acceleration due to gravity	L/T^2	m/s^2	ft/s^2

Parameter	Description	Dimensions	Units	
			SI	Imperial
h, h_0	Hydraulic head	L	m	ft
h_c	Hydraulic head at critical flow	L	m	ft
h_w	Water depth above the breach invert at the time of failure	L	m	ft
H	Total energy head; Reservoir water elevation	L	m	ft
H_b	Total energy head on breach invert	L	m	ft
H_1, H_{1e} H_2, H_{2e}	Upstream head; Downstream head	L	m	ft
H_1	Hydrostatic pressure force			
I_α	Erosion resistance indices	1	-	-
K_d	Soil erodibility or detachment coefficient		$cm^3/N\text{-}s$	$(ft/h)/(lb/ft^2)$
L	Length (general)	L	m	ft
L	Length of (rectangular) weir crest in flow direction	L	m	ft
L	Length of failure plane (block failure)	L	m	ft
L	Length of pipe	L	m	ft
LL	Liquid limit	1	-	-
M	Factor representing soil characteristics and condition			
M%	Percentage silt	1	-	-
M_0	Moment about point 0			
n	Manning's roughness coefficient	1*	–	–
n	Exponent	1	–	–
p	Sediment porosity	1	–	–
P	Height of weir crest above upstream bed level	L	m	ft
PI	Plasticity index	1	-	-
PL	Plastic limit	1	-	-

* From practical point of view n can be considered dimensionless

Parameter	Description	Dimensions	Units	
			SI	Imperial
q	Unit discharge or discharge per unit width	L^2/T	$m^3/s/m$	$ft^3/s/ft$
Q	Discharge	L^3/T	m^3/s	ft^3/s
Q_1	Free or undrowned discharge (Villemonte)	L^3/T	m^3/s	ft^3/s
Q_p	Peak outflow	L^3/T	m^3/s	ft^3/s
r_c	Radial distance (from breach) of critical flow	L	m	ft
R	Hydraulic radius	L	m	ft
R_m	Average hydraulic radius	L	m	ft
S_e	Energy slope	1	–	–
S_c	Critical breach section	1	–	–
SC%	Percentage coarse sand	1	–	–
S_n	Breach cross section number	1	–	–
S_f	Friction slope (Manning equation)	1	–	–
SF%	Percentage coarse sand	1	–	–
S_r	Degree of saturation	1	–	–
SL	Shrinkage limit	1	–	–
t, T	Time	T	s	s
T_b	Time to breach	T	s	s
T_e	Time to erode	T	s	s
T_n	Time of transitions between different breaching processes	T	s	s
U	Depth averaged flow velocity	L/T	m/s	ft/s
U_*	Shear velocity	L/T	m/s	ft/s
US_e	Unit stream power.	L/T	m/s	ft/s
V_w	Volume of water stored above the breach invert at the time of failure	L^3	m^3	ft^3
W	Weight of dry block of soil			

Parameter	Description	Dimensions	Units	
			SI	Imperial
W_s	Weight of saturated block of soil			
W_u	Weight of submerged block of soil			
WC%	Percentage water content	1	-	-
w%	Water content (%)	1	–	–
w_{opt}	Water content (%) for optimum compaction			
w_{LL}	Measure of liquidity in relation to clay and moisture content	1	–	–
w_{PL}	Measure of plasticity in relation to clay and moisture content	1	–	–
x	Distance	L	m	ft
y	Depth at a distance x	L	m	ft
Y	Water level	L	m	ft
ϕ	Soil angle of friction or angle of repose	1	–	–
γ_d	Dry unit weight of soil	M/L^2T^2	N/m^3	$poundal/ft^3$
γ_w	Unit weight of water	M/L^2T^2	N/m^3	$poundal/ft^3$
ρ_d	Dry density of soil	M/L^3	Kg/m^3	$poundal/ft^3$
ρ_s	Density of sediment	M/L^3	Kg/m^3	$poundal/ft^3$
ρ_w	Density of water	M/L^3	Kg/m^3	$poundal/ft^3$
τ_c	Critical shear stress	M/LT^2	N/m^2	$poundal/ft^2$
τ_o, τ_e, τ	Applied or effective shear stress	M/LT^2	N/m^2	$poundal/ft^2$
υ	Kinematic viscosity	L^2/T	m^2/s	ft^2/s
ω_s	Sediment fall velocity	L/T	m/s	ft/s
σ_t	Tensile stress or strength	M/LT^2	N/m^2	lb/ft^2

1. Introduction

Every year, flooding causes damage and disruption to people and economies around the world (Samuels et al., 2010). Flooding is often perceived by the public as something that can be prevented, however it is also increasingly recognised as a risk that can (and should) be managed, and as something that cannot be completely removed (Klijn et al., 2009). There is also growing recognition that the likely effects of climate change will result in more extreme flood conditions occurring more often (Defra, 2010, Environmental Audit Commission, 2010, Wilby et al., 2008). In addition to managing with more severe flood conditions, the extremely wet or extremely dry conditions will also affect the state of flood embankments and embankment dams, potentially weakening the soil structure. A weaker soil structure, for example by fissuring (Dyer and Gardener, 1996, Dyer, 2004, Dyer et al., 2007, Dyer et al., 2009, Frith et al., 1996), will result in flood embankments and dams that are more susceptible to erosion.

1.1 Why predict breach?

When flooding occurs, it is often as a result of overflowing and failure of flood defence structures such as flood embankments, or in the extreme, dams. Being able to predict and subsequently manage flood risk therefore depends greatly upon the accuracy and reliability of models or methods to predict the performance and failure of flood embankments and embankment dams. These are generally referred to as 'breach models'.

The prediction of breach often forms a key part of a flood risk assessment, which in turn provides underpinning data for a range of activities including asset design, asset management, spatial planning and flood risk management including incident management and emergency planning (Figure 1-1). Breach prediction can provide a range of data, comprising the timing and magnitude of flood flows as well as the timing and magnitude of potential breach dimensions. The different

stages of breach development are of greater or lesser interest to different end users, depending upon their need and role within the community (Morris and Hughes, 2008). For example:

- A *designer* is interested in producing a design that will perform according to the project specifications, for example, withstanding certain magnitude flood events without failure;
- an *asset manager* is interested in the initial breaching process and indicators of this, so as to be able to avoid development of a catastrophic breach;
- a *spatial planner* is interested in potential flood conditions (flood risk assessment) that might arise from a breach;
- a *flood risk manager* is interested in what might happen under a range of different load conditions and during a catastrophic event, so as to be able to plan for all eventualities, but also as a means for decision making support during an emergency; and
- an *incident manager* is interested in all stages of the process, and in real time, so as to be able to advise upon the safety of a structure during an incident and to advise on the likelihood, timing and management (including repair) of any potential catastrophic failure.

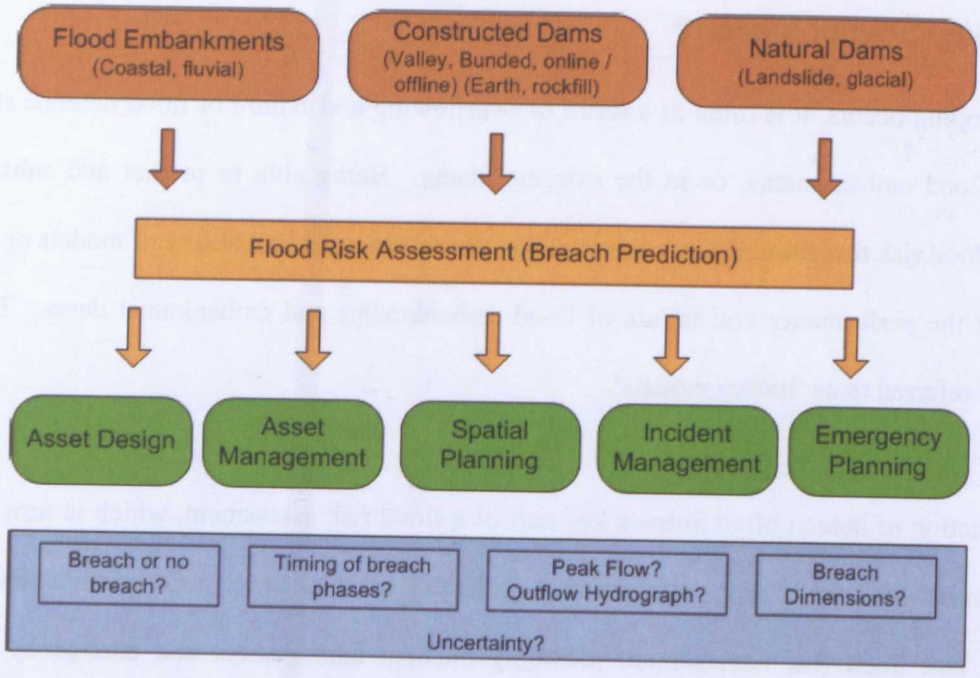

Figure 1-1 The role of breach prediction within flood risk analysis and management

The boxes at the bottom of the diagram in Figure 1-1 give an example of the likely questions that the various end users of breach prediction data are likely to ask. In addition to these there is the

underlying question of uncertainty. The complex interactions that occur during the breaching process mean that there is considerable uncertainty within the predicted results (Morris et al., 2009a). The fact that the breach prediction forms one part within the overall flood risk assessment analysis and that attention is often focussed upon the resulting inundation plans can help to mask very approximate and uncertain estimations of breach condition (Environment Agency, 2009a).

There is a long history of catastrophic dam failures, along with less well publicised, but widespread and relatively frequent breaching of flood embankments and levees, and to a lesser but still notable extent, canals (DoE, 1986, International Commission on Large Dams (ICOLD), 1998). Some of the more recent and famous dam failures include the Teton Dam failure in 1976 (Graham, 2008a, Graham, 2008b) as shown in Figure 1-2, the failure of the Taum Sauk Dam in 2005 (FERC, 2006) (Figure 1-3) and the failure of a mine tailings dam at Ajka, Hungary in 2010 (Figure 3-1). The latter demonstrates the added risk that mine tailings dams pose, whereby failure leads to the release of substantial quantities of sediment and mine waste (e.g. heavy metal pollutants) as well as flood water.

In England and Wales there are approximately 2100 dams registered as retaining more than 25,000m^3 of water above local ground level; this is the current condition for determining whether or not management of the reservoir falls under the UK Reservoirs Act (1975). This excludes mine tailings dams, which fall under different safety legislation (1969, 1971, 1975, Cambridge, 2008). This number rises rapidly if you consider dams retaining smaller volumes such as 10,000m^3 (Goff and Hope, 2008, Goff and Warren, 2008), as likely to be introduced as the Flood and Water Management Act 2010 is enabled.

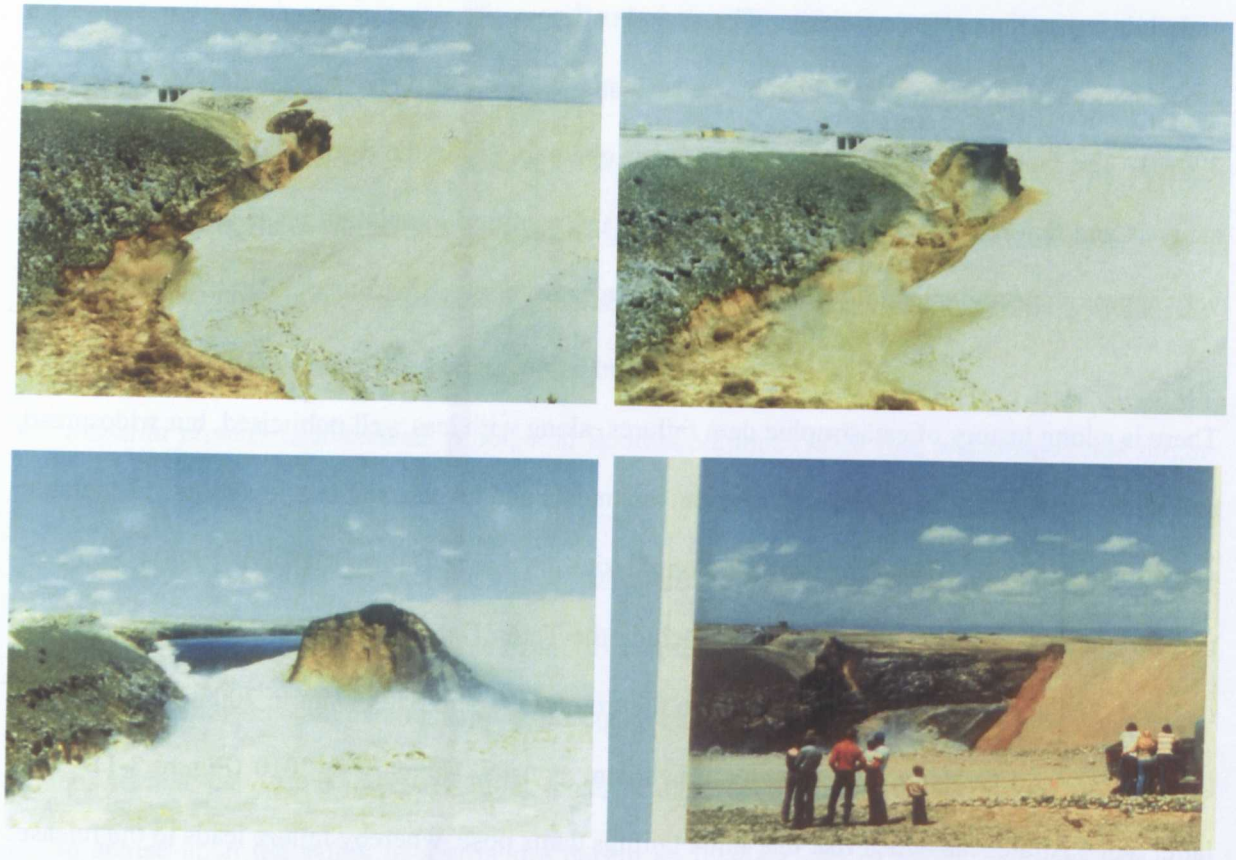

Figure 1-2 Failure of the Teton Dam (Photos courtesy, Gillette, USBR)

Figure 1-3 Failure of the Taum Sauk Dam, 2005

At an international scale, there are many tens of thousands of dams around the world, with construction dating back thousands of years. The oldest according to Kerisel dates from around 4000BC (Kerisel, 1985). Dams built after 1900 are deemed to be constructed in the modern era (Saxena and Sharma, 2006).

About 80% of the dams across England and Wales are made of earth. The oldest dams were built in the 12th century, and many were built during the Victorian era. Extensive canal networks comprising many kilometres of earth embankments were also established during the 18th and 19th centuries. In 2008, the average age of a dam in England and Wales was estimated to be 110 years (Hamilton-King et al., 2008) and concerns are rising as to their long term performance and including the likelihood of breaching (Defra, 2009). The first detailed review of the risks from breach and dam failure in the UK was undertaken in 1986 (DoE, 1986). This was repeated 20 years later (Pitt, 2008) following the extensive 'summer 2007 floods'. On both occasions concerns were raised regarding the need to understand the potential for breach formation and to assess and map flood risk from potential dam or flood embankment failure.

The most notable dam failure in England was that of Dale Dyke near Sheffield in 1864 which resulted in the loss of around 250 lives (DoE, 1986, Pitt, 2008, Smith, 1972). The failure of two dams in Wales in 1925 (Eigiau and Coedty Dams) led to the deaths of 15 people and prompted the introduction of the Reservoirs (Safety Provisions) Act in 1930 (1930) that introduced legislation in the UK on the safety of reservoirs, but not for flood embankments or canals (Morris and Hughes, 2008). The Reservoirs Act, 1975 evolved from this earlier Act, and is now being updated to incorporate risk-based concepts under the new Flood and Water Management Act 2010 (2010). The reason for updating of the Reservoirs Act were events during 2007 when a series of extreme floods occurred in England, resulting in the near failure of the Ulley Dam (Hinks and Mason, 2007) (Figure 1-4).

The subsequent enquiry (Pitt, 2008) highlighted the need for a series of measures, including the introduction of risk based methods for flood risk management and in particular, inundation mapping for all reservoirs to help with emergency planning. Both of these actions require breach prediction as part of any risk analyses (Environment Agency, 2009a). The same need exists worldwide; a review of research priorities supporting dam failure analysis in the US identified the

need for better understanding of breach, identification of breach modelling parameters and the development of improved breach models as key actions (Hanson et al., 2001a).

Figure 1-4 Near failure of the Ulley Dam, UK

The possibility of breach also exists for both flood and canal embankments (Figure 1-5). In England and Wales, it is estimated that there are between 7,500km (Environment Agency, 2007) and 35,000km (Dyer, 2004) of river and costal flood embankment defences. The uncertainty in extent reflects the size of the asset management problem that managing authorities face and the possible confusion in defining and identifying lengths of flood embankment. The extensive network of canals in England and Wales means that there are also many kilometres of canal embankment at risk of breaching and posing a risk to property and life (DoE, 1986, Hughes, 1981). At the peak of canal construction during the 'Golden Age' between the 1770s and the 1830s, the canal network extended to nearly 6500km (Wikipedia Contributors, 2011a). Whilst the size of the canal network has now reduced significantly from the peak, British Waterways still manages more than 3000km of canal channel alone (British Waterways, 2009). Again, the need for more reliable methods of breach prediction as part of improved flood risk analysis and management procedures are emphasised in national reviews such as *Learning to Live with Rivers* (Fleming et al., 2001).

Figure 1-5 Breach of a barrier bank along the River Aire, near Gowdall, UK, 2002 (Courtesy Environment Agency)

On 29th August 2005 Hurricane Katrina wrought havoc along the Mississippi Gulf Coast and in New Orleans as flood defences were breached and large parts of the city were inundated (United States Army Corps of Engineers (USACE), 2007). The breaching of levees here was particularly influenced by wave action and the interaction between water, soil and concrete wall structures (Figure 1-6). The impact of levee failure on communities within the city was catastrophic as widespread flooding and mass evacuation took place.

Figure 1-6 17th Street Canal levee breach (Hurricane Katrina, New Orleans)

Breaching processes can also play a role in determining flash flood conditions. In August 2004 Boscastle (Cornwall, UK) experienced extreme flash floods (Bettess and Bain, 2006). Analysis of

the event suggested that rapidly changing water levels arose through the blockage of bridges by debris and the subsequent failure of the structure or breaching of the blockage. This was consistent with observations from the event (Figure 1-7) and the extreme quantities of debris carried by the flood.

Figure 1-7 Severe flash flood event at Boscastle

Historically, there are many ways in which the results from analyses of breach have been used. The analyses might be undertaken to determine the extent of flooding that would occur (hence prediction of the volume of flood water likely to pass) or perhaps how best to repair a breach should it occur (hence prediction of breach dimensions to plan emergency repair works). Emergency planners are also interested in the speed with which a breach might develop (hence the time before flow through a breach starts to accelerate rapidly). The recent development of risk based approaches for system wide simulation of flood risk (McGahey et al., 2009, Sayers et al., 2002) requires the performance of a flood embankment or dam (Environment Agency, 2009b) to be represented for all possible load conditions, providing probability of failure, rate of breach growth and hence the associated flood hydrograph. Figure 1-8 shows how overall flood risk may be estimated, providing performance and response curves can be calculated. The approach uses the "Source-Pathway-Receptor-Consequences" model for flood risk analysis. Current system risk models use crude or simple representations of breach to limit the computational load. As more accurate breach models are developed, so the uncertainty in flood risk calculation will reduce.

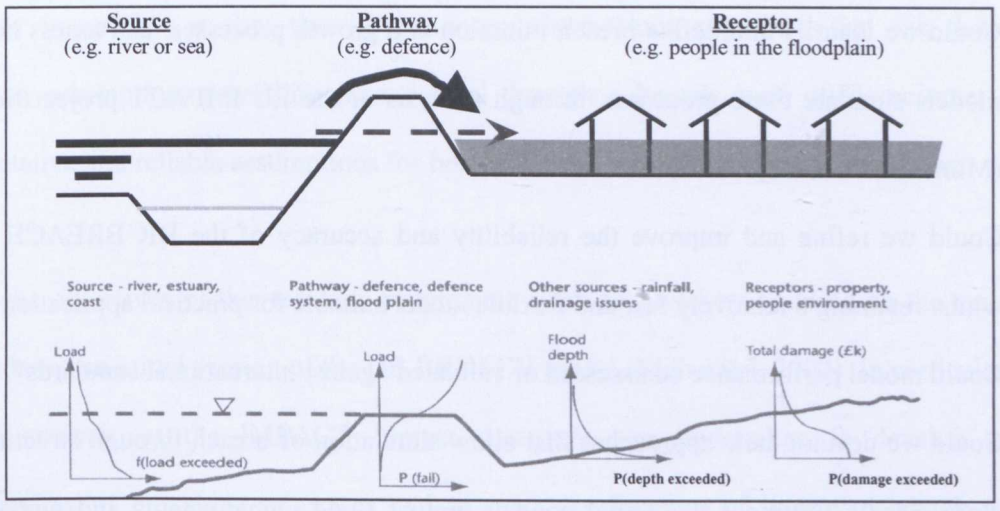

Figure 1-8 The source-pathway-receptor-consequences model for flood risk (Sayers et al., 2002)

This brief introduction has highlighted that a range of different structure types are susceptible to breach formation and that a variety of different end users are often interested in different aspects of the overall breaching process from flow and timing to ultimate breach dimensions. It can also be seen that understanding of breaching processes are relevant during flash floods and dambreak conditions where secondary trash dams may form and then breach, so changing the flood conditions. The development of risk based approaches to flood analysis and management does not change the need for a clear understanding of breach initiation and growth processes along with a range of breach models balancing accuracy of prediction with speed of modelling; these models should provide the reliable, underpinning science for such large scale management tools.

1.2 Aims and research questions

The overall aim of this research is to improve the reliability, scope and accuracy of modelling breach initiation and growth through flood defence embankments and embankment dams. More direct research questions (RQs) may be posed, including:

RQ1 How well do existing breach models, and the HR BREACH model in particular, simulate breach initiation and growth processes?

RQ2 Why has the accuracy and reliability of breach modelling not progressed over the past two decades at the same rate as the development of numerical flood models?

RQ3 Could we identify and define breach initiation and growth processes, and assess how well models simulate these processes, through analysis of the EU IMPACT project field data (Morris and Hassan, 2005a)?

RQ4 Could we refine and improve the reliability and accuracy of the HR BREACH model, whilst retaining a relatively fast and flexible model suitable for practical applications?

RQ5 Could model performance be assessed or validated against international standards?

RQ6 Could we develop new approaches that allow simulation of breach through structures that more closely represent the actual construction of flood embankments and embankment dams?

Hence, in addition to the research community, this thesis should be of interest to engineers and planners working in a range of disciplines related to flood risk management (see Section 1.1).

1.3 Directly linked prior research

At the start of this research, it could be seen that there were a number of breach models which could be used to estimate breach growth and the associated flood flow. However, the accuracy with which just the peak value of the flood hydrograph could be predicted was within perhaps ±30 to 40% of typically observed values (Morris, 2005). The estimation of other breach formation parameters such as timing, breach dimensions etc., was considerably less certain.

Earlier research (Mohamed, 2002) investigated these issues and developed a numerical model to predict breach growth – the HR BREACH model (Mohamed et al., 2002). This work undertook initial steps to integrate concepts and methods from soil mechanics, hydraulics and structures within the predictive approach. Following this research, an extensive programme of research investigating breach growth and breach modelling was undertaken through the European IMPACT Project (Morris, 2002). Under the IMPACT project programme of work (coordinated by the writer) considerable data was collected from field, laboratory and numerical modelling tests. However, whilst initial conclusions could be drawn from this work, a more detailed analysis of the

data was impossible at that time. Preliminary observations suggested that the then current modelling assumptions regarding flow control through a breach were often incorrect and that representative and reliable assumptions for breach growth mechanisms remained elusive.

Hence, the objectives of this research programme were achieved by building on the earlier work that produced an initial version of the HR BREACH model (Mohamed, 2002). In particular, a more detailed analysis of the IMPACT Project data sets was undertaken to develop a greater understanding of breaching processes and to steer development of improved breach modelling capabilities. The analyses used field, laboratory and numerical modelling data sets. The research was undertaken as part of the European FLOODsite Project (Morris et al., 2004) (www.floodsite.net). This project provided a mechanism for collaboration with other researchers and end users operating in this field internationally and extended the range of data and information available for analysis and understanding of the breach initiation and growth processes.

1.4 Structure of this thesis

Chapters 1, 2 and 3 of this thesis provide an introduction to the research, a review of literature and conclusions regarding research gaps, priorities and goals. The research is then divided into breach initiation and growth processes, with factors affecting initiation detailed in Chapter 4. Breach growth processes are considered in terms of flow processes (Chapter 5) and erosion processes (Chapter 6). A new approach for modelling breach through embankments constructed from zones of different materials is presented in Chapter 7. Model performance evaluation is detailed in Chapter 8 and overall conclusions and recommendations in Chapter 9.

Supporting material is included in the appendices covering a summary of the HR BREACH model (Appendix 1), a summary of breach model development versions (Appendix 2), details of test case data used for model evaluation (Appendix 3), results and analysis for application of the new

modelling approach (Appendix 4) and selected supporting papers and publications (Appendix 5 - DVD).

In addition to the material included within this thesis and the associated DVD, there are a series of relevant reports and papers detailed in the research that have been produced on a project by project basis:

- European IMPACT project – see www.impact-project.net (Work packages 2 and 5);
- European FLOODsite project – see www.floodsite.net (Tasks 4 and 6);
- International DSIG breach modelling project – see www.ceati.com (Dam Safety Interest Group R&D programme).

The research reports produced under the IMPACT project detail the programme of field and laboratory breach tests, along with breach model comparison and evaluation. The research reports under the FLOODsite project detail the analysis of physical processes (using the IMPACT project data) along with breach model development. The DSIG breach project reports detail the international programme of breach data collection, model review and selected breach model evaluation against field and laboratory data.

2. Literature review

2.1 Introduction

To gain a clear understanding of the current state of the art, and hence gaps in knowledge and specific research needs, it is important to understand what the different stages of the overall breaching process are and how predicting these processes can be used to support a range of community services, such as asset management and flood event management, as well as spatial planning. It is important to recognise that different aspects of breach prediction, such as the timing or breach dimensions or breach flow, have greater significance for some applications rather than all.

2.2 What is breach?

'Failure' is defined in the FLOODsite project *Language of Risk* Report (Gouldby and Samuels, 2009) as the "Inability to achieve a defined performance threshold (response given loading). Catastrophic failure describes the situation where the consequences are immediate and severe, whereas prognostic failure describes the situation where the consequences only grow to a significant level when either additional loading has been applied or time has elapsed, or both."

In the context of breach modelling, embankment failure is considered to be the situation where erosion or structural failure of the embankment allows the passage of flood water over or through the embankment in an increasingly uncontrolled manner (Figure 1-5). The *breaching process* might relate to any stage of erosion or failure arising from initial seepage through to complete and catastrophic failure. However, *breach*, typically implies that failure has occurred leading to formation of a hole or gap in the embankment or flood defence structure.

2.2.1 Factors affecting breach

A range of factors affect both the rate and size of breach formation. Two primary factors are the *structure type* and the *hydraulic loading*. An additional factor can be human intervention, such as through acts of war or terrorism. During the Second World War, dam breach as a result of placing explosives was instrumental in destroying the Moehne and Eder dams in Germany. The bombs used were derived from research and model tests performed by the Building Research Station (Collins, 1972, DoE, 1986), but were more effective on concrete rather than earth or rock fill dams. The apparent increase in international terrorist activity since 2001 has raised concerns again about the safety of flood defence and dam structures, prompting further government research into the response of earth structures to explosives. However, this aspect of breach initiation is not considered further within this thesis.

2.2.1.1 Structure type

Table 2-1 shows a simplistic listing of different structure types that can be at risk of breaching.

Table 2-1 Main and different types of structure susceptible to breaching

Structure Type	Variations
Flood embankments	Simple, homogenous
	Composite (with clay cores, layers of soil types, etc.)
	Composite (embankments with integrated structures such as wave or crest walls, sheet piles etc.)
Dams	Homogeneous earth fill
	Homogeneous rock fill
	Composite (with clay cores, layers of soil types, etc.)
	Composite (embankments with integrated structures such as spillways, roads, wave walls, outlets etc.)
	Concrete / masonry
	Service reservoirs (water tanks)

The structure type may also be described in greater detail as a function of the basic design, material type and material state. The relevance of material type and state here relates particularly to material erodibility, since this directly affects the various breaching processes. Material erodibility depends on a range of factors including cohesive strength and density (and hence degree of compaction and moisture content – see Section 6.3). The material state arises through a

combination of the construction process, maintenance actions and structure deterioration. The combination of these factors at any given time can lead to significant variation in the breach initiation and growth processes (as demonstrated later in this thesis).

Design of Embankment; Embankment Type

The design of an embankment significantly affects the physical breach process. The simplest embankment design is that from uniform homogeneous material. However, even such embankments, perhaps simply constructed from available local material, typically develop a surface protection layer of grass or other vegetation. The strength and uniformity of this vegetation will also significantly affect the breach initiation process. Designs also vary nationally, with distinct styles adopted by different countries.

Embankments are quite often designed to include additional structural measures for better erosion protection, seepage resistance or structural strength. These measures may include sheet pile cut-offs (within the body or toe), revetment protection (including gabion baskets, mattresses etc) and specific slope surface and crest protection measures. In addition, appurtenances such as pipe outfalls, culverts and sluice gates etc. are often constructed through an embankment creating a higher risk of failure at that location (Foster et al., 2000a, Foster et al., 2000b). General guidance on the function, use, design and operation of flood embankments can be found in, for example, the *Management of Flood Embankments* (Environment Agency, 2007) and the *Surveillance, Maintenance and Diagnosis of Flood Protection Dikes* (Mériaux and Royet, 2007).

Embankment dams can vary significantly in design from small homogeneous embankments through to multilayer structures, sometimes containing a clay core. The effect of multi-layers of soil or rock of differing strength is that the breaching process then comprises a combination of processes at different rates. The effect of layering on the breaching process will depend upon the soil erodibility for each layer, hence the soil type and degree and effectiveness of compaction and soil integration between layers.

Historically, flood embankments have been raised to provide increased levels of flood protection, typically after large flood events have overtopped the defences. Older dikes may have numerous layers and extensions to the original design.

Embankment Material

Significant changes in the physical breaching process can be seen as a result of the use of different construction materials (Morris et al., 2008). Three distinct categories of material typically used to build flood embankments or embankment dams are non-cohesive fill, cohesive fill and rock fill.

Non-cohesive fill, such as sand, will typically erode relatively quickly. The behaviour of erosion will vary according to embankment geometry and initiation process, but the removal of material is broadly through progressive surface erosion. Slopes gradually vary as erosion cuts into the embankment. Negative pore water pressure, created from moisture content within the sand or gravel, will give some degree of cohesion (Pickert et al., 2004). For example, as a breach forms, the sides of the breach will initially remain vertical. Figure 2-1 shows the exposed side of a breach from a large scale test undertaken in Norway as part of the EU IMPACT project (Morris and Hassan, 2005a, Morris et al., 2007). The material used to construct the embankment was non-cohesive. The embankment shows vertical and even undercut sections (near the crest) on the breach face. Material has started to fall and gather at the base of the face. This developed after erosion of the breach, with the fallen material sitting against the breach sides inside the breach section. This behaviour is analogous in some ways to that which can be seen with river bank recession (Damgaard and Mitchener, 1997), although breach formation processes tend to be more dynamic than bank erosion processes.

Cohesive Fill, such as clays, will typically have a lesser rate of erosion in comparison to non-cohesive fill. In addition, the process of erosion can differ significantly. Cohesive fills tend to erode through a process of head cutting. This process leads to the creation of steps in the eroding face of the embankment which progressively erode upstream (Figure 2-2). As the head cuts progress, they

tend to merge into fewer, but more significant steps until erosion through the crest and upstream face occurs.

Figure 2-1 Breach formation through non-cohesive material (showing vertical sides of breach)

Figure 2-2 Breach formation through cohesive material (showing head cut formation)

The development of a head cut occurs as a result of the interaction between the flow and the erosion resistant soil. Erosion of any material will tend to initiate at a discontinuity in the soil, where the flow is disrupted and local turbulence can remove some soil particles or blocks. Once a

depression is formed in the material, the flow increasingly drops into the depression and scours the base, so propagating formation of the step. The erosion resistant nature of the soil means that such steps can form, are stable and can grow. Less erosion resistant soils are unable to support the creation of steps, with the sides of any depression or step tending to slip and erode relatively quickly.

Rock fill material can vary in grading from relatively fine material through to large rocks. The finer material can behave as a non-cohesive fill material. As larger and larger particles (rocks) are used, a transition occurs whereby the interlocking nature of the rock fill can begin to significantly affect the rate at which material can be eroded during the breaching process.

An immediate conclusion that may be drawn from these observations is that any predictive breach equation or model should consider these three erosion processes in a separate manner. Figure 2-3 shows how the different breach physical processes could be broadly related to the soil grading (Morris et al., 2008). However, it should be recognised that this is indicative and that soil properties such as density and moisture content will also play a significant role. As such, regions of overlap, where soils may breach in different ways simply as a function of state rather than particle size are likely to exist.

With a limited choice of predictive breach models available, it is quite common practice to apply one breach model to all soil cases. The potential for errors arising from such an approach should be recognised.

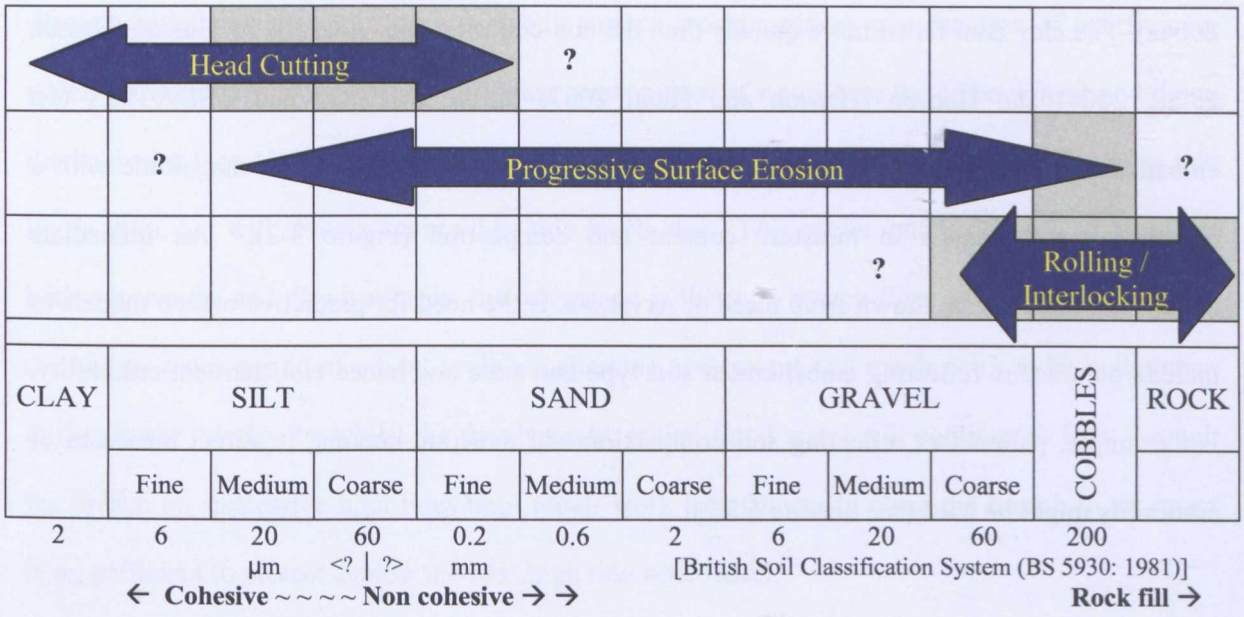

Figure 2-3 Broad division of behaviour by material type

Construction and Condition of Embankment Material

Research (Hanson and Hunt, 2007, Morris and Hassan, 2005a) has begun to highlight the importance of the condition of embankment material in relation to potential breach growth. Both soil compaction and moisture content have been identified as key factors affecting the erodibility of soils, particularly of cohesive soils. Whilst the condition and method of soil placement have been recognised as important factors for effective embankment construction for centuries (Bossut and Viallet, 1764), this has not been recognised until more recently within the flood risk management or breach modelling community. This is problematic since breach modelling requires the integration of expertise from the engineering disciplines of hydraulics, soil mechanics and structures, and it is the writer's experience that there are few breach modelling experts who are equally familiar with the detail of each of these engineering disciplines.

It was notable during the IMPACT project field tests #1 and #2 in Norway (Vaskinn et al., 2004a) that the rate of breach formation between non-cohesive and cohesive was reversed from that which was typically expected due to the construction and moisture content of the test dams. The non-cohesive test dam was constructed with very high compaction, whilst the clay embankment was constructed during a prolonged wet period and had extremely high moisture content (Vaskinn et al.,

2004a). The clay dam failed more quickly than the non-cohesive one. Analysis by Hassan (Hassan et al., 2004) and Hanson (Hanson and Hunt, 2007) of the IMPACT and USDA-ARS test embankments shows that erodibility of cohesive soils can vary by orders of magnitude with a relatively small change in moisture content and compaction (Figure 3-2). An immediate conclusion that may be drawn from these observations is the need for predictive breach models to include parameters reflecting embankment soil type and state and hence embankment erodibility. For example, parameters reflecting soil compaction and moisture content, or direct measures of erodibility might be used (see Section 6.3.2).

2.2.1.2 Hydraulic loading

The type of hydraulic loading on an embankment significantly affects the way in which a breach might occur. For example, a river embankment might be subject to prolonged wet or dry periods, and subsequently to progressive or rapidly varying, flood levels. Actual conditions will depend upon scheme design, catchment size and type (i.e. large or small catchment, rapid or slow rainfall runoff). Different combinations of loading will tend to encourage or discourage certain failure modes, which might in turn lead to breach initiation and growth (Table 2-2).

Table 2-2 A summary of different types of hydraulic loading

Structure location	Variations
Reservoir – online dam	Steady for long periods; varying according to flood; hydropower operation; rapid draw down in emergency; waves
Reservoir – offline storage dam	Steady or even empty for long periods; varying according to release of flood water; hydropower operation; waves
Fluvial embankment	Catchment dependent with occasional loading. Slowly to rapidly varying flood cycle. Approach flow parallel rather than normal
Coastal / estuarine embankment	Tidal (hence potentially cyclic (repeated) loading); surge; waves (including variable impact and flow speed); saline; tidal currents may influence growth. Potential for embankments to be constructed above normal tidal range and only loaded during extreme high tide or surge conditions.

Breach initiation may occur through steady surface erosion arising as a function of overflowing water, or progressively as wave overtopping sends pulses of water over the embankment and down the landward face. When subjected to tidal loading, breach initiation and growth will stop as tide levels drop, but will resume again when tide levels rise. This cyclic nature of the loading offers both advantages and disadvantages; the advantage is that any breach flow will only occur during the higher water period of a tidal cycle, so allowing assessment and repair work to be undertaken during lower tide levels, whilst the disadvantage is that flood water will continue to flow through the breach on successive high tides until repair work is sufficient to close the breach to an invert level sufficient to protect against the next high tide water level.

2.2.2 Defining the basic breach processes

A number of different researchers have analysed the breach problem and attempted to define distinct stages in breach development. Whether quoted as stages or phases of development, none of these definitions have universal acceptance, perhaps due to confusion in understanding the different breach processes that can occur when breach forms through different types of material (i.e. head cut or surface erosion processes as a function of soil type and state).

The advantage of adopting clearly defined phases and mechanisms for breach initiation and growth related to specific material types and condition is that numerical models may be simplified and hence can run faster. The danger, however, is that error in prediction will arise where soil types and state vary and the breaching process deviates from the predefined conditions within the numerical model.

A logical structure may be established by first considering breach in relation to the shape of the outflow hydrograph and secondly by behaviour (as defined by material type). These are outlined below and build upon work by the writer (Morris et al., 2006) and Visser (Visser, 1998a) on non-cohesive breaching and Temple (Temple et al., 2005) for cohesive breaching.

2.2.2.1 The generic breach outflow hydrograph

Figure 2-4 below shows a typical flood hydrograph that might arise from breach through an embankment or dam. In practice, the detailed shape and duration of the hydrograph will be determined by the type of hydraulic loading (i.e. the volume of water retained behind the embankment; the variation in loading such as storm loading, tidal cycles etc.) and the nature of the soil. The initiation flow (period T_1 to T_2) might also vary, for example, showing periodic surges where initiation was prompted by wave overtopping. However the broad features demonstrated in this example are generally common to all breach hydrographs in varying degrees. The series of time markers indicate different stages of breach activity as explained below.

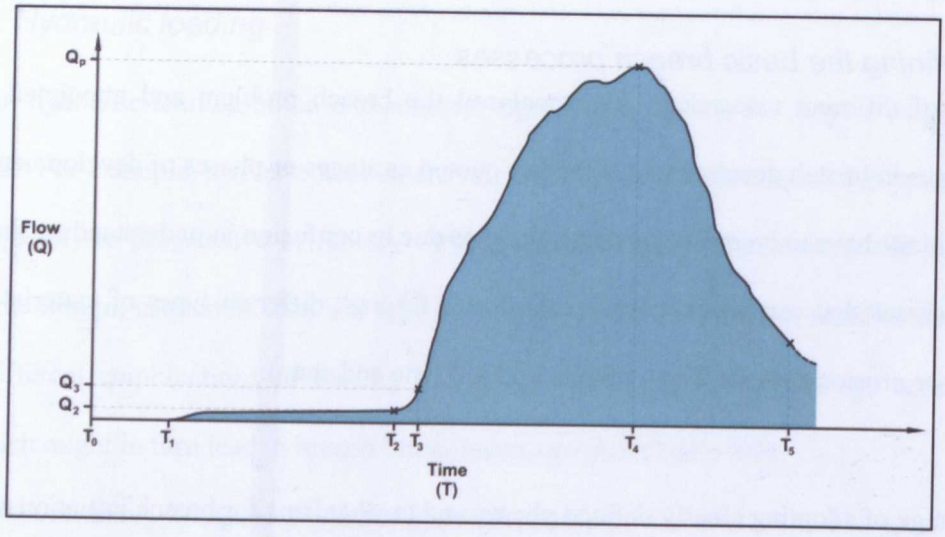

Figure 2-4 Generic breach flood hydrograph

Table 2-3 provides a summary of each stage of the generic breaching process, including relevance to end user, indicators of the process and indicative current modelling ability. The writer's assessment of breach modelling ability is based upon conclusions found during the European IMPACT project (Morris and Hassan, 2005a), the more recent Dam Safety Interest Group (DSIG) breach modelling project (Wahl et al., 2008, Wahl, 2009) and judgement regarding modelling advances as identified through the literature review.

Table 2-3 Generic breaching process stages (Morris et al., 2008)

Time	**T_0**
Process:	Stable – no breach initiation
Indicator:	None
Inspection methods:	Routine – non specific
Relevance:	Flood embankment or dam is performing as intended
Current modelling capability:	Not required.

Time	**T_1**
Process:	Start of *Breach Initiation*. Seepage through or over the embankment initiates.
Indicator:	Damp patches on embankment. Variations in vegetation growth. Cloudy seepage water.
Inspection methods:	Visual (seepage and vegetation); infra red photometry; ground water temp.
Relevance:	It is important to identify the potential for breach before it actually occurs for effective asset management. Seepage is often not visible and difficult to locate.
Current modelling capability:	Limited. Limit state equations exist for surface and internal erosion processes; a high degree of uncertainty exists in any prediction.

Time	**$T_1 - T_2$**
Process:	Progression of *Breach Initiation*. Breach flow increases slowly through either or both increased loading and the progressive removal of material. Flow is typically small and the rate of change can be very slow. The time period may be hours, days or months.
Indicator:	Apparent steady seepage or overtopping. Cloudy seepage water. No signs of rapidly changing flow.
Inspection methods:	As for T1; flow monitoring to detect change in flow rate
Relevance:	Having identified a potential problem, awareness of the timescale for development is often critical in determining the most appropriate action for maintenance, repair, emergency planning etc.
Current modelling capability:	Poor. There is a high degree of uncertainty in both the process and time prediction.

Time	**$T_2 - T_3$**
Process:	Transition to *Breach Formation*. Critical stage where steady (& relatively slow) erosion cuts through to the upstream face of the embankment initiating relatively rapid and often unstoppable breach growth. Transition may occur within hours.
Indicator:	Visibly changing flow conditions and quickening erosion of embankment through upstream face. Cloudy seepage water.
Inspection methods:	Monitoring seepage flow quantity and quality
Relevance:	Knowing when growth transitions to and past T2 is critical for emergency action.
Current modelling capability:	Included in many models, although typically limited representation.

Time	**$T_3 - T_5$**
Process:	*Breach Formation*. Rapid erosion of embankment vertically; continued erosion of embankment vertically and laterally. Extent and rate dependent upon volume of available flood water and design and condition of embankment.
Indicator:	Rapid breach growth; turbulent, sediment laden flow. Continued widening of

	breach after initial formation.
Relevance:	Important for predicting potential inundation downstream. Lateral growth important for planning emergency repair works.
Current modelling capability:	Prediction of hydrograph – moderate. (Peak ±30% (IMPACT project (Morris, 2005)). Ability to predict lateral growth rate and ultimate breach dimensions is poor.

Time	**T_4**
Process:	*Peak Discharge.* Q_p is a function of available flood water and embankment design and condition.
Indicator:	Difficult to identify during rapidly varying conditions.
Relevance:	Often used as a measure of worst case. However, Q_p at the breach does not necessarily relate to worst flood conditions downstream.
Current modelling capability:	±30% (most accurate of all aspects of breach modelling).

Section 6.3 details how different combinations of soil erodibility in relation to reservoir (flood) volume can result in flatter, longer duration flood hydrographs. It should also be recognised that this type of breach represents conditions where the outflow is affected by the breach size. In some situations, such as with canal breaches, where the canal channel is relatively narrow in relation to the breach width, the breach discharge becomes a function of the canal cross section geometry and the pound stored water volume. In this situation, the breach grows predominantly as a function of water flowing along and out of the canal; the breach does not control the outflow and the hydrograph tends to be flat and prolonged, rather than rapid and peaky (Dun, 2007).

2.2.2.2 Breach processes related to structure and material type

The differences between the large scale physical processes that occur for breach through more erodible (typically non-cohesive) soil and less erodible (typically cohesive) soil are significant. Breach formation through non-cohesive material tends to develop through the progressive surface erosion of the material, whilst breach formation through cohesive soil tends to result in the formation of headcuts (steps). Figure 2-5 provides a description of the surface erosion process, using the IMPACT project field test #4 as an example (Morris, 2009). Figure 2-6 provides a description of the head cut erosion process as defined by Temple (Temple et al., 2005).

Stage 1 – Initial overflow and surface erosion This stage relates to flow behaviour T_1-T_2 on Figure 2-4. Erosion of the embankment surface by overflowing water. Most aggressive erosion on downstream face. Slow or no erosion of crest means that discharge across the crest of the embankment is not significantly affected. Flow concentrates erosion at discontinuities in the embankment surface.	
Stage 2 – Continued surface erosion, including crest erosion This stage shows the transition of flow behaviour from T_1-T_2 into T_2-T_3 on Figure 2-4. Erosion on the downstream slope starts to cut into the embankment. Slower erosion of the crest starts to allow an increase in discharge, which in turn increases the rate of overall erosion. A mixture of surface and potential head cut formation can be seen in this photo.	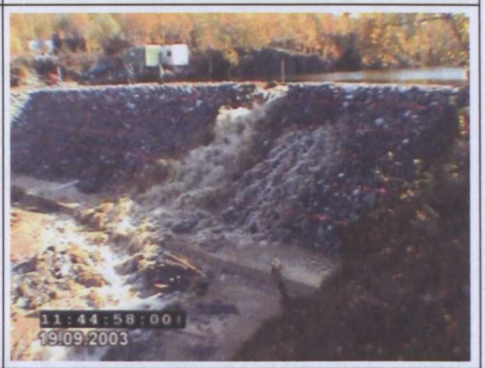
Stage 2 (cont) – Continued surface erosion, including crest erosion This stage relates to flow behaviour T_2-T_3 on Figure 2-4. The cycle of erosion of both the downstream slope and crest cuts deeper into the embankment progressively allowing an increase in discharge. Rapid and widespread surface erosion removes material from the face of the downstream slope, hence the eroding surface retreats upstream.	
Stage 3 – Continued surface erosion, including crest erosion and some breach widening This stage relates to flow behaviour T_3-T_5 on Figure 2-4, (although specifically between T_3-T_4 for this example). As erosion of the downstream slope and crest level becomes more aggressive, the control section for flow through the breach lowers and moves upstream (following the upstream slope). Some widening occurs, but erosion is still mainly vertical.	
Stage 4 – Breach expansion during reservoir drawdown This stage relates to flow behaviour T_3-T_5 on Figure 2-4. Once the embankment section within the breach has eroded towards the bed, the width of the breach then grows. The rate and extent of growth is affected by the volume of reservoir water that can be released and discharge through the breach eventually stops either through the release of all reservoir water, or because downstream flood levels rise and drown out the breach flow).	

Figure 2-5 Stages of surface erosion driven breach growth

Stage 1 – Headcut formation
Erosion of the downstream face by overflowing water leading to the formation of a headcut (step) in the embankment face capable of moving upstream through the embankment to form a breach. Erosion during this stage does not affect discharge across the crest of the embankment.

This stage relates to flow behaviour T_1-T_2 on Figure 2-4.

Stage 2 – Headcut advance through the embankment crest
The headcut advances upstream cutting through the downstream face of the embankment and into the crest. Prior to cutting through the crest and upstream slope, the headcut still has little effect on discharge over the embankment (and through the breach).

This stage also relates to flow behaviour T_1-T_2 on Figure 2-4.

Stage 3 – Breach formation - headcut enters the reservoir
The headcut advances upstream and cuts through the crest and upstream face into the reservoir. This has the effect of lowering the controlling crest elevation into the breach, hence flow increases significantly. As flow increases, so does the headcut erosion process. At this point the embankment or dam is likely to progress to catastrophic failure. Erosion of the upstream face continues down to or below the base level of the embankment.

This stage relates to flow behaviour T_2-T_3 on Figure 2-4.

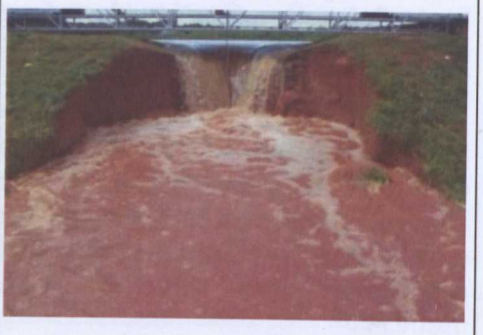

Stage 4 – Breach expansion during reservoir drawdown
Following rapid increase in discharge under Stage 3, the width of the breach then grows as a result of the reservoir discharge. The rate and extent of growth is affected by the volume of reservoir water that can be released. During this stage of growth, discharge through the breach eventually stops either through the release of all reservoir water, or because downstream flood levels rise and eventually drown out the flow through the breach (i.e. up and downstream levels normalise). Temple noted that during this phase of development the eroding breach sides remained more or less vertical, consistent with observations from larger scale tests under the IMPACT project (Vaskinn et al., 2004a)

This stage relates to flow behaviour T_3-T_5 on Figure 2-4.

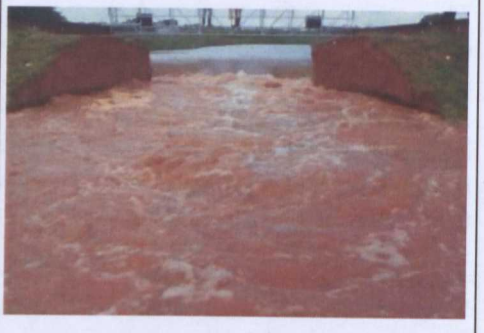

(Photos courtesy Greg Hanson, USDA-ARS-HERU, Stillwater, OK, USA.)

Figure 2-6 Stages of head cut driven breach growth

Case studies and research projects describing breach formation typically describe aspects of either head cut or surface erosion, however the significance of the material type and state in determining the overall process is often missed. Often, there are also conflicting descriptions relating to the surface erosion process where the angle of the eroding slope appears to either steepen or flatten. This is most likely reflecting the response to erosion of different soil erodibility, as shown by Zhu (2006) in a series of laboratory experiments on different soil types. The current state of research therefore allows us to state that this type of process would occur, but we cannot yet be specific as to the angle that the eroding face might adopt (i.e. steeper or shallower than the embankment face) or how significant this is to the overall breaching process.

A critical point during the growth of any breach occurs when erosion starts to affect the crest elevation at the upstream edge of the embankment crest. This region of the embankment typically controls the flow into the breach (at this stage in the breaching process) hence erosion of this crest level will allow greater flow into the breach and acceleration of the breaching process. For a given embankment geometry and loading, the timing at which this point is reached may differ as a result of whether head cut or surface erosion processes occur. This is considered further in Section 6.1.

The differences in erosion behaviour are related to differences in soil strength or erodibility. This difference is often attributed to cohesive or non-cohesive materials, however in reality the different processes can occur within a range of soil types given appropriate compaction and moisture contents that result in different soil states and hence different soil erodibility. This is represented in Figure 2-3 by the overlapping arrows reflecting the zones of soil type relating to different breach processes.

It is the writer's experience that the difference between headcut and surface erosion processes is not widely recognised outside of the research community; even within the research community processes are often attributed as generically applicable, without consideration of how they relate to soil type and state (Morris et al., 2008). Guidance is needed within industry in the selection and

application of breach models to ensure that the particular model chosen simulates soil erosion processes that are appropriate for the particular application (Morris et al., 2009a, Orendorff and Nistor, 2010).

In addition to material, the embankment structure design plays a significant role in determining which breach processes occur and when. Complex interactions occur between water, soil and structure such that even small variations in hydraulic load conditions, soil type and state or structure design, can lead to significantly different breach processes. The effects and implications of these interactions are demonstrated in Section 7.

Many embankments typically have a surface layer of vegetation that binds and protects the surface of the soil. In more exposed conditions, manufactured surface protection layers may comprise rip rap (placed rock) or some form of stone or concrete covering. The effect of a surface layer is to delay the onset of surface erosion and hence breach initiation and formation. The delay in initiation can lead to significantly different breach results such as the timing, breach size, breach outflow and the outflow characteristics. These significant changes can be seen because the altered timing means that the various stages of breach development can occur at different times during a given storm or hydraulic loading event. This can lead to both more or less extreme breach flood hydrographs since a delay in timing does not always result in a slower, less catastrophic breach.

The sensitivity of breach prediction to initiation timing means that predicting the performance of any surface layer is important within the overall prediction of breach. Since grass is a very common form of surface protection for flood embankments and embankment dams, predicting the performance of grass under both overtopping and overflowing conditions becomes important (Figure 2-7). However, modelling accuracy for the prediction of the performance of vegetation is still relatively limited (Morris et al., 2010, Young, 2005) and is a topic for further research between 2009-2013 under the European FP7 FloodProBE project (Morris et al., 2012). The issue of

vegetation performance and how this affects overall breach prediction is considered in more detail in Section 4.

Figure 2-7 Grass erosion: Overflow at a depression in the crest initiating erosion at weak points in landward slope grass cover (left); Grass erosion due to overtopping (right)(Environment Agency, 2007)

When you consider more complex structures (rather than a simple homogeneous embankment) the design permutations grow rapidly. Figure 2-8 and Figure 2-9 show two further examples of embankment design variations. Figure 2-8 shows an embankment with a core, whilst Figure 2-9 shows how embankments can often be raised and extended over decades (or even centuries) to cope with increasing flood water levels. Such design variations can be dependent upon function and availability of local material. Where an embankment or dam is expected to impound water over long periods, then a design such as shown in Figure 2-8 is more likely to be adopted, along with the use of a suitable low permeability material.

The effect of each of these simple design variations on the breaching process can be significant; where the different zones (core or layers) comprise of different material type or state, and hence different erodibility, the rate of headcut or surface erosion will change as erosion cuts through the zones. This change in erosion rate may be sufficient to change the overall breach process – for example, a highly erodible crest layer may allow preferential erosion of the crest, a rapid increase in discharge and hence more rapid overall failure regardless of the state of the rest of the

embankment. This example is particularly relevant where embankments might suffer from fissuring and is investigated in more detail later in Section 4.

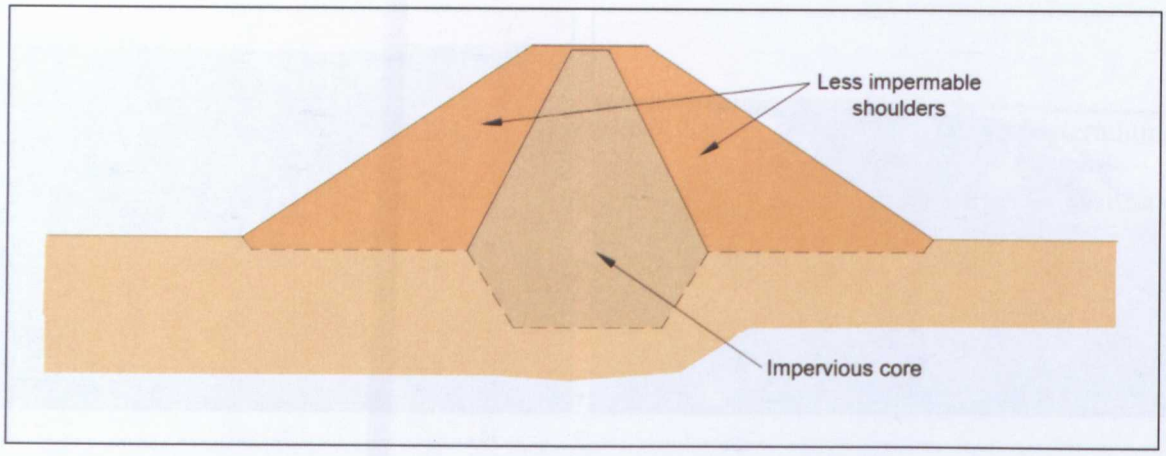

Figure 2-8 Composite embankment – simple earth embankment with core

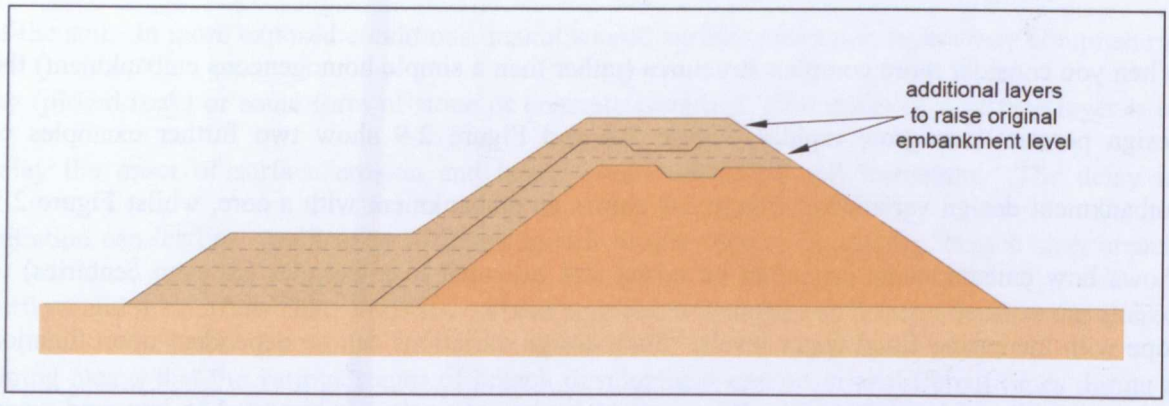

Figure 2-9 Composite embankment – earth embankment built progressively with additional layers or zones of soil

A more complex form of a composite structure is where the embankment is built with additional structures and / or protection measures included. Figure 2-10 shows an embankment within a tidal reach of a river, close to a bridge (off picture to right) (Environment Agency, 2007). The embankment has failing, rigid protection on the exposed river face, an outfall structure through the embankment and concrete capped sheet piling along a length approaching the bridge abutment. This structure already shows numerous signs of distress in terms of erosion. The location and nature of this erosion is dictated by flow interaction with the various structure components. Hence, prediction of breach around such a structure requires careful consideration of these interactions. This is something that deterministic breach models do not currently predict; simulation of breach

through complex structures such as this is an important area for model development in the future along with consideration of stochastic breach modelling approaches. In the meantime, it is important that care is taken in applying existing breach models for the simulation of composite structure failure. Useful results can be obtained by identifying the likely control features of a composite embankment, and simulating failure of that control section. For example, erosion of a large clay core component of a zoned embankment will likely dictate the rate of overall failure of the embankment, with more erodible supporting fill material being eroded simultaneously, but at a rate controlled by erosion of the core. Some earlier breach models, such as the DAMBRK breach code (Fread, 1988b) treated the erosion of zoned materials by combining and averaging soil parameters which may vary by orders of magnitude. This approach does not offer a reliable solution, and can result in significant errors in prediction (Mohamed et al., 2001).

Figure 2-10 Composite embankment – earth embankment with outfall, sheet pile wall and failed rigid surface protection

2.2.3 Common misconceptions in understanding and predicting breach

The complexities of different breaching processes, and their prediction, are not widely or consistently understood. The importance of recognising the applicability of research and models which address different aspects of breaching for different material types and / or states is often overlooked (Morris et al., 2008, Morris et al., 2009c). Table 2-4 provides a summary of common misunderstandings relating to breach processes and breach prediction.

Table 2-4 Misconceptions and misunderstandings relating to breach

Relevance to:			Issue	Misconception	Correction
Breach process	Prediction	Application			
✓		✓	One (breach) model fits all	All embankments breach in the same way	Different mechanisms will prevail driven by material type, construction and design. Core processes apply to non-cohesive, cohesive and rock fill designs.
		✓	Use of simplified breach equations	All embankments breach in the same way	Simplified breach equations will most likely be applicable to a very specific set of test data and hence design of embankment. Use for conditions outside of this data envelope should only be done recognising the uncertainty.
		✓	Use of peak discharge equations	Provides a simple "reliable" method of predicting the "worst case" from a breach	Peak discharge equations have been developed for use in assessing dam failure and are generated by regression analysis using historic dam failure data. The reliability of the equation depends greatly upon the historic data used and specifically the types of dam within the dataset. Typically no allowance is made for variations in dam condition, design, materials etc.
		✓	Use of peak discharge as a measure of the worst case	Assumption that the highest peak value from a breach flood hydrograph will match to the worst case condition downstream	When assessing flood conditions arising from a breach, the downstream flood conditions will be a function of the volume of water released, timing and local topography. Selection of the peak discharge value as correlating to the worst conditions downstream is not always the case. Analysis of the full breach hydrograph is required for a reliable assessment (Morris, 2005)
	✓		Quality of Construction	All embankments breach in the same way	The embankment quality and condition arising from construction can significantly affect the rate of erosion and hence breach growth. A measure of material condition should be incorporated in any predictive model.
	✓		Embankment condition at failure	All embankments breach in the same way	Weather and hydraulic loading conditions can significantly affect the embankment condition prior to breaching. Extreme and prolonged rainfall or prolonged high water levels can affect moisture content and hence erodibility. This aspect is also relevant in relation to potential effects of climate change.
✓			Shape of breach growth (side walls)	Predefined breach shapes such as trapezoidal, parabolic etc. which are then typically used within models to calculate flow through the breach	The shape of the breach opening during growth is a function of material type and erosion process. However, with soil moisture content offering some form of strength through soil suction, both cohesive and non-cohesive breaches tend to develop with vertical side walls.
✓			Flow control (prediction) through a breach	Assumption that the flow through a breach is controlled by a section within the breach opening (typically used in models)	The point of critical flow through a breach is often across the upstream face of the embankment as the breach forms. Erosion typically creates a curved weir that forms upstream of the central part of the breach. This weir is typically wider than the minimum central section of the breach.
✓			Use of standard 2-D, steady flow sediment equations	Assumption that the erosion of material from a (dynamic) breach follows the same laws as applied to morphological modelling in rivers (i.e. long term steady evolution based upon steady flow data).	Breach formation is dynamic and unsteady; morphological river modelling is taken as a long term averaged process. It is by no means clear that the two processes correlate.

2.3 The development of breach models

The following sections introduce the different types of breach model and their application, including a summary of physically based models developed over the last 40 years. A reference system for describing breach processes is given in Figure 2-11 below.

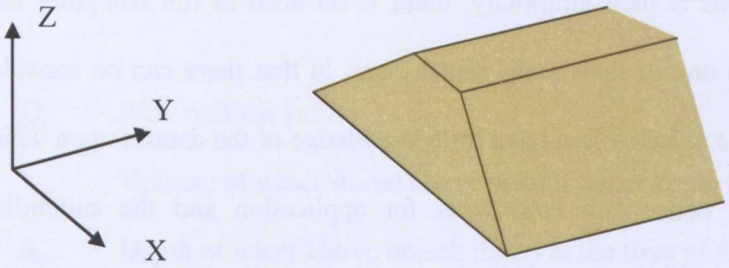

(a) General reference system

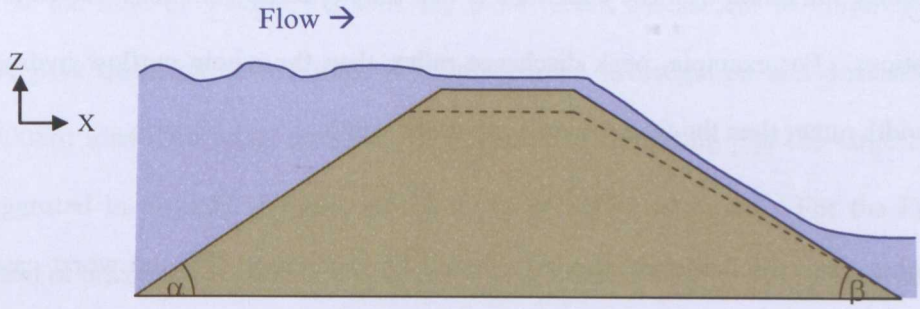

(b) Slope angles in X-Z plane

Figure 2-11 General reference systems for describing breach processes

2.3.1 Breach model types and typical applications

Models used to predict breach formation range in complexity and basis. One common factor is that researchers and engineers have striven to develop improved models for at least the past 50 years. A discussion as to why progress has been slow is given in Section 3.1.

Breach models are typically described as one of three or four types of model, depending upon the writer. These may be summarised as:

- Non-physically based, empirical models;
- Semi-physically based, analytical and parametric models;
- Physically based models.

2.3.1.1 Non-physically based, empirical models

Non-physically based or empirical models are methods usually based upon data collected from a series of documented breach events. Breach parameters (e.g. peak discharge, beach width etc.) are estimated from predictor equations, derived through regression analysis using the available data.

The advantage of these equations is their simplicity; there is no need to run computer models. However, this simplicity is also one of their main weaknesses, in that there can be considerable uncertainty within the predictions. Users often have little knowledge of the dataset upon which the equations were developed and hence any constraints for application and the suitability for application to site specific cases are hidden or unknown.

An additional limitation of these equations is that only specific parameter values are predicted by the equations. For example, peak discharge rather than the whole outflow hydrograph, or final breach width rather than the time varying growth of width.

When using peak discharge equations it should be recognised that the worst case flood extent conditions downstream do not always relate to peak discharge. The Tous case study in the IMPACT project (Morris, 2005) provides an example where the worse case flooding from a dam break does not correspond to the breach peak discharge; flooding is a function of volume and rate of water release, combined with topographic features of the valley downstream of the breach.

An additional source of uncertainty when using peak discharge equations is that users requiring a flood hydrograph will typically then estimate a hydrograph around the peak value given by the equation. This is often done by forming a triangular shaped hydrograph. With care, the estimated hydrograph should ensure conservation of reservoir or flood volume, but it is likely to increase the uncertainty in flow calculation because the rate of breach growth defined by the triangular shaped hydrograph has been specified by the user without a sound basis for the prediction.

Some examples of peak discharge equations are given by MacDonald and Langridge-Monopolis (MacDonald and Landgridge-Monopolis, 1984) and more recently Froehlich (Froehlich, 1995a, Froehlich, 1995b, Froehlich and Tufail, 2004, Froehlich, 2008). The Froehlich (Froehlich, 1995b) equation is given below:

$$Q_p = 0.607(V_w^{0.295} h_w^{1.24}) \qquad (2\text{-}1)$$

Where

Q_p Peak outflow (m^3/s)

V_w Volume of water stored above breach invert at the time of failure (m^3)

h_w Depth of water above breach invert at the time of failure (m)

An extensive review by Wahl (Wahl, 2004) assessed the performance of different breach prediction equations and, at the time of writing, remains the most recent assessment of empirical model performance for peak discharge estimation. A more detailed investigation and discussion with Wahl (Wahl, 2008b) identified some errors in this assessment indicating that the large bands of uncertainty, suggested in original analysis, are likely to be under estimated. For the Froehlich equation, the band of uncertainty around a hypothetical predicted value of 1 was approximately 0.4 to 2.4 for breach width and peak flow, and 0.4 to 7.3 for the timing.

2.3.1.2 Semi-physically based, analytical and parametric models

The large range of uncertainty associated with the non-physically based methods on one hand and the complexity of the physically based methods on the other hand, prompted authors such as (Singh and Scarlatos, 1989) and (Walder and O'Connor, 1997) to develop models based on physical processes, but with simplified assumptions to represent the failure of embankment dams.

The purpose of these models is to improve the prediction capability by including some of the physical processes involved in the failure without unduly complicating the computation procedure. Assumptions usually include use of a weir equation to represent the flow over the embankment, and hence that critical flow conditions exist on the embankment crest. The breach growth process

is also assumed to be time dependent, but with simplifying assumptions.

Models, based on these assumptions, can be used to estimate the outflow hydrograph through a breached embankment. However, these models often also require input of erosion rate for the growth of breach or time to, and the final dimensions of, a breach shape. Some models then simply predict a growth pattern to fit these parameters and subsequently produce a flood hydrograph. However, input parameters are not easy to estimate and can be subjective. Thus their values may vary depending upon the user. Hence, whilst these models appear to provide a more accurate prediction of the flood hydrograph in comparison to empirical equations, they simply reflect the data provided by the user and hence can also include large degrees of uncertainty.

2.3.1.3 Physically based models

Physically based models differ significantly from the empirical, analytical and parametric models described above. Physically based numerical models simulate the failure of embankments based on the processes observed during failure, such as the flow regimes, erosion and slope instability processes. In the last four decades many models have been developed to simulate the failure of embankments. These models differ in their complexity, assumptions involved, and techniques used. A summary of these models is given in Table 2-5.

Some authors (Kahawita, 2007) subdivide physically based models into empirical and theoretical models, based upon the degree of use of empirical relationships within the model versus theoretical processes. A recent example of a physically based, empirical model is given as SIMBA (Hanson et al., 2005c, Temple et al., 2005). SIMBA predicts the growth and progression of headcut advance through cohesive material, so predicting the stages of breach formation, flood hydrograph and breach dimensions. The model is based around the use of an erodibility coefficient for the embankment soil, the value of which is determined experimentally. Four different stages of headcut erosion are predefined in the model simulation (Figure 2-6).

Examples of physically based, theoretical models include FIREBIRD (Wang and Kahawita, 2002, Wang et al., 2006) and HR BREACH (Mohamed, 2002, Morris et al., 2009a). These models endeavour to use theoretical relationships to simulate the physical processes. However, invariably there is always a degree of empirical relationships embedded within the models, since modelling "factors" or coefficients are generally included at the detailed level of model simulation (e.g. weir discharge coefficients).

The advantages of using physically based models include:

- observed breach growth processes are simulated, generally incorporating aspects of hydraulics, sediment transport, soil mechanics and structural behaviour;
- an estimate of the outflow hydrograph and breach growth process are predicted, without (in more recent models (2000 onwards – see Table 2-5)) predefining or constraining the predicted growth process or requiring the user to define critical breach parameters;
- uncertainties within individual processes or parameters may be included within the model.

The disadvantages of using physically based models typically include:

- Computer programs are required; model runtimes can become quite long as the simulation of processes becomes more complex;
- Current computing power means that 1D / pseudo 2D models incorporating hydraulics, sediments, soil mechanics and structural stability are feasible; 2D / pseudo 3D models incorporating all of these elements are being considered and developed, but are not yet practical for industry use in terms of model run time or validated in terms of improved performance (relative to the faster 1D models).

An example of an early, widely used physically based model is given by the NWS (DAMBRK) BREACH model (Fread, 1984, Fread, 1988b). Developments in understanding of breach processes, soil mechanics and computing power mean that more recent models, such as SIMBA, FIREBIRD and HR BREACH now offer more rigorous analyses.

2.3.2 Current state of the art and research initiatives

The history of numerical model development is highlighted well by the summary of models presented in Table 2-5 below. This summarises the development of numerical breach models to 2007, starting with a model produced in 1965 (Cristofano, 1965). Whilst a considerable number of models are listed here, it is inevitable that others exist. The listing provided here builds from the earlier review work by Mohamed (Mohamed, 2002) updated with recent review findings from D'Eliso, Kahawita, Zhu and Morris (D'Eliso, 2007, Kahawita, 2007, Morris et al., 2009a, Zhu, 2006).

The list of models under Table 2-5 reflects the wide number of researchers that have worked to try and provide a reliable method for predicting breach. A number of trends and observations can be identified when looking at this table:

- The method of flow calculation typically varies between solutions of the St Venant equations (typically 1D, but more recently, 2D) and the use of simplified equations or weir flow formulae;
- Until the last 10 years (2000 onwards), most models used equilibrium sediment transport equations rather than sediment erosion equations;
- Many models predefine the shape of the breach which include triangular, rectangular, trapezoidal and parabolic;
- Many models ignore slope stability;
- The model descriptions do not easily reflect the degree of complexity of the model calculations; a mixture of simple and more complex models are listed.

A summary of researchers and initiatives since Fread's work on DAMBRK and the NWS BREACH model in the 1980s (Fread, 1988b) is given in Table 2-6. Note that this focuses on work relating to breach prediction and does not include research on internal erosion.

Table 2-5 Summary of physically based models

Model	Breach Morphology	Flow Over the Dam	Sediment Transport	Geo-Mechanics of the Breach Side Slopes	Comments, Limitations & Deficiencies
CRISTOFANO (Cristofano, 1965)	Trapezoidal with constant bottom width. YZ: Trapezoidal XZ: Constant β	Broad crested weir formula	Empirical formula developed by Cristofano	None	• Constant breach bottom width and shape • No lateral erosion mechanism • No slope stability mechanism • Unrealistic erosion relation
HARRIS-WAGNER (Harris and Wagner, 1967)	Parabolic with top width equal to 3.75 depth YZ: Parabolic XZ: Constant β	Broad crested weir formula	Schoklitsch formula	None	• Constant sediment concentration • No slope stability mechanism • User input breach slope
BRDAM (Brown and Rogers, 1981)	YZ: Parabolic with 45° straight side slopes. XZ: Constant β	Broad crested weir formula	Schoklitsch (1934) bed load formula	Failure of the top wedge above pipe specified by the user	• Developed from Harris-Wagner model • Constant sediment concentration • No slope stability mechanism • No lateral erosion mechanism • User input time for pipe failure
PONCE – TSIVOGLOU (Ponce and Tsivoglou, 1981)	Top width flow rate relation YZ: B = f(Q) XZ: Exner equation	Full Saint Venant equations	Exner equation with Meyer-Peter and Müller bed load formula	None	• First fully physically based model • No slope stability mechanism • The use of the regime concept • No lateral erosion after the peak flow
LOU (Lou, 1981)	Most effective stable section YZ: Cosine shape XZ: Exner equation	Full Saint Venant equations	1. Cristofano's empirical formula 2. Duboy and Einstein formulae 3. Lou's formula	None	• Similar to Ponce-Tsivoglou model • No slope stability mechanism • No lateral erosion after the peak flow • Empirical formula to compute the erosion • Inappropriate method to model the breach growth

Model	Breach Morphology	Flow Over the Dam	Sediment Transport	Geo-Mechanics of the Breach Side Slopes	Comments, Limitations & Deficiencies
NOGUEIRA (Nogueira, 1984)	Effective shear stress section YZ: Cosine shape XZ: Exner equation	Full Saint Venant equations	Exner equation with Meyer-Peter – Müller	None	• Similar to Lou model, hence same limitations as Lou's model
DAMBRK (Fread, 1984)	YZ: Trapezoidal or rectangular XZ: Constant β	Weir formula	Assumed linear erosion	None	• Original NWS DAMBRK code
SMPDBK (Wetmore and Fread, 1984)	YZ: rectangular	Weir formula	None	None	• Simplified DMBRK model
FUJITA & TAMURA Flood Levee Breaches (Fujita and Tamura, 1987)	Rectangular breach shape was above water level and trapezoidal below water level	Broad crested weir	Sediment transport rate was estimated assuming that the energy slope to be consumed only in sediment transport	None	• Uniform erosion of the breach • No slope stability mechanism
EMBANK (Chen and Anderson, 1986)	Erosion in horizontal layers Breach width undetermined	Broad crested weir velocity profile	Duboys formula Lab tests / Shields curve	Lateral collapse effects	• Developed for road embankments • With or without downstream submergence • No mass conservation
NWS BREACH (Fread, 1988b)	Rectangular and trapezoidal. Allows for presence of grass cover. YZ: Rectangular and trapezoidal XZ: Constant β	Broad crested weir formula for overtopping and orifice for piping	Meyer-Peter-Müller modified by Smart	1. Breach side slope stability 2. Top wedge failure during piping or overtopping	• First model to include side slope stability analysis • Uniform erosion of the breach • Incompatible computation method for hydraulics and sediment • Inaccurate slope stability analysis • Simplified modelling of the failure of composite embankment dams

Model	Breach Morphology	Flow Over the Dam	Sediment Transport	Geo-Mechanics of the Breach Side Slopes	Comments, Limitations & Deficiencies
BEED (Singh and Quiroga, 1987, Singh and Scarlatos, 1989)	YZ: Trapezoidal XZ: Constant β and erosion of the crest	Broad crested weir formula	Einstein-Brown Meyer-Peter-Müller	Breach side slope stability (Chugaev method)	• Similar approach to NWS BREACH model • Uniform erosion of the breach • Incompatible computation method • Inaccurate slope stability analysis
GIUSEPPETTI & MOLINARO (Giuseppeti and Molinaro, 1989)	Triangular	Broad crested weir flow formula	Englund and Smart formulae		
HAVNØ (Havnø et al., 1989)	Trapezoidal		Linear predetermined Englund and Hansen Meyer-Peter-Müller formulae		
DEICH_P (Bechteler and Broich, 1991)	YZ: Trapezoidal XZ: Global Exner equation with horizontal channel	Weir formula	Meyer-Peter-Müller, Smart and Bagnold formulae	Core stability	• Simple practical tool
TINGSANCHALI & HOAI (Tingsanchali and Hoai, 1993)		Weir formula	Meyer-Peter-Müller Exner equation	None	
SITES USDA-ARS (USA) www.pswcrl.ars.usda.gov **(National Resources Conservation Service (NRCS), 1997)**	Three stages of failure (XZ): 1. Grass cover failure 2. Headcut formation 3. Headcut erosion	Spillway stage-discharge curve	For stage 1 and 2 a detachment model was used For stage 3 an energy dissipation equation was used	Spillway exit channel stability	• Incomplete modelling of embankment failure • Empirical coefficient to compute erosion
NCP-BREACH (Coleman and Andrews, 1998, Coleman et al., 2002)	YZ: Parabolic XZ: Constant β and then erosion around a pivot point	Weir formula	Assumed empirical erosion rate	None	• Empirical formula completely based on small-scale models • No slope stability mechanism

Model	Breach Morphology	Flow Over the Dam	Sediment Transport	Geo-Mechanics of the Breach Side Slopes	Comments, Limitations & Deficiencies
EDBREACH (Loukola and Huokuna, 1998)	YZ: Trapezoidal	Broad crested weir formula	Meyer-Peter-Müller	Top wedge failure during piping	• Uniform erosion of the breach • Inaccurate pipe stability analysis • No slope stability mechanism
BRES (Visser, 1998a, Visser, 1998b)	Five 5 stages of failure: YZ: trapezoidal XZ: Global Exner equation with rotation up to $\beta = \omega_0$ and then constant β	Broad crested weir formula + Bélanger	Four sediment transport formulae: I Wilson II Engelund & Hansen III Van Rijn IV Bagnold-Visser	None	• First model for river and coastal dikes • Simple slope stability mechanism • No effect of waves
DEICH_A (Broich, 1998)	XY: Trapezoidal XZ: Horizontal channel	Weir formula	Meyer-Peter-Müller	None	• Non predictive capability
DEICH_N1 (Broich, 1998)	XZ: Exner equation	1D shallow water equations	I Meyer-Peter-Müller II Engelund & Hansen III Smart IV Bagnold Differently combined; 9 cases included	None	• Parabolic breach shape • No slope stability mechanism • Unrealistic modelling of the vertical and lateral erosion
DEICH_N2 (Broich, 1998)	YZ: Diffusivity approach XZ: Exner equation	2D shallow water equations	I Meyer-Peter-Müller II Engelund & Hansen III Smart IV Bagnold Differently combined; 9 cases included	None	• First 2D numerical breach model • Parabolic breach shape • No slope stability mechanism • Unrealistic modelling of the vertical and lateral erosion
RENARD (AND RUPRO) (Paquier et al., 1998)	Uniform erosion of the pipe	Orifice equation	Meyer-Peter-Müller	Failure of the material above the pipe	• Unrealistic modelling of the failure of the material above the pipe • No slope stability mechanism

Model	Breach Morphology	Flow Over the Dam	Sediment Transport	Geo-Mechanics of the Breach Side Slopes	Comments, Limitations & Deficiencies
LOUKOLA & HUOKUNA (Loukola and Huokuna, 1998)	Trapezoidal	Broad crested weir flow and orifice flow (Fread, 1988a, Fread, 1988b)	Meyer-Peter-Müller		•
HR BREACH (original) (Mohamed et al., 1999, Mohamed, 2002)	YZ: Effective shear stress dependent XZ: Exner equation & soil wasting	Weir plus 1D steady non-uniform flow equation	Various sediment transport equations, including I Bagnold-Visser II Yang III Chen & Anderson	Slope stability – Osman Core stability	• Includes option for uncertainties in material properties
PEVIANI (Peviani, 1999)	YZ: Trapezoidal XZ: Exner equation	St Venant Equations	Di Silvio & Peviani formula	Slope stability (Peviani model) - critical erosion depth for failure - Plane failure surface with assumed slope angles	• Focussed towards analysis of landslide dams
MACCHIONE – RINO (Macchione and Rino, 1999)	YZ: triangular	Weir formula	Empirical erosion rate	None	•
RIHA & DANECEK (Riha and Danacek, 2000)	Continuous rectangular shape	Analytical solution for breach outflow and reservoir water level	Ponce's approach	None	• Calibrated with laboratory tests
TINGSANCHALI – CHINNARASRI (Tingsanchali and Chinnarasri, 2001)	XZ: Exner equation	1D SWE's	I Meyer-Peter-Müller II Smart III Rickenmann IV Bagnold-Visser V Takahashi	Stability of the downstream slope - Fellenius	•
DAVE_F (Froehlich, 2002, Froehlich, 2004)	Undetermined	St Venant & Exner equations	Erosion formulae from WEPP, USDA	None	• Tested against Norwegian field tests, IMPACT (original data)

Model	Breach Morphology	Flow Over the Dam	Sediment Transport	Geo-Mechanics of the Breach Side Slopes	Comments, Limitations & Deficiencies
ROZOV (Rozov, 2003)	YZ: Rectangular XZ: Exner equation	Weir formula Energy equation	Voinich & Syanojenski formula	None	• Simple practical tool
KRAUS (Kraus, 2003)	YZ: Rectangular XZ: Sediment mass conservation and horizontal channel	Not indicated	Not indicated	None	• Applies to coastal barriers (water on both sides of structure)
RUPRO Cemagref, FR Reported (Paquier, 1998, Paquier et al., 1998, Paquier, 2002)	YZ: Rectangular XZ: Horizontal channel	Bernoulli equation	Meyer-Peter-Müller	None	• Coupled with flood routing model
ERODE (Marche and Fuamba, 2002)	No assumptions	Stream tube formulisation as in GSTAR	Minimum stream power – sediment transport formulae		• Based upon the GSTAR flow model of (Yang and Simoes, 2000)
FIREBIRD (Wang and Kahawita, 2002, Wang et al., 2006)	Variable trapezoidal	St Venant and Exner equations. Unsteady formulation	Exner equation. Sediment transport formulae or erosion rate equations	Lateral breach stability considered	• Limited testing on (original) Norwegian data and two prototype cases
SIMBA (Hanson et al., 2005c, Temple et al., 2005)	Rectangular, trapezoidal	Broad crested weir formula	Parametric relations for headcut advance, bottom and lateral erosion (Hanson erosion formula)	Side slope erosion driven by same erosion concepts. No discrete failures.	• Developed on the basis of flume and larger scale (outdoors) experimental tests on head cut development
DamBreach (Wang and Bowles, 2006a, Wang and Bowles, 2006b, Wang and Bowles, 2006c, Wang and Bowles, 2006d)	Undetermined	2D solution of St Venant equations	Sediment transport formula (Smart) and erosion rate formula		• Non-cohesive; tested on data from laboratory and some IMPACT data

Model	Breach Morphology	Flow Over the Dam	Sediment Transport	Geo-Mechanics of the Breach Side Slopes	Comments, Limitations & Deficiencies
BRES (Zhu, 2006)	Five 5 stages of failure: YZ: trapezoidal XZ: Global Exner equation with rotation up to $\beta = \omega_0$ and then constant β	Broad crested weir formula + Bélanger	Erosion rate formula for cohesive sediment, with soil erodibility coefficient M to be determined experimentally or empirically	None	• Model for river and coastal dikes (developed from earlier 1998 version) • Simple slope stability mechanism. • No effect of waves
DamBreach (Wang & Bowles, 2007)	Undetermined	1D solution of St Venant equations	Sediment erosion rate formula		• Cohesive; tested on data from laboratory and some IMPACT data

Table 2-6 Major research initiatives supporting breach model development

Fread / NWS Breach (National Weather Service (NWS)) (mid 1980s onwards) Fread of NWS developed the original US DAMBRK code in the early 1980s (Fread, 1984). This code included the NWS BREACH model (Fread, 1988b) and revisions to the code were made in later years. Development of this model occurred with the start of widespread use of personal computers and the code proved very popular, particularly since it was freely provided. The code was used worldwide and a variation was adopted in the UK called DAMBRK UK (DoE, 1991) although this did not modify the breach model in any way.
Visser / BRES (Technical University of Delft (TUD)) (1990's onwards) Visser has undertaken a series of research projects investigating breach formation. His work produced the BRES model (Dutch for breach). BRES(1998) (Visser, 1998a) addressed breach through sand dikes whilst BRES(2006) (Zhu, 2006) addresses breach through clay dikes. The earlier work on sand dikes was underpinned by large scale testing of breach through a sand dike constructed across a tidal inlet at Zwin.
Wahl (US Bureau of Reclamation) (1990s onwards) Wahl has worked on a range of dam safety related issues for the last 20 years (Wahl, 1998). His work related to breach initially focussed on the analysis of peak discharge equations from breach (Wahl, 2004, Wahl, 2008b). Between 2005-2010 Wahl coordinated the CEATI (Centre for Energy Advancement through Technological Innovation) facilitated Dam Safety Interest Group (DSIG) project on breach modelling (Wahl et al., 2008). The goals of this work included collation of laboratory and field data on breach (Courivaud, 2007b, Wahl, 2007), identification of promising breach models for evaluation (Kahawita, 2007) and evaluation of breach model performance with the aim of supporting industry development and uptake (Wahl, 2009). Since 2005, research has also focussed on comparing and analysing different erodibility measurement equipment (Wahl, 2008a) (underpinning both breach and internal erosion research).
Mohamed / Hassan & Morris / HR BREACH (HR Wallingford) (Late 1990s onwards) Hassan (formerly referenced as Mohamed) undertook initial research and development of the HR BREACH model (Mohamed, 1998, Mohamed, 2002). This was undertaken in parallel with the European research projects CADAM (1998-2001) and IMPACT (2001-2004) (see below). Morris coordinated the CADAM (Morris, 2000) and IMPACT projects (Morris, 2005) along with breach research under the FLOODsite project (Morris et al., 2009a) which underpinned development of the next generation of the HR BREACH model (as reported in this thesis).
European Framework Research 1998 – 2009 These European funded research projects all included research related to different aspects of breach initiation and growth: **CADAM (1998-2001)** [www.hrwallingford.co.uk] – Concerted Action on Dambreak Modelling: Identified current state of practice and gaps in knowledge **IMPACT (2001-2004)** [www.impact-project.net] – Investigation of extreme flood processes and uncertainty: A programme of research looking at breach formation, flood propagation, debris and sediments and modelling uncertainty. As part of the breach research, 5 large scale field tests (Vaskinn et al., 2004a) and 22 laboratory tests (Hassan et al., 2004) were undertaken. Comparisons of the performance of various breach models were undertaken. **FLOODsite (2004-2009)** [www.floodsite.net] – Integrated flood risk analysis and management methodologies: Breach research here focussed upon wave induced breach initiation processes and detailed analysis of the IMPACT project data. New versions of the BRES and HR BREACH models were produced; research models simulating wave induced breach were also produced. Breach data from the IMPACT project was reviewed and issues identified (Hassan and Morris, 2008).

Temple, Hanson & Tejral / SITES / SIMBA / WINDAM (USDA-ARS-HERU) (1980s onwards)

Temple & Hanson undertook, and continue to conduct, an extensive, long term programme of research into the performance of earth embankments and small dams at the US Department of Agriculture, Agricultural Research Service, Hydraulic Engineering Research Unit centre at Stillwater, Oklahoma, US. Their test facilities allow for construction and testing of embankments typically 2m high, with established vegetation (since most facilities are open air). Research in the 1980/90s covering performance of vegetation and soil erosion; more recently (90s onwards) the work has focussed on soil erosion, headcut growth and most recently pipe formation through embankments. Hanson is responsible for the development of jet testing equipment for measuring soil erodibility, K_d, subsequently used within the Hanson erosion equations (Hanson and Hunt, 2006). This research work underpins the development of breach models simulating headcut advance through embankments. The SITES headcut model was originally developed, and more recently the SIMBA breach model which will be integrated within the WINDAM package (Temple et al., 2006).

Dam Safety Interest Group (DSIG) Breach Modelling Project (2006 - 2010)

The CEATI facilitated DSIG breach modelling project adopts many of the concepts applied under the earlier IMPACT project, but at a larger, more international scale (Wahl et al., 2008). Actions under the project included a review of breach models and identification of the most promising for potential industry use (Kahawita, 2007); review and collation of data available for breach model testing and calibration (Courivaud, 2007b); and evaluation of breach model performance and potential for integration into flow modelling packages for wider industry use (Wahl, 2009).

The IJKDIJK Project (2006 onwards)

The Ijkdijk [www.ijkdijk.eu] is a facility in the Netherlands to test dikes and to develop sensor network technologies for early warning systems. In studies of dike stability, about eighty dikes will be destroyed aiming to, ultimately, derive a relation between the various sensor readings and dike performance. The research on IJKDIJK is not focussed directly at breach model development, but at understanding the soil state and processes that lead to failure and hence processes that future versions of breach models might want to incorporate.

European Framework Research 2009 – 2013

UrbanFlood (2009 – 2012) (www.urbanflood.eu). The UrbanFlood project is an EU funded project under the ICT area of Framework Programme 7. The focus of the research is on the development of a sensor system embedded within flood embankments and linked wirelessly to the Internet and cloud computing facilities to allow real time analysis of embankment state and subsequently, real time analysis of flood risk. The flood risk assessment is made by analysing the probability of embankment failure, linked to breach prediction, flood inundation and flood impact models. The system will support routine asset management, event warning and event management systems.

FloodProBE (2009-2013) (www.floodprobe.eu). The FloodProBE project is an EU funded project under the environment call of Framework Programme 7. The focus is on flood risk management in the urban area, which includes analysis of processes affecting flood embankment performance. Aspects of relevance to breach modelling include analysis of internal erosion processes and soil erodibility, performance of flood defence structure transitions, and the performance of flood embankment grass cover.

2.4 Identifying and understanding key physical processes

In order to develop and assess the performance of a physically based predictive breach model it is important that there is first a clear understanding of the physical processes that occur during real embankment or dam failure. Sections 2.2 and 2.3 have emphasised some of the confusion and misconceptions that exist in relation to predicting breach growth, and in particular to predicting breach shape and the way in which the embankment structure erodes. Since the breaching process depends upon complex interactions between soil, water and structure, evaluation of these three processes simultaneously becomes very difficult in laboratory studies. Hence research performed in laboratories at small scale is particularly at risk of misrepresenting the correct physical processes (Morris and Hassan, 2005a). Missing the significance of soil state on erodibility and hence overall breach behaviour (Section 2.2.2) is also a common failing (Morris et al., 2008, Wahl, 2007). Hence, the most useful data for understanding breach processes is that collected from large scale tests or real events. Since large scale testing is expensive, and data from real events is not often recorded to the degree of detail and accuracy required, such data is difficult to find.

However, the programme of breach research under the European IMPACT Project (www.impact-project.net) comprised a series of five large scale field tests on up to 6m high dams, a programme of 22 smaller scale laboratory tests at 1:10 to field test scale dams, and an extensive programme of numerical breach model testing and comparison (Morris and Hassan, 2005a). A considerable amount of data was collected during this study. This data was not fully analysed during the IMPACT project because the amount of data collected and extent of potential analysis proved far more than had been anticipated and hence budgeted for. The data included survey data, DVDs with video footage, flow and water level data and sensor data reflecting the time when movement occurred at sensors embedded within the body of the dam. Hence, availability of this data provided an opportunity for a more detailed review, which forms part of this thesis. The extensive video footage from 36 project DVDs provided an invaluable record of breach initiation and formation processes for a range of different load conditions, structure type and soil type and state. The video

footage was recorded from various positions up and downstream of the breach, including some from directly above the breach.

A detailed report on this review, including many screen shots detailing specific breaching processes, is referenced in Appendix 5 and is also registered as FLOODsite Report T06-08-11 (Morris, 2009). Key findings are summarised in Section 2.4.2. It should be noted that an additional review of IMPACT Project data quality was also undertaken and a series of issues were identified relating to much of the test data. It was found that there were inconsistencies between the data provided during the IMPACT project, and hence reported within the IMPACT project reports, and that reported after the event by Statkraft Groner, who undertook the field work. The source of error appears to arise from the difference between specified and as built test conditions. In some tests these differences were significant and related to the embankment geometry as well as soil parameters. Findings from this review are reported under FLOODsite Report T04-08-04 (Hassan and Morris, 2008). Any readers wishing to access and use the IMPACT Project data should refer to this report as it provides recommendations as to corrections and clarifications to the IMPACT data sets and additional information regarding the field test conditions.

2.4.1 Analysis of the IMPACT project breach data

Key IMPACT project reports (available from the project website: www.impact-project.net) are:

1. The IMPACT Project: Final Technical Report (Morris, 2005);
2. IMPACT: WP2 Technical Summary Report (Morris et al., 2005);
3. IMPACT: Breach Formation Technical Report (WP2) (Morris and Hassan, 2005a);
4. IMPACT: Summary of breach formation field tests (Vaskinn et al., 2005).

The large scale field tests were undertaken in Norway, at a remote site close to the Arctic Circle (Vaskinn et al., 2004a). The test site (Figure 2-12) comprised a reach of river, where the test embankment was built, with a large reservoir, and hence flow control structure, upstream. Downstream from the test site the river widened into a small lake. The stage-volume relationship

at the test site allowed for a volume of approximately 70,000m^3 of water to be retained behind a 6m high test embankment. Hence, the 70,000m^3 of retained water plus any released from the upstream reservoir could be used during a test to create a breach.

Whilst five large scale tests were undertaken as part of the IMPACT project, additional tests were also undertaken as part of a parallel Norwegian funded national project. The five IMPACT project tests are summarised in Table 2-7.

Figure 2-12 Aerial view of the Røssvass dam breach test site (IMPACT project)

Table 2-7 Summary of IMPACT project breach field tests

No	*Reference*	*Height*	*Description*	*Failure initiation*
1	Test1-02	6m	Homogeneous cohesive structure (clay)	Overtopping
2	Test2C-02	5m	Homogeneous non-cohesive structure (gravel)	Overtopping
3	Test1-03	6m	Composite structure (gravel with moraine core)	Overtopping
4	Test2-03	6m	Composite structure (gravel with moraine core)	Piping (Overtopping)
5	Test3-03	4.5m	Homogeneous structure (moraine)	Piping

The writer coordinated the IMPACT project and hence all the data were readily available. A set of 36 DVDs was provided to the IMPACT project upon completion of the work in Norway by SWECO (formerly Statkraft Groner, a partner within the project). The DVDs provide video footage from cameras in different locations for different tests, but generally provide views from upstream and downstream left or right banks. For one test aerial footage directly above the breach

is also available, which shows the critical point when erosion of the downstream face cuts through the upstream edge of the dam crest. The video footage was analysed in detail as part of this research, with the observations summarised in Section 2.4.2 below. This analysis allowed different stages of the breaching process to be identified. In addition, data from three of the tests was provided to the Dam Safety Interest Group modelling project for use in model performance evaluation (Chapter 8; Appendix 3).

2.4.2 Summary of observed processes

Table 2-8, Table 2-9 and Table 2-10 provide a summary of the processes observed from analysis of the five field tests (Morris, 2005, Vaskinn et al., 2004b). These summarise breach initiation and growth processes observed in relation to flow, erosion and structure response respectively. A series of screen shots showing selected processes referenced in these tables are included in Figure 2-13, Figure 2-14 and Figure 2-15. More detailed versions of these tables, which include links to screen shots for each of the observed processes, are available in FLOODsite report T06-08-11 (Morris, 2009) under Table 8-1, Table 8-2 and Table 8-3. These are then followed by a discussion of the significance of these processes in relation to breach modelling methods and subsequently recommended approaches for future breach model development (as summarised in Section 3 of this thesis).

Table 2-8 Flow related processes observed from IMPACT field test video footage

No.	***Observed flow related process***
1	Broad crested weir flow (in notch)
2	Modified broad crested weir flow, with flow entering breach across embankment side slopes as well as directly through the mouth
3	Round or even sharp crested weir flow – weir shape modifies during crest erosion and as head cut erodes back through upstream crest edge
4	Braided surface flow (around rocks and cutting gullies)
5	Converging flow – flow behaviour as with a point sink (smooth glassy flow surface)
6	Asymmetric converging flow behaviour as approach velocity changes
7	Flow parallel to crest along embankment faces either side of breach opening
8	Turbulent flow (up welling) against face of embankment either side of breach opening
9	Elongated vortices created along base of either face within the breach
10	Central jet emerging through converging flow in breach as embankment erodes down and greater flow can pass directly through the converging and falling flow
11	Seepage and piping through cracks and fissures developing within remaining embankment sections
12	Upstream vortices into mouth of submerged pipe through embankment
13	Culvert / pipe flow behaviour for flow through enlarging pipe (in relation to varying up and downstream water levels)
14	Minor and transient disturbances to breach flow as large blocks collapse into central breach area and are removed

a. Erosion of surface layer; flow eroding fines from between larger rocks

b. Broad crested weir flow cascading into head cut through clay embankment

c. Flow converging to point shortly after erosion cuts through upstream crest

d. Flow vortices and undercutting along the toe of each eroding breach face

e. Central jet of water flattens as erosion removes upstream embankment material

f. Secondary seepage and erosion as breach results in tension cracking and progressive block failure

Figure 2-13 Screen shots showing selected flow related processes

Table 2-9 Erosion related processes observed from IMPACT field test video footage

No.	***Observed erosion related process***
1	Headcut erosion was observed in 3 of the 5 tests; surface erosion was observed in 1 of the 5 tests and piping occurred for the remaining test.
2	Headcut erosion allowed erosion of a stepped or near vertical face to cut back into the upstream crest leading to a relatively sudden and catastrophic collapse of the eroding breach section.
3	Surface erosion allowed progressive erosion of the embankment material leading to (what appeared to be) a less catastrophic failure of the embankment section.
4	Headcut erosion was observed in frozen gravel (non-cohesive) material. The geometry was very rigid with vertical cut sides and a single step back to failure.
5	Three types of sediment erosion / removal were observed, consistent with Mostafa (Mostafa et al., 2008); these were sediment erosion, mass erosion and soil wasting. Sediment erosion occurred through particles within the flow. Mass erosion occurred where small blocks of clay or soil were removed (often during the initial overtopping phase). Soil wasting occurred where large blocks of embankment failed into the breach flow and were rapidly removed by the high energy flow.
6	Significant erosion of the upstream face of the embankment on either side of the breach was observed, with converging flow running parallel to the embankment crest into the breach area.
7	Block failure occurred through undercutting of the breach side faces by highly turbulent, elongated vortex flow which arose due to strong flow convergence through the breach and which ran along the eroding toes of the breach side faces. This is consistent with other research observations (Mingsen et al., 1993).
8	Pipe formation could only be observed from the outside, but demonstrated removal of sediment through 'sediment erosion', arching of the embankment soil and collapse of the downstream embankment progressively from the pipe outlet backwards to the crest.
9	Soil wasting also occurred where the force of flow near to the breach helped to created tension cracks in the remaining embankment sections, allowing erosion within the cracks and shear failure of the blocks in response to the high pressure of flow.

a. Initial surface erosion of sediment

b. Early stages of mass erosion (small lumps being removed)

c. Substantial head cut erosion into 6m high clay embankment

d. Head cut in heavily compacted and potentially frozen (non-cohesive) gravel material

e. Surface erosion at crest – onset of breach formation as erosion cuts through upstream edge of crest

f. Block failure leading to soil wasting – this block completely removed within 3s of frame

Figure 2-14 Screen shots showing selected erosion related processes

Table 2-10 Structure related processes observed from IMPACT field test video footage

No.	***Observed structure related process***
1	Tension cracks develop within the crest and slopes of the embankment as breach formation occurs (prompting soil wasting along these lines)
2	The exposed ends of the embankment (facing into the breach) showed signs of slumping and rotation into the breach. As large blocks were created through cracking, those most exposed to the breach flow also showed signs of sliding before eventual failure.
3	Breach sides remained vertical, near vertical or undercut. Erosion within the breach leading to soil wasting created undercut sections just prior to failure.
4	Arching of the soil structure was observed during the piping test (and also obscured erosion during the failed piping tests). During the single test, no signs of crest disturbance were observed right up to the point of crest failure.
5	Pipe migration from the base of the embankment towards to top of the embankment occurred for the failed piping test.

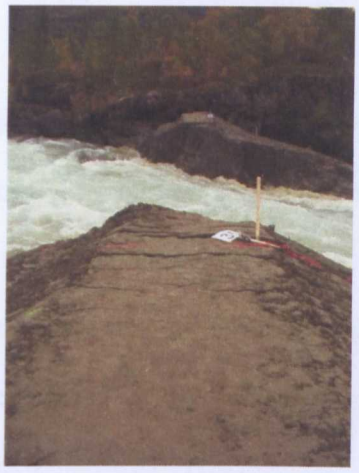

a. Tension crack forming in crest; embankment ends rotating into breach

b. Tension cracks develop into block failure. Pressure of flow sliding and rotating blocks

c. Soil block fails and rotates into breach flow (removed completely within 10s)

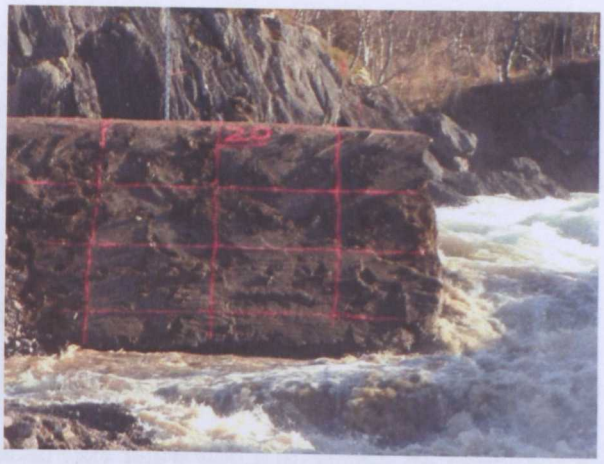

d. Breach sides remain vertical or undercut during the breach formation process

e. Overhanging remains of embankment made from non cohesive material at test completion

f. Arching effect during pipe formation delays roof collapse

Figure 2-15 Screen shots showing selected structure related processes

Based upon the review of processes observed from the field tests, the following points may be concluded:

1. The flow processes that occur during breach initiation and growth are complex and three dimensional. Elongated vortices tend to form along the breach faces, actively eroding and undercutting the breach sides;
2. The flow processes vary according to the different stages in breach initiation and growth and depend upon the eroding embankment geometry, size of breach and up and downstream water levels;
3. A range of flow processes and controls can occur at any given time during the formation process, as embankment and breach geometry is rarely regular, and approach flow conditions are not normally symmetric and uniform;
4. Overall erosion behaviour falls into one of two main categories: head cut erosion or surface erosion;
5. Factors dictating whether head cut or surface erosion occurs are not clear, but seemingly related to soil strength or erosion resistance;
6. The rate of release of flood water (i.e. nature of failure event) differs between head cut and surface erosion (but also probably as a function of upstream storage volume and water level);
7. Most of the erosion processes occur simultaneously at any given time;
8. Soil wasting through block failure appears to be a significant physical process through which breach formation and widening occurs;
9. Sediment erosion and removal is not uniform or steady. High energy flow typically removes soil blocks that fall into the breach within seconds;
10. The structure response to breach formation appears to guide where subsequent block failure will occur (through the creation of tension cracks). The tensile strength of the material therefore plays an important role here;
11. The sizes of soil blocks tend to follow the embankment geometry, comprising blocks (the full depth of the embankment to undercutting flow) that are the width of the crest section, upstream or downstream slope sections, or a combination of two or all of these.

Considering these points in relation to breach model development:

Complex Interactions

It can be seen that the processes of breach initiation and growth comprises complex interactions between flow, soil erosion and structure response processes. An error in predicting any of these 'components' can significantly affect the results of breach modelling. This error might arise from the modelling methodology itself or the data used to describe the embankment and hydraulic conditions.

An alternative approach to the deterministic prediction of these specific processes is to adopt a probabilistic approach in the simulation of breach. Hence a distribution of possible answers will be provided rather than a single deterministic solution. This approach is better suited to situations with complex interactions and a lack of knowledge of embankment soil parameters and state.

However, there are likely to be conflicting demands from industry for different types of breach model. Predictive breach models will be required to work in parallel with predictive flow models, whilst probabilistic breach models will provide additional information and understanding for situations where in-depth breach studies are appropriate.

Model development: Two broad lines of model development can be envisaged; deterministic and probabilistic, or a combination of the two. For predictive models an appropriate balance between all three processes (flow, erosion and structure) needs to be established within the breach model, so that a consistent level of detailed inputs that are of adequate accuracy is adopted throughout the model leading to the final breach prediction.

To date probabilistic approaches related to breach have tended to focus on breach location within flow systems, rather than detailed analysis of a single breach case (Sayers and Meadowcroft, 2005). In these cases, even simpler breach models or assumptions tend to be used because of limitations in

computing power. Research under the Flood Risk Management Research Consortium 2 programme is investigating this aspect of breach (Spagni et al., 2009, van Damme, 2010). Hassan developed a Monte Carlo option within the original HR BREACH model that allows the user to specify breach parameter distributions and then analyse result distributions (Mohamed, 2002) and application of this is demonstrated on the Tous Dam case study within the IMPACT project research (Morris and Hassan, 2005b). Development of more refined probabilistic methods for breach analysis has not been undertaken; uncertainty regarding true breach physical processes and the selection of relevant soil parameters may have influenced this.

Flow Simulation

3D flow simulation would be most appropriate for simulating the complex flow conditions within a breach. However, to predict overall breach behaviour requires flow, erosion and structure response to be simulated; full 3D simultaneous simulation of these processes is not yet possible within a reasonable (industry acceptable) model run time, hence simplifications remain necessary in practice. (This conclusion is drawn from initial observations of model run times for simple breach conditions conducted by EDF as part of the Dam Safety Interest Group breach modelling project (Theriot, 2008)).

Where 2D flow simulation is possible, either 2D-H or 2D-V will provide a refinement upon 1D simulation, but will also miss key processes. 2D-H will allow for flow contraction into the breach but will miss flow dropping through the breach and the vortex behaviour leading to soil wasting within the breach. 2D-V will miss flow contraction and vortex behaviour.

Where only 1D flow simulation is practicable, then modifications to allow for contraction and evolving weir profile may allow some improvement of the flow calculation.

It is clear from all of the tests that the earlier, traditional assumption of trapezoidal breach flow is unrealistic; breaches have vertical or undercut sides, hence flow should be calculated accordingly.

Model development: Whilst 3D simulation of flow is appropriate for breach conditions, it is recognised that this is not yet practicable (in conjunction with 3D erosion processes and 3D structure response). Where possible 2D flow simulation (2D-H) should be adopted to account for flow contraction when approaching the breach. If 1D flow is adopted, then calculation should take into account the varying flow conditions and the evolving breach section.

Erosion Simulation

A number of different types of erosion have been observed (sediment erosion, mass erosion and soil wasting). All occur within a very transient and dynamic environment. Soil erosion occurs – not equilibrium sediment transport – hence mass conservation is not observed for numerical modelling.

The rate of breach growth and widening would appear to depend upon the rate of soil wasting. This in turn depends upon the size and frequency of block failure, dependent upon the breach toe erosion process and tension cracking within the embankment. Erosion also depends (of course) upon the erodibility of the soil in question and hence erodibility and how this may vary within a soil, or through different layers of soil, needs to be included within the model.

Model development: A better understanding of structure response, tension cracking and soil wasting is required in order to refine model prediction. Current state of the art models that consider soil wasting do so on an individual section by section basis (i.e. 2D analysis of stability rather than 3D) whilst tests show that failure tends to occur by geometric regions such as within the crest or slope areas, implying a 3D process. Breach models should be developed to allow for variations in soil erodibility to be considered.

Structure Simulation

The susceptibility and response of the structure to breach formation needs to be considered as an integral part of the breach model. This is linked closely to the simulation of erosion processes, since processes such as tension cracking, soil wasting, block sliding etc. arise in response to the preceding erosion.

The accuracy of predicting breach formation and widening might be improved by a closer inspection and more detailed analysis of the embankment sections adjacent to the breach. In particular, how these sections erode during the early dynamic flow stages, crack due to loss of structural integrity and slide through pressure of the approaching flow. Understanding how these processes occur and support breach development would allow a better representation of the processes to be developed. Links between field observations (site inspections), measured data and the risk of breach could also be developed to support flood risk management activities. Research under the EU UrbanFlood project is currently developing real time modelling systems to predict flood risk based upon measured field data, collected in real time by sensors embedded in the flood embankments (Krzhizhanovskaya et al., 2010). Cost effective methods for the provision of real time embankment data makes the inclusion of these breach processes within future models feasible.

Structural behaviour of an embankment is also highly dependent upon soil type and state. Simulation of soil erodibility and how it may vary within a homogeneous embankment, or change between different material layers or construction layers, may help to improve breach model accuracy.

Model development: Breach models should include greater detail regarding the response of the structure to breach formation. Analysis should include an assessment of when and where soil blocks might form. Rates of erosion should also relate to varying soil erodibility as a function of soil type and / or state.

2.4.3 Effect of freezing on breach growth

The IMPACT project field test on a dam constructed from non cohesive material provided an interesting special case because of the freezing conditions under which the test was undertaken. The dam showed very clear headcut erosion despite, in theory, being a non cohesive and potentially highly erodible material. Whilst heavy compaction helped to improve resistance to erosion, the freezing conditions most likely significantly affected behaviour (Figure 2-16). Breach formation through headcut rather than surface erosion changes the timing and shape of the breach flood hydrograph.

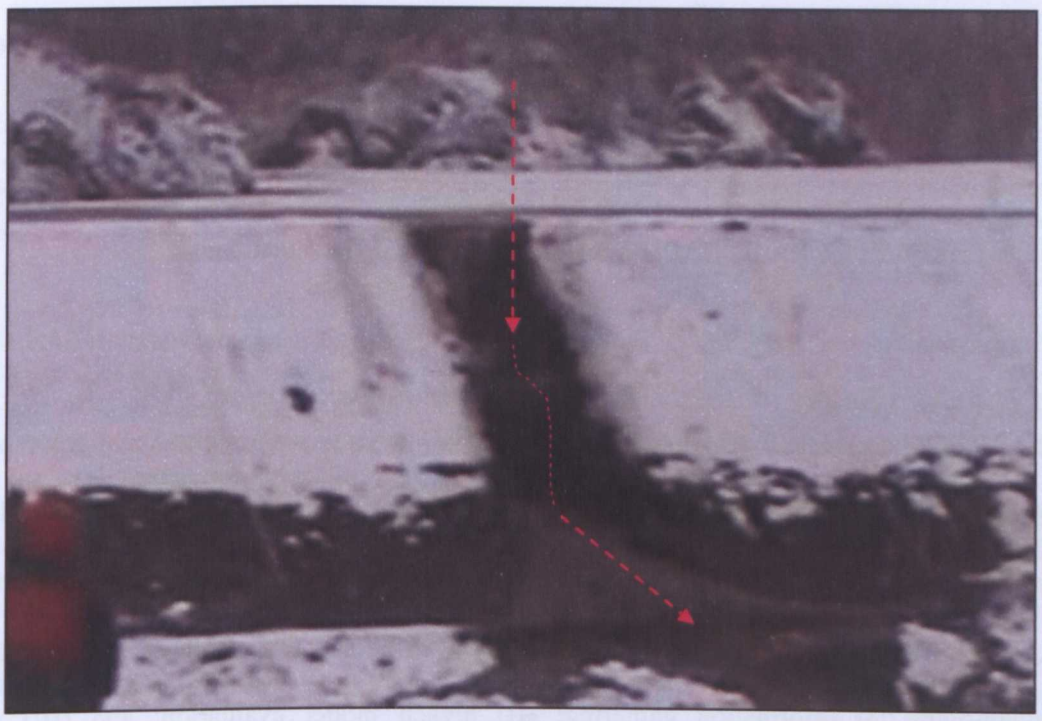

Figure 2-16 Enlargement of Figure 2-14d showing headcut through frozen non cohesive material

This finding has implications for breach modelling under extreme climatic conditions and hence should also be of interest when considering potential climate change effects on breaching processes. Extremes of temperature will affect soil state by changing moisture content. Under very hot conditions, moisture will reduce and cracking will be an increased risk. Under very low temperatures, as shown here, there is the potential for freezing the moisture within the soil structure. Climatic changes will also affect any surface vegetation, which will in turn affect soil moisture retention and hence erosion behaviour. Whilst specific climate change impacts such as these are not considered further within this thesis, they will require closer analysis in future in order

to determine the real effect that climate change has, or will have, on the performance of flood embankments and dams, and hence allow the assessment of future variations in flood risk.

2.5 Evaluating breach model performance

In undertaking any model development it is necessary to evaluate model performance to establish an absolute measure of performance and to ensure that any developments have made a positive contribution. During the IMPACT project, considerable work was undertaken to try and assess the relative performance for a number of breach models against the various field and laboratory test data. This concept was recently adopted and taken further by the Dam Safety Interest Group (DSIG) Breach Modelling project (Wahl et al., 2008). The writer participated in this project, using the international expert meetings to discuss and develop breach modelling concepts and the selected test case data for HR BREACH model development and evaluation.

2.5.1 The Dam Safety Interest Group Breach Modelling project

The CEATI facilitated Dam Safety Interest Group (DSIG) comprises an international group of dam owners that undertakes collaborative research on a wide range of topics. Since 2004 the DSIG has been working to facilitate the development and deployment of a physically-based embankment dam breach model. A working group and project was initiated in 2004 with a plan for three phases of work comprising (I) information gathering; (II) breach model evaluation; and (III) model refinement and integration. These actions are consistent with recommendations from a US review of dam failure analysis needs (Hanson et al., 2001a) and efforts under the IMPACT project to review and evaluate breach models (Morris and Hassan, 2005a).

In Phase I, three activities were completed comprising (1) development of a database of case studies suitable for use in breach model testing; (2) a review of laboratory and field testing programmes to identify data sets that could be used for breach model testing and evaluation, and (3) a review of computational breach models to identify those models which could serve as the foundation for a next-generation breach modelling tool (Wahl et al., 2008)

The conclusion from Activity 3 of the Phase I work (Kahawita, 2007) was the recommendation to evaluate the performance of 3 specific breach models (Table 2-11), namely:

- SIMBA – Under development at the USDA-ARS Hydraulic Engineering Research Unit, Stillwater, Oklahoma. (Hanson et al., 2005c, Temple et al., 2005);
- HR-BREACH – Under development at HR Wallingford, UK. (Mohamed, 2002, Mohamed et al., 2002);
- FIREBIRD BREACH – Under development at Montréal Polytechnic. (Wang and Kahawita, 2002, Wang et al., 2006).

Table 2-11 Summary of basic model characteristics (Wahl et al., 2008)

Model	***Embankment types***	***Erosion modes***	***Erosion processes***
SIMBA	Homogeneous cohesive	Overtopping	Head cut formation, deepening, and upstream advancement; lateral widening
HR-BREACH	Homogeneous cohesive, or simple composite embankments with non-cohesive zones, surface protection (grass or rock) and cohesive core	Overtopping, piping	Surface erosion or head cut erosion. Variety of sediment transport / erosion equations and multiple methods for application. Discrete breach growth using bending, shear, sliding and overturning failure of soil masses
FIREBIRD BREACH	Homogeneous, cohesive or non-cohesive	Overtopping	Surface erosion. Coupled equations for hydraulics and sediment transport

Evaluation of these models was undertaken using a set of seven test cases, drawn from a variety of data sources, comprising 2 tests from the US Department of Agriculture, Agricultural Research Service laboratory (USDA-ARS, Stillwater, Oklahoma), 3 tests from the European IMPACT project and 2 real dam failure case studies (Courivaud, 2007b). These data sets are summarised in Table 2-12 and presented in more detail in Section 8 and Appendix 3.

These tests provide a range of challenges for the models, since they cover a range of material types and condition plus additional factors that will have affected the breach initiation and growth processes.

The ARS tests provide very reliable data (both for construction and test conditions) relating to the failure of earth embankments via the head cut process. Whilst the first test comprises a sandy soil that is relatively erodible, the second contains a higher degree of clay, is far less erodible and does not reach the breach formation stage during the test. Both embankments include grass cover which delays the onset of surface erosion and head cut formation.

Table 2-12 Summary of DSIG test data used for model evaluation

Name & Source	*Description*	*Comment*
ARS#1	2m high, homogeneous embankment constructed from silty sand. Includes grass cover.	Controlled construction. Head cut failure occurs
ARS#2	2m high, homogeneous embankment constructed from clay-loam. Includes grass cover.	Controlled construction. Head cut starts, but failure does not occur within timeframe
IMPACT Clay (Field Test#1 / Test1-02)	5.9m high homogeneous embankment with ~25% clay content. No surface protection (grass etc.)	Very wet construction. Variable compaction. Head cut failure.
IMPACT Gravel (Field Test#2 / Test2C-02)	5.0m high homogeneous embankment constructed from gravel (D_{50} 4.75mm)	High degree of compaction. Freezing conditions. Head cut failure occurs
IMPACT Composite (Field Test#3 / Test1-03)	5.9m high composite embankment constructed from moraine core with rock fill cover layer	Mixture head cut and surface erosion failure
Oros Dam (Brazil)	35.5m high zoned dam with mass clay core, sand and rock fill shoulders	Real dam failure case study Uncertainty within data means test data are calculated / estimated
Banqiao Dam (China)	24.5m high zoned dam with clay core and earth shoulders. Failed during construction - condition at failure uncertain.	Real dam case study. Limited data (for example, core geometry unknown) hence test data are calculated / estimated

The IMPACT project tests were at a large scale but have a higher degree of uncertainty regarding soil state (Hassan and Morris, 2008). In particular, the clay test was constructed during a very wet period, hence the clay was soft with a very high moisture content. The gravel test was constructed with a very high degree of compaction, but was conducted during late autumn during freezing conditions. It was clear that this affected at least the surface layer of the dam. Analysis of the composite test construction geometry suggests that this was more akin to a homogeneous embankment with a surface layer of rock protection as compared to a rock fill dam with a moraine core (Appendix 3).

Finally, both the Oros and Banqiao cases (Courivaud, 2007a, Courivaud, 2007c, Wikipedia Contributors, 2011b) were real dams that failed and demonstrate the typical problems associated with dambreak prediction, namely considerable uncertainty in all data describing the event. Test conditions for these two cases were estimates based upon an analysis of limited recorded data combined with observations from the event. For example, details of the material used for dam construction are poor, and restricted to an indicative soil type. Details of the breach outflow are back calculated from recorded and observed reservoir water levels. This means that small errors in estimating the reservoir level with time result in large errors in estimated outflow due to the large reservoir surface area.

2.6 Investigating the original HR BREACH model

A detailed review of the original HR BREACH model (Mohamed, 2002) was undertaken. A summary of the key modelling processes covering flow calculation and sediment and section erosion, including breach side slope stability, is provided in Appendix 1.

During this review a number of model performance issues were noted, modifications to the code and run settings undertaken and rules established regarding use of the model. This, and later research activities address some of the future research recommendations from Mohamed

(Mohamed, 2002). Key issues and actions arising from the initial review of the original model were as follows:

Explicit Modelling Solution – Space and Time Step Dependency

The modelling process of Mohamed (Mohamed, 2002) uses an explicit solution, which means that the solution depends upon space and time steps defined by the modeller. Achieving an implicit modelling solution that simultaneously solves for hydraulics, sediment transport and breach side slope instability and soil wasting would require a far more complex modelling approach. At this stage in model development and testing, it was thought appropriate to continue with the explicit approach, but to check for any model performance limitations.

Testing the model for a range of space and time steps showed that there are zones of space and time value combinations that result in poor model performance. In this instance, 'poor' is taken to be the point where results from using the combined values of space and time show a significant trend away from the observed test results. Within the 'acceptable' range of space and time values the model results show slight dependency, but cluster around the observed test results. A basic rule to ensure acceptable performance was found to be selection of a uniform section spacing (in metres) that was, at most equivalent to the embankment crest width, but ideally half crest width. From a physical perspective this is necessary in order to define the embankment crest profile. The associated time step (in seconds) should be broadly equivalent to the section spacing (in metres). Increasing the time step by a factor of 2 or 3 can be accepted where model run times become limiting. The Courant-Friedrichs-Lewy condition (Courant et al., 1928) applies in principle here, but is complicated through the inclusion of soil wasting from block failure within the breach.

Simplified Section Profiles

In order to optimise model run speed, the various combinations of hydraulic load condition and potential flow section evolution and block failure were identified and then simplified to a minimum number of section description points (Buchholzer, 2007).

Modelling Tolerances

The breach model incorporates a series of tolerance factors that define the degree to which iterations continue to achieve numerical solutions at each time step. Some of these tolerances were found to have a marked effect on modelling results; hence the values were revised to ensure minimal influence. These tolerances were then set as default values within the modelling software. It was noted that where model simulations showed no breach development or progression, yet hydraulic load conditions were applied, the lack of initiation could relate to the use of specific tolerance values. For example, where erosion at a section is found to be below the selected tolerance level, then no section profile update is undertaken and hence no change to the breach section will be seen. This will remain the case until tolerance values are exceeded by the load condition.

2.6.1 HR BREACH model limitations

Evaluation of the HR BREACH model (Mohamed, 2002) under the IMPACT project concluded that it was one of the better performing breach models at that time (Morris and Hassan, 2005a, Morris et al., 2005). This conclusion was endorsed two years later by the selection of this model (and two others) for further evaluation under the DSIG project (Kahawita, 2007). The approach taken within the model to integrate flow, sediment erosion and structural behaviour has been built on by others (Wang and Bowles, 2006b, Wang and Bowles, 2006c, Wang and Bowles, 2006d) but significant improvements in performance have yet to be demonstrated. For example, Wang (Wang and Bowles, 2006d) presents excellent performance of his model against the EU IMPACT project data (Vaskinn et al., 2004b) but this was prior to published warnings about potential errors in the IMPACT project data sets and test case conditions (Hassan and Morris, 2008). Hence, the model performance appears to have been fitted to the data, rather than evaluated against it.

Whilst the original breach model (Mohamed, 2002) performance has been considered to be good in comparison to many other breach models, there were a number of areas where the modelling

process could be extended and improved. The initial review of model performance identified the dependence of the modelling results upon the flow and sediment model used (1D explicit rather than, say, 2D implicit scheme). However, it also highlighted the complexity of interactions that occur between flow, erosion and structure behaviour; the timing of initiation, controlled by the performance of surface layers, could also have a significant impact.

Since the underlying concept for original model development was to integrate flow, erosion and structural processes to broadly the same degree of analytical complexity, any improvements should try to maintain this concept. This approach supports the fact that the entire breach initiation and growth process comprises complex interactions between different physical processes. Consequently, the focus for model development should adopt a wide ranging approach, looking at improvements in all process simulations rather than focussing just on, say, flow or erosion prediction.

A more fundamental issue to consider, given the complex interdependencies, is whether a physically based deterministic model is the best approach for simulating breach processes? It might be argued that a probabilistic based approach to breach modelling is more appropriate given the large number and magnitude of uncertainties spread throughout the modelling process. This approach has been investigated by researchers such as (Morris and Hassan, 2005b, Yang, 1996b) and can produce a spectrum of results as shown in Figure 2-17 below. This plot shows the number of breach simulation results distributed by peak discharge value. The grouping of results to the left demonstrates a large number of scenarios where the modelled outflow is significantly lower than the distribution of results to the right. This group of results represents the scenarios where catastrophic breaching did not occur, and hence the peak discharge value arises from overtopping only. The group of results to the right show a wider distribution of peak outflow values. These reflect different breach scenarios where the unique combination of parameter values for each run results in a slightly different breach scenario. In this example, the peak outflow value varied from around 15,000m^3/s to 23,000m^3/s. The inset image shows an enlarged scale plot of these breach scenarios. By providing a distribution of potential breach scenarios in this way the dam owner is

able to appreciate the uncertainty within the breach prediction and perhaps use a range of scenarios for emergency planning. Closer analysis of the data may also allow dependence of the predictions on certain parameters to be identified and hence steps to be taken through which the likelihood of catastrophic breach may be reduced. Such an approach can form part of risk analysis and management for dam safety (Morris et al., 2011a). In practice, it is likely that both deterministic and probabilistic approaches will be of value to meet the range of industry needs (see Section 1.1).

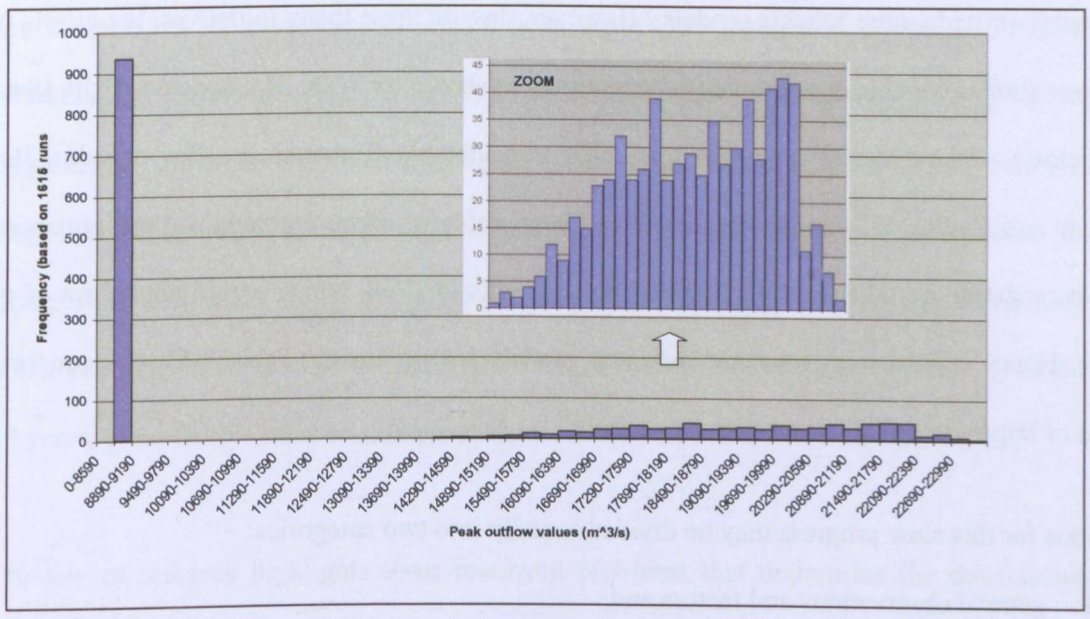

Figure 2-17 Example of Monte Carlo analysis of breach formation

3. Identifying gaps in knowledge and research priorities

3.1 Observations and conclusions from the literature review

Many of the publications produced emphasise the importance of accurately predicting breach to support flood risk analysis for dams or flood embankments (Wahl, 1997) and then proceed to develop a new model or method. The review of breach models (Section 2.3; Table 2-5) shows that research into breaching processes and prediction has been undertaken for many decades in an attempt to provide more reliable models. However, despite these many initiatives, the efforts often uncover similar conclusions and recommendations, as shown by Wahl, Ralston and White (Section 3.2 below). This cycle of repetition goes back considerably further than a few decades; Bossut (Bossut and Viallet, 1764) gave descriptions of how soil type affects embankment performance and how care should be taken in selecting and placing soils in 1764, which would not be out of place today. Hence, whilst numerous methods and models are produced (Table 2-5), real progress in terms of improving prediction accuracy, is slow.

Reasons for this slow progress may be divided broadly into two categories:

1. general observations and factors and;
2. specific factors relating to the influence that material properties and condition have on the breaching process (Morris et al., 2008).

3.2 General factors influencing progression of breach modelling capability

Similar observations relating to beach growth processes may be seen in publications dating back over the last six decades (Ralston, 1987, Wahl, 1997, White and Gayed, 1943). All authors agree on the need to reliably predict breach in order to manage flood risk; Wahl (Wahl, 1997) starts with the statement that "simulation of embankment dam breach events and the resulting floods are crucial to characterizing and reducing threats to potential dam failures". The authors also describe similar observations for the breaching processes. Wahl refers to the "predominant mechanisms of headcut erosion, geotechnical slope failure and lateral erosion" whilst Ralston (Ralston, 1987)

states that "it is necessary to understand the mechanism of embankment erosion", that "erosion of cohesive soil occurs in single or a series of stair step cascades" and that "hydrodynamic and soil mass wasting processes are involved". Ralston also recognises that "interest (in predicting breach)...has existed for years, even centuries". However, subsequent investigations to produce a better model rarely consider the full range of load conditions and soil types, resulting instead with a model or method that offers a solution for only certain, limited breach conditions.

During the past few decades there have also been significant changes in science and technology that should allow improvement in our ability to model or predict breach growth. These include the development of concepts, tools and techniques in the field of geotechnical engineering and the development of computers to aid predictive modelling. It is clear that both of these areas play an integral part in our present ability to predict breach growth, however, improving capabilities within both of these disciplines are not similarly reflected in breach modelling progression over the last 10-20 years; other factors must be dominant here.

The review of research highlights three recurring problems that undermine the development of more reliable, generic breach modelling solutions. These are the:

i. Limitations in model applicability;
ii. Use of incorrect modelling assumptions;
iii. Misapplication of models.

Limited model applicability

It has been shown in Section 2 that the overall breaching process is complex, with a number of different stages and processes that are dependent upon the type of embankment design, material and construction, and which are more or less relevant to different types of end user. Key differences between breach initiation and growth processes related to material type (primarily rock fill, non-cohesive and cohesive earth fill) have not always been clearly identified by researchers. Many researchers focus on overtopping breach of non cohesive material, undertaking tests with

sand in laboratory flumes. Results of this work are then published as a new breach modelling solution without emphasising the limited scope of applicability of such a model. Such a model will only simulate a surface erosion process, ignoring the headcut process that occurs with less erodible material. In addition, unless details of the way in which the sand has been compacted are analysed, the process of embankment surface flattening, steepening or parallel retreat may be reported as a generic breach model solution, rather than a solution for those specific conditions. Consequently these are often dismissed by later researchers who identify that the earlier model performs poorly in comparison to new methods, when applied to a different data set. This does not necessarily mean that the models are poor, rather than there is a failure to recognise the importance of material state as well as type when developing and validating models, and that such models have very specific limitations for application. It should be recognised that a majority of dams or flood embankments are made from either cohesive or a mixture of cohesive and non cohesive material, hence a model that simulates only sand erosion, only offers part of a generic solution for breach prediction.

Use of incorrect modelling assumptions

A common error with many models is the use of a predefined shape for the eroding breach section. As shown in Table 2-5, the cross section of the breach used for flow calculation in models is often given as trapezoidal or even triangular, when in practice it can see seen as very nearly rectangular, with vertical or undercut breach side slopes. The effect of this error on breach prediction accuracy will be 'site specific' since, as the breach widens, the error contribution from incorrect side slope representation to the overall outflow prediction, reduces. However, changes in the breach initiation process also affect the timing of overall breach development, which in turn can have a significant impact on overall results (see Section 4.1).

The recent failure of a Hungarian tailings dam (Figure 3-1) provides a clear example of vertical sides to a recent breach whilst the British Waterways archive of canal breach data also confirms observations that breach sides are typically vertical during breach formation (British Waterways, 2005, British Waterways, 2010). Collapse of the side slopes after breaching has occurred helps to

support the incorrect assumption of triangular or trapezoidal shape during the breach formation process. Publications past and present (Froehlich, 2008, Illes, 1977) propagate these perhaps mistaken concepts. Naturally, use of a trapezoidal rather than rectangular flow section within a breach model can noticeably affect the discharge calculation; complex interactions between soil, water and structure mean that such changes can result in significantly different end results.

Figure 3-1 Vertical sides to breach through Hungarian tailings dam (BBC, 2010)

A further problem with some models is the inappropriate use of case study data to validate the model. A good example of this is use of the Teton Dam failure which is often cited because it is one of a few rare data sets that exist regarding the real failure of a large dam. However, the Teton failure arose through a very specific failure process of seepage across a rock abutment (Muhunthan and Pillai, 2008), leading to pipe formation and complete dam failure. The significance of breach development against a rock abutment rather than in the body of the dam often appears overlooked. As reported by Mohamed (Mohamed, 2002) and the IMPACT Project (Morris and Hassan, 2005a, Morris and Hassan, 2005b) the location of a breach does noticeably affect the breach evolution rate and hence the outflow hydrograph. One of the IMPACT Project laboratory tests investigated the difference in the nature of breach growth between initiation at a central location and initiation

adjacent to non erodible material (i.e. the flume side). The tests showed a measurable difference in peak discharge (for the given test geometry) of approximately 13%, with the centrally located breach resulting in the higher discharge (since the rate of breach growth was higher because erosion could occur in both directions simultaneously). A similar effect might be envisaged for the Teton Dam failure which had non-erodible rock abutments. Hence, validation of a breach model assuming unrestricted breach growth, but using the Teton data to validate, will lead to a systematic error in the model.

Misapplication of models

Since breaching processes in relation to soil and structure type do not appear to be well understood by researchers, model users, who may have far less detailed knowledge of the physical processes, often misapply models in the search for a quick and easy solution.

A recent example of how modelling approaches can be misapplied is given by Tucker (Tucker and Spencer, 2010) for the analysis of potential breach for the Herbert Hoover dike. In this paper, the authors review different parametric equations, which are based upon dam rather than levee failure, and consider how they might perform for the Herbert Hoover Dike (HHD). The HHD comprises 143 miles of levee, encircling Lake Okeechobee. The levees have an average height of 35ft (10.7m) and the lake has a large surface area of 720 miles^2 (1,865km^2) with an average retained depth of 10ft (3m) resulting in an average (and very large) retained volume of 5.6×10^9 m^3. The authors review a range of parametric equations, developed through analysis of historical dam failure, rather than levee data, and choose to apply one of these equations rather than adopting a predictive model as detailed in various European research initiatives (for example the work on dike breach by Verheij (Verheij, 2002)) or the DSIG project (Wahl, 2009). Further to this, the MIKE11 model (DHI Software, 2004) is also applied, apparently because it offers an integrated breach and flow model, rather than because of the accuracy of the breach model. The author states "...it is probably impossible to say it is the most accurate of all other prediction models, its dynamic link to MIKE21 FM (flexible mesh) makes it convenient and efficient to produce the products as tasked". This

suggests selection of the model for ease of use rather than quality of performance. Having listed a large number of possible analysis methods, a comparison of only Pugh (Pugh, 1985) and MIKE11 is made, giving similar results. However, it is clear from earlier discussion that use of some of the other methods would have given significantly different results. Finally, a comparison between the analysis and a local breach event is given, showing very similar outflow hydrographs, but with no discussion regarding the significant differences in key parameters – notably the lake surface area – which, combined with soil erodibility, would have a affect major influence on the breach conditions.

3.3 Specific factors (material properties) influencing progression of breach modelling capability

More recent research into the effect of material properties on breach, particularly for cohesive materials, highlights some specific factors that could explain why many models initially appear to perform well, but are subsequently discredited by others who find their performance not to be as good in comparison to (yet) another new breach model. As early as the 1940s it was observed that clay and water content had a significant effect on physical modelling of breach failure of small scale embankments (White and Gayed, 1943). At that point no conclusions physically or numerically were made because it was deemed too complex to offer a solution. Research over the last decade by Hanson and others (Hanson et al., 2001b, Hanson and Cook, 2004, Hanson et al., 2005a, Hanson et al., 2005b, Hanson et al., 2005c, Hanson and Hunt, 2007, Hunt et al., 2005) at USDA-ARS has focussed on the erodibility of cohesive material and how this affects breach growth. Three key factors affecting erodibility have been identified, namely material texture, compaction moisture content, and compaction energy. The influence that these parameters have on erodibility and hence the rate of breach initiation and growth is extremely high, extending to orders of magnitude for relatively small changes in moisture content or compaction. Erodibility studies conducted by Hanson and Hunt (Hanson and Hunt, 2007) on a series of soil material samples prepared at three compactive efforts over a range of water contents provide an insight into the importance and complexity of compaction (Figure 3-2). The different compaction efforts shown in

Figure 3-2 relate to American standard ASTM D698A (ASTM, 2003) whereby 'standard compaction' equates to 25 blows per layer (B/L) using a standard defined force and layer thickness. Hanson and Hunt observed that the soil erodibility coefficient K_d (see Equation 4-2), can clearly vary by several orders of magnitude as compaction water content and effort is varied. Additional observations from Figure 3-2 include that:

1. each compaction effort results in a unique curve dry of the optimum water content (w_{opt});
2. each curve merges at water content values greater than w_{opt}; and
3. small changes in water content dry of w_{opt} can result in vary dramatic changes in erodibility.

The variations of erodibility are a result of the influence of compaction effort and water content on the complex interaction of soil particles, material structure, and water. It is recognised that the extent of erodibility sensitivity to variations in these parameters will vary according to material type and tests are ongoing to widen the range of available data. Hanson and Hunt (Hanson and Hunt, 2007) also observed that material properties (i.e. gradation) also have an important influence on erodibility. These observations have important practical implications relative to construction practices of earthen embankments and the resulting erosion resistance, and for assessing (i.e. testing and measuring erodibility resistance) and understanding the state of existing embankments.

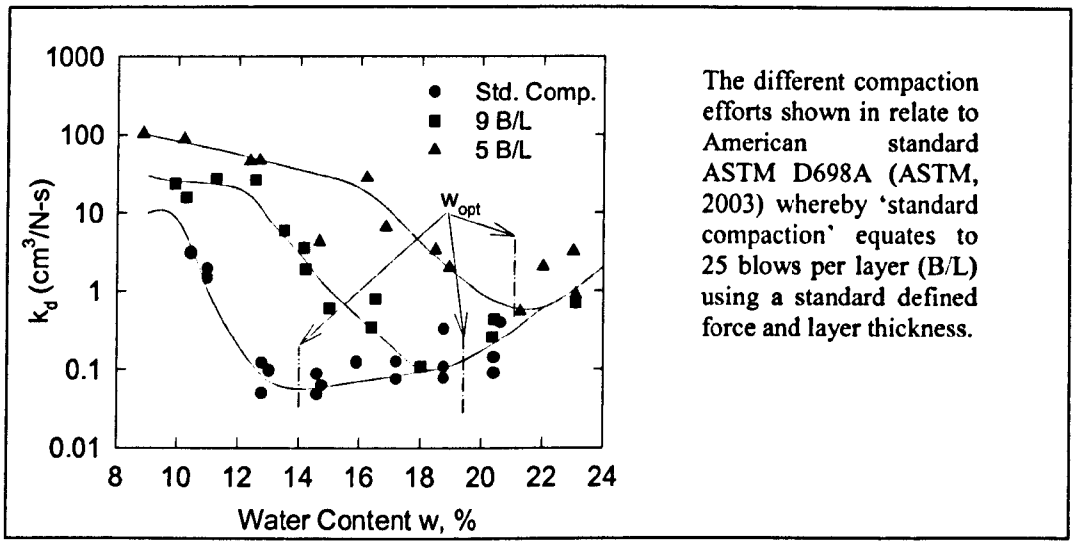

Figure 3-2 Measured variation of erodibility for a soil over a range of compaction water contents and compaction effort (Hanson and Hunt, 2007)

If K_d, as a measure of erodibility, is a dominant factor contributing to soil behaviour during erosion (i.e. determining whether the dominant erosion mechanism is by surface erosion or head cut processes), then re-drawing Figure 2-3 using erodibility along the x axis might allow identification of the exact transition point between these two erosion processes. This could have significant implications for embankment performance and hence design if it can be shown that the timing and nature of catastrophic breach for a given embankment geometry differs significantly between breach arising from surface erosion or breach arising from head cut erosion.

Having established the importance of understanding material type and state in relation to erodibility and hence breach growth, a number of questions may then be considered:

Does embankment size affect the breaching process?

A further issue that arises in considering potential transitions between or conditions relating to head cut and surface erosion, is how the embankment size might affect the erosion processes. For example, is there a transition in process when the head cut height on large embankments approaches the limits of the physical strength of the material? Does this result in catastrophic movement or does the process continue as a form of steep sloped movement dependent upon hydraulic stress and erodibility? Dependencies of scale such as this will affect the applicability of models developed using smaller scale tests or field data. In this context, 'large embankments' might be considered to be in the range of 20-100m, hence 'smaller scale tests or field data' refers to most, if not all, tests undertaken to date and results in another aspect of uncertainty and another reason for the present slow rate of progress in this field. Aspects such as this are only likely to be addressed once researchers recognise and agree upon the relationship between materials, erodibility and breaching processes.

Do existing models use the right parameters/material characterisation?

If one accepts the significance of these parameters (material type, compaction moisture content; compaction effort, erodibility) in addition to soil strength as relevant to the breach formation

process, then an immediate question that arises is whether or not they are adequately reflected within the various breach models that are presented by researchers.

The answer to this is not always simple, since whilst a majority of models do not directly incorporate these parameters, some breach models include a representation of material type, moisture content, and compaction energy through the use of other soil parameters such as soil strength, density, and porosity. This raises the question as to whether this is enough to represent the real effects of varying material state on failure processes within the model. To answer this, we have to look at the failure processes that are associated with breach development and which may be simulated by a model. We can broadly split the modelling processes into two main categories, namely soil erosion and slope instability. All models simulate some form of erosion whilst some, such as that by Mohamed (Mohamed, 2002), include analysis of block failure and soil wasting. If the model representation cannot account adequately for the soil state reflected by moisture content and compaction energy in the calculation of each of these processes, then the representation is insufficient. It is clear that the soil strength, and density, form key parts in slope stability analysis but it is not certain what the degree of influence this aspect of the modelling has on the overall breach prediction results (see Section 6.3.4).

Looking at traditional sediment transport equations, which have been typically used within a majority of breach models, we can see that the effect of density or porosity on the rate of transport is not significant as the equations are mostly based upon applied shear stress, water velocity and particle diameter and specific gravity, which do not reflect soil strength, density, porosity or erodibility. This is because these equations were not developed for predicting conditions within a breach, but rather the long term, near steady state conditions found within rivers. Therefore, we could say that at least one of the main breach processes is not well represented by many of the existing models that use sediment transport rather than soil erosion based equations.

Section 3.2.2 of Mohamed (2002) provides an overview of different sediment transport equations investigated and used by different researchers. One example of a sediment transport equation that has been used for non cohesive materials, but which fails to allow for variations in density, erodibility etc. is the Yang formula (Yang, 1979). The Yang (1979) formula for non-cohesive soils can be expressed as follows:

$$\log C_t = 5.435 - 0.286\log\frac{\omega_s D_{50}}{\nu} - 0.457\log\frac{U_*}{\omega_s} + (1.799 - 0.409\log\frac{\omega_s D_{50}}{\nu} - 0.314\log\frac{U_*}{\omega_s})\log(\frac{US_e}{\omega_s}) \quad \textbf{(3-1)}$$

where: C_t : Total sediment concentration (parts per million by weight).
US_e : Unit stream power (U: Average water velocity, S_e: Energy slope) ([(ft-lb/lb)/s].
D_{50} : Median particle diameter (mm)
ω_s : Sediment fall velocity (ft/s)
ν : Kinematic viscosity of Water (ft^2/s)
U_* : Shear velocity (ft/s)

If the effect of material type, compaction moisture content and compaction effort is so great, it is clear that any models developed without these parameters or direct input of erodibility based on specific measurements will struggle to provide reliable predictions over a range of embankment types and conditions. Whilst these parameters are particularly relevant to cohesive materials (of which many flood embankments and embankment dams are constructed) the concepts are also relevant to breaching through non-cohesive materials. Analysis of the European IMPACT project field test data (Morris, 2009) shows both headcut and surface erosion processes occurring in non-cohesive materials, arising as a result of the material state.

Why is there a frequent cycle of new model development?

A third question that then arises is why new research models initially appear to work well, and are subsequently criticised by others? It is suggested by the writer that this relates to the way in which models are often calibrated and validated. Breach models are often calibrated to a laboratory data set rather than based purely on theoretical analysis. Calibration is often done using a specific set of data arising from laboratory, and in some cases, field tests. Where directly calibrated, the model should invariably perform well against the data sets. Fundamentally, if material state arising, for

example, from intentional or default compaction effort and moisture content conditions are not recorded, then the value of the data reduces significantly since there is no means to determine where within the differing orders of magnitude of erodibility the test data resides. Whilst the calibrated model may reproduce those test conditions well, there can be no guarantee of prediction for other material types or conditions.

Model validation is also typically accomplished using different data sets (but often drawn from the same test series) or by using case study data. Test data from the same experimental setup is likely to use material in a similar state (i.e. similar compaction effort or moisture control processes during model construction) as the data used for initial numerical model calibration. Hence the importance of material state is unlikely to be highlighted here. This is demonstrated well by the recent DSIG project review of breach modelling data sets (Courivaud, 2007b) which shows that very few recorded laboratory experiment data sets include details of material state (such as moisture content and compaction detail); real dambreak or breach case study data sets contain even less information and often do not include a clear record of material type and in some cases little information on embankment geometry.

As with the earlier Teton Dam example (Figure 1-2; Section 3.1), the error that would arise in model prediction is a result of generally applying a model which, in fact, is only really valid for a limited set of soil type and conditions.

How useful is case study data?

Validation against case study data then raises a fourth question, namely that if construction history, defining material state, plays such a significant role in determining erodibility and breach growth, how can model performance be validated against case study data where this information typically does not exist? The answer has to be that models cannot be reliably validated against such data, yet that is exactly what is done. It seems that the attraction of comparing model performance against a

real event is strong and tends to blind many to the question of the real uncertainties associated with the case study data.

A more general problem with case study data is related to the uncertainty surrounding the event itself. This is due to uncertainty in obtaining reliable data related to the as built embankment materials, construction history, condition, geometry, reservoir inflow and storage failure timing, process and outflow. Often, the combined magnitude of these uncertainties makes detailed model performance evaluation very difficult, if not impossible. This is one of the challenges that faced the DSIG project on breach model evaluation (Courivaud, 2007b, Wahl et al., 2008).

Without better certainty in the actual case study data, and the limited number of such cases, there can then be a reluctance to improve physically based breach models or to rely on the results of such models. In order to solve this problem there is a need for improved data gathering and forensics of actual failures and increased physical modelling of breach processes at large rather than laboratory scales.

3.4 Knowledge gaps, and research priorities

The need to improve the performance and availability to industry of predictive breach models is clear, with calls for research to address this problem continuing from different sectors of academia and industry (DoE, 1986, Environment Agency, 2003, Fleming et al., 2001, Hanson et al., 2001a, Hinks and Mason, 2007, Pitt, 2008, Simm, 2006).

The review of breach modelling has highlighted a range of issues relating to breach modelling. There is clearly a demand from industry for improved models (Morris et al., 2009b) but conflicting publications from academia and industry as to how reliable different breach models are and their suitability for different applications. This stems, to some extent, from confusion within the research community, but also a tendency within industry to find and apply a quick solution with lesser regard to the applicability and uncertainty that may be introduced by such a method

(Environment Agency, 2009a, HR Wallingford, 2009). An example of this is given by Orendorff (Orendorff and Nistor, 2010) which claims to provide an assessment of the current (2010) state of the art in breach modelling. There are a range of statements in this paper which are misleading. The most significant include:

1. That the size of initiation notch affects the time to peak discharge, but that the magnitude of peak discharge remains similar. *This fails to recognise the link between upstream stored water volume, soil erodibility and flood outflow;*
2. That eroding downstream slopes will steepen. *This fails to recognise the range of different processes that can occur during surface erosion;*
3. Quoting "The manner in which a cohesive embankment breach slope progresses is also thought to be highly different from that of a non cohesive structure, owing of course to the large difference in erosion characteristics. However, they may in fact be more similar". *Fails to identify the real difference in processes, namely surface and headcut erosion, and then implies little difference between the two. For the surface erosion, the paper states that the downstream slope steepens as it erodes back upstream. This can be compared to work by Schmocker (Schmocker and Hager, 2009) who shows plots of sand and gravel embankment slopes flattening as they erode back upstream. Both fail to emphasise the relationship between material type and state (erodibility) and the overall physical process.*

The Orendorff paper also concludes that little progress has been made in recent years, yet fails to reference any recent research programmes on breach modelling, such as the EU FLOODsite project (Morris et al., 2009a), the DSIG project (Wahl et al., 2008) or ongoing work by USDA-ARS (Visser et al., 2010).

The review (in this thesis) has highlighted that a better understanding of the role of soil type and state within the breaching processes is needed. This affects both the rate at which soil is removed and the overall physical process of breach growth.

The review has also highlighted complex interactions between soil, water and structure, noting that relatively small changes to any of these can significantly affect the overall breaching process. These dependencies mean that breach initiation processes, such as initial grass or rock cover erosion, also play an important role in the overall prediction process.

The approach taken previously with the HR BREACH model development to integrate simulation of the three physical processes (soil, water, structure) provides a logical basis for breach modelling upon which to build.

Hence the goals for the research will be to:

1. Investigate the prediction of physical breach processes to establish how well existing models, and the HR BREACH model in particular, simulate breach initiation and growth processes, noting that complex interdependencies between processes exist (Figure 3-3). Identify and define the breach initiation and growth processes and understand why the accuracy and reliability of breach modelling has not progressed over the past two decades at the same rate as the development of numerical flow models. [This addresses research questions RQ1 and RQ2 introduced in Section 1.2];
2. Building from the initial review and analysis of physical processes through use of the EU IMPACT project data, refine, enhance, restructure and extend modelling capability, whilst retaining a relatively fast and flexible model suitable for practical applications. In particular investigate:
    a. ways in which flow processes within breach initiation and growth may be better represented, including the suitability of 1D, 2D or 3D simulation;
    b. soil erosion processes, including the suitability of using sediment or erosion equations, initiation processes and structure response (head cut versus surface erosion; soil wasting etc.).

    [This addresses research questions RQ3 and RQ4 in Section 1.2];
3. Consistent with these research goals, build upon the existing HR BREACH model through:

a. evaluation of model performance – where possible against internationally recognised data and standards

b. development of a new modelling approach to provide a model that can simulate breaching of structures that more accurately reflect real, rather than simplified, structures;

[This addresses research questions RQ5 and RQ6 in Section 1.2].

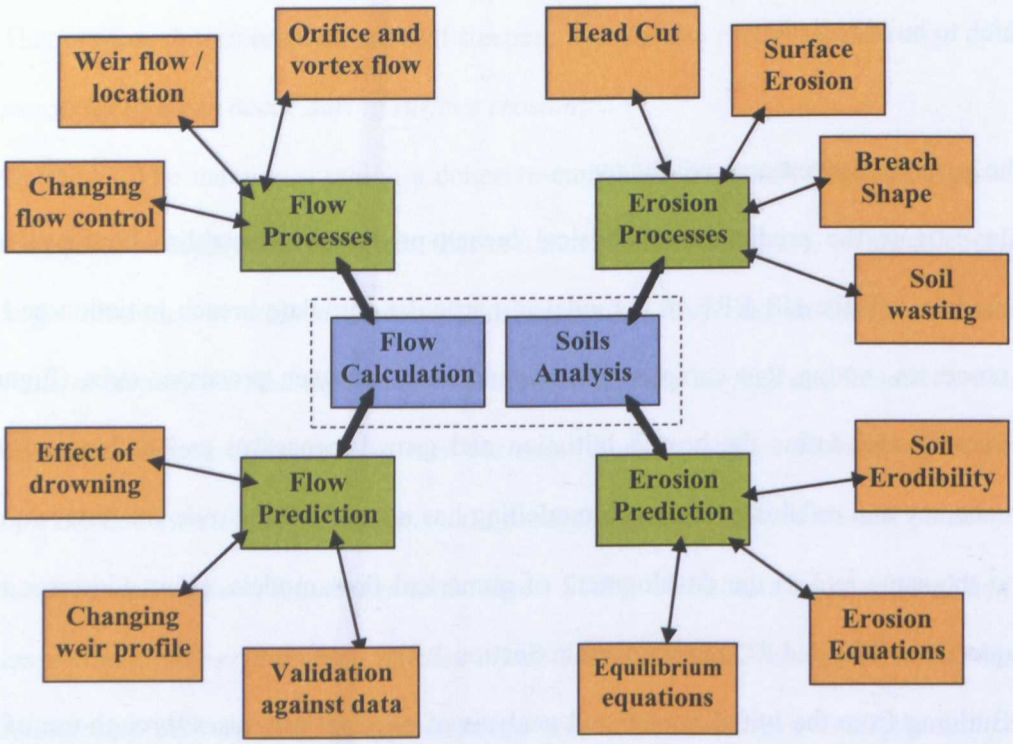

Figure 3-3 Physical processes associated with breach formation and factors influencing breach modelling

4. Breach initiation processes

Breach initiation is defined under Section 2.2.2 as that period of erosion occurring before breach formation, leading to initial flow between times T_0 and T_2 on Figure 2-5. Breach initiation processes can be difficult to observe in the early stages since this is the point where a stable embankment starts to erode as a result of flow over or through the embankment. The erosion of soil particles from the embankment can be delayed or hidden by surface protection layers, such as grass cover or a surface cover of rocks. The rate at which the initiation erosion progresses can be extremely hard to predict since it requires accurate prediction of both the initiation of sediment erosion, which will depend greatly upon soil type, state and variability, as well as the performance of any surface protection layers, which are also subject to local variability in terms of condition performance.

Whilst breach initiation (leading to 'open' breach formation) can arise from either overflow erosion or internal erosion arising from seepage flow, subsequently leading to a collapse of the soil above the erosion area, research here focuses upon the process of overflow erosion. Ongoing research by teams in the European FloodProBE project (Benahmed and Philippe, 2012) and the ICOLD European Club working group on internal erosion, aim to make significant advances in clarifying and defining internal erosion processes.

4.1 The significance of breach initiation

Where breach initiation depends upon the erosion of soil by a small overtopping flow, then small changes in soil structure or soil erodibility can result in significant changes in the time before breach formation occurs (breach formation being the point where erosion and discharge start to rapidly increase (T_2-T_3, Figure 2-4). Hence, the breach initiation process can significantly affect the timing when breach formation occurs. The impact on timing is further increased when surface protection measures, such as grass or rock cover, are added to prevent or limit surface erosion.

With these measures in place, the timing of breach formation then depends both upon soil erosion and the performance of the surface protection measures.

Since the breach formation process depends upon the close interaction of hydraulic load with soil state and structure response, a change to one or more of these parameters can lead to a change in the breach growth process. Where the breach initiation process results in either a faster or slower progression towards the point of breach growth, the change in timing means that breach formation initiates at a different point in the load flood hydrograph. This, in turn, affects the volume of potential outflow water available to erode the breach and the rate at which that water can pass through the breach. This change in timing can therefore result in either a greater or a less severe flood outflow hydrograph, depending upon the nature of the loading and the timing of initiation.

Figure 4-1 shows an example of how the breach outflow prediction can change by varying the breach initiation timing relative to the flood load conditions. Two sets of three runs are presented. One set of runs has a steady inflow which leads to embankment overtopping whilst the second set of runs has a small flood event added to the steady inflow. Three curves are shown for each set of results, which relate to poor, average and good quality grass cover. The quality of the grass cover affects the rate of erosion and hence the timing of initiation.

For the set of runs with a steady inflow, it can be seen that two runs result in breach whilst one (with good grass cover) does not breach. The flow predicted for this case simply arises through water flowing over the embankment crest. For the runs with a flood event imposed, the interaction between the timing of the flood event and the timing of initiation, affected by the quality of grass cover, leads to results that show a difference in peak discharge of nearly 40%. For this set of runs, the only difference between the three results is the grass condition.

The reliable prediction of the breach initiation process is therefore an essential part of overall breach prediction.

The small spikes and steps shown in the modelling results of Figure 4-1 arise when the control section within the model changes. This is normally triggered by block failure within the breach section which affects the section flow capacity and hence the predicted location of critical flow control through the breach. This process of critical flow control moving around within the breach area can be seen in video footage of some of the IMPACT project field tests (Morris, 2009).

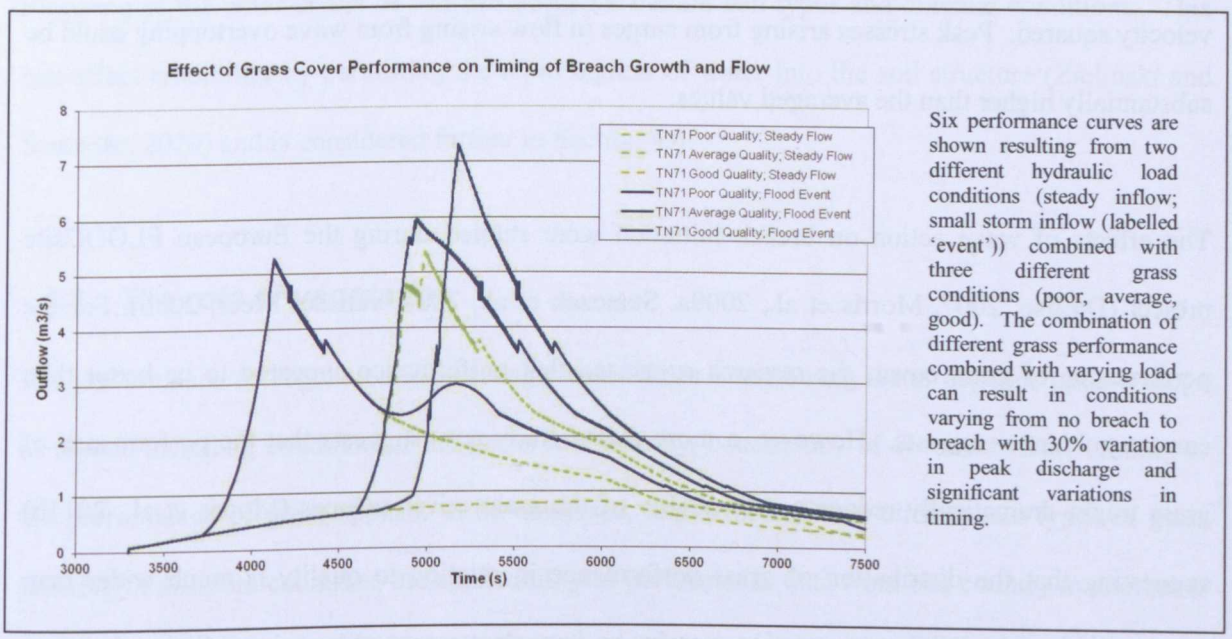

Figure 4-1 Impact of breach initiation timing on breach formation

4.2 Factors influencing breach initiation processes

The following sections provide an overview of factors influencing breach initiation processes. More detail on the performance of grass cover is subsequently provided in Section 4.3 and on soil erodibility and fissuring in Section 4.2.3 and Chapter 6.

4.2.1 Hydraulic loading, including wave impact and overtopping

The magnitude of hydraulic load on an embankment affects the rate at which surface protection layers fail and soil erosion begins. Where embankments are exposed to wave action, then both wave impact and wave overtopping can lead to breach initiation processes that would not have occurred with static water loading. Wave impact can result in more rapid destruction of the surface

protection, and subsequent removal of the soil beneath through repeated wave action. Wave overtopping provides a periodic pulse of water over the crest and down the landward face of the embankment. The acceptability of overtopping has often been assessed by calculating an average overtopping flow and comparing this against surface protection performance criteria. However, the pulsed nature of the flow will mean that flow shear stresses will likely be higher than the averaged values, particularly since the shear stress at the soil or grass surface is a function of the flow velocity squared. Peak stresses arising from surges in flow arising from wave overtopping could be substantially higher than the averaged values.

The effects of wave action on breach initiation were studied during the European FLOODsite project (D'Eliso, 2007, Morris et al., 2009a, Stanczak et al., 2007, van der Meer, 2006). For the performance of grass cover, the research suggested that performance appeared to be better than current guidance suggests. However, a more recent study now suggests that the performance of grass might dramatically reduce as the quality of the grass cover reduces (Morris et al., 2011b) suggesting that the distribution of grass performance in relation to quality is much wider than previously thought. Whilst wave action remains an important aspect of breach prediction for wave exposed embankments, they are not considered further here.

4.2.2 Surface protection measures

A range of different surface protection measures are used in the design of flood embankments and embankment dams (Environment Agency, 2007, Mériaux and Royet, 2007). A large proportion of earth dams and flood embankments are covered with grass. Some design guidance is available for predicting the performance of grass cover (Hewlett et al., 1987). The impact of grass protection on breach initiation is considered in more detail in Section 4.3. The performance of stone layer protection (revetment design) can also be assessed through different design methods (Escarameia, 1998) but is not considered further within this thesis.

4.2.3 Soil erodibility and fissuring

The soil state affects how breach initiation occurs since the soil state affects soil erodibility, and hence the rate of erosion. The soil erodibility also determines larger scale processes such as whether head cut or surface erosion processes dominate; these processes are considered in more detail in Section 6.

Fissuring of the outer layers of soil can occur for certain soil types and climatic conditions. This can affect erodibility by permitting the rapid ingress of water into the soil structure (Zielinski and Sentenac, 2010) and is considered further in Section 4.4.

4.3 The role of vegetation

The performance of vegetation in resisting erosion from overflowing water depends upon a range of factors including condition of the grass, root density, consistency of cover etc. Data relating to the performance of grass appears to be dispersed, and with different climate and types of grass growing in different countries, the applicability of performance data from one country to another is unclear and the extent of knowledge regarding performance relatively limited (Young, 2005). In the UK it is common to use design guidance provided by CIRIA (Hewlett et al., 1985) since this provides a simple method for predicting the duration that grass might withstand surface flow of a certain velocity.

4.3.1 CIRIA grass performance curves

When a closer investigation into the CIRIA design data (Hewlett et al., 1987) was undertaken by the writer it was found that the data was based upon earlier analysis undertaken at the Hydraulics Research Station by Whitehead (Whitehead et al., 1976). The quantity of data supporting the grass performance curves appears to be quite limited but there are also differences between the original research data and the performance curves, suggesting that a factor of safety has been introduced into the CIRIA curves (Figure 4-2).

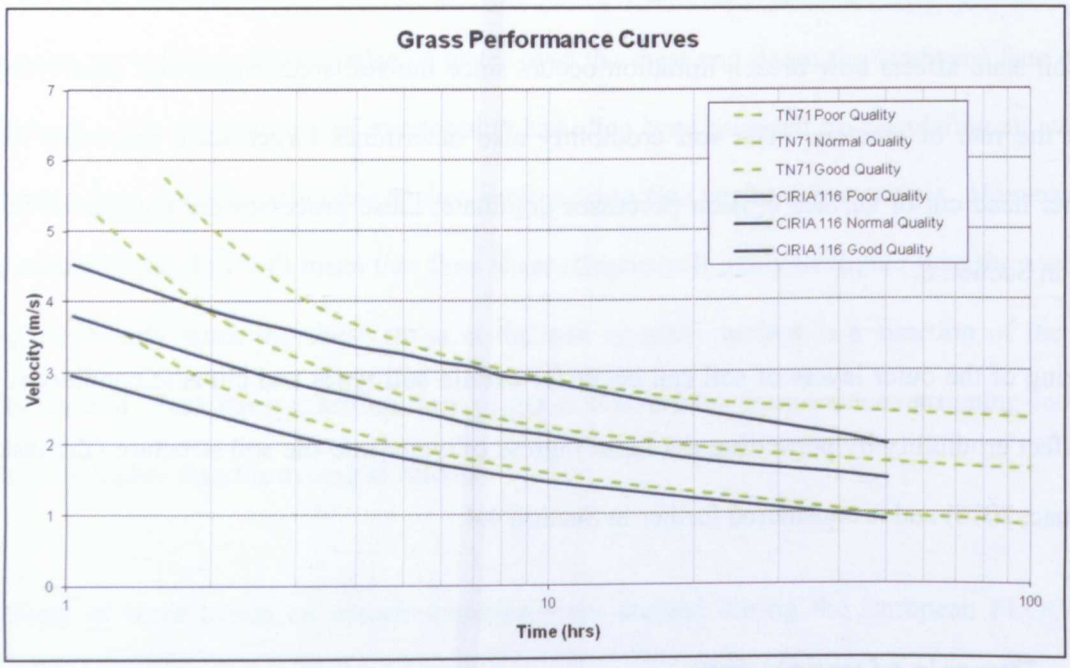

Figure 4-2 Comparison between CIRIA 116 grass performance curves (Hewlett et al., 1985) and the original Technical Note 71 field test data (Whitehead et al., 1976)

It is important to remove factors of safety from any stages of analysis used for modelling breach initiation and growth since these factors will bias the true model predictions. Instead, it is more appropriate to consider uncertainty within any parameters and process predictions to allow a realistic range of solutions to be simulated that are not affected by embedded factors of safety.

Whilst the suggested factor of safety within the CIRIA curves would have been intended to provide assurance in the use of the performance curves for surface protection design, the effect on breach prediction is very significant. Figure 4-3 shows model predictions for breach outflow using the CIRIA design guidance (CIRIA), original data (TN71) and a delayed onset of erosion (Delay) against observed data from a controlled field test on a 2m high embankment. The difference in timing between the CIRIA and TN71 plots (i.e. approximately 800s peak to peak) accounts for more than half the error in timing between the CIRIA prediction and the observed data (i.e. 1200s peak to peak).

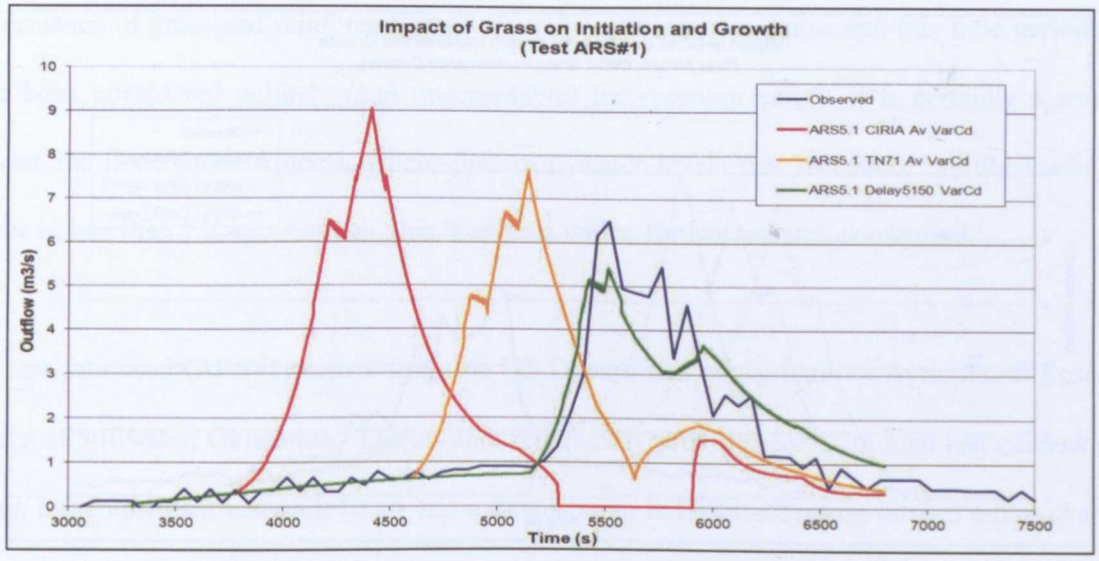

Figure 4-3 Comparison of HR BREACH model performance using CIRIA116 performance curves or TN71 original data

Another aspect of the CIRIA grass performance curves is that they provide predictions for the performance of 3 different types of grass condition (poor, normal, and good). Figure 4-4 and Figure 4-5 show how breach predictions vary when using these different grass condition grades and the different CIRIA and TN71 performance data respectively. Figure 4-4 shows that all of the predictions made using the CIRIA curves predict breach initiation much earlier than the observed event. However, Figure 4-5 shows the observed test results sitting within the distribution of results provided from the TN71 predictions. Note that the prediction for TN71 Good quality grass suggests that breach does not occur, with the overflowing water being of insufficient intensity to erode the grass cover and allow breach initiation. However, using the CIRIA performance curves containing the factors of safety, lead to predictions of breach that occur much earlier than the observed data.

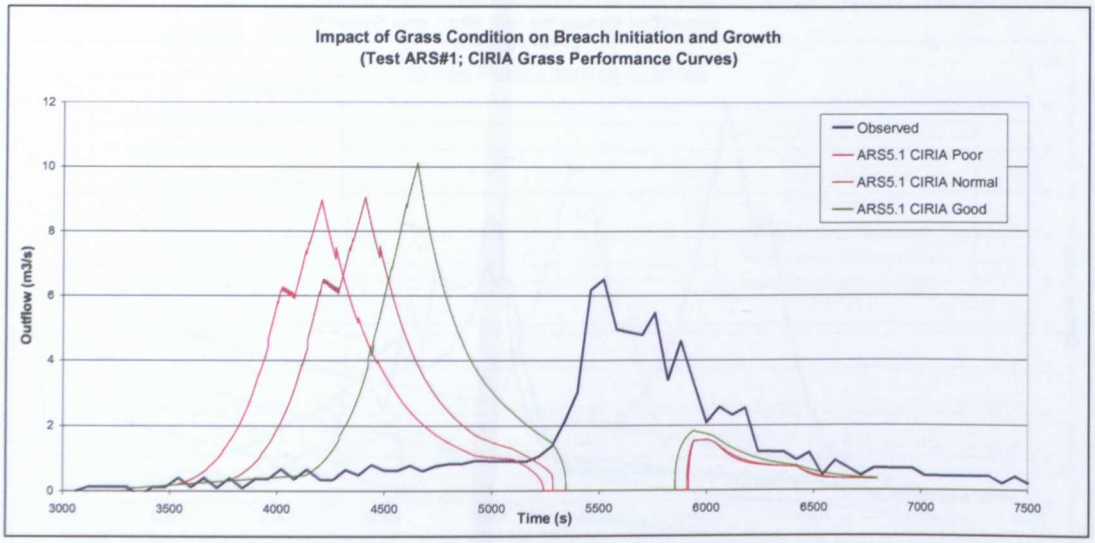

Figure 4-4 Impact of grass condition on breach initiation and growth (CIRIA performance curves)

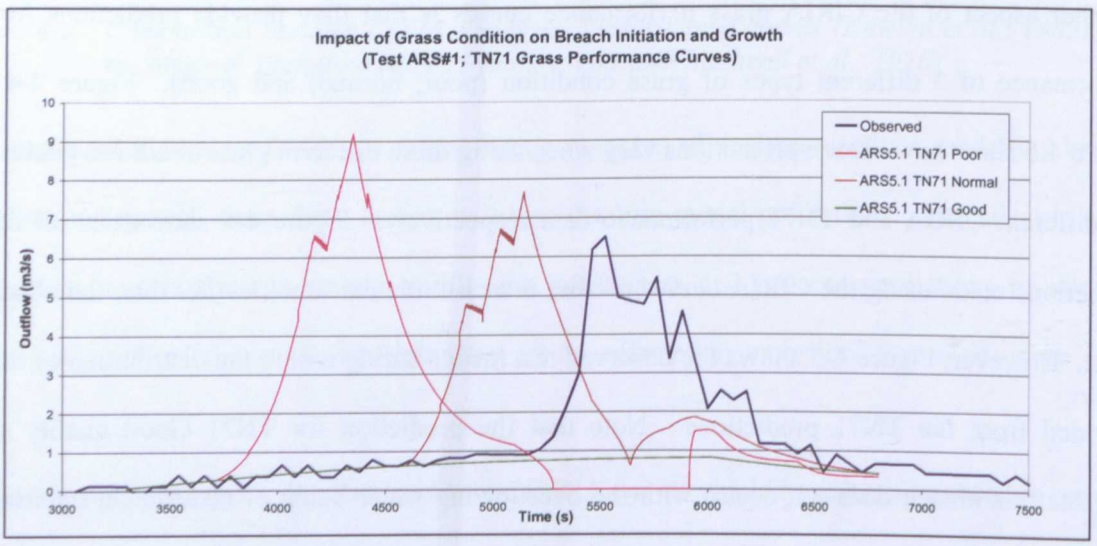

Figure 4-5 Impact of grass condition on breach initiation and growth (TN71 performance curves)

These findings emphasise the difference between the use of design guidance data and data for performance evaluation. The former assumes use of the data for design and may embed factors of safety which can bias the results. The latter provides unaltered data against which performance may be directly evaluated.

A further limitation of the CIRIA 116 data shown in Figure 4-2 is that there is no data for the period 0 to 1 hour. Whilst the original goal of the CIRIA research was to investigate the

performance of grass and reinforced grass cover for embankment dams, and this time period may have been considered unlikely (and unacceptable) for reservoir safety, it is certainly a zone of interest for flood embankments, where upstream water levels can rise more rapidly leading to failure in less than 1 hour. As such, this is an area where further research is required.

The test data used (ARS#1) comes from the US Department of Agriculture Agricultural Research Station at Stillwater, Oklahoma. The outdoor test facility provided for a 2m high test embankment with a large upstream reservoir basin and a downstream basin, discharging into an outlet channel. As the test embankment breached and flow rapidly increases, the water level in the downstream basin rises above the embankment base invert level. Consequently, this affects growth of the breach during the breach formation and widening stages.

The effect of the downstream level on modelling results needs to be understood since this is a further factor affecting overall model performance. The test data presented in Figure 4-3 to Figure 4-5 above uses observed downstream water levels as a model boundary condition. Hence, if the model prediction deviates from the observed timing, the imposed downstream boundary conditions make predictions worse. The effect of the downstream conditions can be seen in all three figures where the breach model predicts failure too quickly; a second small peak of water can be seen later in the simulation. This small surge reflects flow through the already formed breach that occurs after the (imposed) downstream levels rise (sometime after the model prediction of breach), so raising the upstream reservoir water level via backflow through the breach, and subsequently allowing the reservoir to drain again through the breach.

Section 5.3 includes a detailed assessment of the effects of drowning on breach growth, along with analysis of the difference in breach model prediction achieved by using predicted downstream boundary conditions rather than the simple imposition of observed data.

4.4 The role of fissuring in breach initiation

Soil erodibility dictates the rate at which erosion and hence breach initiation can occur. Soil fissuring affects the structure of a soil and can permit the rapid ingress of water within the soil structure as well as influencing the process of block failure during breach formation. The ingress of water could affect both soil moisture content and the pore water pressure. Whilst changing the pore water pressure within a soil can significantly affect the embankment stability, changing the soil moisture content will affect the soil erodibility.

Analysis of embankment fissuring processes (Dyer et al., 2007, Dyer et al., 2009, Zielinski and Sentenac, 2010) showed the propensity of some soil and climate conditions to result in the development of a fissure network, extending over 600mm into the surface of a flood embankment (Figure 4-6). Under such conditions, the embankment soil becomes susceptible to water ingress and greater erodibility of the soil in the crest area that in itself is most critical for overall embankment performance under extreme flood conditions.

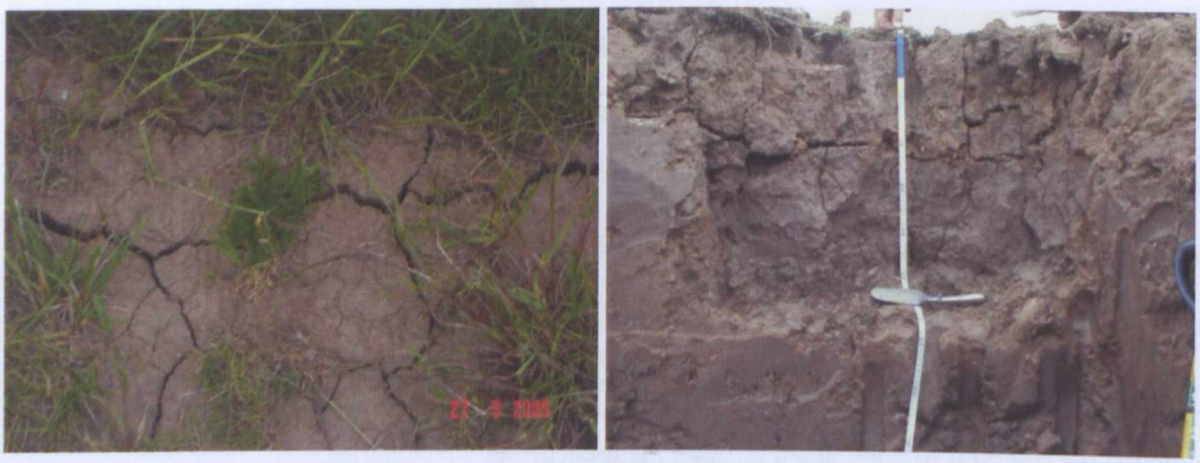

Figure 4-6 Embankment fissuring: Surface cracking in new embankment at Thorngumbald (left); Depth of cracking in original embankment at Thorngumbald (right) (Dyer et al., 2007)

The potential impact of different layers of soil erodibility on embankment performance has been considered later in the thesis through the use of a newly developed breach model that simulates breach erosion through different zones of soil (Section 7). An example of potential behaviour predicted by this new model is given below. Figure 4-7 shows the generic form of the zoned

embankment used for breach modelling. In this example two layers were used with two significantly different values for soil erodibility. Figure 4-8 shows predicted flood hydrographs (Type 2 – 2 layers), also including a comparison against predictions for the same embankment constructed entirely of one or other of the two soil types (Homo). The 2-layer simulations give results that are significantly different, depending upon whether the outer layer has a higher or lower soil erodibility (i.e. whether it is a fissured embankment or not).

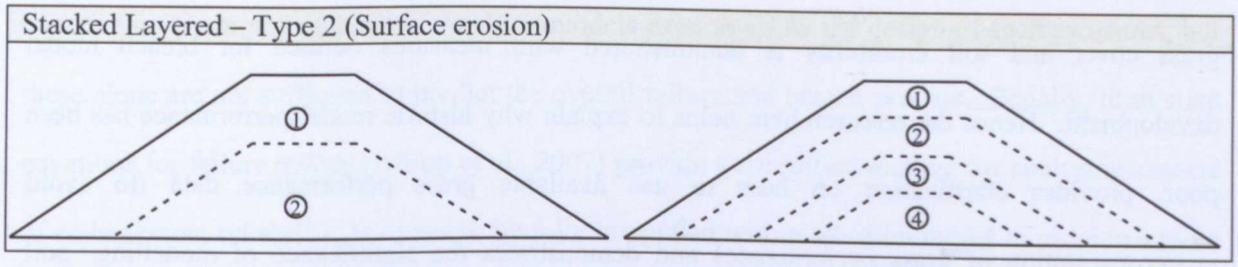

Figure 4-7 Generic geometry for Type 4layered embankment

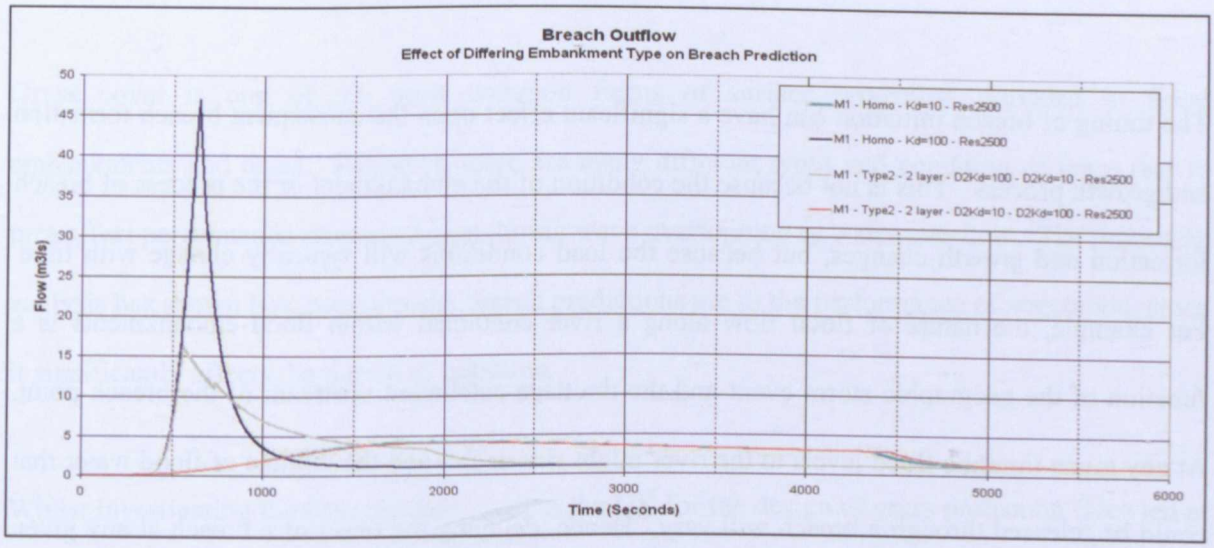

Figure 4-8 Breach outflow: Type 2, 2 layer embankment

These results confirm the importance of fissuring in affecting the breach initiation process through permission of water ingress and the subsequent adjustment of soil moisture and hence soil erodibility. The results also demonstrate the importance of simulating zones of material when predicting breach through real structures. More detail on soil erodibility processes is given in Section 6, the new modelling approach in Section 7 and the detailed modelling results in Appendix 4.

4.5 Discussion

The issues highlighted here all affect the time to breach initiation, which in turn was shown to affect the way in which breach formation might develop. Factors affecting the initiation timing include surface protection layers (such as grass cover) and the structure soil type and state, and hence erodibility, in conjunction with the magnitude and timing of the hydraulic load. A failure to recognise these processes and their significance will result in poor model performance; historically, many models have ignored or poorly represented these processes. In particular, the significance of grass cover and soil erodibility is demonstrated with measures defined for breach model development. Hence the research here helps to explain why historic model performance has been poor, provides clarification on how to use available grass performance data (to avoid misrepresentation of grass performance) and demonstrates the significance of modelling soil erodibility and soil layers, supporting the new modelling approach outlined in Chapter 7.

The timing of breach initiation can have a significant effect upon the subsequent breach formation and growth process. This is not because the condition of the embankment or the process of breach formation and growth changes, but because the load conditions will typically change with time. For example, the nature of flood flow along a river contained within flood embankments is a function of the geographic storm event and the drainage catchment upstream of the breach point. At any given time the flood levels in the river might rise or fall and the volume of flood water that could be released through a breach will vary. Hence, delaying the onset of a breach at any given time does not necessarily result in a less extreme flood hydrograph when the breach eventually occurs. In practice, what is and is not acceptable for flood risk management can only be determined by undertaking careful analysis that covers a range of possible initiation timings. It is important to understand this for breach model research and development since model performance is quite often assessed against field or case study data where the same issues apply.

Since surface protection layers play a significant role in delaying the start of breach initiation, understanding and being able to predict the performance of such measures becomes an important part of breach modelling of real structures. However, the multitude of protection measures and complexity of different design solutions make this a challenging task. In order to simulate the initiation process correctly, it is necessary to integrate a failure model of the surface protection layer with the breach model. The performance of both grass and rock protection has been included within the breach model, but more complex protection measures such as interlocking stone or concrete units are not simulated. Analysis models exist to allow the design of such measures, but these alone are not sufficient to predict the overall failure and breach process. Equally, limit state equations for failure modes (Allsop et al., 2007) provide a simplified method for analysing aspects of embankment reliability, but need to be fully integrated within a breach model to provide a more accurate prediction of the combined failure and breach growth process.

Grass cover is one of the most common forms of surface protection provided to flood embankments and dams. However, there are many different types and condition of grass that in turn affect performance against erosion during wave overtopping or water overflow. The preceding analysis has shown how sensitive the breach predictions are to the performance of vegetation, since it significantly affects the timing of initiation.

Whilst investigating the data typically used in the UK for the design of grass protection (Hewlett et al., 1985, Young, 2005) it became clear that the extent of available data was limited and that safety factors had probably been incorporated into the design curves. Since this work was produced more than 20 years ago, detail regarding the inclusion of safety factors is now unavailable and the design curves used as given. Whilst this provides for a safer design, this has the opposite effect when used directly within breach modelling or system risk modelling. Within the design curve, an added safety factor has the effect of suggesting that grass will fail more quickly than observed. For breach modelling, this results in predictions where breach initiation occurs too quickly and for reliability analysis, a fragility curve that suggests that failure will occur when years of experience

show that it does not. This was consistent with findings from a study into flood defence performance in England and Wales after the 2007 floods, where a number of defences breached, but a significant number did not fail, despite fragility curve predictions that they should (Flikweert and Simm, 2008, Flikweert and Underwood, 2008).

For more accurate breach and reliability modelling, it is therefore important to use the original grass performance data (Whitehead et al., 1976), referred to within this thesis as Technical Note 71 (TN71) data. However, the need for more reliable data covering a wider range of grass types, grass conditions and load conditions is clear. With climate change effects likely to influence soil moisture content and hence vegetation condition and type, such research becomes even more urgent. A review of such data and research needs is being undertaken as part of the European FloodProBE project (www.floodprobe.eu) (Morris et al., 2011b).

The rate of breach initiation also depends upon the rate at which soil starts to erode and hence the soil erodibility. Whilst soil erodibility is addressed in more detail in Chapter 6, the potential effects of fissuring on breach initiation are demonstrated. Fissuring affects soil moisture, the soil erodibility and hence the rate at which breach initiation can occur, which in turn affects the predicted breach flood hydrograph. This is particularly relevant when the embankment is under extreme flood conditions where the flood water levels impinge upon the fissured areas, hence it becomes clear that for breach modelling of real embankments it is necessary to consider potential variations in the embankment soil state and the way in which this can vary within the embankment body. As such, the breach model needs to have the capability of predicting breach behaviour through zones of different soil type (erodibility). Development and testing of a new modelling approach to achieve this is detailed in Chapter 7.

5. Breach flow processes

The nature of flow over an embankment during the breach initiation, formation and growth stages changes as the geometry of the embankment and breach evolves. At times, the flow approximates to different forms of weir flow, orifice, flume and open channel flow (Ackers et al., 1978). Hence, the validity of any single simplifying assumptions made for modelling breach flow will vary according to the stage of breach initiation and growth being considered.

The downstream water level also plays a key role in the breaching process. As discharge through the breach increases, and the breach invert level erodes downwards, a point at which flow through the breach is affected by the downstream conditions is reached (i.e. drowning after the modular limit is reached). The effect of drowning is to reduce the discharge and flow velocity, and hence the rate of erosion and of breach growth. In some situations, such as dambreak conditions in steeply sloped valleys, drowning may never occur and hence not be an issue. However, in other situations such as breaches through flood embankments where flood levels on the other side of the breach can rapidly rise, drowning effects may stop breach growth all together. It is therefore very important to allow for the potential effects of drowning within any general purpose breach model.

5.1 Observed flow behaviour

As flow through the breach increases, the nature of the flow control changes. These changes may be broadly related to the different stages of the generic breach hydrograph (Figure 2-4) and can be seen in the analysis of IMPACT Project field data and the images in Figure 2-13, Figure 2-14 and Figure 2-15, also explained in Table 2-8, Table 2-9 and Table 2-10. The phases of flow are summarised in Table 5-1.

Table 5-1 Summary of the phases of breach flow

Stage (Figure 2-4)	***Breaching Stage / Process***	***Flow Magnitude***	***Flow Control Type***	***Potential Variations***
T_1-T_2	Initial, shallow depth of water crossing embankment crest	Low flow	Simple broad crested weir flow	Little - None
~T_2	Initial stages of erosion into embankment crest, reshaping profile.	> Low flow	Broad crested weir flow plus variations. Higher water levels may lead to side flow into the breach area across the upstream face of the embankment. Flow contraction effects might start as discharge increases.	As erosion changes the embankment crest profile, the type of flow control may change. Most likely change will be from broad crested weir flow to ogee weir flow, as the crest is 'rounded'. This will increase the discharge per unit width, compared to broad crested weir flow. A high flow depth across a narrow embankment crest may briefly allow for thin crested weir behaviour (but likely to be rare)
T_2-T_3	Severe erosion of the embankment crest into the upstream face. Profile likely to erode towards a triangular or rounded crest profile.	Medium flow	Triangular or Ogee weir control. Higher discharge means that flow contraction is likely. Drop through breach creates elongated vortices along the base of each eroding side of the breach.	Weir flow to suit the crest profile, with allowance for flow contraction. High levels may result in flow across the upstream embankment face into the breach.
~T_3 (---T_4)	Collapse of the eroding crest opening breach through the embankment	Medium flow	Orifice – Converging flow Extreme flow convergence discharging through a relatively small hole in the embankment. Very smooth surface profile dropping near vertically through the breach	None – this phase of flow occurs briefly just after initial break through and before wider erosion of the breach occurs.

Stage (Figure 2-4)	*Breaching Stage / Process*	*Flow Magnitude*	*Flow Control Type*	*Potential Variations*
T_3-T_5	Rapid erosion and widening of the breach	High flow	Transition from converging orifice flow to weir (if embankment control sections remain) or open channel flow	Exact nature and location of the flow control will vary across the breach as areas within the breach erode preferentially leaving an irregular control profile. Mass failure of embankment blocks may remain within the channel as flows reduce. Tension cracks forming in the embankment will dictate nature of the mass failures and may allow seepage and piping prior to mass failure.
$>T_5$	Flow decreases as upstream reservoir or river drains through breach	Drops to low	Weir or open channel flow	

It can therefore be seen that the flow behaviour changes considerably during the breaching process. Consideration is given in Section 5.2 below as to how these different phases of flow may be modelled more accurately within a 1D simulation, or whether a 2D or 3D flow model is needed.

5.1.1 Converging flow

More detailed consideration was given to the flow conditions that occur around the point of collapse of the upstream slope of the embankment, and when flow through the breach rapidly increases. This flow is characterised by rapidly converging flow that is semi elliptical or semi-circular in plan, with flow dropping near vertically through a narrow slot (breach) in the embankment (Figure 2-13c). This phase of breach flow does not appear to have been analysed by other researchers into breach modelling and was identified during analysis of the IMPACT project field test video footage.

This phase of flow has been termed *Converging Flow* and an approximate analysis by Samuels (Samuels and Morris, 2010) (Appendix 5) suggests that the position of the critical flow point is a function of the discharge, and independent of the breach and bed geometry. Critical flow occurs at a radial distance inside the reservoir of r_c given by:

$$r_c^2 = \frac{27Q^2}{8g\pi^2 \mathrm{E}^3} \qquad (5\text{-}1)$$

with discharge given by:

$$Q = (2/3)^{3/2} r_c \pi \sqrt{g} h_0^{3/2} \qquad (5\text{-}2)$$

which only differs from a broad crested weir flow equation by the term πr_c replacing the weir crest width B. Hence, the discharge during converging flow conditions will exceed that calculated for broad crested weir flow by a factor of $\pi/2$.

Two key points may be concluded from this analysis:

1. The discharge calculated using a normal weir flow equation for this phase of flow may underestimate the true rate of flow;
2. At the point where the critical depth occurs, flow rapidly accelerates and drops nearly vertically through the breach. At this point the assumption of shallow water flow with negligible vertical acceleration in the approximate analysis, breaks down and a 3D flow analysis is required. This is also the point when strong vortex action is generated along the edges of the breach, leading to rapid undercutting of the breach sides and subsequent side block failure (see Figure 2-13d).

However, whilst it can be demonstrated that converging flow occurs, it can be seen that during the earlier stages of breach initiation where the head over the crest is small, broad crested weir flow occurs and at later stages, once the breach opening has widened and water levels dropped, weir, orifice or open channel flow occurs. The duration of converging flow is therefore site specific and could vary (in terms of Figure 2-4) between T_2, T_3 and T_4. Analysis of the IMPACT field test videos suggest that (for these tests) the duration of converging flow is relatively short with the timing of occurrence closer to T_3 than T_4 In this situation, the error arising from the use of a weir equation instead of converging flow equation will be smaller. However, it is not clear whether this would be the case for all or a majority of breach events, hence further analysis of this flow phase is required.

5.2 Improving 1D flow simulation

Many breach models use weir equations as the method for calculating flow through the breach opening. All models reviewed to date (that use a weir equation) use fixed discharge coefficients within the weir equation. The use of a fixed discharge coefficient is an approximation representing continually changing conditions.

5.2.1 Rationale

The magnitude of error generated through use of fixed weir coefficients could be very significant given that weir coefficients can change by over 40% according to different weir geometries. This error in flow prediction (by 1D flow simulation) may be reduced by finding a way of adapting the simple weir flow calculation (Equation A1-1) to better match the changing weir profile that controls the flow during breach development.

5.2.2 Use of weir discharge coefficient curves

The behaviour of flow over a weir varies according to the weir shape, the up and downstream channel geometry and the local approach flow conditions. As a breach develops through an embankment, the type of weir flow varies since the weir geometry and the hydraulic loading changes with time. When you consider different breach flow and profile conditions, different types of weir flow may be identified (Table 5-2).

Table 5-2 Potential forms of weir equation that might be used to predict flow through a breach

Type of flow and embankment profile	Potential Form of Weir Equation
Small flow overtopping embankment crest	Broad crested weir flow
Moderate flow overtopping embankment crest	Broad crested flow → tending to round or ogee crested flow as crest geometry erodes
Moderate flow overtopping narrow crest width embankment	Triangular profile weir flow → tending to ogee flow if crest erodes?
Moderate flow overtopping narrow embankment crest with headcut step downstream of crest	Sharp crested weir equation → tending to ogee if crest becomes rounded
Moderate flow with small, eroded embankment section	Drowned weir flow – ogee or broad crested, with modified discharge coefficient based upon ration of up and downstream heads of water

Ackers (Ackers et al., 1978) provides a comprehensive review of weirs and how they may be used for flow measurement. Ackers considers different types of weir, different weir equations and in particular, potential variation in discharge coefficients for different weir types and conditions. The

comparison of different equations goes back to reviewing and analysing source laboratory and field data in order to provide an objective assessment. Recommendations are made as to the use of different equations for various flow conditions, as well as variation in discharge coefficient in relation to various flow and structure parameters.

Figure 5-1 shows a plot which relates the discharge coefficient to the up and downstream slope of a triangular weir. This shows the discharge coefficient varying in the extreme between approximately 1.5 and 2.2 – consistent with the upper and lower bound behaviour of sharp and ogee crested weirs. This is consistent with the changes in the up and downstream slopes of the weir, in effect between a steep, near vertical faced weir and a low flat weir. It is suggested that these shapes can approximate towards a sharp crested weir and an ogee weir, hence by extracting the time evolving breach model surface slope angles, the time varying weir discharge coefficient may be estimated.

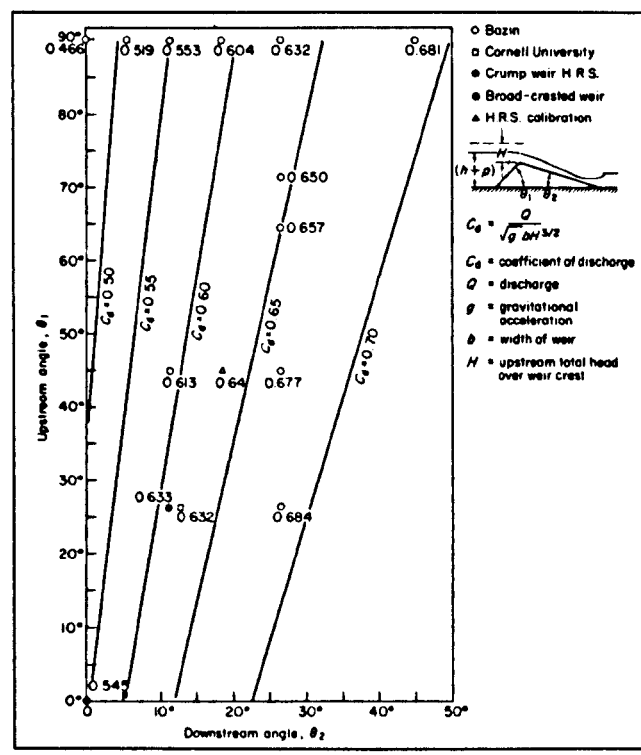

Figure 5-1 Approximate coefficients of discharge for triangular-profile weirs (Ackers et al., 1978)

A similar approach may be adopted for adjusting the discharge coefficients relating to broad crested weir flow. The weir flow equation (Equation A1-1) may be written as:

$$Q = (2/3)^{3/2} C_p b g^{1/2} H^{3/2} \qquad (5\text{-}3)$$

where

Q	Flow through breach
C_p	Discharge coefficient depending upon weir geometry
b	Crest breadth (across channel)
H	Total energy head

This may be extended to

$$Q = (2/3)^{3/2} C_b F b g^{1/2} H^{3/2} \qquad (5\text{-}4)$$

Where

C_b	Base coefficient
F	Coefficient adjustment factor (depending upon head and geometry)

The base coefficient is fixed and defined as 0.848 (Singer, 1964) or 0.855 (Crabbe, 1974). Whilst the former was used in British Standards, the latter seems to be recommended by subsequent researchers.

A value of C_b of 0.855 equates to a value of C_d in Figure 5-1 above of 0.465. This is at the lowest end of the variable range of C_d and is consistent with a transition to variable coefficient. This value also relates to an overall 'combined' coefficient (as use in Eq.5-3) of 1.456. This is consistent with use of a typical coefficient value of 1.5 for (sharp edged) broad crested weirs.

The adjustment factor F depends upon the head of water on the weir crest, h, and the weir geometry (namely, P, the crest level above upstream bed level). The correction factor F, is generally greater than 1. Singer plotted this correction factor for a limited range of h/L and h/(h+P) (Figure 5-2) and this range was extended by Crabbe (Figure 5-3). Note that the Singer plot (Figure 5-2) shows just the correction factor F whilst the Crabbe plot (Figure 5-3) shows the product of C_bF.

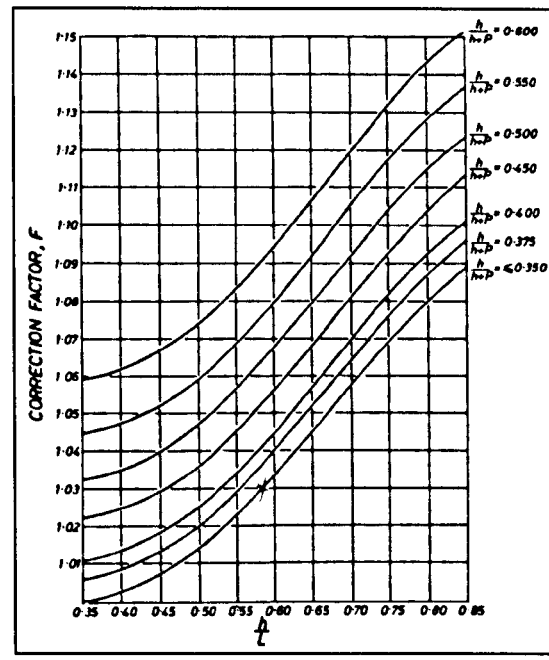

Figure 5-2 Correction factor F in terms of h/L and h/(h+P) after Singer (Ackers et al., 1978)

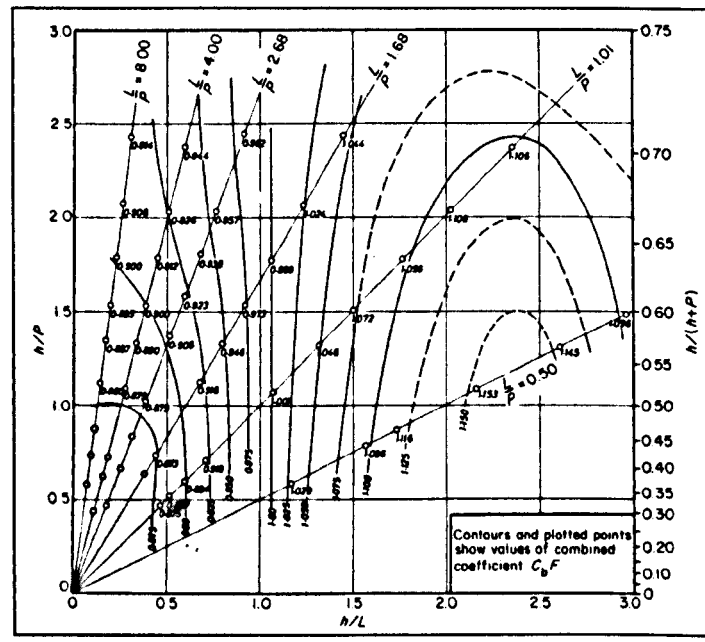

Figure 5-3 Combined coefficient C_bF in terms of h/L and h/P, after Crabbe (Ackers et al., 1978)

The maximum adjustment factor F (Singer, 1964) is 1.15, suggesting a 15% increase in weir capacity as a combination of head and geometry. This translates to a C_d value in Figure 5-1 of approximately 0.535. This value relates to a relatively contained area of the plot.

Variation of the combined coefficient C_bF in Figure 5-3 ranges between 0.875 and 1.15. This correlates to a range of F (comparing the Singer plot, Figure 5-2) of 1.02 to 1.35, so extending the range of the adjustment factor and giving up to 35% increase in estimated discharge. The upper end of this range correlates to a C_d value in Figure 5-1 of approximately 0.626. This value relates to a larger but still relatively contained area of the plot.

5.2.3 Effect of application within the breach model

In order to implement the variable coefficient approach within the model, parameters regarding the eroding crest profile shape need to be extracted and rules developed for changing between coefficient sets. The following logic was applied to select between coefficient sets and to define a minimum C_d value:

1. Calculate the Head to Weir width (in the direction of the flow) ratio;
2. If the ratio >= 0.5 use the triangular curves;
3. If the ratio < 0.5 use alternate set of curves;
4. If the calculated value of C_d is less than 1.7, then default to 1.7.

The default minimum value of C_d set to 1.7 is based upon the difference between a purely rectangular broad crested weir (C_d=1.5) and a round nosed rectangular broad crested weir (C_d=1.7). Even slight rounding of the weir nose moves the discharge coefficient rapidly towards 1.7 hence, even for initial overflow of an embankment, the crest profile can be considered as a round nosed broad crested weir.

Figure 5-4 shows how use of different weir coefficients, including a variable coefficient approach, effects breach prediction. Results are presented for three fixed weir coefficient values and for the variable coefficient approach. The effect of using discharge coefficient values of 2.2, 1.7 and 1.5 are shown. It can be seen that changing the coefficient value (for this particular example) affects the timing of breach formation as well as the peak outflow, with a higher discharge coefficient

resulting in breach initiation earlier than for a lower coefficient value. Peak outflow is affected by approximately 10%. Results from using the variable discharge coefficient differs only slightly (in this example) from results for the fixed coefficient value of 1.7.

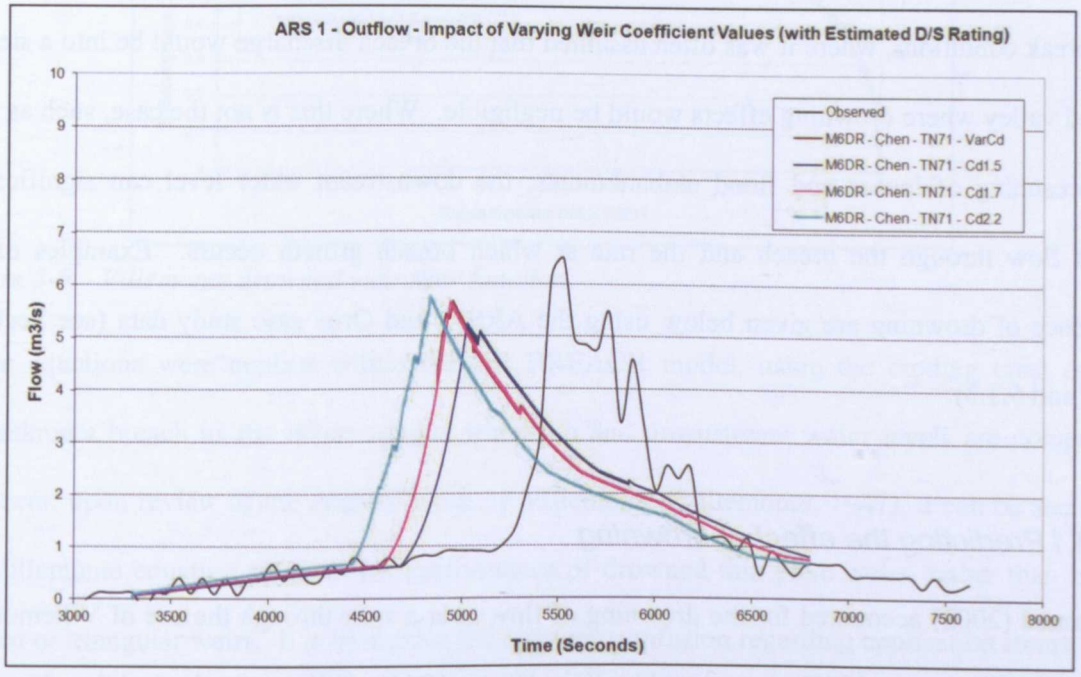

Figure 5-4 Example impact of using different (and variable) weir discharge coefficients

The value of the results shown in Figure 5-4 is to demonstrate that varying the weir discharge coefficient can noticeably affect the timing and shape of the breach flood hydrograph. The extent to which this will happen will be very case specific. Hence in some situations use of a variable weir coefficient will make little difference to model predictions as compared to use of a fixed coefficient (such as C_d=1.7), whereas in other cases the impacts could be significant. Hence, where breach modelling is being undertaken using a simplified 1D flow modelling approach, use of a variable weir coefficient will improve the model prediction. Use of an integrated 2D or 3D flow model would offer a better solution for flow prediction, but at an increasing cost in terms of model run time.

5.3 The significance of drowning

The importance of including the effects of drowning within a breach model is shown in the following section. In the past, many breach models did not take potential drowning effects into account. This perhaps reflects the fact that many breach models were developed to simulate dambreak conditions, where it was often assumed that the breach discharge would be into a steeply sloped valley where drowning effects would be negligible. Where this is not the case, such as with the breaching of levees and flood embankments, the downstream water level can significantly affect flow through the breach and the rate at which breach growth occurs. Examples of the influence of drowning are given below using the ARS#1 and Oros case study data (see Sections 5.3.2 and 5.3.3).

5.3.1 Predicting the effect of drowning

Mohamed (2002) accounted for the drowning of flow over a weir through the use of Villemonte's equation (Villemonte, 1947), as reported by King (King, 1954). Villemonte showed that drowning (for thin plate weirs) could be represented by the single equation (Equation 5-5 and Figure 5-5)

$$\frac{Q}{Q_1} = \left[1 - \left(\frac{H_2}{H_1}\right)^n\right]^{0.385} \qquad (5\text{-}5)$$

Where

n	is the exponent in the free discharge equation (Equation 5.3)
Q	is discharge for the submerged or drowned condition
Q_1	is discharge for the free or undrowned condition
H_1	is upstream head of water (relative to weir crest)
H_2	is downstream head of water (relative to the weir crest)

and

$$Q_1 = CH_1^n \qquad (5\text{-}6)$$

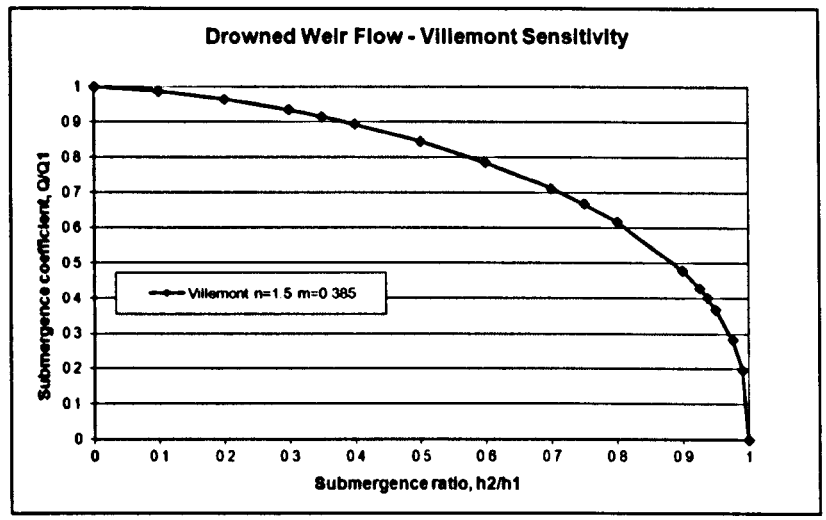

Figure 5-5 Villemonte drowned weir flow function

These equations were applied within the HR BREACH model, using the eroding crest of the embankment breach as the invert against which up and downstream water levels are compared. However, upon review of the original work by Villemonte (Villemonte, 1947), it can be seen that the Villemonte equation refers to the performance of drowned thin plate weirs, rather than broad crested or triangular weirs. It is likely that the apparent confusion regarding application stems from the use of descriptions by Villemonte such as rectangular and triangular shaped weirs, for thin plate rectangular and thin plate triangular shaped weirs (Figure 5-6).

WEIR NO.	DESCRIPTION	SHAPE AND SIZE	HEAD DATUM HEIGHT, P, FT.	FREE FLOW DISCHARGE FORMULAS, CFS	EXPONENT USED IN COMP.	NUMBER OF TESTS
1	SYMMETRICAL PROPORTIONAL	$\frac{X}{b}=1-\frac{2}{\pi}\tan^{-1}\sqrt{\frac{Y}{a}}$ WHERE: a=.003 FT. b=1.00 FT. WITH X & Y IN INCHES	1.01[6]	$Q_e=.0863\,h_e^{2.50}$	1.00	42
2	RECTANGULAR FULL-WIDTH	3.02'	2.00	$Q_e=3.35L\,h_e^{1.49}$	1.50	59
3	RECTANGULAR CONTRACTED	.25' .050 .25'	1.00	$Q_e=2.96L\,h_e^{1.44}$	1.44	36
4	RECTANGULAR CONTRACTED	1.00 1.00 1.00	1.25	$Q_e=3.00L\,h_e^{1.45}$	1.45	9
5	PARABOLIC	$Y=3X^2$, IN FEET	0.83	$Q_e=2.04\,h_e^{1.98}$	2.00	33
6	90° TRIANGULAR	$Y=X$, IN FEET	2.00	$Q_e=2.54\,h_e^{2.51}$	2.50	40
7	CUSP PARABOLIC	$Y=\sqrt{25X}$, IN FEET	0.83	$Q_e=0.594\,h_e^{3.32}$	3.32	58
NOTE	For all weirs h_1 was measured 3.00 ft upstream from weir and h_2 6.00 ft. downstream. Three piezometer holes on a transverse line in the flume floor were connected to each point gage stilling tube. [6]Head datum 0.010 ft. above weir crest.					

Fig. 2. Seven types of weirs were tested in this series of experiments.

Figure 5-6 A summary of tests performed by Villemonte showing the different weir types (Villemonte, 1947)

A review of guidance on drowning functions (Ackers et al., 1978, Chadwick and Morfett, 1993, Chow, 1959, French, 1986, Henderson, 1966, King, 1954) identifies two main sources of information, namely *Weirs and flumes for flow measurement* (Ackers et al., 1978) and the British Standards (British Standards Institution (BSI), 1986, British Standards Institution (BSI), 1990, British Standards Institution (BSI), 2008a, British Standards Institution (BSI), 2008b, British Standards Institution (BSI), 2008c).

The difficulty in identifying a single drowning function for use within a breach model is that the function varies according to the weir geometry; in turn the weir geometry changes as the breach evolves. Hence, any function that is selected either needs to cope with significant geometry changes, or multiple functions are used and selectively applied as the geometry changes.

The guidance on drowned weir flow by British or International Standards varies in format according to the weir type under consideration. A plot that combines the drowning functions from different sources was produced (Figure 5-7) to allow a direct comparison of the different guidance.

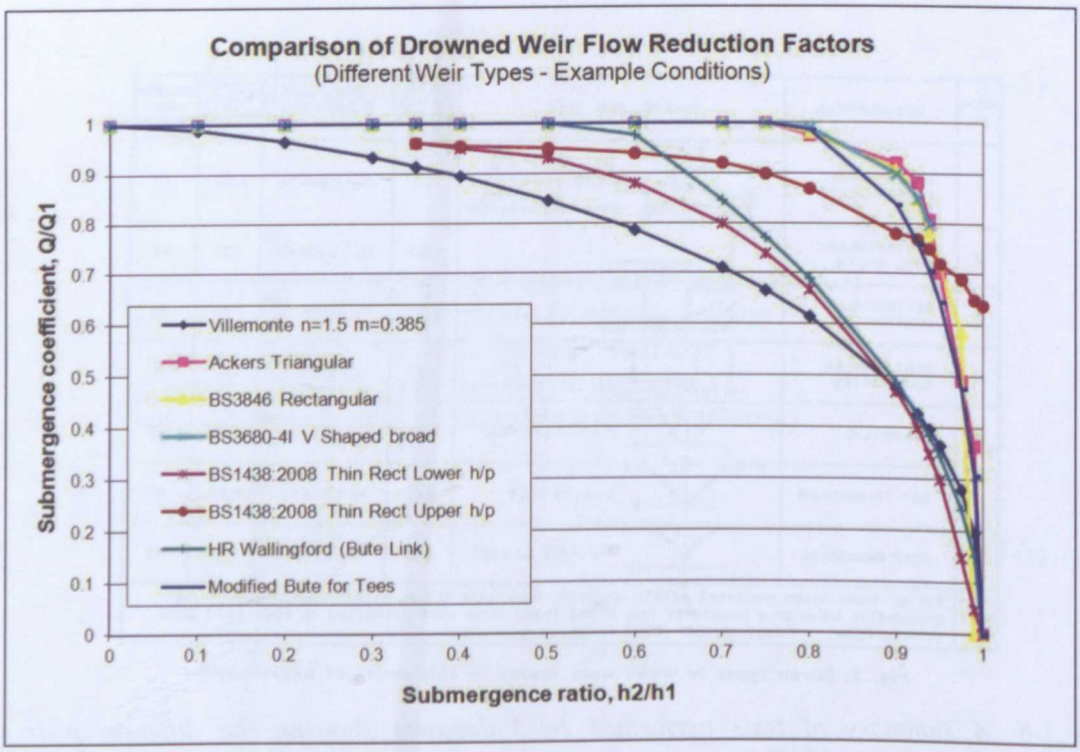

Figure 5-7 A comparison of weir drowning functions

Additional weir drowning functions were also developed by HR Wallingford for weir design studies undertaken in the 1980s (HR Wallingford, 1989). These offer a more generic approach to the drowning equation, incorporating the weir modular limit as a variable. These are included for comparison against selected drowning functions in Figure 5-8.

BS1438:2008 (British Standards Institution (BSI), 2008c) relates to flow measurement using thin plate weirs. The guidance here should correlate with the work by Villemonte. However, as shown in Figure 5-7, there is a difference between the drowning functions. BS1438:2008 makes it clear that the drowning function depends upon a range of geometric parameters as well as simply the crest and relative water levels; the two curves plotted show upper and lower bound functions.

The three remaining plots in Figure 5-7 appear very similar, but originate from different sources and for different weir shapes. These comprise:

- Drowning function for triangular weirs (e.g. Crump) from Weirs and flumes for flow measurement (Ackers et al., 1978);
- Drowning function for V shaped, broad crested weirs from BS3680-4I (1986);
- Drowning function for rectangular broad crested weirs from BS3846 (2008).

Care should be taken to recognise whether gauged heads (h_2/h_1) or the ratio of total head (H_2/H_1) are used:

Villemonte uses gauged heads	h_2/h_1
Ackers uses total head	H_1/H_2
British Standards use total head	H_1/H_2

The approach velocity for breach could vary from low to moderate, whilst the downstream velocity is likely to vary from moderate to very high. Hence, the (mis)use of total head instead of gauged could make a significant difference.

The Ackers equation comprises a modular limit at H_{2e}/H_{1e} = 0.75, with the following equation applicable to $0.75 < H_{2e}/H_{1e} \leq 0.93$ (i.e. when $0.87 \leq f < 0.99$)

$$f = 1.035\left[0.817 - \left(\frac{H_{2e}}{H_{1e}}\right)^4\right]^{0.0647} \tag{5-7}$$

and the following equation is applicable to $0.93 < H_{2e}/H_{1e} \leq 0.985$ (i.e. when $0.40 \leq f < 0.87$)

$$f = 8.686 - 8.403\left[\frac{H_{2e}}{H_{1e}}\right] \tag{5-8}$$

BS3846 (Broad Crested Weirs) gives guidance on a specific, but typical geometry of rectangular broad crested weir where the length (in the direction of flow) to height ratio is approximately 3:

$$Q = (2/3)^{3/2} g^{1/2} bfCh_1^{3/2} \tag{5-9}$$

Where f, the drowned flow reduction factor is defined in terms of total head as follows:

in the range $0.750 < H_2/H_1 < 0.925$:

$$f = 1.045[0.76 - (H_2/H_1)^{4.2}]^{0.0645} \tag{5-10}$$

in the range $0.925 < H_2/H_1 < 0.975$:

$$f = 5.70 - 5.245(H_2/H_1) \tag{5-11}$$

The HRW equation (HR Wallingford, 1989) was developed to allow simulation of drowning of a gated weir structure. The gates were initially angled with the flow, providing a sharp crest, but could be pivoted into a horizontal position whereby flow could pass both over and under the gates. The drowning function comprises:

$$f = \sin\left[\left(\frac{\pi}{2}\right)\left(\frac{1-x}{1-A}\right)^{0.5}\right] \tag{5-12}$$

Where:

$X = H_2/H_1$

A = Modular limit ($0 < A < 1$)

Figure 5-8 shows a comparison of how this equation compares to the Ackers and Villemonte equations. Note that Villemonte uses gauged heads whilst the others use total head.

It can be seen that the HRW equation offers a range of solutions that can be set to match either of the other equations. Consideration also needs to be given to the dependency of the overall weir behaviour on geometric parameters, which are not reflected here. A further variation in discharge of the order of 20% might be experienced as a function of head relative to geometry (within the given weir type).

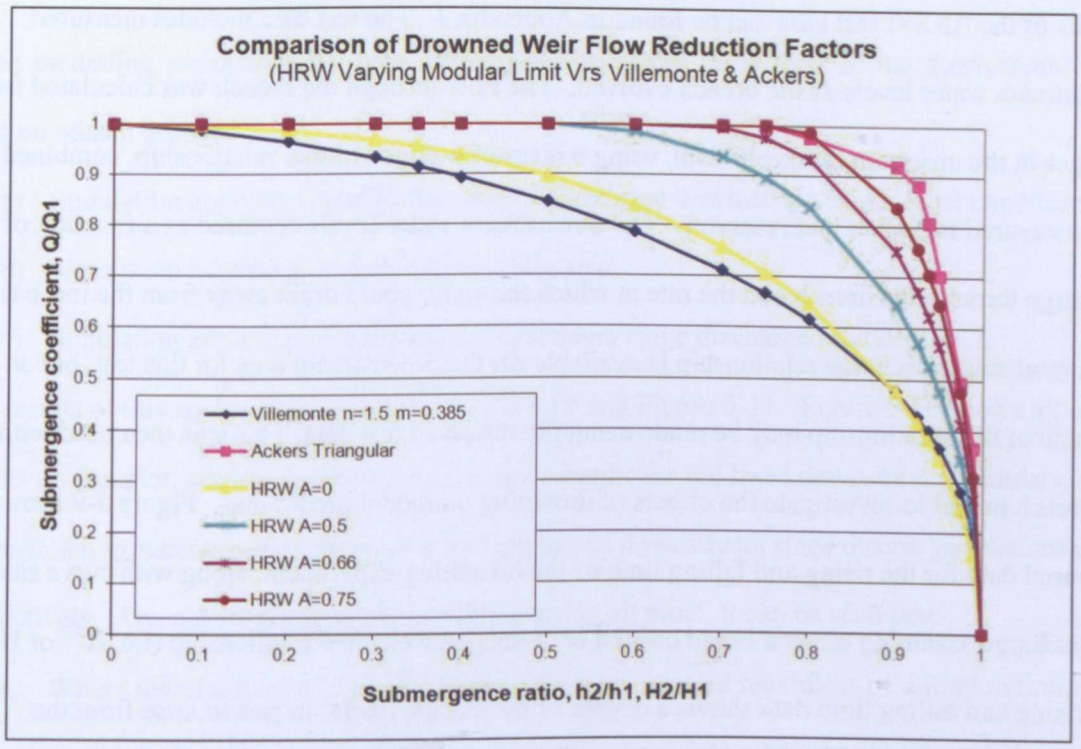

Figure 5-8 Comparing HRW (varying modular limit) to Ackers and Villemonte drowning functions

Based upon the comparison of guidance on weir drowning functions for different types of weir in relation to the typical shape of embankments as breach formation occurs, it would seem that the most appropriate function to apply is that of Villemonte, or HR Wallingford if there is greater confidence in knowing the shape of the eroding weir section. Whilst the Villemonte equation has been shown to be derived from the analysis of thin plate weirs, it can be argued that the drowning process is most important at the breach formation stage where the embankment body can be

eroding fast in relation to the head of water. Under these conditions the potential difference between thin plate and ogee weir flow is less, hence the potential error in applying Villemonte is less.

Examples of the impact of the weir drowning function are provided for two case studies in the following Sections 5.3.2 and 5.3.3.

5.3.2 Influence of drowning on the ARS#1 test case

Details of the ARS#1 test case can be found in Appendix 3. The test data includes measured downstream water levels as the breach evolved. The flow through the breach was calculated from changes in the upstream reservoir level, using a measured stage volume relationship, combined with measured inflow to that reservoir. The downstream water levels occurred as a function of discharge through the breach and the rate at which the water could drain away from the test basin. No formal stage discharge relationship is available for the downstream area for this test, but an estimate of this relationship may be made using the observed test data. This was then used within the breach model to investigate the effects of drowning on model predictions. Figure 5-9 shows measured data for the rising and falling limb of the breaching experiment, along with curve fits for the discharge assuming either a broad crested or V-shaped weir flow relationship (i.e. $H^{3/2}$ or $H^{5/2}$). The rising and falling limb data shows a degree of hysteresis, likely, in part to arise from the calculation method for breach discharge. Assuming some form of weir control for discharge out of the downstream reservoir, it can be seen that a V-shaped weir equation (i.e. $H^{5/2}$) fits the data better than a rectangular weir equation (i.e. $H^{3/2}$).

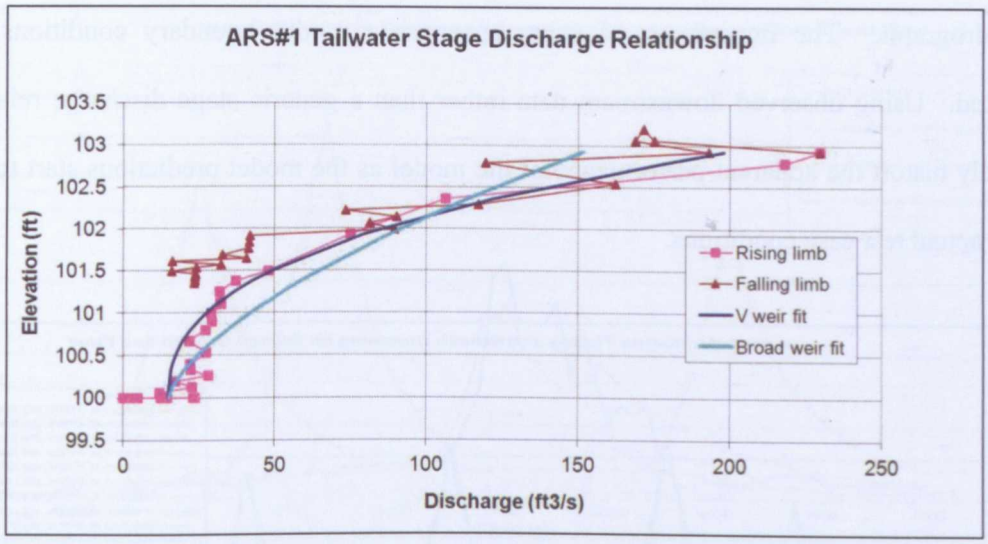

Figure 5-9 Analysis of downstream stage discharge relationship for test ARS#1

Three modelling scenarios have been investigated to assess the effects of the downstream water level on breach growth:

a) Simulation applying (rigidly) the observed test case downstream water level conditions;

b) Simulation assuming no downstream influence;

c) Simulation applying the calculated downstream stage discharge relationship.

The results of this analysis are shown in Figure 5-10 and Figure 5-11. Figure 5-10 shows all of the results on one plot, whilst Figure 5-11a, b, c show results for the fixed downstream boundary, no downstream influence and application of the calculated downstream stage discharge relationship respectively. The observed test discharge is shown on all plots. It can be seen that:

- Where the observed test boundary conditions are applied regardless of initiation timing, the model predictions rapidly deviate from the observed data when the model prediction timing varies from the observed conditions;
- Without considering the effects of downstream water level on breach growth, the breach outflow predictions are significantly greater than observed;
- Application of the estimated downstream boundary conditions gives a far more consistent prediction that is significantly less dependent upon the initiation timing.

The importance of including drowning effects within a breach model is clearly demonstrated by these results. Drowning effects can significantly affect the rate of erosion and the magnitude of the

flow hydrograph. The importance of using appropriate model boundary conditions is also highlighted. Using observed downstream data rather than a generic stage discharge relationship can rapidly distort the apparent performance of the model as the model predictions start to deviate from the actual test case conditions.

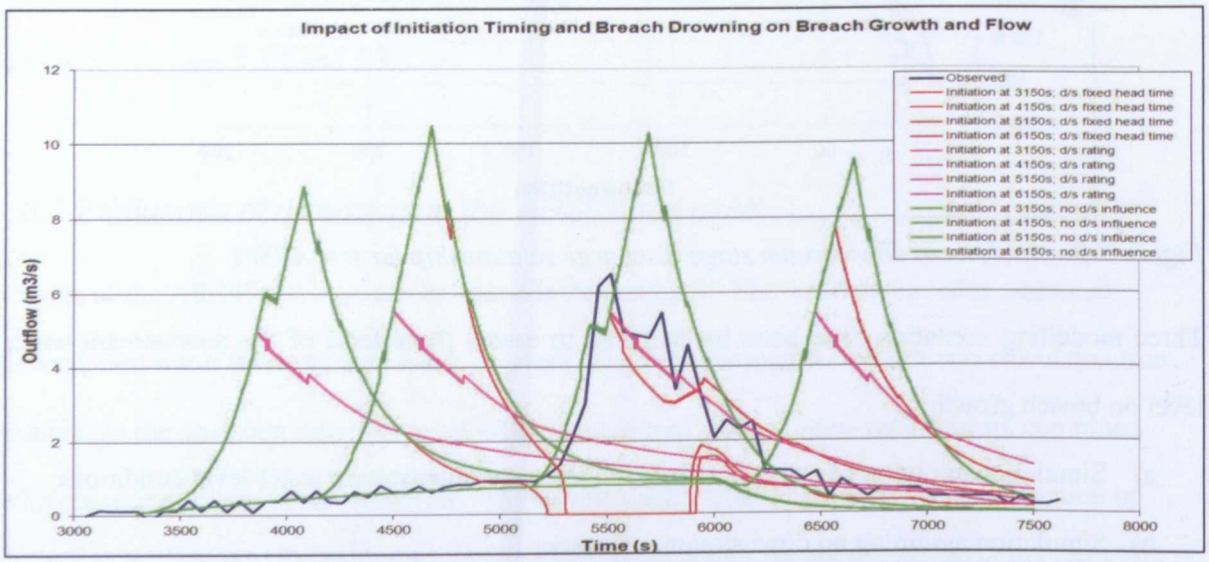

Figure 5-10 Model predictions with varying downstream boundary conditions: all boundary conditions (fixed head time; no downstream influence; estimated rating)

It is noticeable that the observed flow data shown in Figure 5-10 and Figure 5-11shows fluctuations in comparison to the model predictions. These most likely arise from two sources. Firstly, the breach discharge is calculated from the change in measured upstream water level, hence any error or oscillation in this level will be reflected in the 'observed' discharge. Oscillations can be seen in the predicted values leading up to the point of breach formation. These errors are indicative of estimated flow error for relatively stable, slowly changing conditions; during breach formation when conditions change more rapidly, it is reasonable to assume that these errors might become larger, which is what can be seen as the breach flow surges. The second cause of fluctuation arises when blocks fail and fall into the breach as part of the breach widening process. Block removal below the water level increases the flow area, whilst block failure into the breach comprising material from both above and below the water level may briefly reduce the flow area. Hence the influence of block failure can be to both reduce and then increase discharge, as can be seen in the observed results.

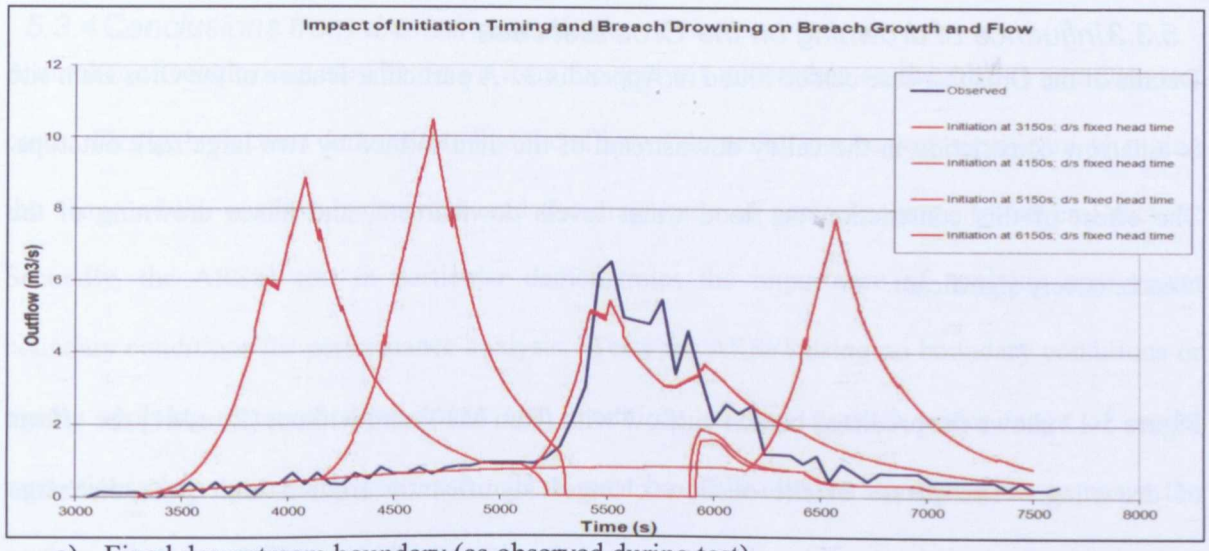

a) Fixed downstream boundary (as observed during test)

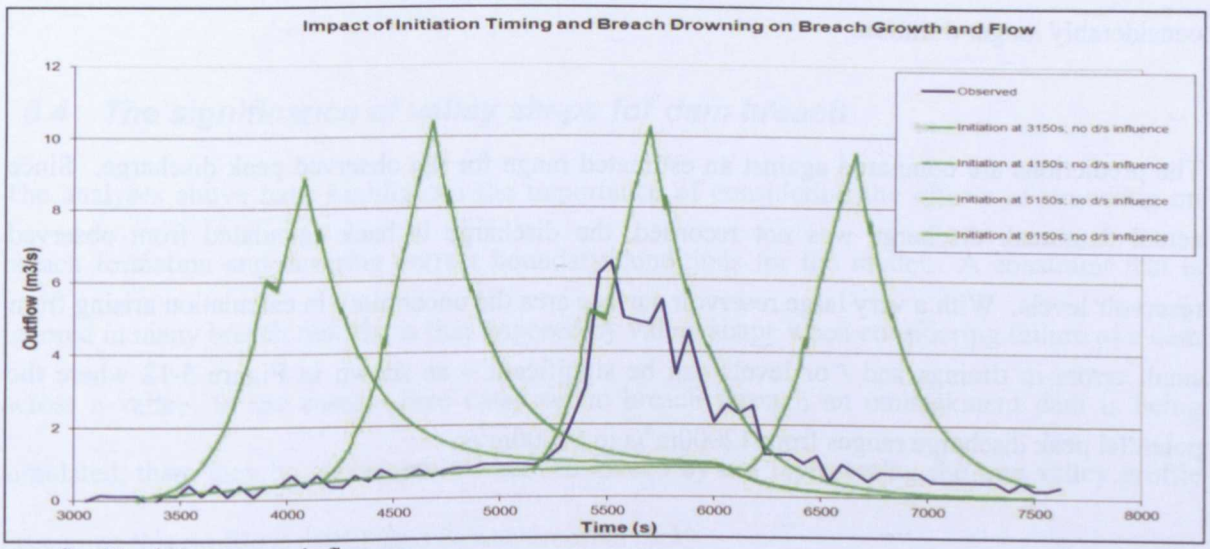

d) No downstream influence

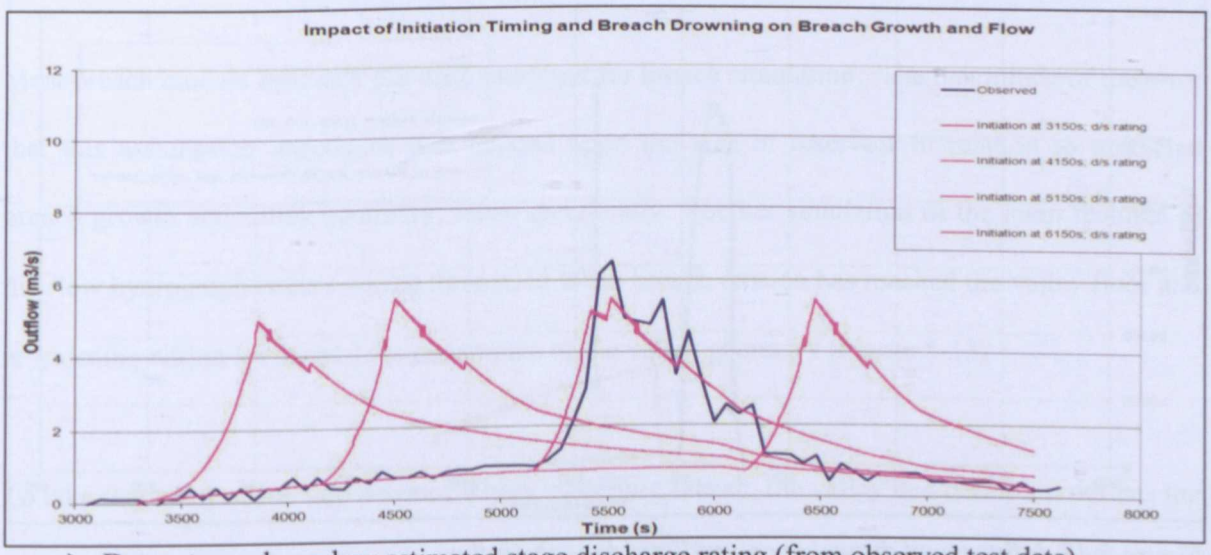

e) Downstream boundary estimated stage discharge rating (from observed test data)

Figure 5-11 Comparison of model predictions with varying downstream boundary conditions (separate plots)

5.3.3 Influence of drowning on the Oros test case

Details of the Oros test case can be found in Appendix 3. A particular feature of the Oros Dam site is a narrow constriction in the valley downstream of the dam formed by two large rock outcrops. The effect of this constriction on flood water levels downstream, and hence drowning of the breach, is very significant.

Figure 5-12 shows the predicted breach outflow with (Run M10) and without (Run M1) the effects of drowning. The nature of the outflow changes significantly from a high peak discharge hydrograph of relatively short duration, to a much lower peak discharge hydrograph but over a considerably longer duration.

The predictions are compared against an estimated range for the observed peak discharge. Since actual dambreak discharge was not recorded, the discharge is back calculated from observed reservoir levels. With a very large reservoir surface area the uncertainty in calculation arising from small errors in timings and / or levels can be significant – as shown in Figure 5-12 where the potential peak discharge ranges from 12000m^3/s to 58000m^3/s.

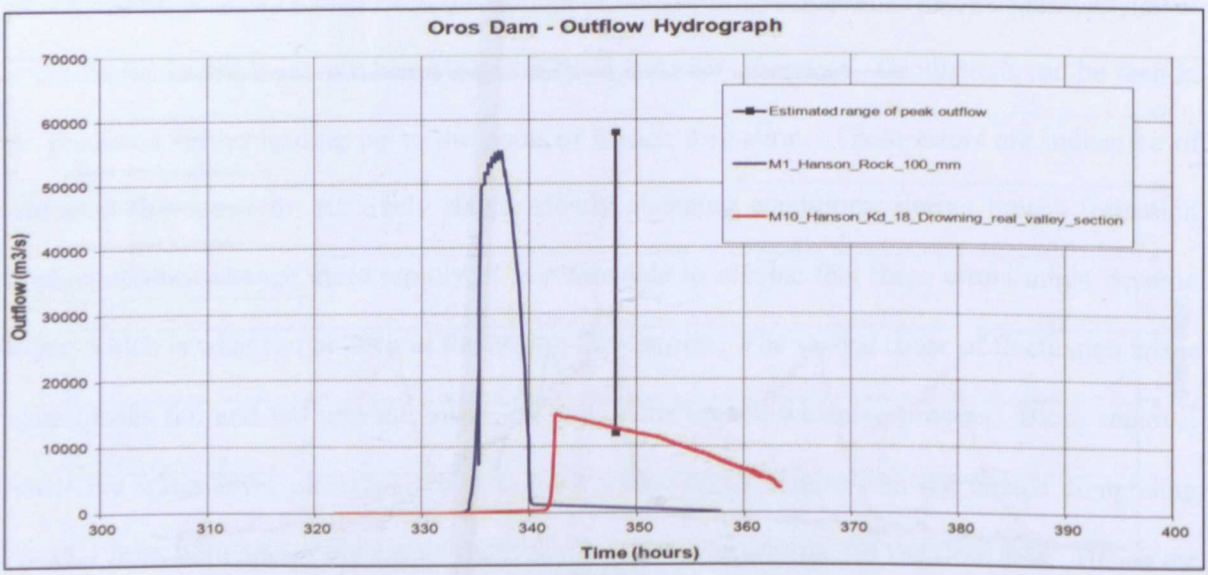

Figure 5-12 Influence of drowning on predicted breach outflow

5.3.4 Conclusions from drowning analysis

A number of conclusions may be drawn from the analysis undertaken on the ARS#1 and Oros test cases. Firstly, both cases demonstrate that the effect of drowning can be very significant, changing the shape of the outflow hydrograph and the magnitude of peak discharge by several factors. Secondly, the ARS#1 test in particular demonstrates the importance of applying appropriate boundary conditions for performance analysis. Tests for ARS#1 using no boundary conditions or rigidly applying observed downstream test conditions suggest a much wider range of model predictions than is actually the case. This may be misleading when trying to compare the performance of a number of models together.

5.4 The significance of valley shape for dam breach

The analyses above have highlighted the importance of considering the effects of drowning on breach formation and ensuring correct boundary conditions for the model. A constraint that is ignored in many breach models, is that imposed by valley shape when considering failure of a dam across a valley. In the cases where catastrophic breach through an embankment dam is being simulated, there may be considerable error introduced by not representing the true valley profile (assuming this profile is established by non erodible rock).

Most breach models assume a flat base as a limit for breach simulation. The magnitude of the error that this assumption introduces will depend upon the size of reservoir in relation to predicted breach growth and valley geometry; more specifically, whether simulation of the main features of the flow hydrograph occurs during the period when breach erosion has reached the valley floor and is widening within (or across) the constraints of the valley geometry (Figure 5-13).

To take the valley shape into account whilst modelling breach, the valley bed definition defines the non erodible base to the embankment. This is considered to be fixed through the X direction – i.e. the same for all sections through the breach. However, the non erodible bed may vary in the Y and Z directions in order to define a valley shape. The objective is how and when to introduce the

valley shape within the breach shape definition, whilst maintaining fast and efficient breach computation.

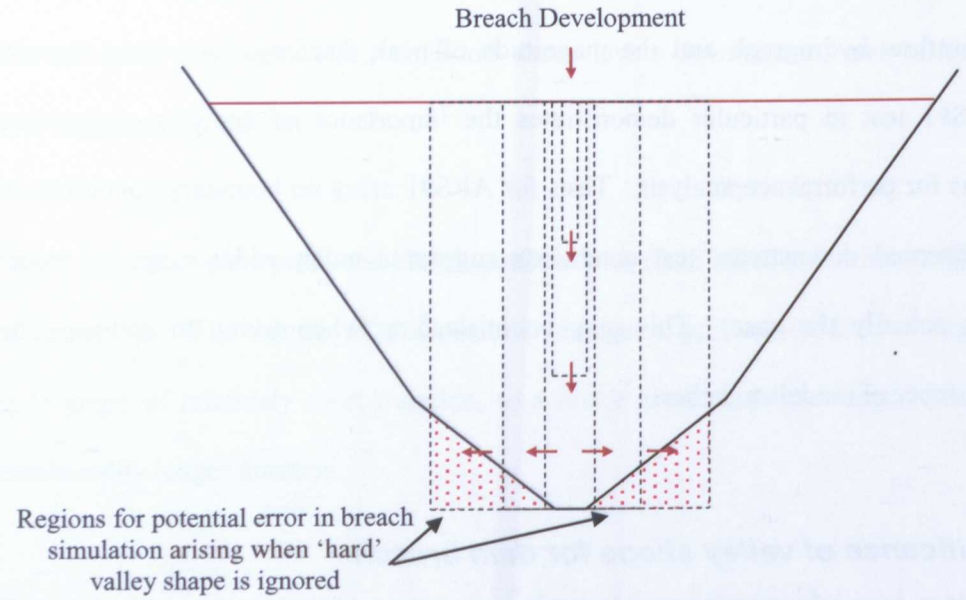

Figure 5-13 Potential error in calculation when ignoring valley shape for dambreak analysis

The valley shape needs to be defined by as small a number of points as possible in order to keep the model run time as low as possible. A simple valley can comprise a river channel with flood plains on either side before reaching the valley sides. This geometry may be defined by 11 points as shown in Figure 5-14.

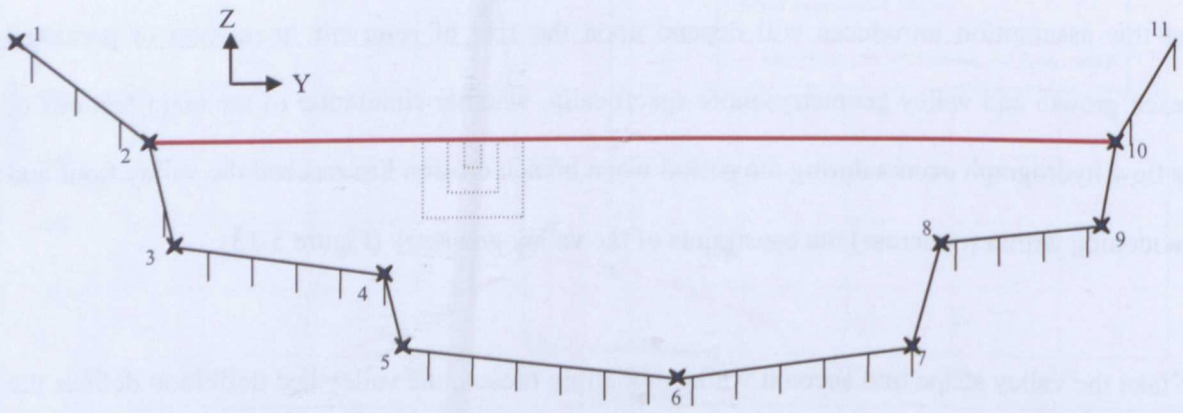

Figure 5-14 Breach growth through an embankment with a fixed (rock) valley profile

Checking whether the growing breach profile has intercepted the valley sides at every time step complicates and slows the computational process, hence it was considered that initial zones of 'safe breach growth' could be established (for each model section) prior to the model run. This could be done, for example, by extending a profile from the initiation notch vertically down until it intersects the valley, horizontally until intersection and then back vertically. This may be done for a single vertical drop (line A-B-C-D in Figure 5-15) or for additional lines such as a 45 degree drop (line A-E-F plus A-E-G-H in Figure 5-15).

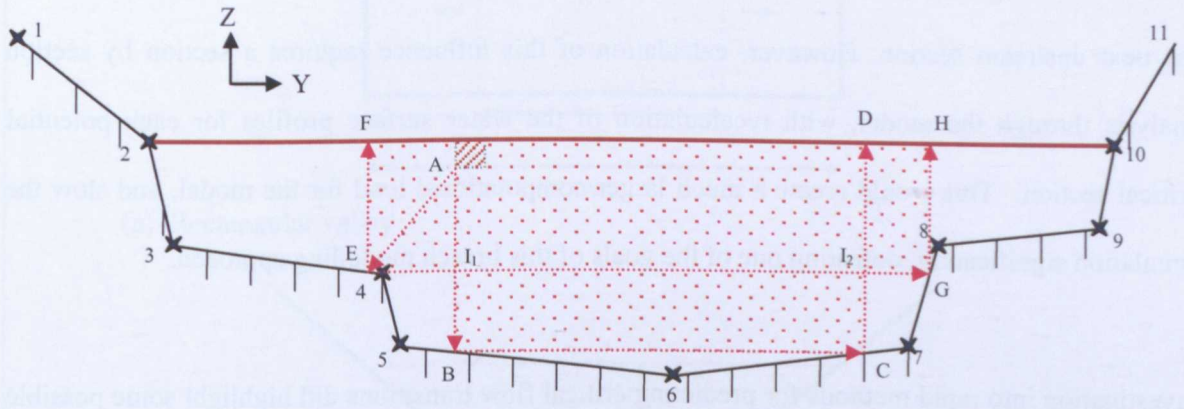

Figure 5-15 Defining a safe growth zone within a valley profile

With the two projections shown in Figure 5-15, the safe breach growth zone is defined by line F-E-I_1-B-C-I_2-G-H (shaded). An initial check on valley profile data will allow identification of the valley low point; a rule may be defined ensuring that a valley shape can only be defined by horizontal or sloping lines leading to a single low point – this makes calculation of the safe breach growth zone and subsequent breach – valley side interaction significantly easier with minimal limitation on the modeller.

The method outlined above focuses upon how to resolve the evolving breach profile at each section through the embankment. However, when tested, a greater problem was found relating to the way in which critical flow conditions through the breach are calculated. The current analysis method (Mohamed, 2002) assesses the flow capacity of each cross section through the breach and identifies the minimum flow section as the control point and hence where subcritical flow transitions to

supercritical. This flow capacity is calculated independently of flow conditions at other sections. This is acceptable for conditions where a breach channel evolves progressively through the embankment, but becomes a problem when there are abrupt changes, such as the fixed valley shape boundary conditions, imposed, generally from the downstream section back towards the crest. By fixing the breach cross section, the method of identifying the critical flow section by calculating the minimum flow section becomes trapped at the valley imposed section, generally near the toe of the breach. Considering the physical situation, it is recognised that this section would not control flow conditions through the breach unless it created a backwater effect sufficient to influence or drown the next upstream section. However, calculation of this influence requires a section by section analysis through the model, with recalculation of the water surface profiles for each potential critical section. This would create a much larger computational load for the model, and slow the simulation significantly, defeating one of the goals of this breach modelling approach.

Investigation into rapid methods for predicting critical flow transitions did highlight some possible approaches (Castro-Orgaz et al., 2008, Montes, 1998) but the complexity of analysis seemed more appropriate to smoother, more stable flow transitions rather than the dynamically changing and relatively uncertain processes that develop during the breaching process. Consequently, this line of investigation was stopped and the valley shape adjustment not implemented within the model.

Allowing for the effect of valley shape does, however, remain an important area that should be addressed in future breach model developments. Figure 5-16 highlights where errors may be induced when calculating breach conditions with a 'flat base' breach model rather than one that can adapt to fixed bed profiles, such as a rock valley. A simple example of the potential error in flow calculation, and hence breach growth calculation is given by comparing calculated flow for a rectangular breach, 10m deep and 20m wide (i.e. Figure 5-16a) against a triangular valley profile that is 10m deep and 20m wide at the crest (i.e. Figure 5-16c) using simple rectangular and triangular weir flow equations with approximate, but accepted coefficient values (Webber, 1971):

Rectangular valley flow:

$$Q = CLH^{3/2} = 1.7 \times 20 \times 10^{3/2} = 1075 m^3/s$$

V shaped valley flow:

$$Q = C_e\ 8/15\ (2g)^{1/2} \tan(\theta/2)\ H^{5/2} = 0.59\ 8/15\ (2g)^{0.5} \tan(45)\ 10^{5/2} = 441 m^3/s$$

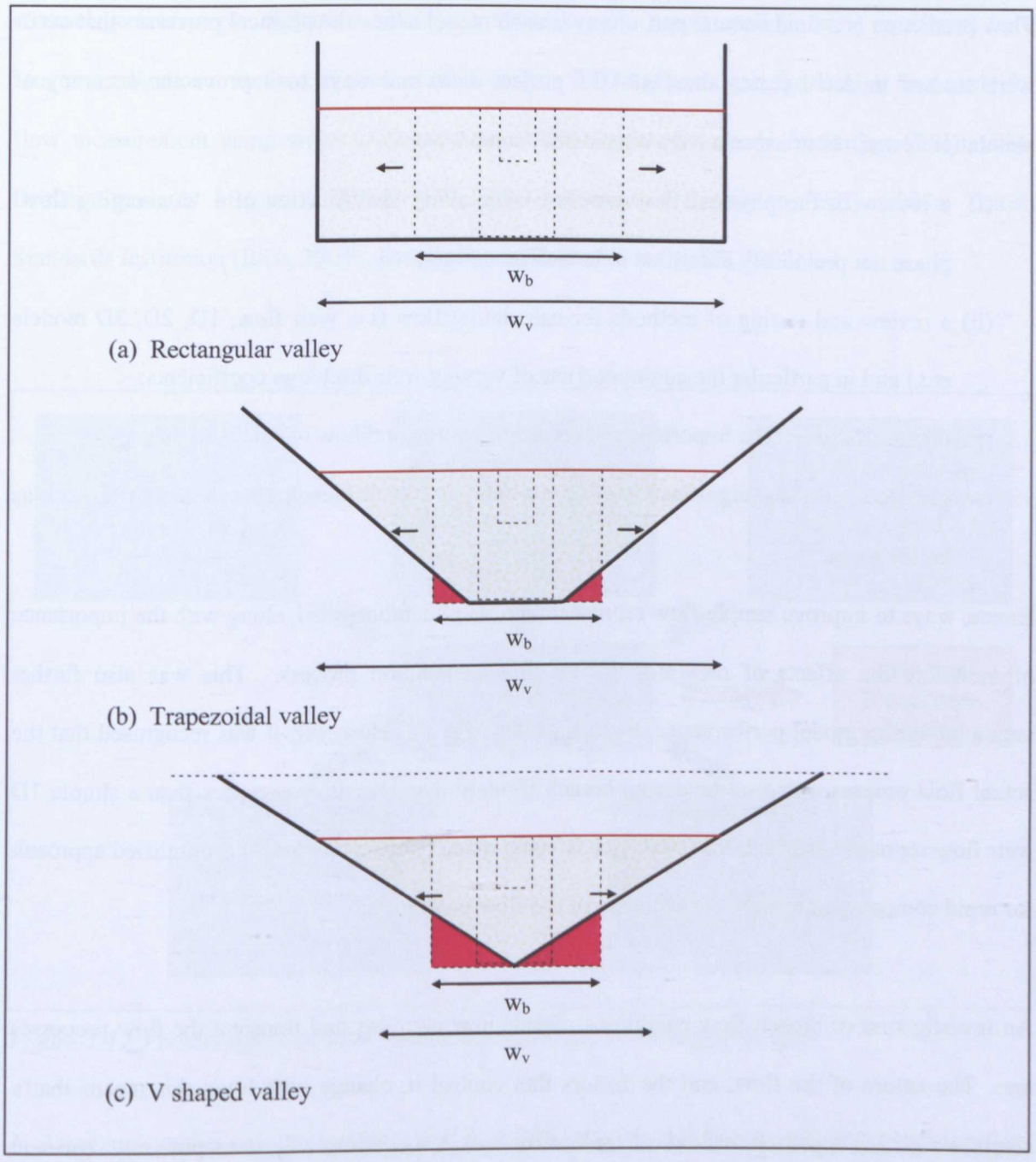

Figure 5-16 Examples of how different valley shape may affect the accuracy of flat bed breach model prediction

The potential effect of valley shape on the formation of a large breach can therefore be significant. At the time of writing, no breach models contain the ability to predict breach evolution over a fixed, non rectangular bed profile.

5.5 Discussion

Flow prediction is a fundamental part of any breach model hence the physical processes that occur were studied in detail (using the IMPACT project data) and ways to improve the accuracy of simulation tested. Four aspects were considered, comprising:

(i) a review of the physical flow processes, including identification of a 'converging flow' phase not previously identified in breach modelling;

(ii) a review and testing of methods for calculating flow (i.e. weir flow, 1D, 2D, 3D models etc.) and in particular the automated use of varying weir discharge coefficients;

(iii) demonstration of the importance of breach drowning and how to calculate this;

(iv) clarification of the significance of constraints on overall breach growth and flow, such as valley shape.

Hence, ways to improve simple flow representation were demonstrated, along with the importance of including the effects of drowning in the flow calculation process. This was also further validated during model performance evaluation (Chapter 8). However, it was recognised that the actual flow processes that occur during breach formation are far more complex than a simple 1D weir flow representation and that a balance is being made between the use of a simplified approach for rapid computation against the accuracy of the flow prediction.

An investigation of breach flow conditions reveals how complex and transient the flow processes are. The nature of the flow, and the factors that control it, change with time; this means that a single, simplified approach to flow calculation for breach modelling will never precisely represent the true breach flow for all phases of breach development. The issues are firstly, whether the impact on accuracy implicit within a simplified approach is really understood and secondly, whether this impact is acceptable for the given use of modelling results.

Analysis of the IMPACT project video footage allowed the different stages of flow and breach evolution to be highlighted. Initially, the breach flow is controlled by the eroding shape of the embankment and a number of different types of weir flow can be seen as the control section and conditions change. Hence, there are several factors that will affect the accuracy of flow calculation using a simple weir flow approach, including weir geometry, water depth on the weir, upstream channel geometry, etc. (Figure 5-17). These influences are represented (in weir equations) by a range of adjustment factors, as presented in various different texts and the British Standards for flow measurement using weirs (Ackers et al., 1978, British Standards Institution (BSI), 1986, British Standards Institution (BSI), 1990, British Standards Institution (BSI), 2008a, British Standards Institution (BSI), 2008b, British Standards Institution (BSI), 2008c).

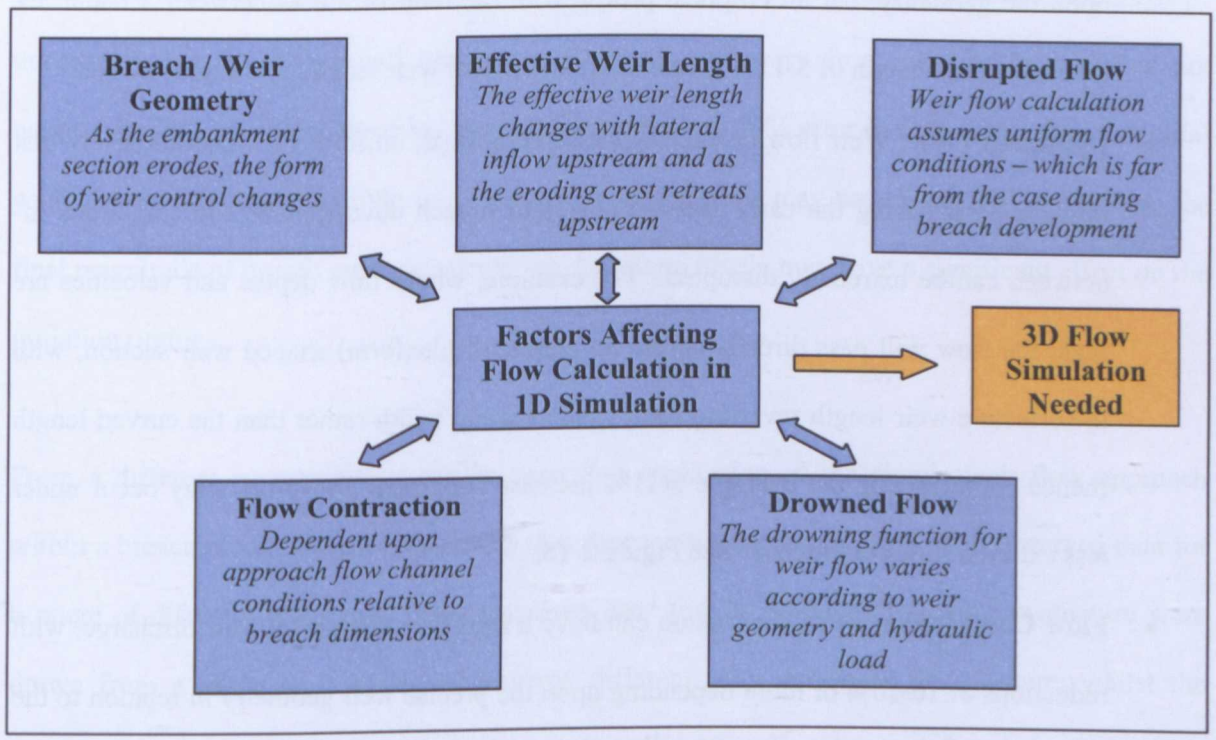

Figure 5-17 Factors affecting weir based calculation of flow through a breach

A closer look at the various flow phases also reveals specific conditions such as converging flow where flow is independent of weir control, and a retreating weir crest that offers a control section longer than the minimum width of the breach. Analysis of the effects of drowning also reveals a similarly complex dependency upon a range of geometric and hydraulic parameters.

The magnitude of variation in flow calculation from each of these different factors can be significant. For example, considering each of the factors shown in Figure 5-17:

- **Weir Geometry**: the weir discharge coefficient can vary by as much as 50% between broad crested and ogee weir shapes. As the embankment section erodes non hydrostatic pressure distributions also develop due to the steep water surface curvature and vertical accelerations. Flow vortices also form along each side of the breach. See Figure 2-13a,f and Figure 2-14a, e;
- **Effective Weir Length**: as the flow control section erodes the embankment it moves upstream (Samuels and Morris, 2010). In the latter stages of erosion (through the upstream embankment slope) the control section moves out of the narrower embankment crest area and can form an elliptical weir control on the upstream face. Effective weir lengths depend upon the geometry, but an elliptical profile with the ratio of a:b as between 5:1 and 3:1 gives a control length of 5-11% greater than the normal weir length. See Figure 2-14e;
- **Disrupted Flow**: Weir flow calculations assume normal, uniform flow conditions. Whilst this can exist during the early and late stages of breach development, the conditions in-between can be extremely disrupted. For example, where flow depths and velocities are high, the flow will pass directly across an elliptical (planform) shaped weir section, with the effective weir length reverting back to the normal width rather than the curved length (hence counteracting the example 5-11% increase suggested above that may occur under less extreme flow conditions). See Figure 2-15;
- **Flow Contraction**: Flow contraction can have a significant effect on weir discharge, with reductions of 10-20% or more depending upon the precise weir geometry in relation to the approach flow and flow channel conditions. These effects will change as the breach shape evolves and widens. See Figure 2-13e-f;
- **Drowned Flow**: as the downstream water level rises and drowning occurs, the flow through a breach and hence the rate of growth can slow or even stop. The onset of drowning and the rate at which flow is reduced is a function of the breach geometry. Modular limits (h_2/h_1) may be considered anywhere between 0 and 0.85, with 0.66 or 0.75

often used. The difference in the rate of drowning (due to geometry and use of different functions) at a given point in the submergence range say 0.7-1.0, could be as much as 30-40%. See Figure 1-5 and Figure 1-6.

Alongside these uncertainties within the model flow calculation process is the additional uncertainty introduced by defining horizontal and vertical boundaries to modelling the breach growth. It can be seen that introducing natural geometry boundary conditions, such as valley shape for dambreak modelling, can have a significant effect on modelling predictions.

However, whilst a long list of uncertainties in flow calculation using simple weir flow calculation can be presented, it should be recognised that the magnitude and range of application of each of these uncertainties varies during the breaching process. The influence that each component of uncertainty has on the overall prediction of breach will vary from case to case and is not necessarily independent of the other factors. For example, a 50% error in flow calculation for initial weir flow conditions when little or no erosion is taking place may have a negligible effect on the final magnitude of breach outflow calculation, but alternatively may have a significant effect on the initiation timing.

From a different perspective, it can be seen that application of the simple weir flow approach within a breach model can provide results that appear reasonably consistent with observed data for a range of different test cases. The test cases used for the DSIG performance evaluation were drawn from a range of sources and covered different sizes and types of structure; whilst the predicted results are far from perfect, they do broadly reflect the observed flow behaviour. This suggests that the uncertainties discussed above do not occur simultaneously or combine to give widely differing answers.

Whilst the simplified weir flow approach might offer an indicative solution to breach flow, a simple observation of the true flow processes during breach evolution demonstrates a complex and

changing 3D flow structure. In particular, the converging flow phase shows near vertical dropping of water through the breach and the later erosion and undercutting along the toes of the breach sides are driven by flow in the form of elongated vortices, which in turn arise through the combination of flow contraction and 'dropping' through the breach. To simulate these flow conditions and the associated erosion processes will require a 3D flow model. Application of a 2D flow model may improve flow predictions relative to 1-D weir flow however a 2D (H) analysis will not be able to simulate the vertical flow accelerations through the breach and in forming the erosive vortices.

In conclusion, it is recognised that use of a weir equation to predict breach flow contains many approximations and a significant degree of uncertainty. Analysis of physical flow processes show that breach flow is a complex 3D process that evolves throughout the breaching process. This suggests that a time varying 3D flow model is required to reproduce these conditions within a breach model. However, whilst 3D flow modelling is possible, it will require significant development to integrate 3D flow, erosion and structure stability analysis, as would be required for a true 3D breach model. In comparison, the performance evaluation of the 1D weir flow approach shows that this offers a pragmatic indicative solution for breach flow conditions. However, attempts to refine the 1D weir flow calculation method simply emphasise the number of dependent parameters and the degree of uncertainty within this approach and it is considered that following this line of analysis further is not practical in the context of this research. Instead, integration of 2D or 3D flow, erosion and stability processes is recommended. This approach should also lend itself to the easier definition of natural boundary profiles, such as valley shape or bedrock boundaries.

6. Breach erosion processes

The erosion processes that occur during breach initiation and growth vary according to the hydraulic loading, soil type and state and structure response (Morris et al., 2009a). Much of the past research into breach formation processes has been undertaken with only a limited, if any, analysis of soil state (Wahl, 2007). This leads to confusion as to the validity and applicability of different breach models (Morris et al., 2008, Zhu, 2006). It is therefore important to clarify what erosion processes can occur, when and how these might be simulated in a breach model. In particular, when breach formation might occur through headcut erosion as compared to surface erosion. This difference is important because the nature of the erosion affects the timing at which the upstream edge of the crest might be eroded; since this typically controls flow driving the breach initiation stage, a change in timing here could significantly affect the overall breach formation timing and hence the rate of flood water release and the ultimate size of the breach.

6.1 Observed behaviour

6.1.1 Breach erosion behaviour: Head cut versus surface erosion

As introduced in Figure 2-3, two 'large scale' physical processes can occur that affect the rate and way in which erosion dictates the breach formation and growth process. These mechanisms are:

1. Headcut formation;
2. Surface erosion.

Headcut formation occurs when the erosion of material forms steps in the downstream face of the embankment. These steps tend to deepen and migrate upstream, progressively forming a smaller number of larger steps. Eventually the steps (or step) cuts through the upstream edge of the crest, where control of the flow into the breach takes place, and rapid failure ensues (Figure 6-1; also see Figure 2-6). The process of headcut formation tends to occur in cohesive materials with a low erodibility (in comparison to say, a sandy non cohesive and highly erodible material). The nature of the material is such that it can support the creation of steps, without rapid collapse and erosion of

the surface material. This process leads to the creation of a series of cascading jets of water, which impact the embankment surface and erode back into the step (embankment) as well as the step surface.

a. Initial stages of headcut formation (11:55) – erosion at weak point near toe of slope

b. Formation of small headcut (12:07) near toe of embankment

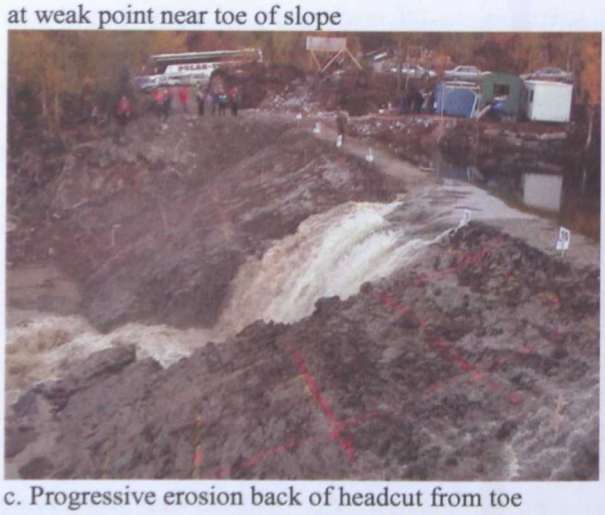

c. Progressive erosion back of headcut from toe (12:32)

d. Erosion of headcut into single large step (12:39)

e. Progressive erosion of headcut (12:59)

f. Failure of upstream crest / slope (13:03)

Figure 6-1 Stages of headcut development (EU IMPACT Project clay test 1-02) (Morris, 2009)

When surface erosion occurs, material is eroded from the embankment face and the crest area rather than just from the downstream face (Figure 2-5). The occurrence of this process is significant since erosion of the crest area will affect the control of flow into the breach. Hence, erosion of the crest could be expected to increase the speed with which catastrophic breach might occur when compared to erosion via a headcut process. Surface erosion tends to occur in non cohesive, more erodible materials which, by their nature, tend not to support the creation of steps. Unlike headcut erosion, surface erosion appears to be driven by tangential flow stresses.

Analysis of the IMPACT field data test data in relation to physical processes (Morris, 2009) shows that headcut processes clearly occurred in Field Test #1 (Test1-02 – Clay embankment) and Field Test #2 (Test2C-02 – Gravel embankment). Field Test #2 demonstrated unusual behaviour by eroding through a headcut process for non-cohesive gravels; this was attributed to the effects of freezing conditions and ice in the gravel, creating a more erosion resistant material. Field Test #3 (Test1-03 – Composite embankment) demonstrated both headcut and surface erosion processes, whilst Field Test #4 (Test 2-03 – Composite embankment; initial attempts at piping failure, followed by overtopping failure) demonstrated predominantly surface erosion processes.

A similar mixture of headcut and surface erosion processes is reported in more recent laboratory based research looking at how the type and state of fill material affects the breach erosion process (Malisa et al., 2010). In particular, Malisa reports behaviour of a cohesive soil that initially shows surface erosion (referred to as 'stress detachment') and subsequently headcut (Figure 6-2). Plots of time varying erosion show the critical stage of erosion through the upstream edge of the crest occurring as surface erosion rather than headcut, for this particular soil and embankment type.

This mixture of erosion processes suggests that, for improved breach process prediction, a breach model should be capable of simulating both headcut and surface erosion processes in order to cope with structures built from a range of different material types and state; the challenge is in identifying when and why these large scale processes change as a function of soil type and state.

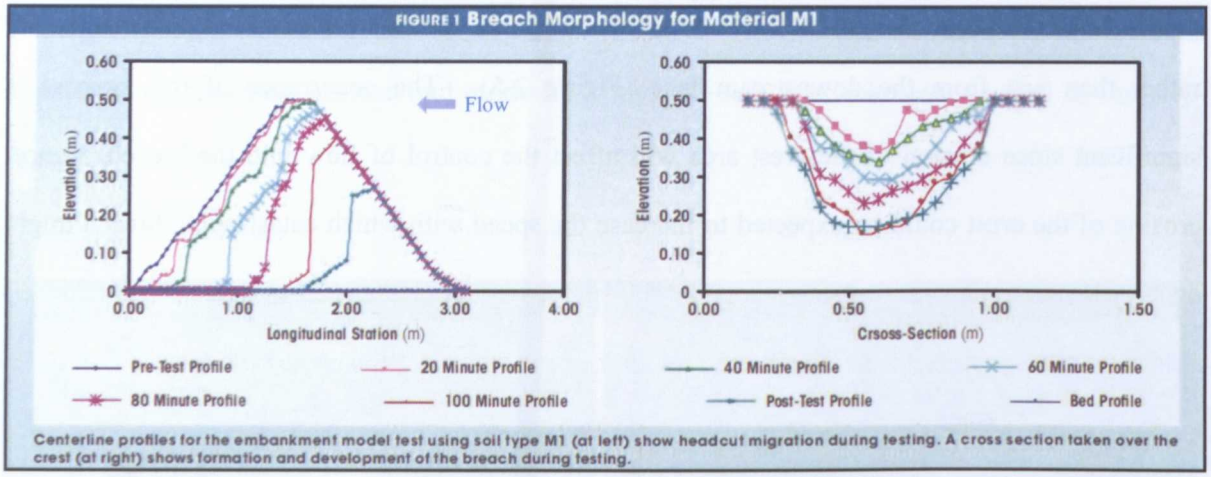

Figure 6-2 Laboratory modelling of breach (as reported by Malisa) showing mixed phases of surface and then headcut erosion (Malisa et al., 2010)

6.1.2 Breach erosion mechanisms

The processes of headcut or surface erosion are fuelled by the removal of sediment from the embankment body. This can occur via the three mechanisms listed below (de Vroeg et al., 2002, Mostafa, 2003, Mostafa et al., 2008); this is also supported by observations from the IMPACT field test data (Morris, 2009). These mechanisms comprise:

1. Sediment erosion;
2. Mass erosion;
3. Soil wasting.

Sediment erosion occurs when sediment is removed from the surface of the embankment and held in suspension by the flow. Mass erosion occurs when small lumps of soil, rather than individual particles, are removed from the embankment surface by the flow. This process is particularly affected by the structure of the soil, including any fissuring that may have occurred. Soil wasting occurs when large blocks of soil are undercut and collapse into the breach flow. These are then quickly removed via a mixture of sediment and mass erosion (Figure 6-3).

a. Sediment erosion by turbulent flow along base of breach sides

b. Mass erosion – small lumps of soil / clay being removed

c. Soil wasting – block failure on left face of breach

d. Soil wasting – block failure on left face of breach 2s after failure of block into breach (i.e. block has been removed)

Figure 6-3 Smaller scale erosion mechanisms

The process of soil wasting occurs most clearly during the breach formation stage. At the entrance to the breach the flow contracts and drops into the breach. This tends to create three flow zones, as shown in Figure 6-3a, comprising (i) a central jet of water that is relatively free from sediment and (ii) two highly erosive, elongated vortices that cut along the base of the breach sides. These vortices erode and undercut material at the breach sides until failure occurs whereby a block of soil will break away from the embankment body and either rotate into or slide into the breach. These blocks tend to crumble into smaller units as they fall into the breach and are then removed very rapidly by the high energy flow (Figure 6-3c,d). This process of breach formation and growth is very complex and dynamic. Flow processes are three dimensional and soil erosion is not in equilibrium. The flow zones and vortex erosion processes shown in Figure 6-3 can also be seen at a much larger

scale in photos of the El Guapo dam which failed in December 1999 due to spillway failure, followed by headcut erosion through the earth dam (Figure 6-4).

a. Headcut erosion back through dam after failure of the spillway (El Guapo Dam, Venezuela)

b. Vortices undercutting the breach sides just after failure of the spillway crest (El Guapo Dam, Venezuela)

Figure 6-4 Failure of the El Guapo Dam (Venezuela)

6.2 Approaches for simulating erosion

Until recently (~2005), a majority of breach models have used equilibrium sediment transport (EST) equations. This can be seen from Table 2-5 where there are frequent references, for example, to formulae such as the Meyer-Peter and Müller, Yang, Bagnold-Visser and Smart equations (Mohamed, 2002, Smart, 1984, Visser, 1998a, Yang, 1979, Yang, 1996a). The problem with the use of EST equations is that they have been developed for the long term prediction of river bed morphology rather than the prediction of short term, dynamic conditions arising from a breach. EST relationships have typically been established by studying equilibrium sediment transport conditions in a flume, where sediment is fed into and collected from a flume under steady state flow conditions in order to establish what bed load and wash load transport rate occurs for a given sediment and flow condition. This process relies upon a balance being established between sediment inflow and outflow; it is also based upon flow over a sediment bed, rather than flow through a breach where erosion may occur along the breach sides resulting in soil wasting, where a mass of sediment is injected into the flow.

Some of the problems encountered whilst investigating different sediment equations and numerical solutions for breach modelling, included:

- The need to adapt sediment transport rate to account for potential erosion of the breach sides, rather than for the bed only;
- Modelling instabilities arising from application of the transport equation to breach sections without any balancing inflow of sediment, often leading to unsustainably high rates of erosion at the first eroding flow section. (This problem could be countered by the introduction of erosion 'smoothing' for the initial erosion sections of the model);
- Uncertainty in selection of the most appropriate transport equation, given that none were truly applicable to flow conditions found in a breach.

Critically, the rate of formation of breach can be seen to be highly dependent upon soil state – for example, a highly compacted soil as compared to a loosely placed soil, will take much longer to erode. EST equations do not offer the flexibility of allowing for soil state, since the equations are based upon the soil being in flux along a river bed.

The use of erosion equations rather than EST equations for simulating erosion during breach would appear to offer a better solution that more closely represents the physical processes that occur. Unlike EST equations, erosion equations relate the rate of sediment removal to the shear stress applied by the surface flow and are applicable to non equilibrium conditions. This concept is not new, and derives from early work on sediment transport. Early research proposed a relationship between sediment size, critical shear or velocity and sediment transport (Henderson, 1966, Hjulstrom, 1935). This was extended by later researchers who started to highlight the significance of soil state on sediment transport (de Vroeg et al., 2002, Sundborg, 1956). Partheniades (Partheniades, 1965) subsequently proposed the following general relationship;

$$e = 0 \qquad \text{for } \tau < \tau_c$$

$$e = M\,[(\tau / \tau_c) - 1] \qquad \text{for } \tau \geq \tau_c \qquad (6\text{-}1)$$

Where:

e is the erosion rate for cohesive soils

τ is the effective shear stress

τ_c is the critical shear stress

M is a factor representing soil characteristics and condition

Examples of more recent use of this form of equation for breach modelling is given by Chen (Chen and Anderson, 1986) and Hanson (Hanson et al., 2005c) in the form below:

$$E = K_d b(\tau - \tau_c)^a \tag{6-2}$$

Where:

E is the erosion rate in $m^3/s/m^2$ (bulk volume hence rate of bed elevation change or retreat)

K_d is the erodibility or detachment coefficient

τ is the effective shear stress

τ_c is the critical stress

a and b are empirical coefficients dependent upon soil properties.

The use of such an erosion equation has two advantages; firstly, the equation reflects a dynamic erosion process and is not based upon steady state equilibrium conditions which clearly do not apply; secondly, the erodibility parameter, K_d, can be used to reflect variations in erosion as a function of soil state (which has been identified as an important issue for breach modelling and is impossible to do using equilibrium sediment transport equations).

The drawback to using an equation based upon an erodibility coefficient, such as K_d is the need to define a value for K_d. To date this has been undertaken through laboratory or field testing (Hanson and Cook, 2004) but there are several different methods by which this might be done and results are not yet consistent between approaches (Regazzoni et al., 2008b, Wahl, 2008a, Wahl et al., 2009).

Simple guidance on the likely range of erodibility for a given soil and state is available, but this needs to be refined in order to support breach modelling accuracy. Nevertheless, it should be recognised that the accuracy of breach prediction offered by this approach (predictive breach modelling based upon erosion equations) is far more accurate than the application of simple peak discharge equations and offers a better long term solution for model development than use of traditional sediment equations.

The recognition that erosion equations should be used in preference to equilibrium sediment transport equations means that a majority of breach models developed previously have used incorrect erosion relationships to simulate breach initiation and growth (Morris et al., 2008).

6.3 The significance of erosion behaviour and modelling approach on breach prediction

The effect of soil state and choice of modelling approach on breach prediction was investigated by the writer in relation to variations in embankment geometry. Figure 6-5 shows the assumed test layout.

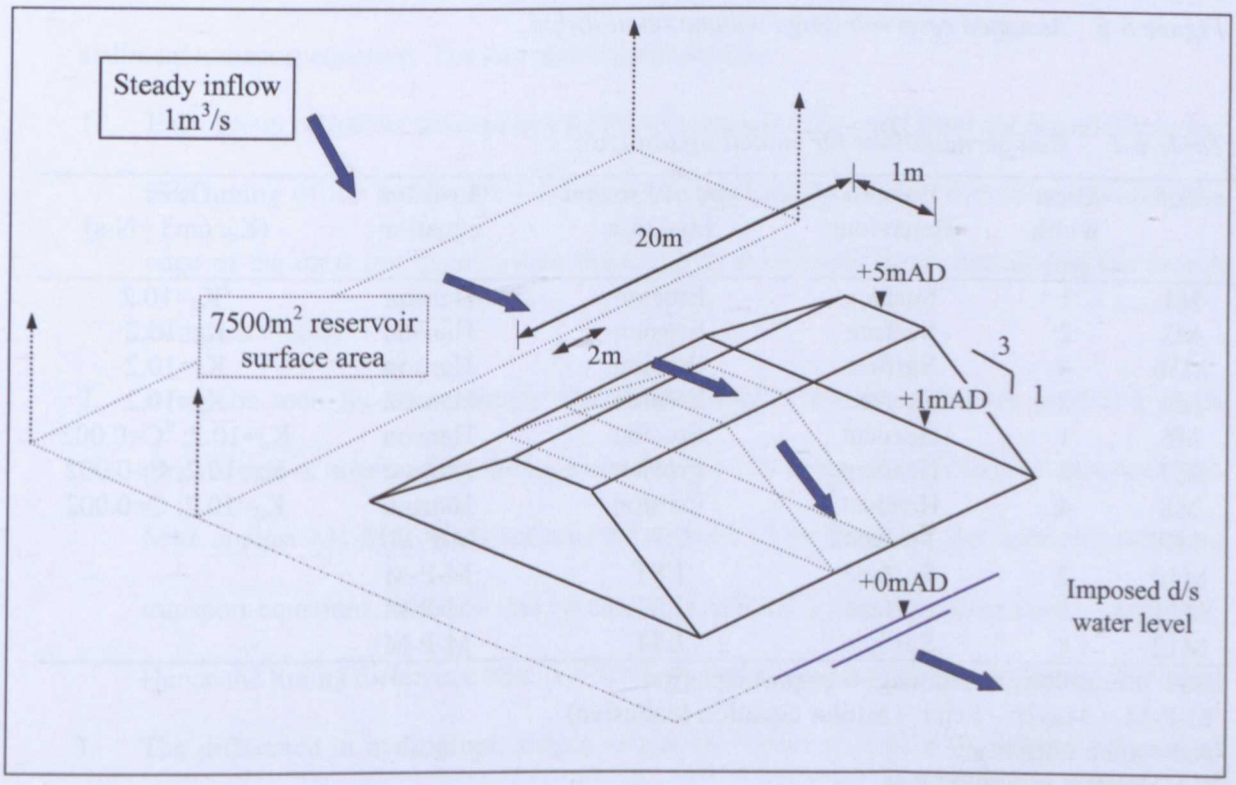

Figure 6-5 Simple embankment scenario for analysis of effect of erosion behaviour, modelling approach and embankment geometry

Table 6-1 summarises the different test conditions, namely different permutations of embankment crest geometry with different breach mechanism (erosion behaviour) and approach for modelling sediment erosion. The results (outflow hydrographs) are compared in Figure 6-7. The upstream reservoir has a constant surface area with depth of 7500m^2 resulting in the reservoir stage volume relationship shown in Figure 6-6 below.

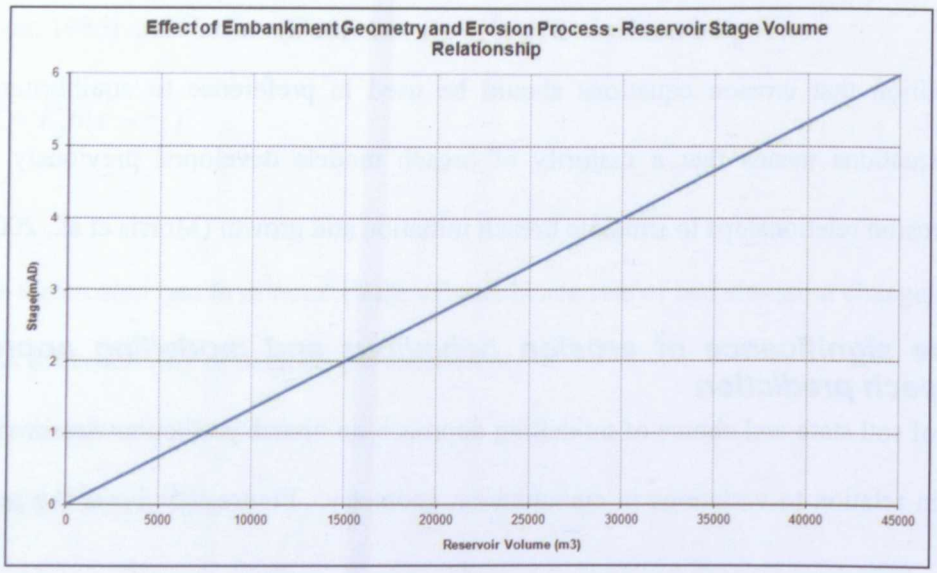

Figure 6-6 Assumed reservoir stage volume relationship

Table 6-1 Run permutations for modelling test case

Ref	Crest width (m)	Erosion Behaviour	Type of Erosion Equation	Erosion equation	Other (K_d: cm3 / N-s)
M1	1	Surface	Erosion	Hanson	[3]K_d=10.2
M2	2	Surface	Erosion	Hanson	K_d=10.2
M3b	4	Surface	Erosion	Hanson	K_d=10.2
M4	8	Surface	Erosion	Hanson	K_d=10.2
M6	1	Headcut	Erosion	Hanson	K_d=10.2; [4]C=0.002
M7	2	Headcut	Erosion	Hanson	K_d=10.2; C=0.002
M8	4	Headcut	Erosion	Hanson	K_d=10.2; C=0.002
M9	1	Surface	EST[1]	M-P-M[2]	
M10	2	Surface	EST	M-P-M	
M11	4	Surface	EST	M-P-M	
M12	8	Surface	EST	M-P-M	

[1]EST = Equilibrium sediment transport equation
[2]M-P-M = Meyer – Peter – Muller equation (cohesive)
[3]K_d = soil erodibility
[4]C = Headcut migration rate

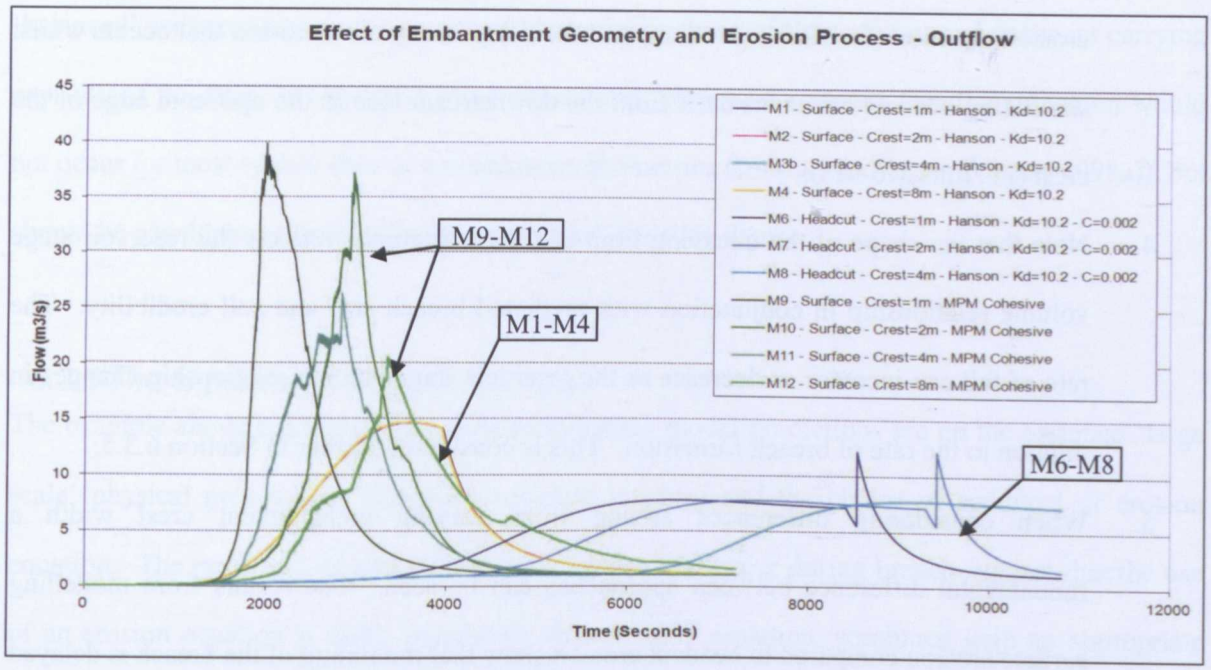

Figure 6-7 Effect of embankment geometry, erosion process and modelling approach on breach prediction

The results shown in Figure 6-7 provide an example of how the different modelling approaches affect the breach prediction. Three groups of results can be seen, labelled M1-4, M6-8 and M9-12 and representing surface erosion behaviour using a sediment erosion equation, headcut erosion behaviour using a sediment erosion equation and surface erosion behaviour using a sediment transport equation. The key differences are that:

1. Each group of results clusters in a different area and with a different characteristic shape. The timing of the results are a function of how quickly erosion occurs at the upstream edge of the crest (the point where breach flow is typically controlled during the breach initiation stage);
2. It can be seen for this example that the sediment transport equations predict a much quicker rate of erosion than the erosion equation (i.e. comparing surface erosion runs M9-M12 against M1-M4). This reflects the in built assumption of soil state for sediment transport equations, whereas this parameter is defined by K_d within the erosion equation. Hence the timing difference here is a function of the assumed parameters for the test case;
3. The difference in hydrograph shapes reflect the rapid onset of crest erosion for surface erosion using the sediment transport equation, the slower rate of crest erosion using the

erosion equation (for surface erosion) and the delay in any crest erosion that occurs whilst simulating headcut advances back from the downstream face to the upstream edge of the crest (i.e. runs M6-M8);

4. Note that the shape of the decaying limb of the hydrographs reflects the reservoir stage volume relationship in conjunction with predicted breach size and soil erodibility. The rate of fall can increase or decrease as the reservoir stage volume relationship changes in relation to the rate of breach formation. This is considered further in Section 6.3.5;
5. When considering differences arising from varying embankment crest width a fundamental difference between approaches can be seen. The results from modelling surface erosion compared to headcut erosion show that the timing of the breach is delayed as the crest width widens for headcut, but not significantly for surface erosion. This is because the surface erosion process occurs rapidly and across all areas of the embankment, including the crest, whilst the headcut process starts on the downstream face of the embankment and cuts back through the embankment. Breach formation only occurs once the upstream edge of the crest area starts to erode, so allowing flow through the breach to increase.

Point 5 above reflects the fact that the application of a sediment erosion equation in surface erosion mode, neglects continuity of sediment. This is acceptable for a breach where the flow path into and through the breach is relatively short, and sediment is "instantly" removed. However, as the embankment crest width increases, say tending to infinity, it is physically inconsistent that no change in the rate of breach initiation occurs. An example of this breaching situation could be where a landslide into a valley has created a very wide blockage to flow. In this situation, where surface erosion occurs, a process tending towards equilibrium sediment transport will probably develop. Whilst the flow energy through an undrowned dam or embankment breach is sufficient to remove large blocks of sediment "instantly", this could not be sustained continuously over an indefinite length and sediment would eventually be dropped by the flow, or the flow would have insufficient energy to move it. Identifying the point where the transition between rapid erosion and

'balanced' sediment transport occurs would require analysis of flow energy and sediment carrying capacity of the flow, but physical observations and judgement suggests that this transition would not occur for most typical dam or embankment geometries (contrary to Visser (Visser, 1998a)), but should be considered carefully for the analysis of landslide dams.

6.3.1 The significance of soil erodibility

The example above highlights how dependent breach model predictions are on the assumed 'large scale' physical process (i.e. headcut or surface erosion) and the choice of sediment or erosion equation. The rapid and dynamic physical processes that occur during breach suggest that the use of an erosion equation is more appropriate than an EST equation, combined with an appropriate representation of the physical processes to replicate either headcut or surface erosion. However, in using an erosion equation (for example, Equation 6-2), it is necessary to define a value for K_d which reflects the embankment soil in the conditions that would occur during the breaching process. Depending upon the soil and speed of breach, K_d might also vary with time (although this is not considered further within this thesis). The dependence, and hence importance of defining K_d as accurately as possible is shown in Figure 6-8.

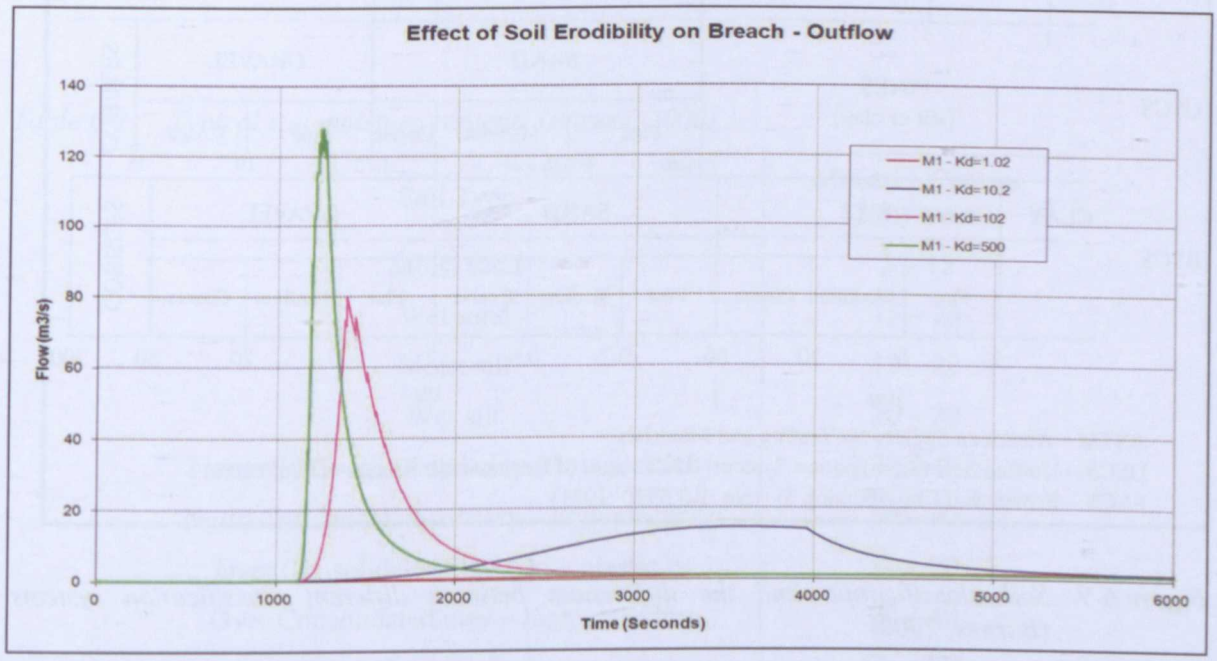

Figure 6-8 Effect of different soil erodibility on breach growth

The results in Figure 6-8 show outflow hydrographs for four different breach simulations, made using the test setup shown in Figure 6-5. Four different soil erodibility values are used – 1.02, 10.2, 102 and 500cm^3/N-s. The runs use the same setup / soil parameters (except for varying K_d) as run M1 in Table 6-1 and Figure 6-7. The impact on breach rate and hence outflow hydrograph is very significant. Hence it is important to limit the uncertainty associated with erodibility prediction.

6.3.2 Defining and describing soil erodibility

In order to relate the breach model prediction to specific field measurements and to construction design specifications, it is necessary to be able to define and describe erodibility, ideally through the use of easily measurable parameters. The basic classification of soils varies subtly from country to country. Figure 6-9 shows how three different soil classification systems compare. Figure 6-10 shows how a soil can be represented on a 'soil triangle'. The soil triangle maps different descriptions of soil type to different component percentages of clay, silt and sand.

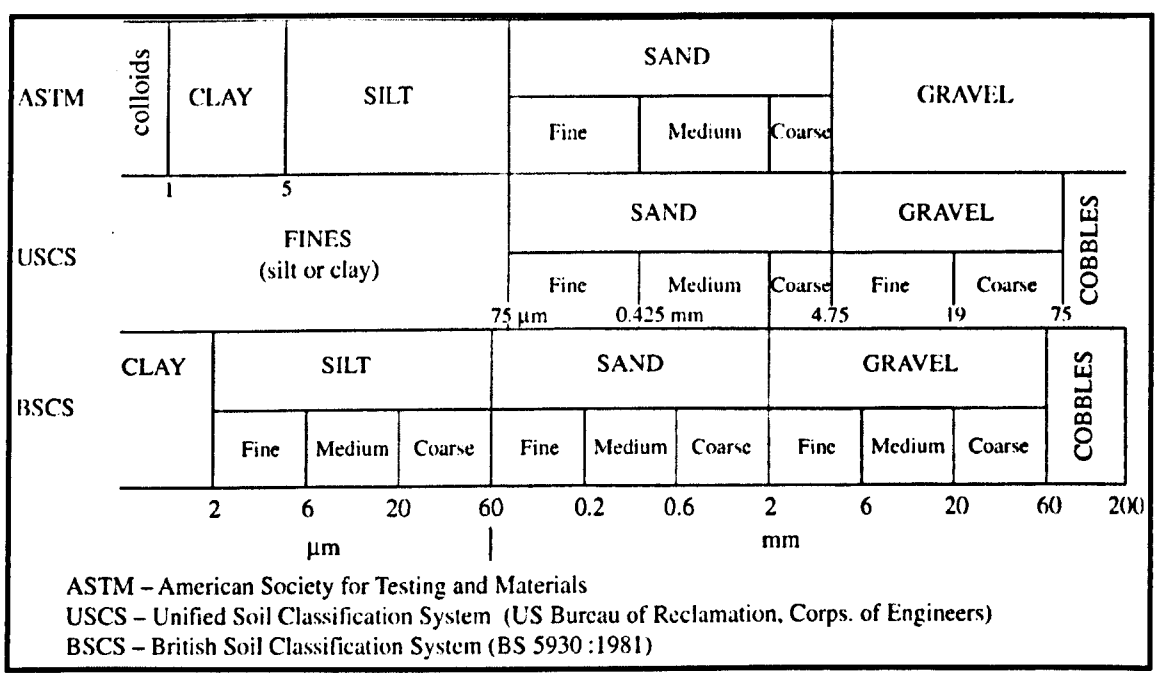

Figure 6-9 Soil classification and the differences between different classification systems (Barnes, 2000)

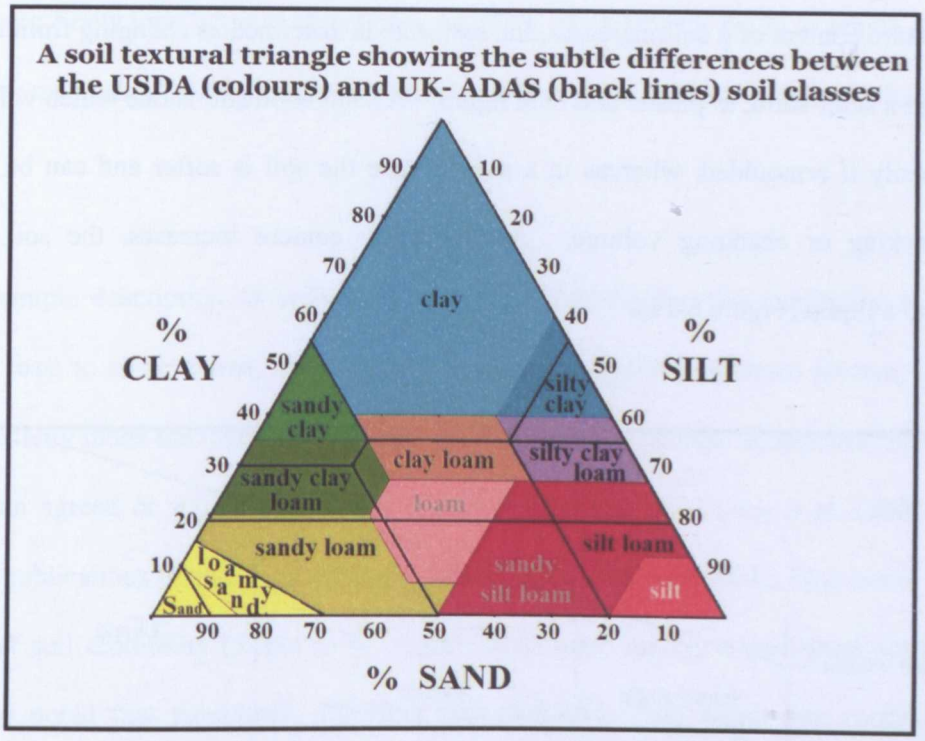

Figure 6-10 Soil textural triangle

Soils containing silts and clay can have the properties of plasticity and cohesiveness. The degree of these properties depends upon the mineralogy of the clay and the moisture content of the soil. Typical soil moisture contents (ratio of mass of soil to mass of water) for different soil types are listed in Table 6-2.

Table 6-2 Typical soil moisture contents (Barnes, 2000)

Soil Type	Moisture Content % (by mass)
Moist sand	5 – 15
Wet sand	15 – 25
Moist silt	10 – 20
Wet silt	20 – 30
Normally Consolidated clay – low plasticity	20 – 40
Normally Consolidated clay – high plasticity	50 – 90
Over Consolidated clay – low plasticity	10 – 20
Over Consolidated clay – high plasticity	20 – 40
Organic clay	50 – 200
Extremely high plasticity clay	100 – 200
Peats	100 - >1000

As the moisture content of a soil increases, the soil state is described as changing from a solid (dry soil) through a semi-solid, to plastic and then liquid. A semi solid soil is one which will crack and break up easily if remoulded, whereas in a plastic state the soil is softer and can be remoulded without cracking or changing volume. As the water content increases, the soil eventually transitions to a liquid (Figure 6-11).

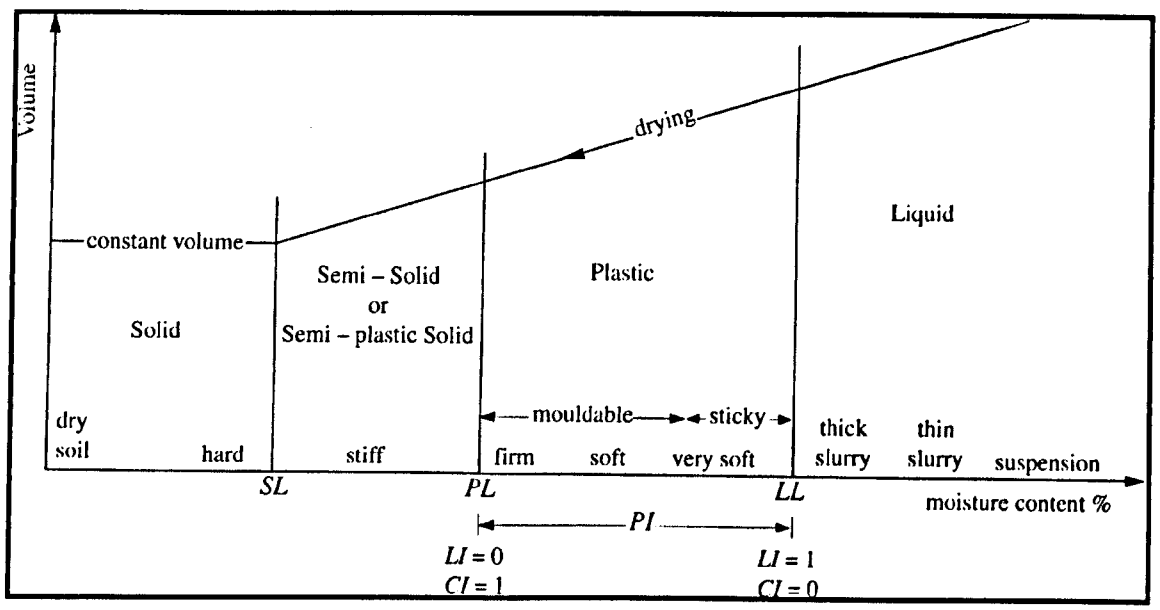

Figure 6-11 Transition between soil states – consistency limits (Barnes, 2000)

The limits between different consistencies are defined as the liquid limit (LL), plastic limit (PL) and the shrinkage limit (SL). These (Atterberg) limits provide useful descriptors for the soil type and state, such as the Plasticity Index (PI) and Activity, as defined below:

$$PI = LL - PL \tag{6-3}$$

$$Activity = \frac{PI}{C\%} \tag{6-4}$$

Where

PI = Plasticity index
LL = Liquid limit
PL = plastic limit
C% = Percentage clay content

The Atterberg limits may be used to create a plasticity chart (Figure 6-12) to which different soil types can be mapped. Clays (marked C) typically sit above the Activity Line and silts (marked M) sit below.

From the simple description of soils given above, it follows that the erodibility of a soil will depend, at least to some extent, upon the soil state and hence the moisture content. Descriptors such as plasticity index are therefore also likely to influence erodibility. In practice, however, there is not yet an agreed or simple description of soil erodibility. de Vroeg et al. (2002) reviews a number of publications on this topic dating from the 1980s and identified a long list of factors that might affect soil erodibility (Table 6-3). Conclusions were mainly drawn from work by Kruse (1996) who noted that parameters affecting soil erodibility "are many and complex and that literature is often not unambiguous about the effects".

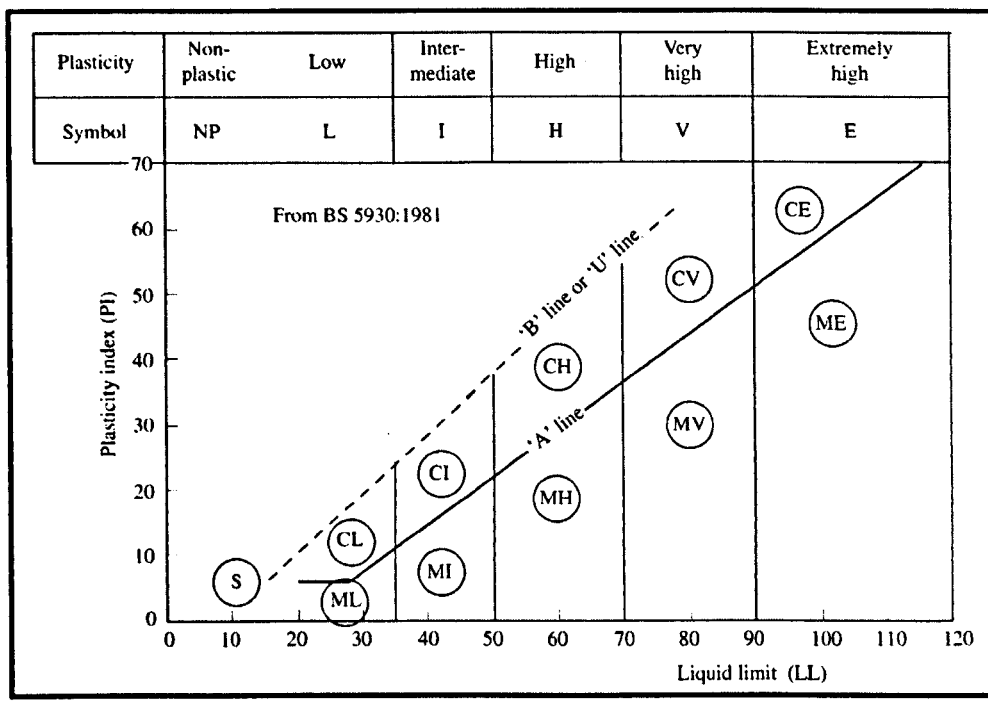

Figure 6-12 Plasticity chart (Barnes, 2000)

Table 6-3 Factors affecting soil erodibility

Factors affecting soil erodibility (de Vroeg et al., 2002)		
• Soil structure	• Initial salt content of pore water	• Other elements (Fe, Al)
• Soil density	• Salt content of eroding water	• Temperature (for fresh water)
• Clay silt sand percentage	• Na+ content	• Roots
• Moisture content of soil	• Lime content	• Rabbit burrows
• Type of clay minerals	• Organic content	• In-homogeneities (such as sand layers parallel to slope)

De Vroeg also noted that other factors commonly listed include hydraulic stress, plasticity index, dispersion / SAR, cementation, slaking and permeability. However, de Vroeg also concluded that some factors could be identified as more significant than others. These include:

- Soil structure;
- Density;
- Clay content;
- Water content.

In particular, the soil structure affects the way in which mass erosion might occur. Where the structure comprises fine or large fissuring, this can also allow rapid ingress of water, which in turn can affect the soil erodibility (de Vroeg et al., 2002). This is consistent with observations by Marsland and Cooling (1958) following the 1953 north sea storm surge which resulted in numerous coastal embankment breaches along the east coast of England.

Later work by Hanson (2007) reiterates these potential links. Temple and Hanson have undertaken programmes of research into soil and vegetation performance at the USDA Agricultural Research Service centre in Stillwater, Oklahoma, US. As part of this work they have produced some indicative and qualitative descriptions of soil erodibility, as shown in Equation 6-5 and Table 6-4 and Table 6-5 below. Equation 6-5 provides an approximate method for estimating erodibility (K_d) based upon percentage clay content and soil density (Temple and Hanson, 1994).

$$K_d = \frac{10\gamma_w}{\gamma_d} \exp\left[-0.121(C\%)^{0.406}\left(\frac{\gamma_d}{\gamma_w}\right)^{3.10}\right] \quad (6\text{-}5)$$

Where:

K_d - erosion rate in units of [(cm^3/N-s)]
$C_\%$ - percent clay
γ_d - dry unit weight in Mg/m^3
γ_w - unit weight of water in Mg/m^3

Equation 6-6 (Hanson, 2007) provides an (unpublished) indicative equation relating K_d to compaction energy and moisture content of the soil

$$k_d = 8.11x10^9 E_c^{-0.5} WC\%^{-7.0} \quad (6\text{-}6)$$

Where

K_d - erosion rate in units of [ft/hr/(lb/ft^2)]
E_c = compaction effort [ft-lb/ft^3]
WC% = compaction water content per cent

When using Equation 6-2, a value of τ_c is also required. An approximation is to assume that τ_c=0 or to use Equation 6-7 (Hanson and Simon, 2001, Hanson and Hunt, 2007).

$$K_d = 0.2\tau_c^{-0.5} \quad (6\text{-}7)$$

Where

K_d - erosion rate	(cm^3/N-s)
τ_c - critical shear strength	(Pa)

Given the uncertainty associated with a clear description and measure of erodibility, an alternative approach is to adopt qualitative descriptions of erodibility and to allow for this uncertainty when considering modelling results. Table 6-4 and Table 6-5 (Hanson, 2007) provide examples of such qualitative descriptions.

Table 6-4 Qualitative descriptions of values for K_d

Qualitative description of values for K_d (modified from (Hanson, 2007)		
K_d (ft/h)/(lb/ft^2)	**Description**	**K_d** (cm^3/N-s)
> 10	Extremely Erodible	> 18
1 - 10	Very Erodible	1.8 - 18
0.1 – 1	Moderately Erodible	0.18 – 1.8
0.01 – 0.1	Moderately Resistant	0.018 – 0.18
0.001 – 0.001	Very Resistant	0.0018 – 0.0018
< 0.001	Extremely Resistant	< 0.0018

Table 6-5 Factors affecting soil erodibility(Hanson, 2007)

% Clay	Well Compacted (ft/h)/(lb/ft^2)		Poorly Compacted (ft/h)/(lb/ft^2)	
	At Optimum Moisture Content	Dry of Optimum Moisture Content	At Optimum Moisture Content	Dry of Optimum Moisture Content
	K_d	K_d	K_d	K_d
>25	0.1	1	1	10
10 – 25	0.5	5	5	20
5 – 10	2	10	10	50
0 - 5	10	20	20	100

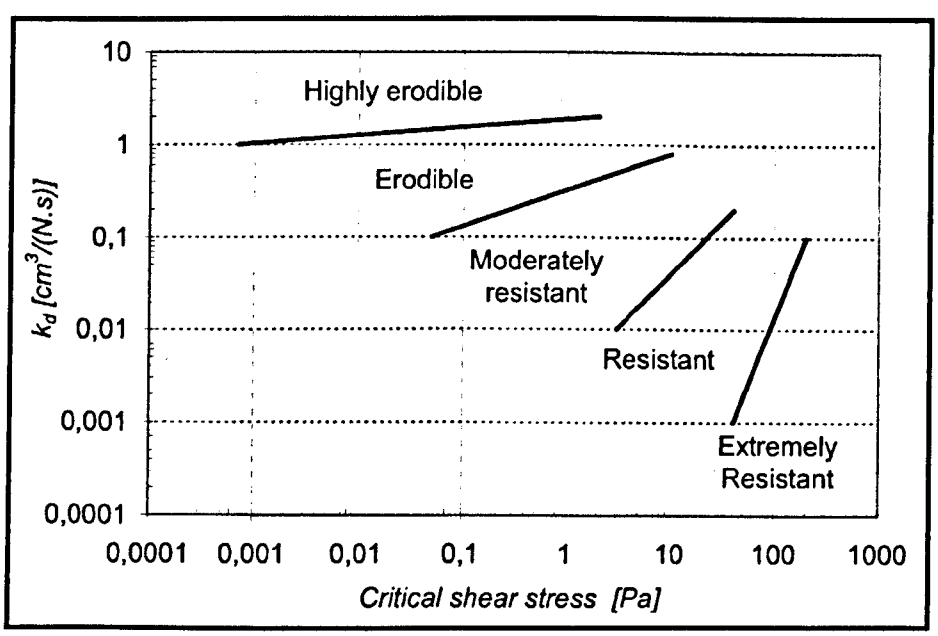

Figure 6-13 Erodibility of soil (Hanson and Simon, 2001)

Embankment Test	Soil Classification[1]	Sand[1] > 75μm (%)	Fines[1] > 2μm (%)	Fines[1] < 2μm (%)	PI[2]
P1	SM	64	29	7	NP
P4	CL	25	49	26	17

Note: Based on ASTM : [1]D 2487, [2]D 4318.

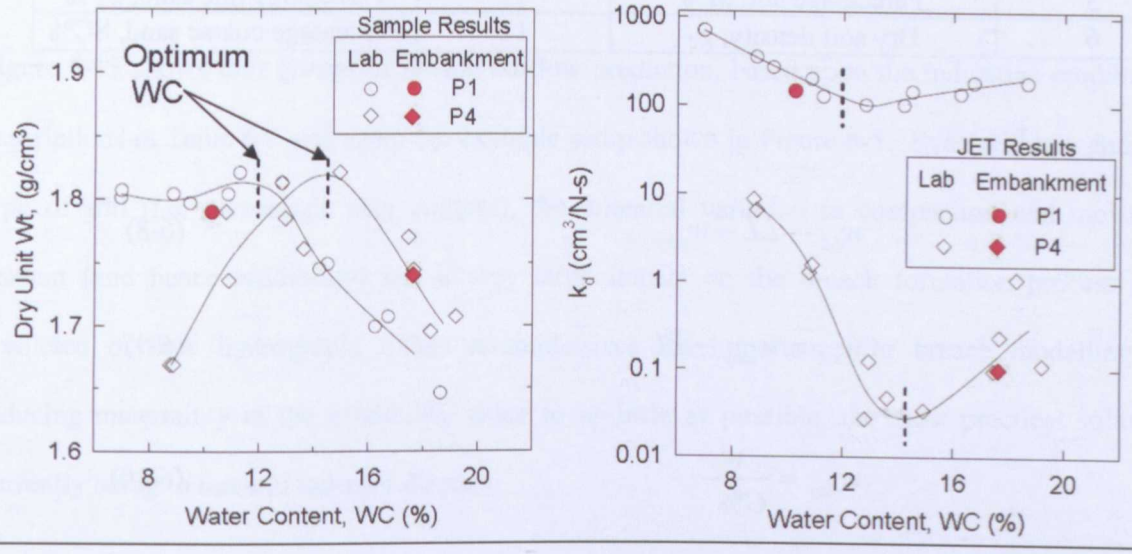

Figure 6-14 Example analyses showing relationship between soil erodibility (K_d) and soil type, density and water content (Hanson et al., 2010)

The variation in K_d shown in Figure 6-14 is similar to the range of K_d values listed in Table 6-5 by Hanson (2007). This shows that a small change in moisture content can give rise to large changes in the value of soil erodibility. Similar findings were reported by Regazzoni (Regazzoni et al., 2008a). [Note that within Figure 6-14 the soil classification terms relate to the Unified Soil Classification System (USCS) (ASTM, 2011), where SM = silty sand and CL = clay. The reference to ASTM relates to codes D2487 and D4318 under the American Society for Testing and Materials (ASTM International, 2013)].

However, more recent research by Regazzoni (Regazzoni, 2009) includes a statistical analysis of parameters affecting erodibility. Regazzoni looked at the influence of 12 variables on soil erodibility. By undertaking principal component analysis (PCA) (Wikipedia Contributors, 2011c) these were reduced to the main contributors. The original 12 variables are listed in Table 6-6 below:

Table 6-6 Potential parameters affecting soil erodibility (Regazzoni, 2009)

Parameter No	Parameter	Parameter No	Parameter
1	w_{LL}	7	Degree of saturation, S_r
2	w_{PL}	8	Degree of compaction, c%
3	w_{clay}	9	$Log(S_c,\rho_d)$
4	Percentage clay, C%	10	Moisture content, w%
5	Percentage silt, M%	11	Percentage fine sand, SF%
6	Dry soil density, ρ_d	12	Percentage coarse sand, SC%

Where:

$$w_{LL} = LL - w_{clay} \tag{6-8}$$

$$w_{PL} = w_{clay} - PL \tag{6-9}$$

$$w_{clay} = \frac{w}{C\%} \tag{6-10}$$

Regazzoni develops relationships between soil parameters and erodibility for soils in general (Equation 6-11), soils excluding dispersive clays (equation 6-12) and soils including dispersive clays (Equation 6-13). The linear correlation factor (R^2) for each of these equations was found to be 0.35, 0.81 and 0.62 respectively. It is notable that the correlation excluding dispersive soils is significantly better than those including dispersive soils. The work by Hanson tends to focus on soil density and moisture content rather than soil chemistry; both would appear to have a significant impact on soil erodibility and advancing knowledge in either field will help improve the accuracy of breach models using the soil erodibility parameter.

$$I_\alpha = -0.97 + 0.47w_{LL} - 0.37c + 5.41S_r \tag{6-11}$$

$$I_\alpha = -1.36 + 8.69w_{LL} + 2.68c + 2.08S_r \tag{6-12}$$

$$\begin{aligned} I_\alpha &= -0.665 + 0.166C\% + 0.138M\% \\ &- 1.971w_{LL} - 8x10^{-3}w_{clay} \\ &- 5.645\log(S_d) + 34.237w \\ &+ 34.996c - 3.877S_r \end{aligned} \tag{6-13}$$

The indicative methods of Hanson plus the equations developed by Regazzoni now provide the breach modeller with a means of estimating soil erodibility based upon soil type or specific soil parameters. Where greater certainty is required, however, these equations should not replace physical testing of soil samples.

Figure 6-15 shows four groups of breach outflow prediction, based upon the indicative erodibility descriptions in Table 6-5 and using the example setup shown in Figure 6-5. Even within a defined type of soil (i.e. percentage clay content), the potential variation in compaction and moisture content (and hence erodibility) has a very large impact on the breach formation process and predicted outflow hydrograph. This re-emphasizes the importance for breach modelling of reducing uncertainty in the erodibility value to as little as possible; the most practical solution currently being to test soil samples directly.

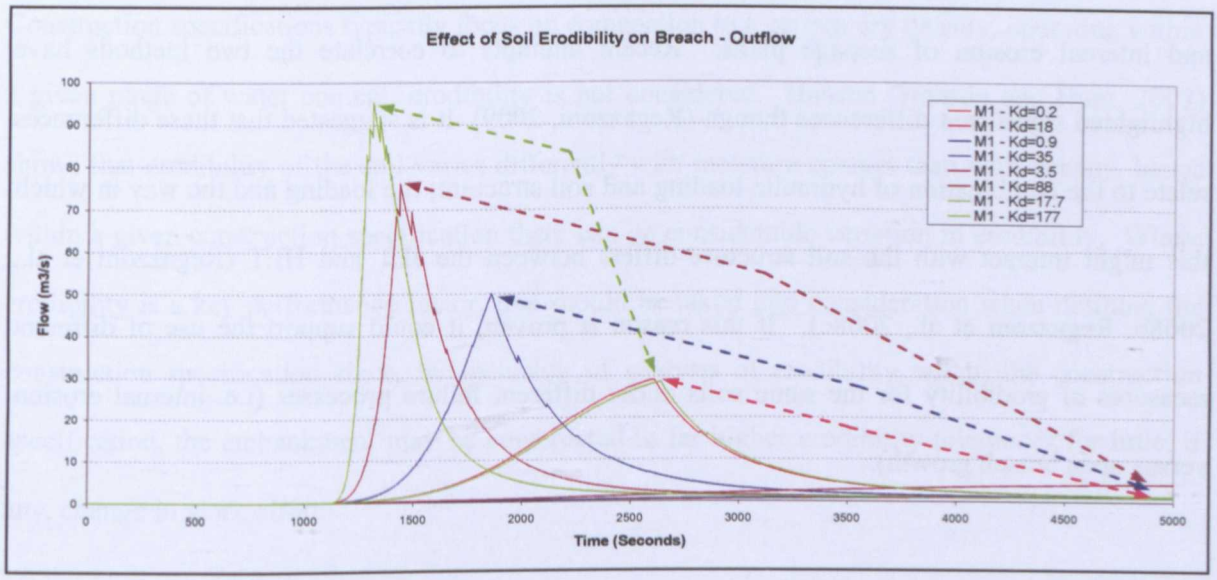

Figure 6-15 Indicative range of breach outflow uncertainty arising from the use of qualitative descriptions of erodibility

Research into the physical processes and prediction of internal erosion through dams and embankments has also found similar conclusions, identifying the rate of internal erosion growth as highly dependent upon soil erodibility (Hanson et al., 2010). For internal erosion, Equation 6-2 can be written as Equation 6-14:

$$E_t = C_e(\tau_e - \tau_c)^a \qquad (6\text{-}14)$$

Where:

C_e is the detachment / erodibility coefficient (s/m) [$C_e = K_d/\rho$; ρ = dry density (kg/m^3)]

τ_e is the effective shear stress (N/m^2)

τ_c is the critical shear stress (N/m^2)

a is a dimensionless exponent (assumed =1 in this form of equation)

Direct laboratory and field measurement of soil erodibility has been developed by various researchers using different forms of equipment. The two most popular approaches are to use the jet erosion test (JET) developed by Hanson (Hanson and Cook, 2004) and the hole erosion test (HET) developed by Wan and Fell (Wan and Fell, 2004). The difference in approaches (JET applying a water jet to a soil sample; HET applying a flow of water through a hole in a sample) directly reflects the physical processes seen within their respective research areas of open breach formation and internal erosion of seepage paths. Recent attempts to correlate the two methods have highlighted significant differences though (Regazzoni, 2009). It is suggested that these differences relate to the combination of hydraulic loading and soil structure; the loading and the way in which this might interact with the soil structure differs between the JET and HET (Regazzoni et al., 2008b, Regazzoni et al., 2008c). If this reason is proven, it could support the use of different measures of erodibility for the same soils under different failure processes (i.e. internal erosion versus open breach growth).

6.3.3 The significance of soil state in relation to erodibility

Soil type and state dictate the soil erodibility and Table 6-3 lists different parameters suspected of having varying degrees of influence. Soil state can either result through natural processes or as a result of construction. In either case, there will also be uncertainties associated with the homogeneity of the soil. This may take the form of natural variations or arise from differing levels of construction quality. These local variations in soil erodibility can provide points at which soil erosion may initiate and subsequently provide the focus for breach formation. As such, the

performance of the embankment as a whole is dependent upon these potential variations in soil erodibility.

The effect of varying compaction energy with soil moisture content for constructing an embankment can significantly alter the properties of that structure. Soil parameters such as volume, strength, flexibility, permeability and crucially, erodibility, are all influenced. A strong correlation between maximum soil density (for a given moisture content and compaction energy) and minimum soil erodibility can be seen (Figure 6-14). The range of interest relates to a few percentage point changes either side of optimum moisture content. The effect on erodibility is greater for a reduction in moisture content relative to optimum – potentially orders of magnitude increase in erodibility for a 2-3% reduction in moisture content (Burns, 2006, Hanson et al., 2010). Increasing content has a slower rate of impact on erodibility.

Construction specifications typically focus on compaction to a certain dry density, operating within a given range of water content; erodibility is not considered. Hanson (Hanson and Hunt, 2007) shows that erodibility of the soil varies differently with moisture content than with density, hence within a given construction specification there can be considerable variation in erodibility. Where erodibility is a key performance factor, this should be taken into consideration when defining the construction specification since, by inclusion of analysis of erodibility within the construction specification, the embankment may be constructed to far higher erodibility tolerances for little, if any, change in work effort.

6.3.4 Discrete block failure simulation

Analysis of breach formation processes (Morris, 2009) clearly shows that erosion within the breach occurs through aggressive undercutting of the breach sides, failure of soil blocks into the breach and their subsequent removal by the highly turbulent flow. This process is clearly an important part of the physical breaching process and Mohamed (2002) introduced this as part of his model. Whilst Mohamed confirmed the importance of including this process within the model, he did not

investigate in detail the significance of this in terms of modelling accuracy and the optimum degree of resolution for modelling. This has now been investigated further, with findings outlined below.

6.3.4.1 Current approach

Mohamed (Mohamed, 2002) considered the stability of the breach sides for each individual cross section within the model (see Appendix 1; Figure A1-1 to Figure A1-11). This means that the analysis for the stability of each section is independent of those adjacent. In reality the process is 3 dimensional and the impact of this simplifying assumption is unclear, hence analysis was undertaken.

6.3.4.2 Analysis and revised approach

Observations of block failure show that blocks tend to fail either throughout the entire length of the eroding section or 'regionally' associated with the crest area or up or downstream slope areas. To assess the sensitivity of the model to the simplified (2D) analysis, a model version that allowed analysis by zone was developed (Figure 6-16). Three failure zones were considered; the upstream slope, crest and downstream slope areas.

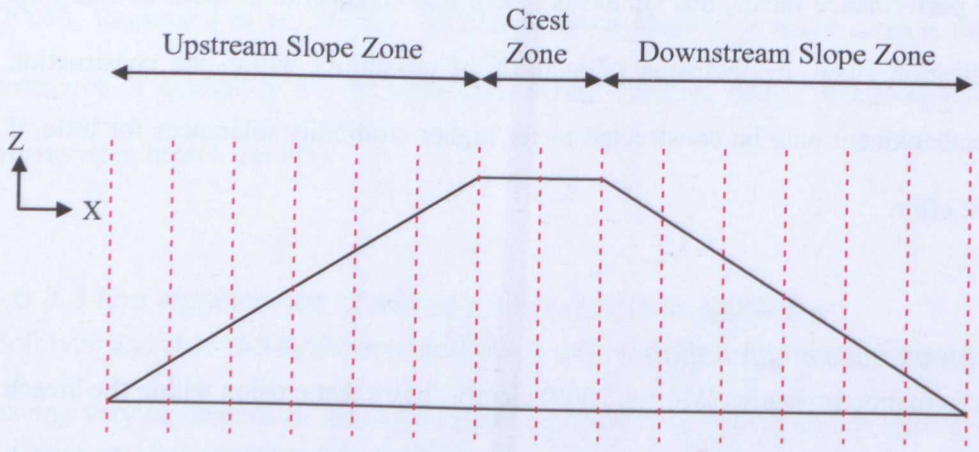

Figure 6-16 Model zoning for block failure stability analysis

Zone analysis was implemented by introducing an additional modelling parameter to define the percentage of sections (within a chosen zone) for which the failure condition should be exceeded

before assuming that all sections within that particular zone had failed. For example, by defining this condition as 40% for the upstream zone, this meant that the model would analyse the failure condition section by section (as before) but not allow any section slope failure to occur until more than 40% of the individual sections in that zone had exceeded their failure condition. At this point, all sections in that zone would be considered to have failed, representing failure of a block covering that zone, and the breach profile would be updated.

6.3.4.3 *Findings*

Initial results from this analysis were far less conclusive than expected and prompted closer consideration of the physical and modelling processes. Figure 6-17, Figure 6-18 and Figure 6-19 show initial results for a range of soil erodibility, macro instability and erosion mechanisms. The tests were undertaken using the modelling example detailed in Section 6.3 above. Figure 6-17 shows breach predictions for 3 different magnitudes of erodibility (K_d). Macro failure mechanisms ranging from 0% (i.e. section by section) to 100% (i.e. all sections must fail before block area is deemed to have failed) were considered. Whilst the characteristics of the breach outflow hydrograph change with the value of K_d, little variation was seen as a result of % macro instability analysis. Figure 6-18 shows results for one test case, but with different erosion processes enabled. The four plots relate to erosion assuming (i) sediment erosion plus block failure through shear failure plus block failure through rotational failure; (ii) sediment erosion only; (iii) sediment erosion plus shear failure only; (iv) sediment erosion plus rotational failure only. Again, it can be seen that the difference between runs is small (for this example). On the assumption that the range within which the macro failure rules might affect results would be between simulations created using only sediment erosion and sediment plus all block failure processes, Figure 6-19 shows this range for the three different soil erodibility values. This shows only small envelopes for each K_d run result within which the macro instability rules could have any effect.

These results appear to contradict the suggestion by Mohamed (2002) that it was important to include simulation of block failure within the breach model. Personal communication with Mohamed confirmed, however, that he originally simulated conditions that showed significant value to the breach modelling results from inclusion of the block failure process. However, the specific model simulation files that were created to demonstrate this point are no longer available for review.

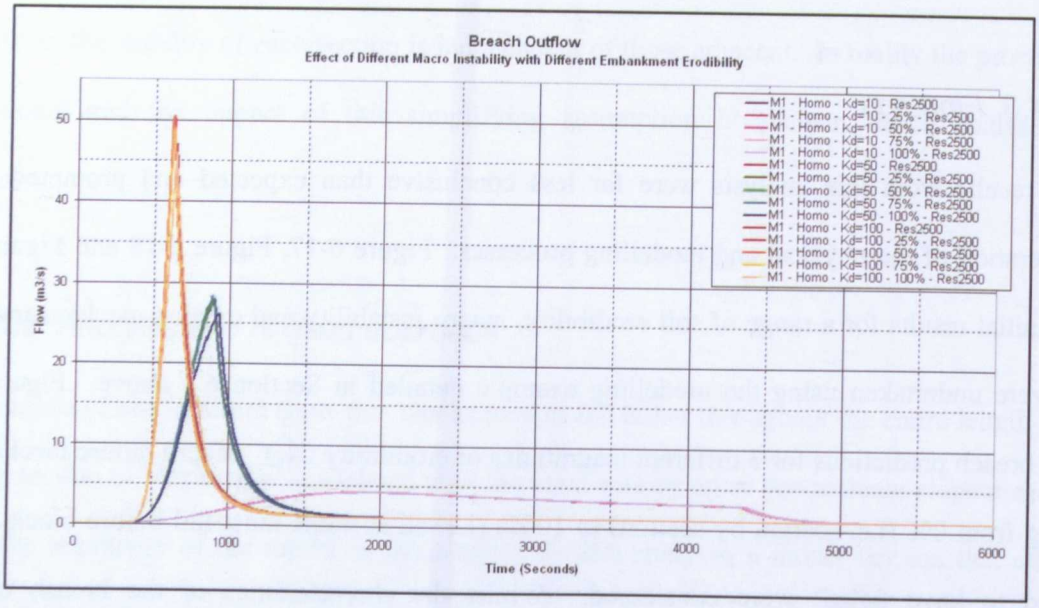

Figure 6-17 Variation in breach outflow with different soil erodibility and macro instability

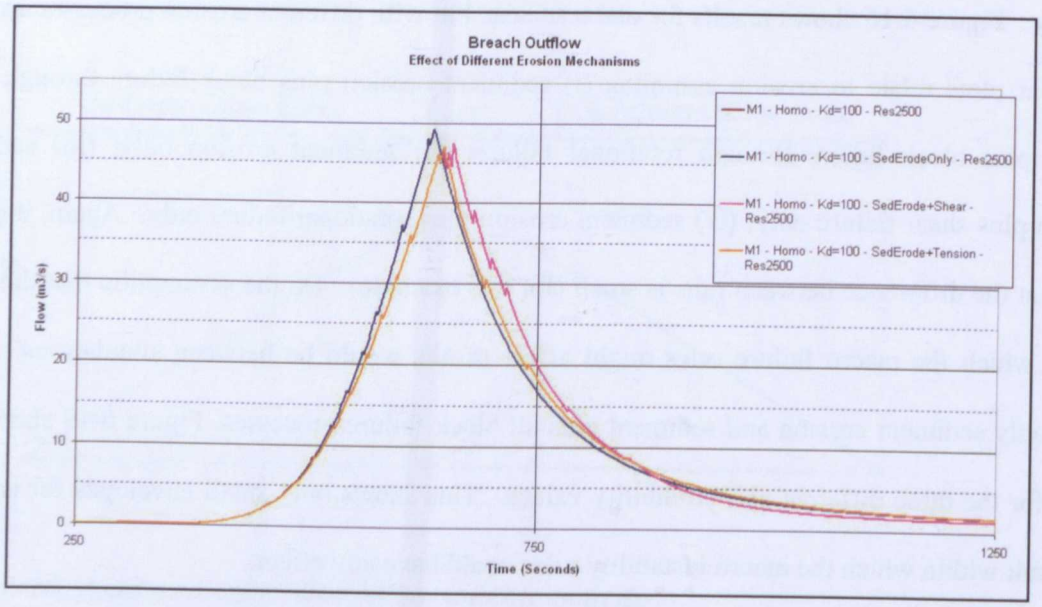

Figure 6-18 Variation in breach outflow with different erosion mechanisms

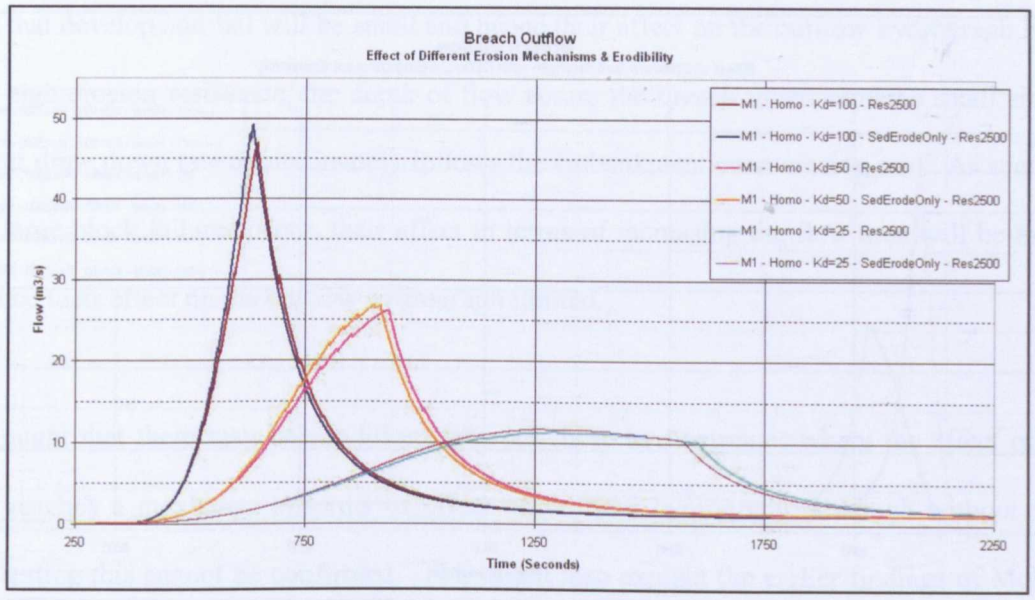

Figure 6-19 Variation in breach outflow with different erosion mechanisms and erodibility

Further analysis of the macro instability problem was undertaken to try and resolve these apparently inconsistent findings. The breach side slope stability analysis uses Equations A1.4, A1.5 and A1.6 (See Appendix 1). A range of values for the various strength parameters required within these equations were identified by reviewing typical soil parameter ranges. These are summarised in Table 6-7. Modelling results using this data for a range of erodibility values are shown in Figure 6-20.

Table 6-7 Extreme range of parameters assumed for macro instability analysis

	Base Run	Min Strength	Max Strength	Extreme Max
D50 (mm)	0.156	0.156	0.156	0.156
Bulk unit weight (KN/m^3)	16.8	16.8	16.8	16.8
Cohesion (KN/m^2)	10	5	50	100
Tensile strength (KN/m^2)	1	0.1	5	10
Internal angle friction (Degrees)	25°	20°	10°	40°

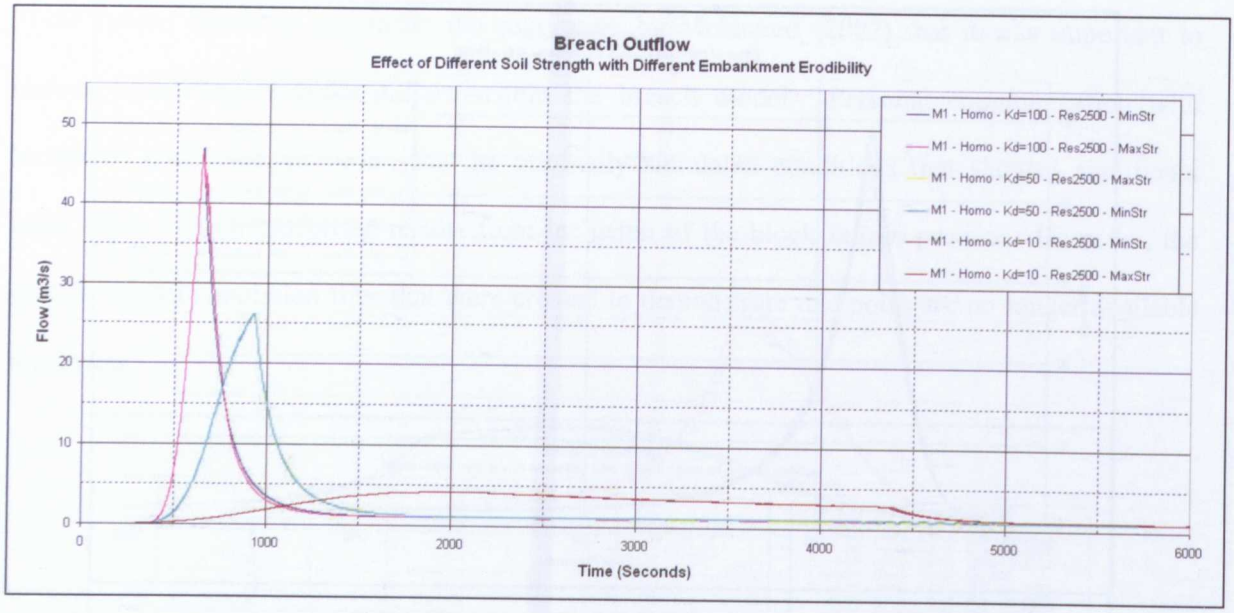

Figure 6-20 Effect of different soil strength parameters on breach prediction for different soil erodibility

The results in Figure 6-20 again suggest that there is only a small range for variation in model predictions as a result of macro instability analysis.

Further investigations into macro stability analysis were not undertaken and the issue of why the original analysis by Mohamed showed significant dependency upon block failure, yet recent model testing shows limited dependency, remains unresolved. However, it is suggested that the degree of dependency is likely to arise from the combination of reservoir stage-area and soil erodibility. Figure 6-20 shows two distinct hydrograph shapes, related to the value of K_d and assumed reservoir size. It can be seen that for a high K_d value, the breach hydrograph is rapid and peaked. This corresponds to the rapid erosion of a highly erodible material, leading to catastrophic breach failure. The hydrograph relating to the low K_d value shows a long, slow erosion process, with an almost steady, but prolonged discharge associated with the failure process. This corresponds to the slow erosion of an erosion resistant material, whereby the reservoir drawdown follows the slow erosion of the embankment crest, resulting is a near steady depth of flow across the breach and hence near steady discharge. If each of these physical conditions is considered, it can perhaps be seen why macro instability analysis has only a limited affect. Under high erodibility conditions, the speed with which normal erosion takes place and the instability of the soil means that any

blocks that develop and fail will be small and hence their affect on the outflow hydrograph limited. Under high erosion resistance, the depth of flow across the breach invert remains small since the reservoir draw down rate approximately follows the embankment crest erosion rate. As such, even where large block failures occur, their effect in terms of increasing the flow area will be minimal and hence their effect on the outflow hydrograph limited.

It is thought that there may be conditions between these two extremes where the effect of block failure reaches a maximum in terms of effect on outflow hydrograph, although without further model testing this cannot be confirmed. This might also explain the earlier findings of Mohamed (2002) who suggested significant value in including the breach block failure process. Further analysis was not undertaken during this study, hence this area requires further investigation.

6.3.5 Implications of reservoir geometry and soil erodibility on breach formation

The previous sections describe two physical conditions resulting in the significantly different breach outflow hydrographs shown in Figure 6-20. A closer look at these processes was undertaken in order to understand why breach results could vary so significantly between different test case conditions.

The two extremes of breach formation appear to comprise the cases where (i) the breach develops very rapidly and before the reservoir (or upstream hydraulic load) has a chance to really respond (i.e. to drain down) and (ii) where the breach formation process is so slow, that the upstream reservoir has ample time to respond, by drawing down as the breach develops. By considering the physical processes involved, it can be suggested that:

$$T_b \propto \frac{A_s}{B_b\sqrt{gh}} \qquad (6\text{-}15)$$

$$T_e \propto \frac{1}{K_d \rho_w g} \qquad (6\text{-}16)$$

Where

T_b	Time of breach development (s)
A_s	Reservoir surface area (m^2)
B_b	Breach width (m)
g	Gravity (m/s^2)
h	depth (m)
K_d	Erodibility (cm^3/N-s)
ρ_w	Density of water (kg/m^3)
T_e	Time of erosion (s)

and hence

- Using constant values of K_dA_s should represent conditions with similar breach behaviour
- The gradient of the breach width growth should be proportional to K_d

A range of breach cases were modelled using a mixture of reservoir area (A_s) and soil erodibility (K_d). Results were reviewed and allocated as either reservoir area controlled or erosion controlled. Where unclear, a question mark was allocated. Table 6-8 shows the initial modelling results whilst Table 6-9 shows the same results ordered according to ascending value of A_sK_d.

The results clearly show a pattern of breach behaviour that is dependent upon the product A_sK_d. This finding is also consistent with the physical constraints described by Walder (Walder and O'Connor, 1997) when developing an earlier simplified breach model. Walder and O'Connor noted that a large volume reservoir could form a breach without significant drawdown of the reservoir, leading to a high discharge, whilst a small volume reservoir allows significant drawdown as the breach develops and hence the erosion rate must play a significant factor in affecting the peak outflow. This point was noted by Wahl (Wahl, 2004) but the significance of performance in comparison to other equations was diminished by the type of data used to assess the performance of the equations (i.e. not a fair distribution between small and large reservoirs). Consequently, the significance of the reservoir stage area relationship with soil erodibility for breach characteristic seems to have been overlooked – at least certainly within industry practice and application of such

Table 6-8 Summary of model runs for varying erodibility (K_d) and reservoir area (A_s)

Run Ref: (VarErod_M1_Homo...)	Res Area A_s (m2)	Erodibility K_d	A_sK_d	Res Area Control	Rate Erosion Control
Kd10_Res250_v5.11_nbm	250	10	2,500		✓
Kd10_Res500_v5.11_nbm	500	10	5,000		✓
Kd10_Res750_v5.11_nbm	750	10	7,500		✓
Kd10_Res2500_v5.11_nbm	2500	10	25,000	~?	✓
Kd10_Res7500_v5.11_nbm	7500	10	27,000	?	✓
Kd10_Res30000_v5.11_nbm	30000	10	300,000	✓	
Kd50_Res250_v5.11_nbm	250	50	12,500		✓
Kd50_Res500_v5.11_nbm	500	50	25,000		✓
Kd50_Res750_v5.11_nbm	750	50	37,500	?	
Kd50_Res2500_v5.11_nbm	2500	50	125,000	✓	
Kd50_Res5000_v5.11_nbm	5000	50	250,000	✓	
Kd50_Res30000_v5.11_nbm	30000	50	1,500,000	✓	
Kd100_Res250_v5.11_nbm	250	100	25,000		✓
Kd100_Res500_v5.11_nbm	500	100	50,000	?	
Kd100_Res750_v5.11_nbm	750	100	75,000	?	
Kd100_Res2500_v5.11_nbm	2500	100	250,000	✓	
Kd50_Res5000_v5.11_nbm	5000	100	500,000	✓	
Kd50_Res30000_v5.11_nbm	30000	100	3,000,000	✓	

Table 6-9 Summary of model runs for varying erodibility (K_d) and reservoir area (A_s) ordered according to ascending A_sK_d value

Run Ref: (VarErod_M1_Homo...)	Res Area A_s (m2)	Erodibility K_d	A_sK_d	Res Area Control	Rate Erosion Control
Kd10_Res250_v5.11_nbm	250	10	2,500		✓
Kd10_Res500_v5.11_nbm	500	10	5,000		✓
Kd10_Res750_v5.11_nbm	750	10	7,500		✓
Kd50_Res250_v5.11_nbm	250	50	12,500		✓
Kd10_Res2500_v5.11_nbm	2500	10	25,000	~?	✓
Kd50_Res500_v5.11_nbm	500	50	25,000		✓
Kd100_Res250_v5.11_nbm	250	100	25,000		✓
Kd10_Res7500_v5.11_nbm	7500	10	27,000	?	✓
Kd50_Res750_v5.11_nbm	750	50	37,500	?	
Kd100_Res500_v5.11_nbm	500	100	50,000	?	
Kd100_Res750_v5.11_nbm	750	100	75,000	?	
Kd50_Res2500_v5.11_nbm	2500	50	125,000	✓	
Kd50_Res5000_v5.11_nbm	5000	50	250,000	✓	
Kd100_Res2500_v5.11_nbm	2500	100	250,000	✓	
Kd10_Res30000_v5.11_nbm	30000	10	300,000	✓	
Kd50_Res5000_v5.11_nbm	5000	100	500,000	✓	
Kd50_Res30000_v5.11_nbm	30000	50	1,500,000	✓	
Kd50_Res30000_v5.11_nbm	30000	100	3,000,000	✓	

equations. These findings have significant implications for the use of regression (peak discharge) equations since these equations typically take no notice of the value of soil erodibility, which is shown here to not only directly affect the rate of breach formation, but in turn, and in conjunction with the reservoir area (or load condition), to significantly affect the nature and shape of the outflow hydrograph.

6.3.6 Predicting head cut or surface erosion processes

The review of breach models and breach modelling processes has shown that two different 'large scale' physical processes dominate the breaching process (Section 6.1.1). For flood embankment and embankment dam failure these may be described as surface erosion and headcut processes. Soil erodibility is a key parameter in determining which of these two processes occurs. In turn, soil erodibility depends upon a number of other soil parameters such as density, moisture content, etc. Breach simulation using one or other of these processes can give quite different results. The degree of difference is not simply due to the physical process, however, but also dependent upon site specific conditions such as embankment size, reservoir area, flood inflow etc. This complicates the process for demonstrating the significance of one process over the other for any given site.

However, since the 'choice' of physical process appears to be highly correlated to soil erodibility, where soil erodibility is very low (i.e. a very strong resistance to erosion) it is most likely that head cut will occur. Where soil erodibility is very high (i.e. a very poor resistance to erosion) it is likely that surface erosion will occur. For conditions in-between, it is difficult to predict one way or another, hence model simulation using both head cut and surface erosion should be undertaken to determine the potential range of outcomes. Indicative guidance on soil erodibility is given in Table 6-4 and Table 6-5. Where greater confidence is required in the breach prediction, it is recommended to first undertake laboratory or field analysis of the soils to determine the actual soil erodibility and subsequently to undertake model sensitivity analysis.

6.4 Discussion

This research into erosion processes identified a range of issues and processes that are fundamental to the way in which breach initiation and formation develops. Many processes were identified through analysis of the IMPACT project data, with their significance subsequently demonstrated through development and testing of the breach model. Some of the processes, such as headcut versus surface erosion and the relationship between soil erodibility and the upstream reservoir stage area relationship (A_sK_d) provide mechanisms through which quick assessments may be made of the likely nature of the breach outflow (i.e. rapid, peaky versus slow and steady). Whilst it is clear that adopting some processes within the breach model (e.g. headcut and surface erosion; use of soil erodibility rather than sediment transport equations) makes a significant improvement, the value of simulating some processes in detail (e.g. block failure) remains less clear and requires further research. However, a failure to recognise or differentiate many of these processes in earlier breach models does help to explain why modelling accuracy has not advanced more rapidly over the past two decades.

The role of soil erodibility (soil type and state) in dictating the dominant physical process through which breach occurs has been presented. The difference in predicted outcomes arising through either headcut or surface erosion processes can also be very large, yet many breach models to date have ignored the different processes and also ignored the parameter of soil erodibility in the erosion process. The dynamic nature of breach formation, plus the clear dependence on soil erodibility, means that the use of sediment erosion equations (which incorporate a measure of soil erodibility) rather than equilibrium sediment transport equations is far more appropriate. Equally, a model which is able to simulate both head cut and surface erosion processes offers a tool which can simulate breach through a range of materials likely to be found in embankment dams and flood embankments.

One breach scenario may warrant a variation on this modelling approach. Landslide dams will have a breach length that is potentially so long that equilibrium sediment processes may start to become important for the simulation of erosion. Care is therefore required when considering these particular breach processes.

These findings significantly undermine the value of many of the earlier breach models and the associated laboratory data, all of which typically ignore soil erodibility. Further analysis of the link between soil erodibility and reservoir size (surface area) shows a clear dependence between the magnitude of A_sK_d and breaching behaviour. This reinforces earlier criticism of the use of regression equations for the prediction of breach, since these equations fail to take into account the soil erodibility and typically rely only on measures of dam height and stored water volume; the nature of the breach formation rate and hence the outflow hydrograph can vary greatly depending upon the parameter A_sK_d.

Block failure was identified as one of three mechanisms for soil erosion that occur during breach initiation and growth; the other two comprised mass erosion and sediment erosion. Most breach models do not differentiate between these processes. It is clear from the detailed analysis of physical processes and images of recently failed structures, that the shape of the eroding breach section is with either vertical or undercut sides, and not trapezoidal as many earlier modellers have suggested. This is consistent with the observed process of erosion, whereby the base of the breach section sides are eroded, leading to block failure into the breach. A trapezoidal shape may arise after the breach event when the exposed soil faces dry and crumble. This is significant since it affects the area used for flow calculation within the breach model.

The model developed by Mohamed (2002) incorporates block failure as part of the prediction of breach growth. Analysis of this process has failed to demonstrate the significance of this process on end results (as compared to using an average erosion rate), despite earlier validation of this approach by Mohamed. Again, however, consideration of the physical interaction between

reservoir and rate of breach erosion may provide an explanation for conditions where block failure will have minimal effect; more detailed analysis of conditions between these bounds is required to see whether there are conditions where the influence of block failure becomes significant.

Two significant challenges remain; namely the reliable prediction of soil erodibility without the need for laboratory testing of samples and the exact dependence of the physical process (headcut or surface erosion) on soil erodibility. Current knowledge allows only for indicative value estimation which depends significantly upon judgement, or laboratory testing. Whilst we can predict with some confidence that highly erodible (probably non cohesive) materials will breach through surface erosion, and highly resistant (probably cohesive) materials through headcut, the point of transition between these two extremes is unclear. Within this transition zone, other parameters affecting erodibility such as compaction, chemical composition, etc. (Regazzoni, 2009) will help to change erosion behaviour from one form to another. The IMPACT gravel field test is a clear example of this, where a non cohesive material demonstrated head cut behaviour due to high compaction, moisture content and freezing conditions. A solution would be to progressively build a database of test and field cases covering a range of different soils and soil states which would show which processes dominate for given conditions. However, as highlighted in Section 2, very few existing sets of test or case study data include such detailed data, hence building such a database would depend upon collation of future test data, rather than review of existing data.

7. A new approach for modelling variable soil state during embankment breaching

7.1 Motivation

One cause of flood embankment or embankment dam failure is the presence of a layer or zone of poor quality material within the structure (Dyer and Gardener, 1996, Environment Agency, 2011, Saxena and Sharma, 2006). This may be as a result of the use of sub standard materials or poor quality or inappropriate construction technique, or both. Historic development of flood embankments and embankment dams also results in structures with layers or zones of different material, or at least material with different properties (i.e. different compaction and / or moisture content). Embankments can form fissures perhaps up to 0.6m deep, due to shrinkage and can allow the rapid ingress of water affecting soil state and possibly stability (Dyer et al., 2007, Dyer et al., 2009).

In order to simulate breach mechanisms for these types of real embankment structures it is necessary to modify the modelling approach to provide a more flexible approach for defining the structure. The model, as developed by Mohamed (2002), restricts the user to either a homogeneous structure or a composite structure with a thin erosion resistant core. A new modelling approach was developed to allow far more flexibility in defining the structure, with multiple zones of different soil type permitted, and hence the ability to predict breach development through complex mixes of soil layers and zones.

The purpose of this new approach was to develop a model that could simulate breach growth through more realistic structures (i.e. layered or zoned structures), including those suffering from fissuring, whilst still retaining a relatively simple modelling approach.

7.2 Simulating zones of variable erodibility

In order to model breach growth through different erodibility zones it is necessary to first consider the physical processes that might occur and subsequently how these processes might be represented within the model.

7.2.1 Variable erodibility – physical processes

The introduction of layers or zones of different erodibility introduces complexity into the way in which erosion and block failure might occur during breaching. Using the general reference system shown in Figure 2-11, we can consider a simple example of an embankment that is built from 3 layers of different erodibility soil (Figure 7-1). These layers might reflect construction of an original embankment (layer 3) and raising of the original embankment (layers 2 and 1). However, layer 1 represents fissuring in the crest of the embankment, creating a separate layer of increased erodibility.

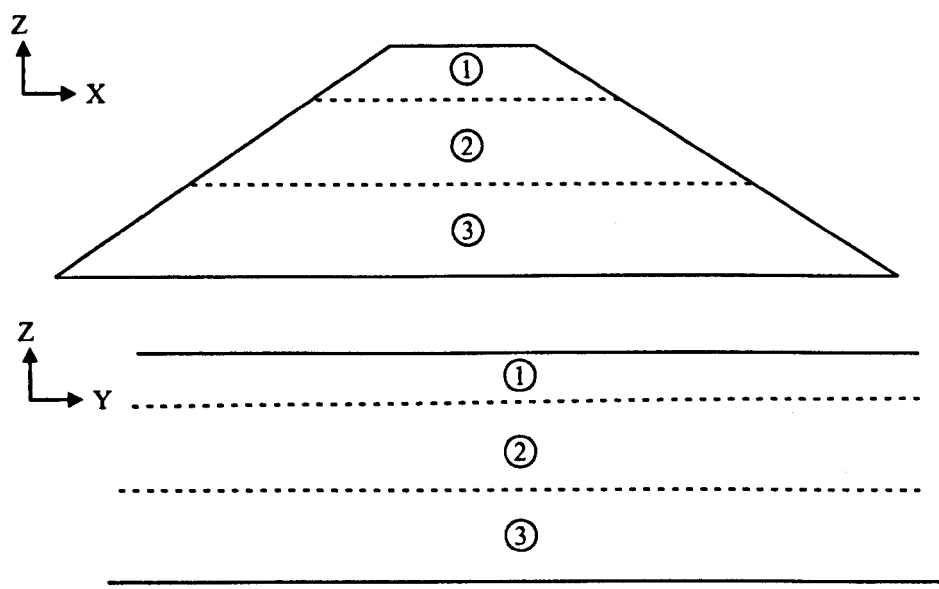

Figure 7-1 Side and front elevations of a layered embankment – regions 1, 2 and 3 reflect layers of material with different erodibility

If we consider how breach might occur through the different zones of erodibility, then the following questions need to be answered:

- How and what do we typically model at the moment?

- What happens if you allow different layers to erode at different rates?
- What do we actually see in practice?

At the moment most breach models (including Mohamed (2002)) simulate erosion through single zones of material (i.e. a homogeneous soil structure). The model of a composite structure does not allow for erosion of the core material (only structural failure) hence we do not consider how erosion of two adjacent zones of material should behave. Additionally, the existing approach distributes the erosion of material around the eroding section so as to erode the bed and undercut the sides of the breach. This always results in breach side erosion that can lead to either shear or rotational failure (or a combination of both) of the undercut section.

If we consider how layers or zones of material might erode at the sides of a breach, we can imagine a series of different permutations of soil layer erosion (and erodibility) that might lead to a variety of breach side profiles. Some examples (A to E) are shown Figure 7-2 below. The lines represent how the exposed side face of the breach might erode, varying as the soil erodibility within each layer (1 to 3) increases or decreases relative to the adjacent layer.

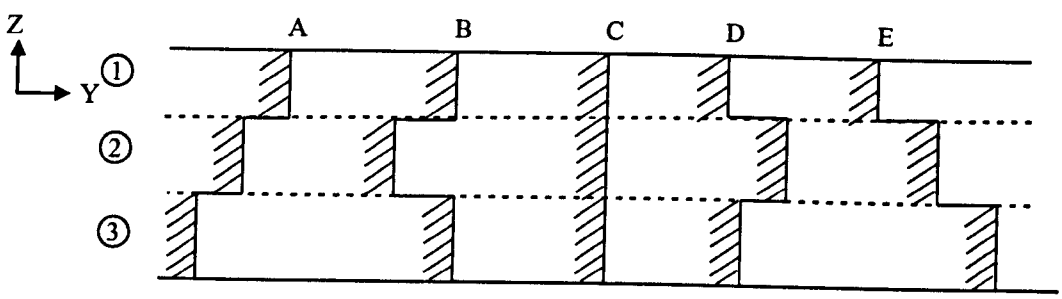

Figure 7-2 Different permutations (A to E) of breach side face erosion for an embankment with 3 layers of soil with differing erodibility

Whilst the profiles in Figure 7-2 may appear logical in terms of the potential rate of soil erosion, they are not consistent with observations of breach erosion in practice. In practice, breach erosion

always occurs through undercutting of breach side material, with discrete losses of side material (soil wasting). The resulting breach shape typically has vertical or near vertical sides and no examples are available that show significant preferential erosion of a particular layer or zone through the breach (e.g. Figure 7-2 B or D), hence it is proposed that the process of erosion and failure differs from this simplistic representation.

The real process of erosion differs from the simplified sections shown in Figure 7-2 due to the 3 dimensional distribution of flow through the breach. It can be seen (Figure 2-13d) that during the process of breach formation and lateral growth there is typically strong flow convergence into the breach. This convergence results in the creation of elongated vortices which aggressively erode along the toe of the breach sides, undercutting the side material and resulting in side failures. It is suggested that this process is so dominant that it dictates the overall rate of erosion that might occur if you assumed uniform flow conditions in conjunction with layers of different material. This process results in vertical or undercut side slopes (almost) regardless of material erodibility, and is more consistent with field observations. This approach is also consistent with research findings in the field of river bank erosion, where basal erosion is found to dominate and dictate the rate of lateral bank erosion (Simon et al., 2008, Watson and Basher, 2006). Accepting these assumption has significant implications for our approach to breach modelling with variable erodibility.

7.2.2 Variable erodibility – modelling approach

A new approach for modelling that is consistent with the conclusions of Section 7.2.1 is to adapt the approach by Mohamed (Mohamed, 2002), but to use soil properties for erosion calculation based only upon the conditions found at the base of the eroding breach section. This approach is consistent with the observation that the rate of erosion is driven by the highly turbulent and erosive flow found to follow the bottom corners of the breach (i.e. the vortices arising from flow converging and dropping through the breach) and consistent with research findings in relation to river bank and gully erosion (Bennett and Alonso, 2004, Gordon et al., 2007, Robinson and Hanson, 1994). Figure 7-3 shows the approach. Breach growth is first calculated using soil

properties from Zone 1. At the point where the eroding base of the breach (line B_1-C_1-D_1) crosses the soil 1-2 zone boundary, the calculations swap to using soil zone 2 properties. The same process occurs at the boundary between soil zones 2 and 3, and so on for multiple layers. The erosion equations allow calculation of a rate of vertical erosion based upon flow conditions and (breach) bed material. Lateral erosion is subsequently calculated from the bed erosion rate.

Whilst the rate of breach erosion from flow shear stress may be calculated using one set of soil properties, the stability of the breach side slopes is calculated using multiple zone soil properties (Figure 7-4).

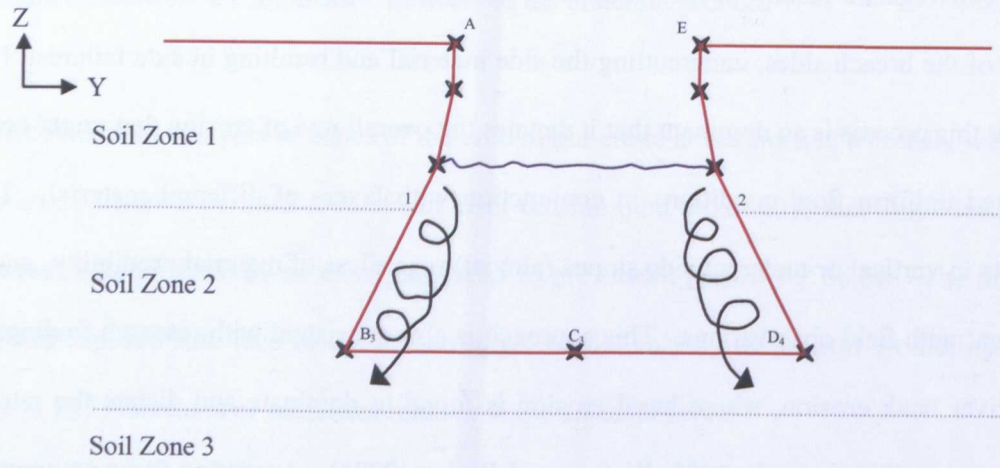

Figure 7-3 Proposed approach for predicting breach growth through layers of soil with different erodibility.

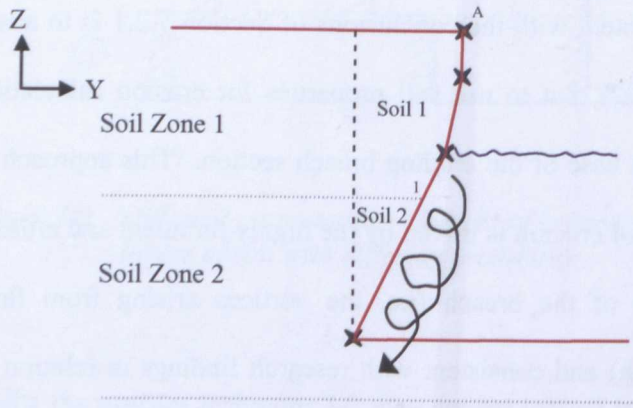

Figure 7-4 Use of different soil properties within side slope wedge stability calculations

This new approach will maintain the current calculation procedure (Mohamed, 2002) whereby, regardless of soil erodibility, the breach side slope profile will always be one that is vertical or undercut. Hence the existing calculation procedures for side slope stability in terms of slip or rotational failure (Mohamed, 2002) remain valid for a multi zoned embankment.

As an initial step, simulation of breach with up to 4 zones of erodibility was implemented. One of these zones may be used to reflect fissuring in the crest or crest and landward slope with the remaining 3 zones reflecting different construction permutations. The generic zone combinations shown in Figure 7-5 were developed to meet a large number of structure combinations found in practice.

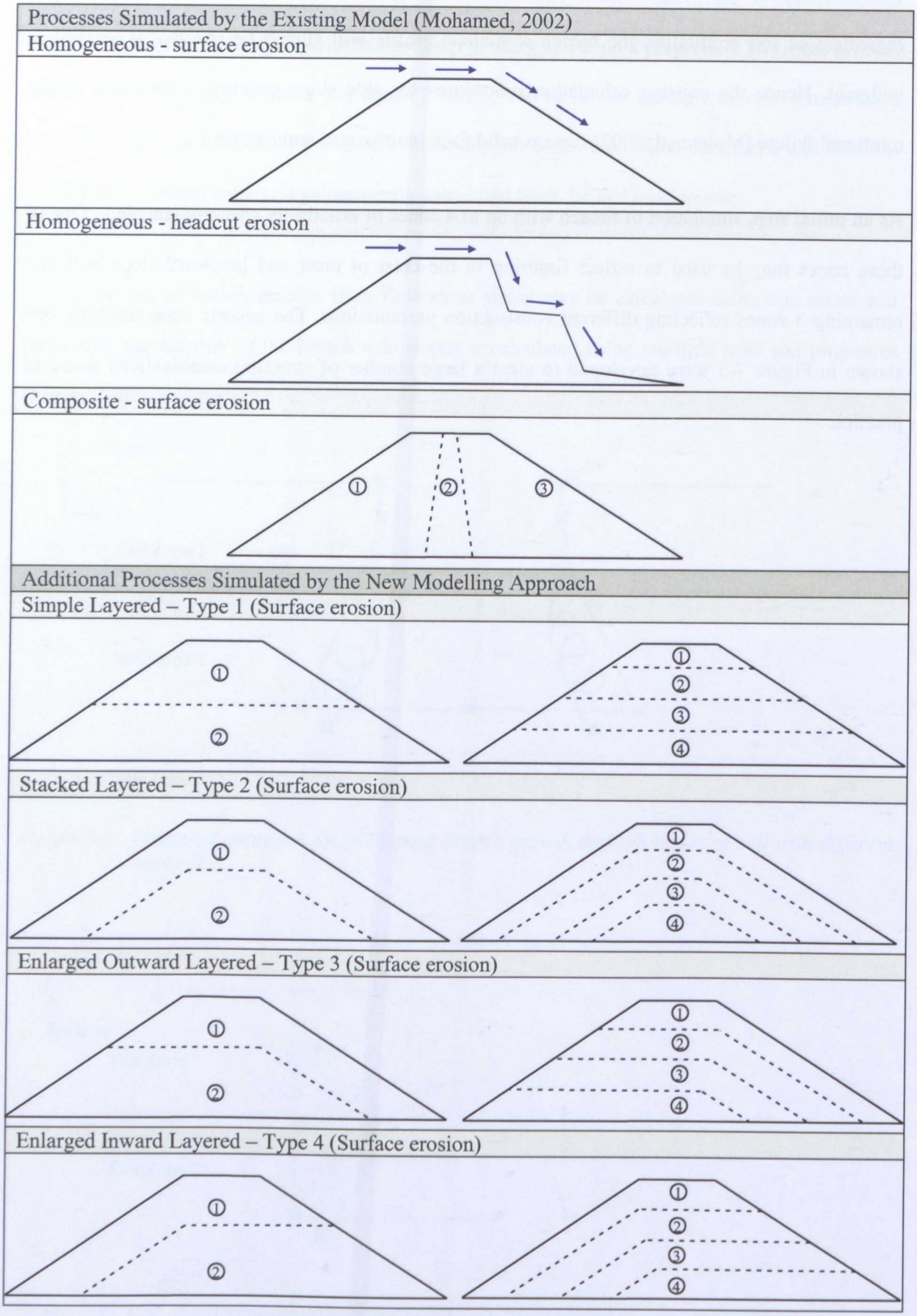

Figure 7-5 Generic options for simulating different zoned geometries

7.3 Variable erodibility – model test programme and key findings

A series of model tests were undertaken to assess model performance for a range of conditions. These tests are summarised in Table 7-1 below with the run reference relating to the generic structure types as listed in Figure 7-5. The results from all of these runs are presented in detail in Appendix 4; key findings and run results are summarised in the following sections.

Table 7-1 Summary of erodibility model testing

No.	Description	Run Reference
1	Homogeneous embankment; Erodibility K_d=10	*M1-Homo-Kd10-Res2500*
2	Homogeneous embankment; Erodibility K_d=10	*M1-Homo-Kd100-Res2500*
3	Two horizontal layers; Upper layer 2m thick with K_d=100; Lower layer 2m thick with K_d=10	*M1-Type1-2layer-D2Kd100-D2Kd10-Res2500*
4	Two horizontal layers; Upper layer 2m thick with K_d=10; Lower layer 2m thick with K_d=100	*M1-Type1-2layer-D2Kd10-D2Kd100-Res2500*
5	Two horizontal layers; Upper layer 1m thick with K_d=100; Lower layer 3m thick with K_d=10	*M1-Type1-2layer-D1Kd100-D3Kd10-Res2500*
6	Two horizontal layers; Upper layer 1m thick with K_d=10; Lower layer 3m thick with K_d=100	*M1-Type1-2layer-D1Kd10-D3Kd100-Res2500*
7	Raised embankment landward side; Extra layer 1m thick with Kd=100; base 3m thick with Kd=10	*M1-Type3-2layer-D1Kd100-D3Kd10-Res2500*
8	Raised embankment landward side; Extra layer 1m thick with Kd=10; base 3m thick with Kd=100	*M1-Type3-2layer-D1Kd10-D3Kd100-Res2500*
9	Raised embankment load side; Extra layer 1m thick with Kd=100; base 3m thick with Kd=10	*M1-Type4-2layer-D1Kd100-D3Kd10-Res2500*
10	Raised embankment load side; Extra layer 1m thick with Kd=10; base 3m thick with Kd=100	*M1-Type4-2layer-D1Kd10-D3Kd100-Res2500*
11	Centrally raised embankment; Extra layer 2m thick with Kd=100; base 2m thick with Kd=10	*M1-Type2-2layer-D2Kd100-D2Kd10-Res2500*
12	Centrally raised embankment; Extra layer 2m thick with Kd=10; base 2m thick with Kd=100	*M1-Type2-2layer-D2Kd100-D2Kd10-Res2500*
13	Three horizontal layers; All layers 1.3m thick with K_d=100, 50, 10 respectively.	*M1-Type1-3layer-D1.3Kd100-D1.3Kd50-D1.3Kd10-Res2500*
14	Three horizontal layers; All layers 1.3m thick with K_d=10, 50, 100 respectively.	*M1-Type1-3layer-D1.3Kd10-D1.3Kd50-D1.3Kd100-Res2500*
15	Three horizontal layers; All layers 1.3m thick with K_d=100, 10, 100 respectively.	*M1-Type1-3layer-D1.3Kd100-D1.3Kd10-D1.3Kd100-Res2500*
16	Three horizontal layers; All layers 1.3m thick with K_d=10, 100, 10 respectively.	*M1-Type1-3layer-D1.3Kd10-D1.3Kd100-D1.3Kd10-Res2500*

Note:
All tests were performed using the same modelling scenario, as described in Section 6.3. A reservoir surface area of 2500m^2 was used in conjunction with erodibility (K_d) values of 10 and 100 respectively. This provided examples where the breach behaviour was controlled by soil erodibility and lake size (See Section 6.3).

Figure 7-6 to Figure 7-10 show modelling results for all of the runs listed in Table 7-1, comprising breach outflow, reservoir level, breach width, breach depth and depth on breach invert respectively. Results for breach width, depth and depth on invert show oscillations. This is not modelling instability and occurs because the data presented is for the modelled critical flow section rather than from a fixed physical section. The critical flow section changes as the breach evolves, with varying combinations of breach width and depth providing the critical flow control. As would be expected, neither Figure 7-6 or Figure 7-7 (reach outflow and reservoir level) show these oscillations.

Each set of modelling results is considered in the sections below. A key feature to note from Figure 7-6 (breach outflow) is that firstly, the two distinct characteristics of breach relating to reservoir volume dominated or erosion controlled breach can be seen (i.e. rapid, peaky hydrograph or long, low steady discharge) but that secondly, transitions between these two cases can be seen, with results initially following one trend and then changing to the other. These transitions relate to the way in which layers of different soil behave as the breach erodes through a multilayer structure.

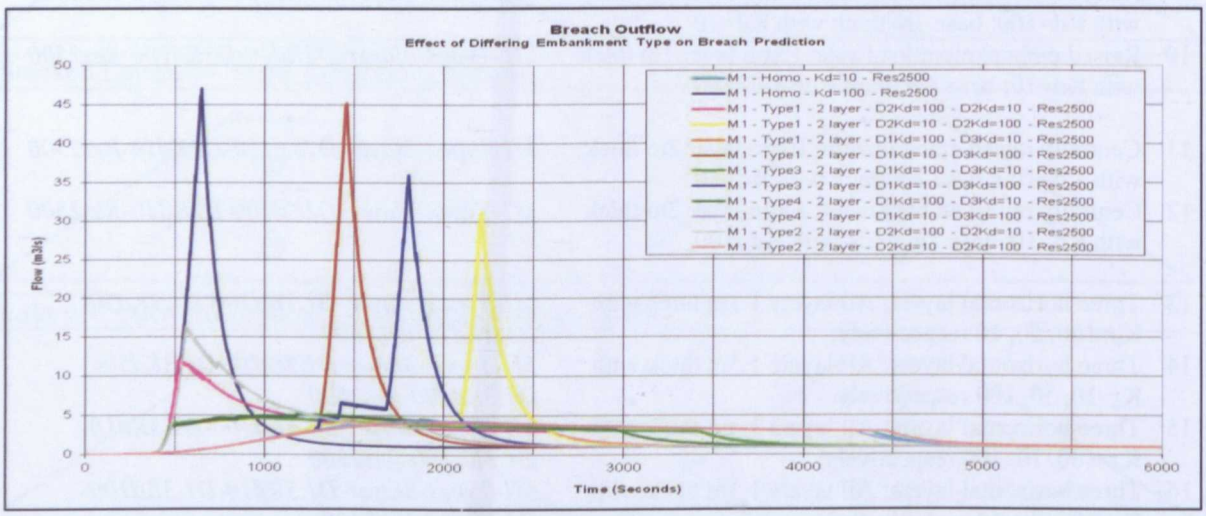

Figure 7-6 Breach outflow – comparison of all erodibility zone runs

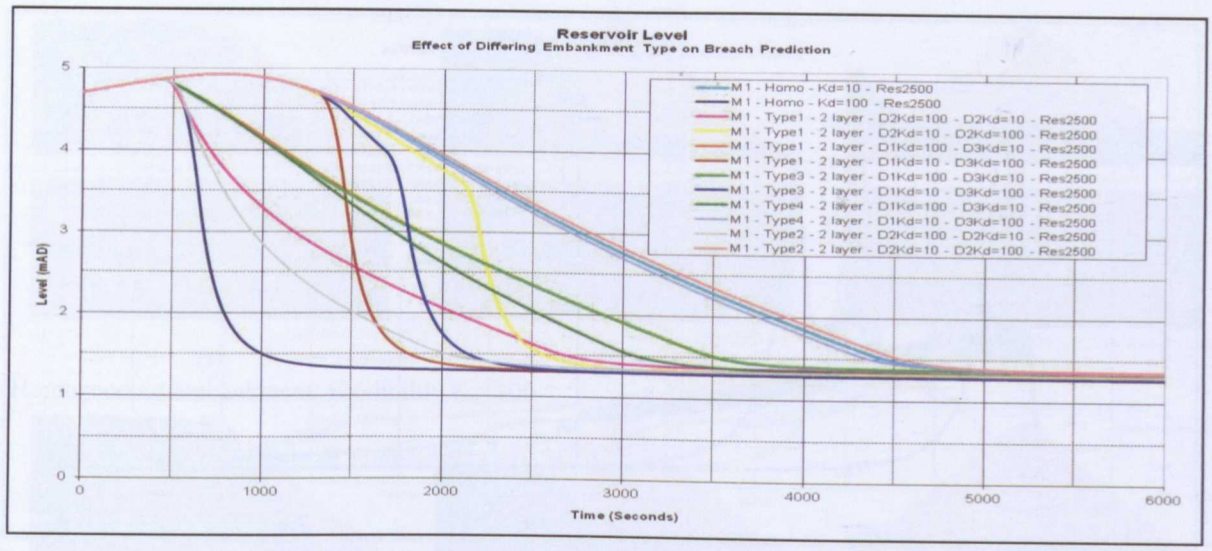

Figure 7-7 Reservoir level – comparison of all erodibility zone runs

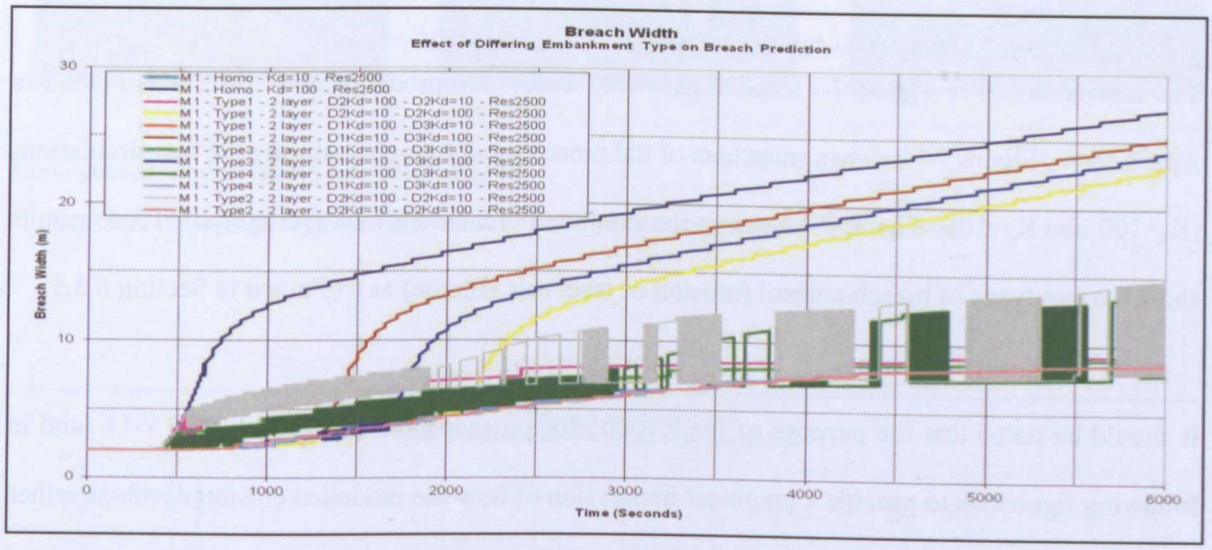

Figure 7-8 Breach width – comparison of all erodibility zone runs

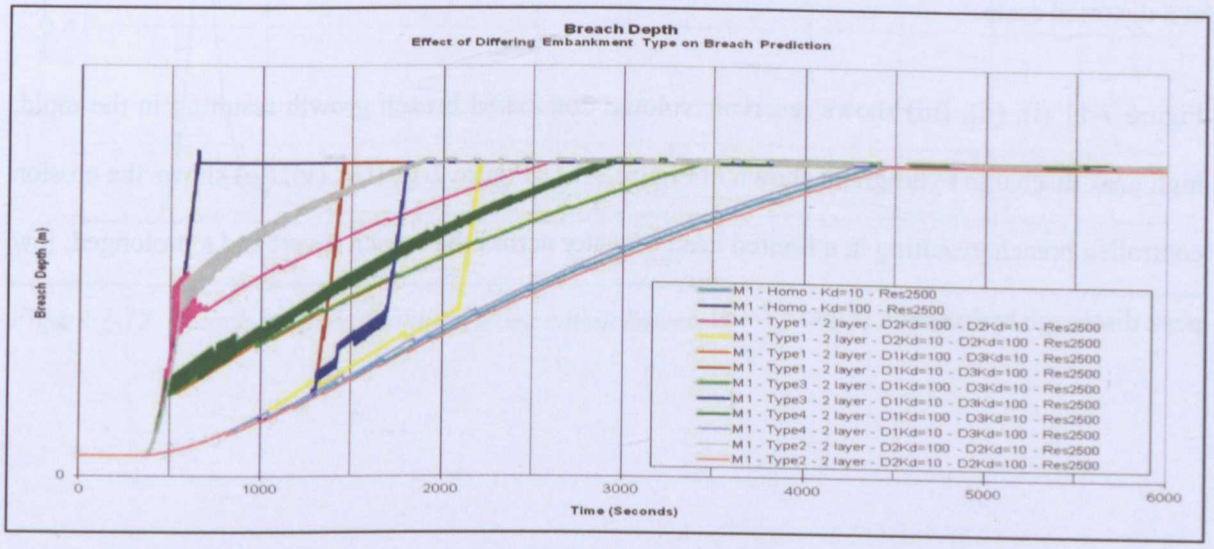

Figure 7-9 Breach depth – comparison of all erodibility zone runs

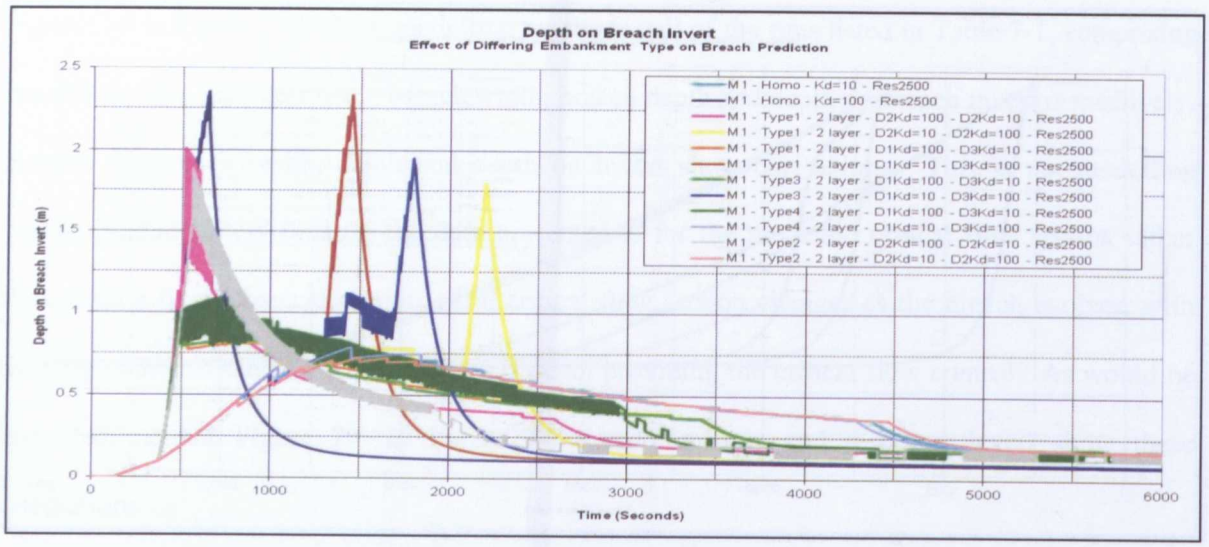

Figure 7-10 Depth on breach invert – comparison of all erodibility zone runs

7.3.1 Modelling results – homogeneous embankment

The results shown in Figure 7-11 and Figure 7-12 below are produced and discussed in detail in Appendix 4. Figure 7-11 shows snapshots of the breach model graphics during the two simulations (K_d=100 and K_d=10). Figure 7-12 shows the predicted breach outflow hydrograph. These results show the two types of breach control (erosion or reservoir volume) as explained in Section 6.3.5.

It should be noted that the purpose of the breach erosion snapshots shown in Figure 7-11 (and in following figures) is to provide a graphical impression of how the modelled erosion develops rather than specific data for a given breach time. Also note that the plan section, showing breach width, is at a distorted scale.

Figure 7-11 (i), (ii), (iii) shows reservoir volume dominated breach growth resulting in the rapid, high peak discharge hydrograph shown in Figure 7-12. Figure 7-11 (iv), (v), (vi) shows the erosion controlled breach, resulting in a limited head of water across the breach invert and a prolonged, low peak discharge hydrograph (Figure 7-12).

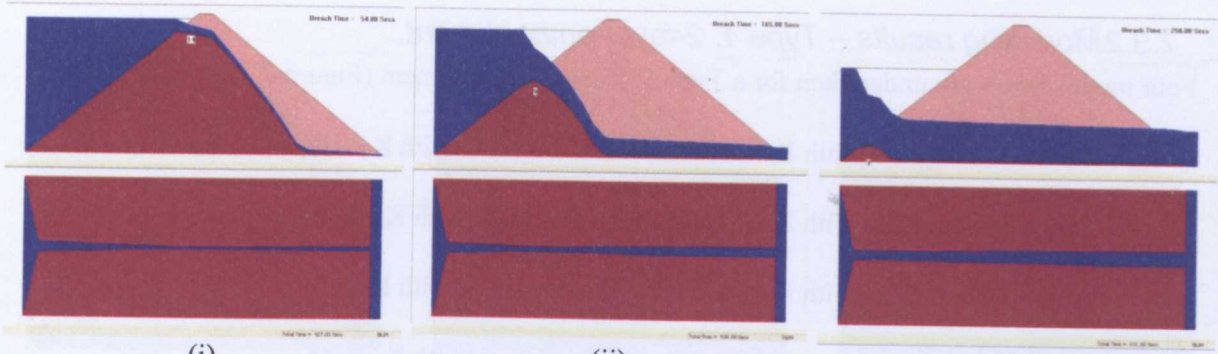

(i) (ii) (iii)

Homogeneous embankment; Erodibility K_d=100

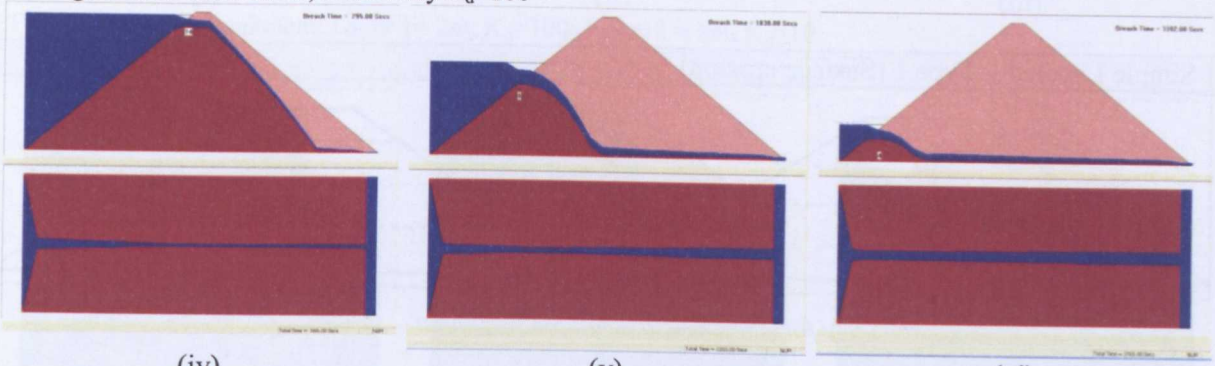

(iv) (v) (vi)

Homogeneous embankment; Erodibility K_d=10

Figure 7-11 Model simulation of breach growth for homogeneous embankment

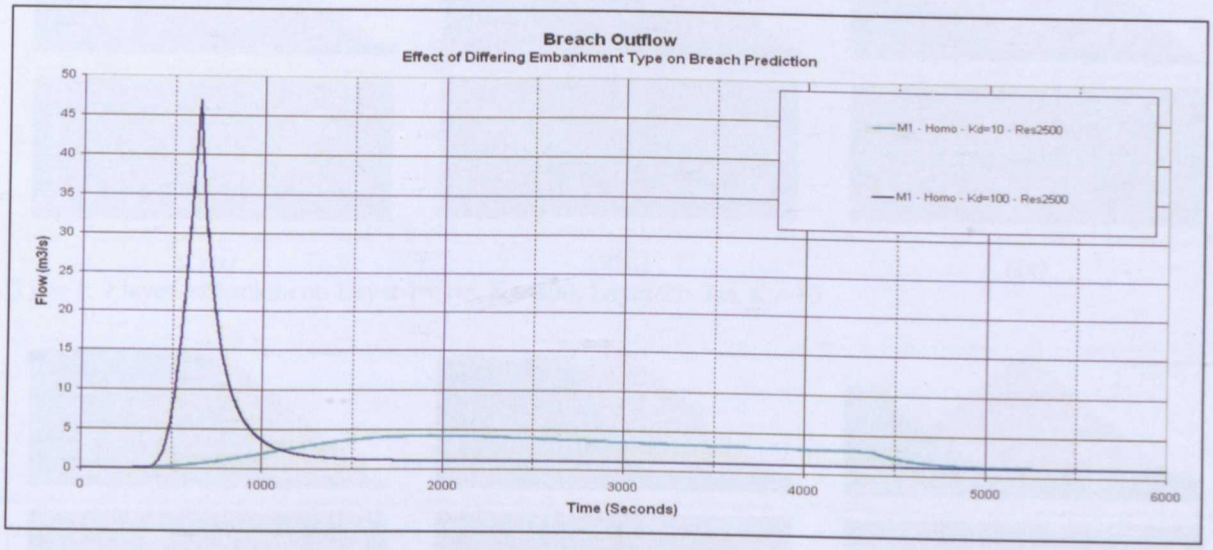

Figure 7-12 Breach outflow: Homogeneous embankment

7.3.2 Modelling results – Type 1, 2-layer embankment

Four model runs were undertaken for a Type 1, 2-layer embankment (Figure 7-13) as follows:

- Layer 1 – 2m thick with K_d=100; Layer 2 – 2m thick with K_d=10;
- Layer 1 – 2m thick with K_d=10; Layer 2 – 2m thick with K_d=100;
- Layer 1 – 1m thick with K_d=100; Layer 2 – 3m thick with K_d=10;
- Layer 1 – 3m thick with K_d=10; Layer 2 – 1m thick with K_d=100.

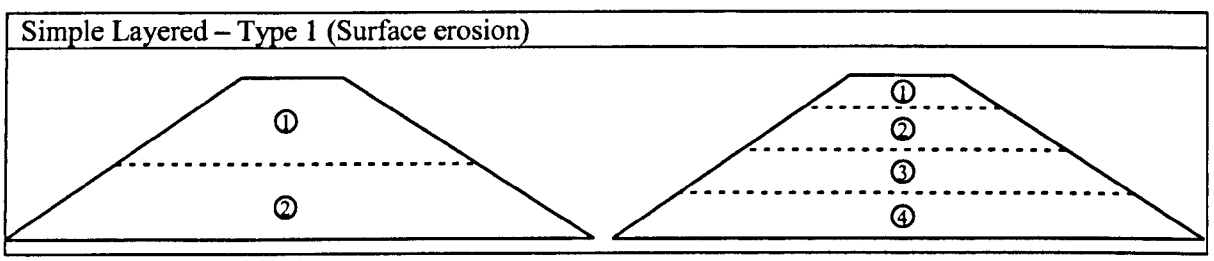

Figure 7-13 Generic geometry for a Type 1 layered embankment

Figure 7-14 shows snapshots of the breach model graphics from the four simulations and Figure 7-15 shows the predicted breach flow hydrographs.

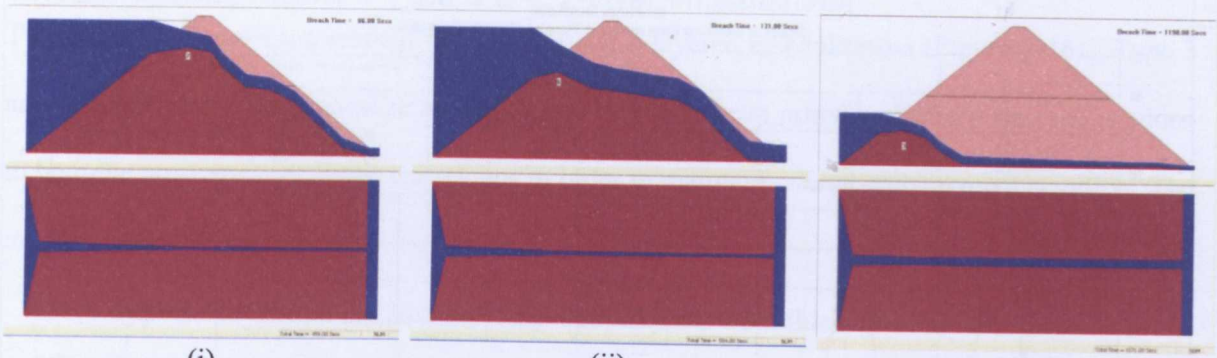

(i) (ii) (iii)

Type 1, 2 layer embankment: Layer 1= 2m, K_d=100; Layer 2 = 2m, K_d=10

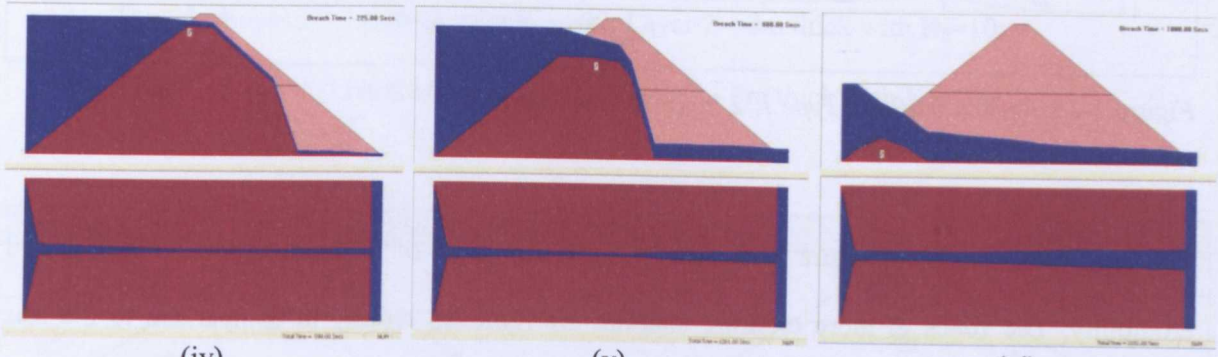

(iv) (v) (vi)

Type 1, 2 layer embankment: Layer 1= 2m, K_d=10; Layer 2 = 2m, K_d=100

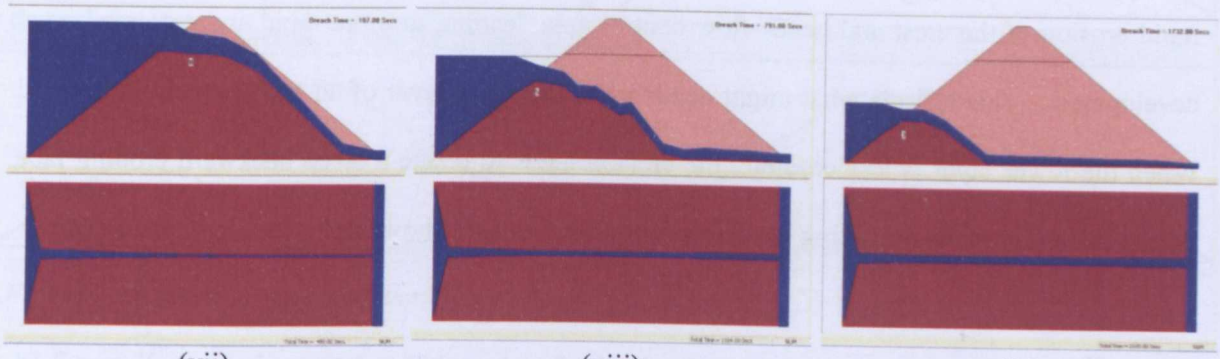

(vii) (viii) (ix)

Type 1, 2 layer embankment: Layer 1= 1m, K_d=100; Layer 2 = 3m, K_d=10

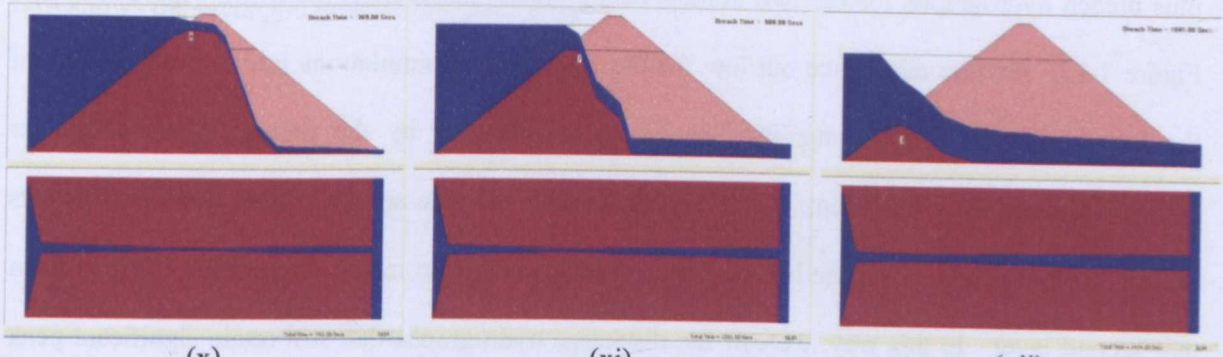

(x) (xi) (xii)

Type 1, 2 layer embankment: Layer 1= 1m, K_d=10; Layer 2 = 3m, K_d=100

Figure 7-14 Model simulation of breach growth for homogeneous embankment

7.3.3 Modelling results – Type 3 & 4, 2-layer embankment

Two model runs were undertaken for Types 3 and 4 layered embankments (Figure 7-16). Type 3 and 4 embankments are typical of embankments that have been raised and where material is added to both the crest and one of the side slopes in order to maintain overall embankment stability. The model simulations comprised:

- Type 3 - Layer 1 – 1m thick with K_d=100; Layer 2 – 3m thick with K_d=10;
- Type 3 - Layer 1 – 1m thick with K_d=10; Layer 2 – 3m thick with K_d=100;
- Type 4 - Layer 1 – 1m thick with K_d=100; Layer 2 – 3m thick with K_d=10;
- Type 4 - Layer 1 – 1m thick with K_d=10; Layer 2 – 3m thick with K_d=100.

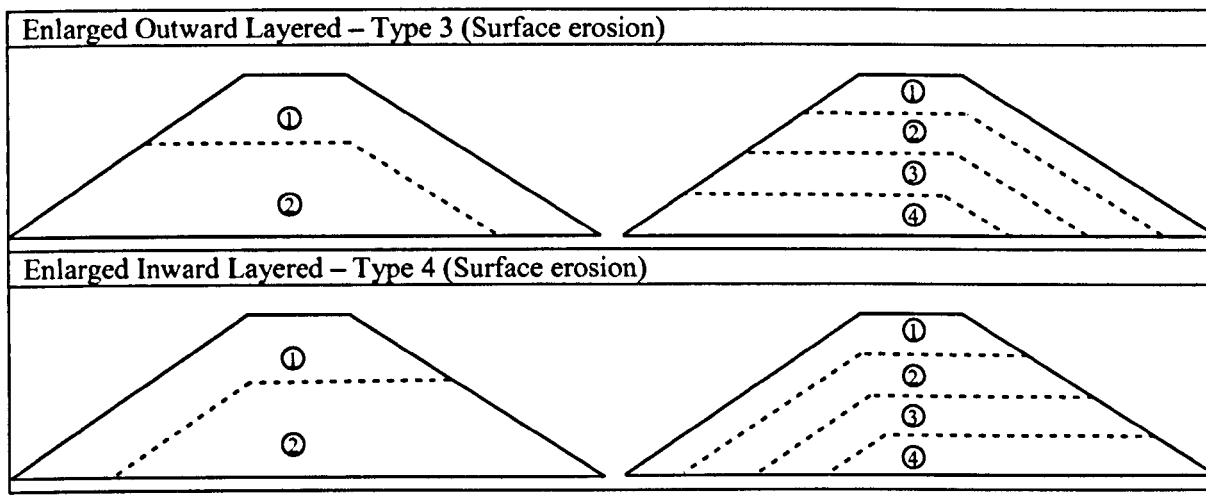

Figure 7-16 Generic geometry for Type 4layered embankment

Figure 7-17 shows snapshots of the breach model graphics from the four simulations and Figure 7-18 shows the predicted breach flow hydrographs.

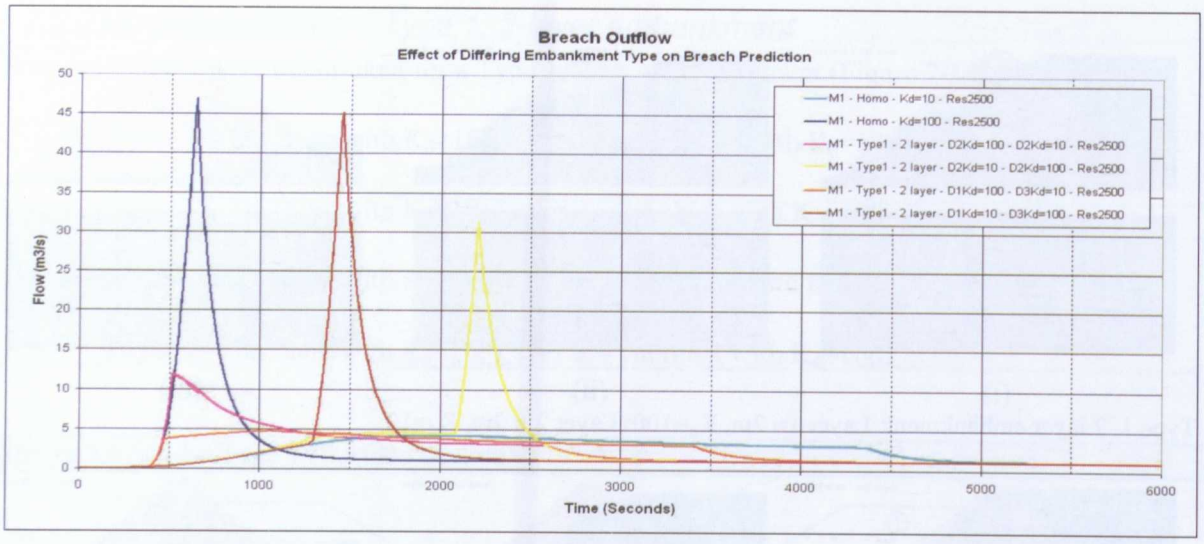

Figure 7-15 Breach outflow: Type 1, 2 layer embankment

The modelling results in Figure 7-14 clearly show the effect of different layers (zones) of soil erodibility. The zones of more erodible material are removed rapidly in comparison to the less erodible material. Where the more erodible material forms the outer or upper layer, this results in a rapid erosion of the crest and hence flow control area, leading to more rapid and extreme breach development. This reflects what might occur when the outer layer of an embankment is fissured. When the lower layer is less erodible, the erosion tends to create a steep backward eroding face. Whilst this is not simulated using headcut assumptions, it does show similarities in characteristics.

Figure 7-15 shows the outflow hydrographs for the four breach simulations shown in Figure 7-14, plus breach hydrographs for the two homogeneous breach simulations shown in Figure 7-11 and Figure 7-12. Erosion and hence outflow for the four, layered simulations initially follows one of the two homogeneous characteristic behaviours, as dictated by the nature of the soil layer controlling the flow at that point. However, when erosion (in the area of critical flow control) cuts through to the second layer, the breach characteristic changes to match the response offered from that second layer. In this way, we can see discharge hydrographs that still retain significant peak values (in comparison to the erosion controlled case) yet which are delayed significantly. In terms of peak discharge behaviour, it would appear to be controlled by the condition of the lower layer which is consistent with the modelling assumptions outlined in Section 7.2.

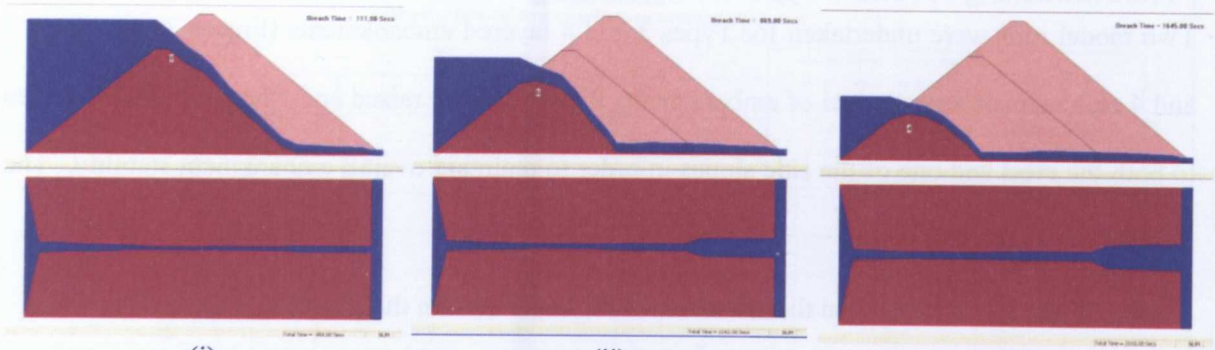

(i) (ii) (iii)

Type 3, 2 layer embankment: Layer 1= 1m, K_d=100; Layer 2 = 3m, K_d=10

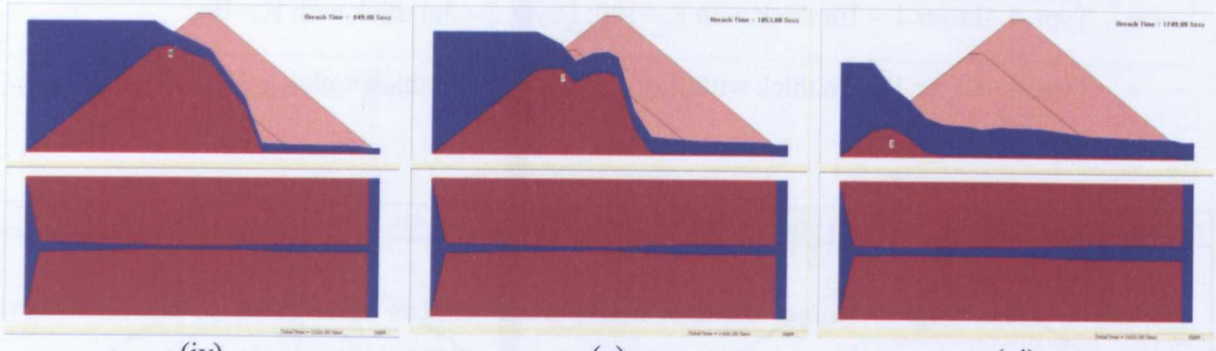

(iv) (v) (vi)

Type 3, 2 layer embankment: Layer 1= 2m, K_d=10; Layer 2 = 2m, K_d=100

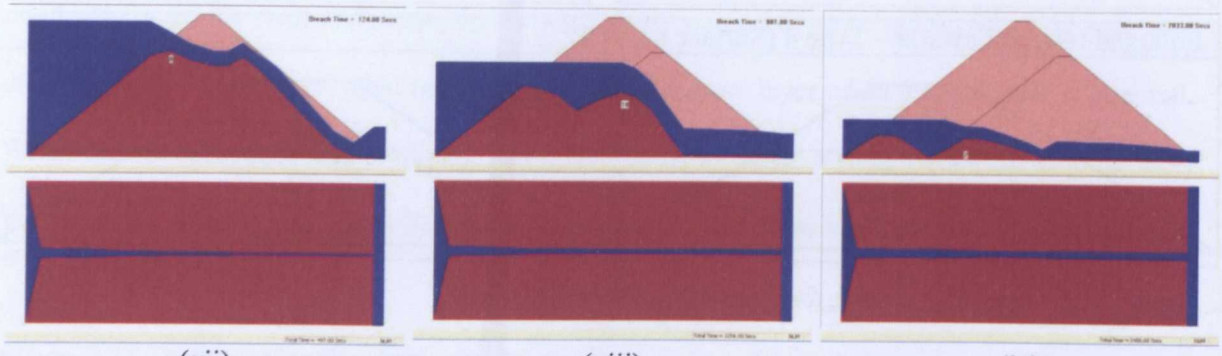

(vii) (viii) (ix)

Type 4, 2 layer embankment: Layer 1= 1m, K_d=100; Layer 2 = 3m, K_d=10

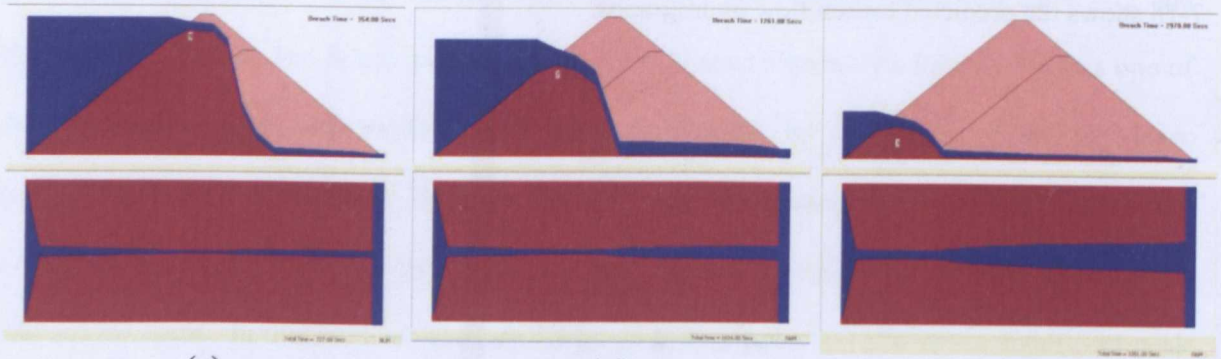

(x) (xi) (xii)

Type 4, 2 layer embankment: Layer 1= 1m, K_d=10; Layer 2 = 3m, K_d=100

Figure 7-17 Model simulation of breach growth for homogeneous embankment

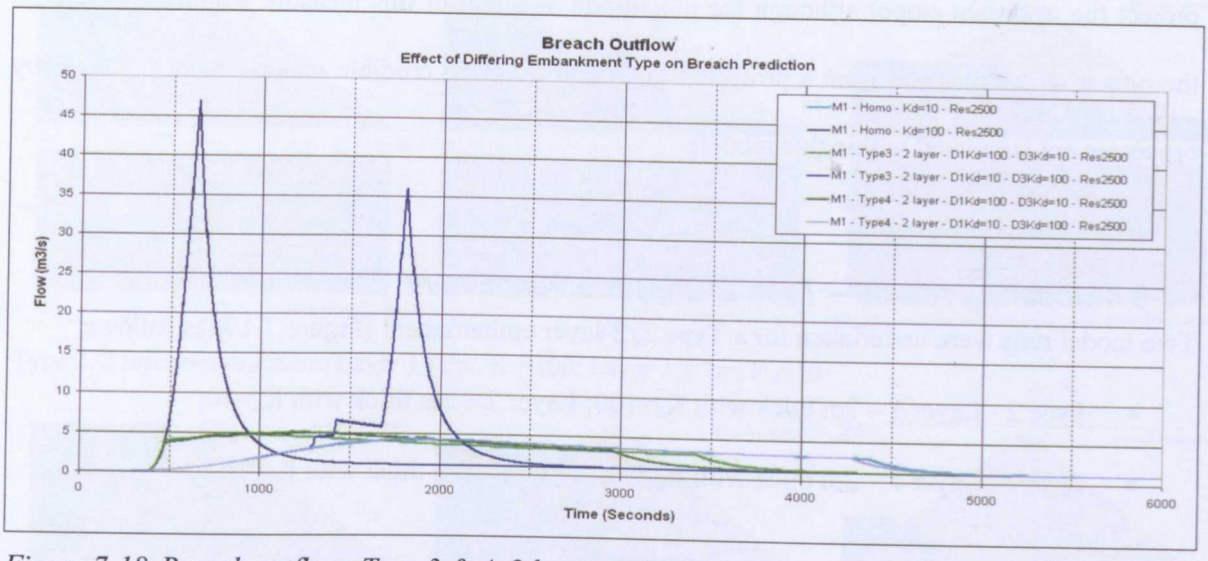

Figure 7-18 Breach outflow: Type 3 & 4, 2 layer embankment

The modelling results show an interesting interaction between the layers of different erodibility material. Whilst the more erodible material is rapidly removed when exposed to flow, the less erodible material typically dictates the rate of breach formation.

The Type 4, K_d=100 / K_d=10 results show physical behaviour against the limits of processes simulated within the breach model. The erosion creates a steep, near vertical wall (headcut) on the downstream face. This is simulated by surface erosion, but would in practice, become undercut and unstable, probably leading to more rapid failure. Undercutting would also induce more rapid failure of the upper, less erodible layer. Addition of some form of slope stability analysis – as already performed for the breach side bank stability – would be sensible for this condition. This would take the process simulation for this condition very close to head cut analysis.

An interesting feature of the Type 4 geometry is that where the outer layer is less erodible, this dictates the overall rate of breach, and a high peak in discharge is not observed for either combination of layer erodibility. This is because the critical flow control point always follows the upstream crest point, hence the path that this control point takes as breach erosion develops always remains within the outer layer of (less erodible) material. This has implications for practical design solutions that might limit the rate at which overtopping breach development could occur (i.e.

protect the upstream slope) although the magnitude of effect of this measure would depend upon the rate at which material from a protected inner core of more erodible material was removed (by processes not simulated within this model).

7.3.4 Modelling results – Type 2, 2-layer embankment

Two model runs were undertaken for a Type 2, 2-layer embankment (Figure 7-19) as follows:

- Type 2 - Layer 1 – 2m thick with K_d=100; Layer 2 – 2m thick with K_d=10;
- Type 2 - Layer 1 – 2m thick with K_d=10; Layer 2 – 2m thick with K_d=100.

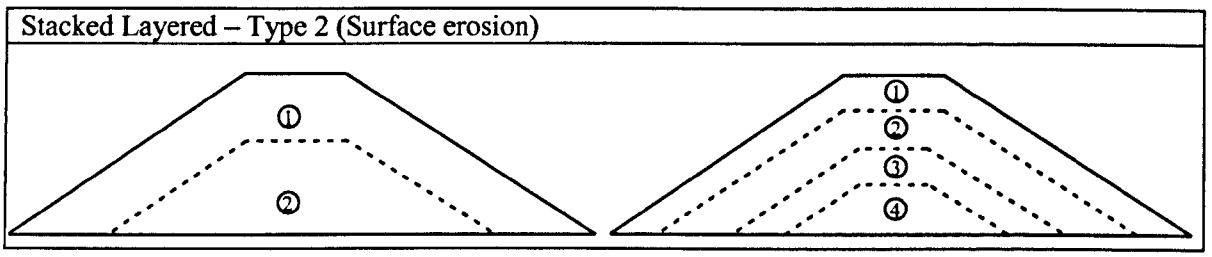

Figure 7-19 Generic geometry for Type 4 layered embankment

Figure 7-20 shows snapshots of the breach model graphics from the four simulations and Figure 7-21 shows the predicted breach flow hydrographs.

Trends are similar to those seen with the Type 3 & 4 embankments (Figure 7-17 and Figure 7-18) and can, again, be compared against the boundary conditions provided by the two homogeneous embankment tests. Performance of the outer layer of soil in the crest and upstream face area has the greatest effect in delaying overall breach growth. (This assumption is valid where headcutting or erosion underneath the less erodible outer layer is not considered). This would suggest that when raising an embankment with less erodible material, the greatest impact will be had if the raised material covers at least the crest and upstream slopes.

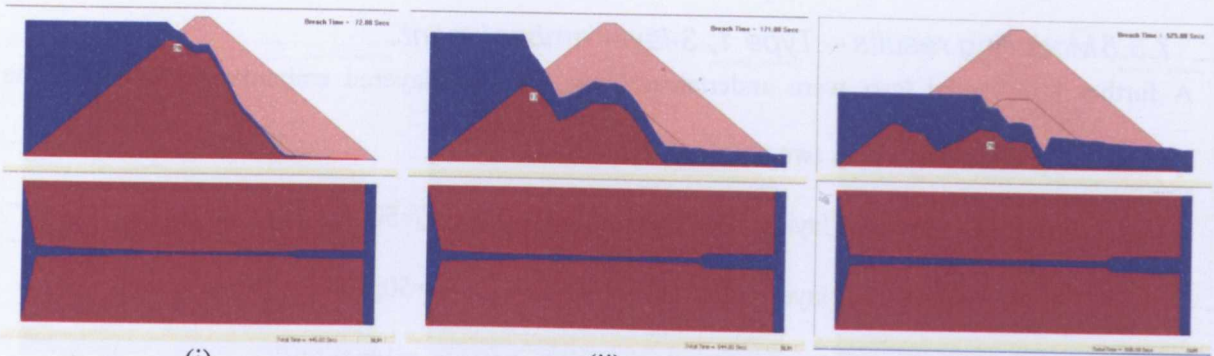

(i) (ii) (iii)

Type 2, 2 layer embankment: Layer 1= 2m, K_d=100; Layer 2 = 2m, K_d=10

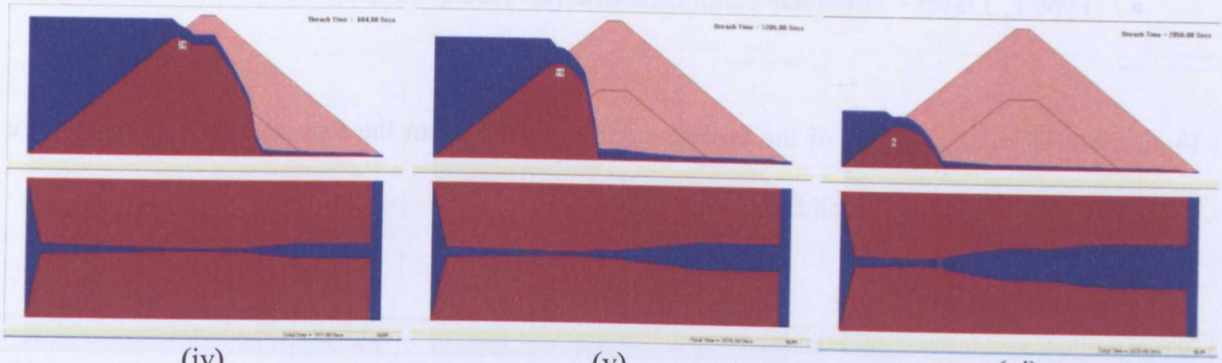

(iv) (v) (vi)

Type 2, 2 layer embankment: Layer 1= 2m, K_d=10; Layer 2 = 2m, K_d=100

Figure 7-20 Model simulation of breach growth for homogeneous embankment

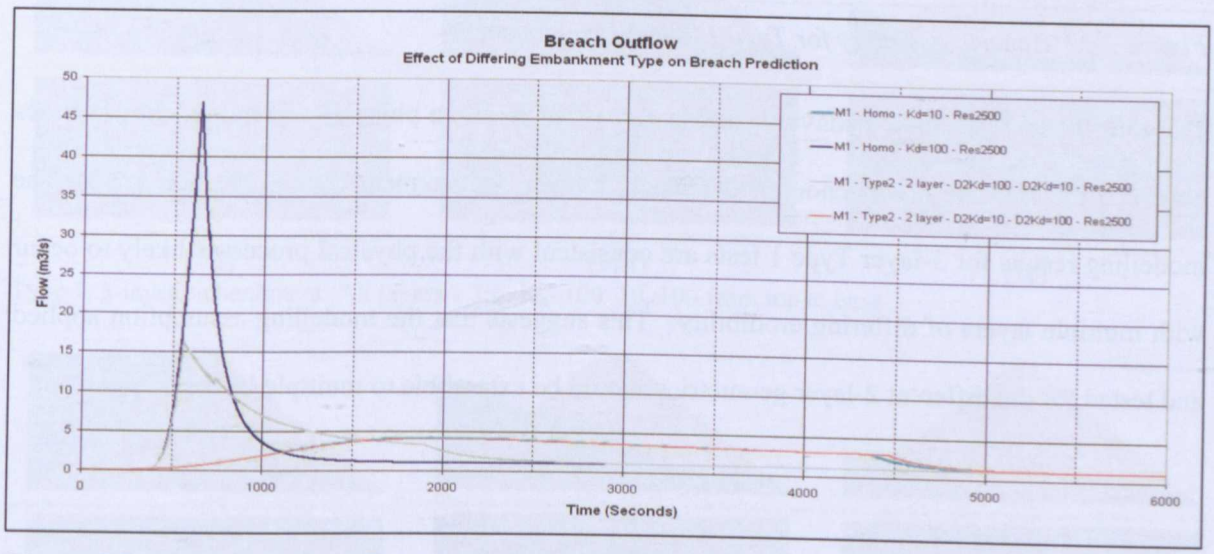

Figure 7-21 Breach outflow: Type 2, 2 layer embankment

7.3.5 Modelling results – Type 1, 3-layer embankment

A further four model tests were undertaken for a 'Type 1' layered embankment but this time incorporating three rather than two soil layers (Figure 7-22):

- Type 1, 3 layer – All layers 1.3m thick with K_d=100; K_d=50; K_d=10;
- Type 1, 3 layer – All layers 1.3m thick with K_d=10; K_d=50; K_d=100;
- Type 1, 3 layer – All layers 1.3m thick with K_d=100; K_d=10; K_d=100;
- Type 1, 3 layer – All layers 1.3m thick with K_d=10; K_d=100; K_d=10.

Figure 7-23 shows snapshots of the breach model graphics from the four simulations and Figure 7-24 shows the predicted breach flow hydrographs.

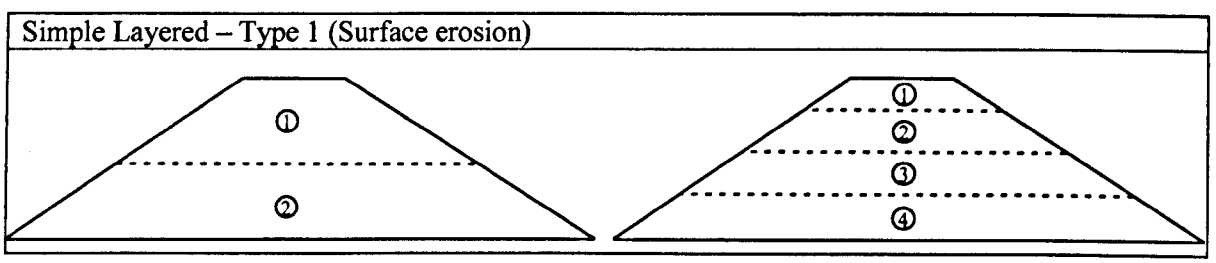

Figure 7-22 Generic geometry for Type 1 layered embankment

The four model tests show behaviour that is consistent with the physical and numerical processes observed for both the homogenous and Type 1, 2-layer embankment testing (Section 7.3.2). The modelling results for 3-layer Type 1 tests are consistent with the physical processes likely to occur with multiple layers of differing erodibility. This suggests that the modelling assumption applied and tested for the different 2-layer geometries should be extendible to multiple layers of soil type.

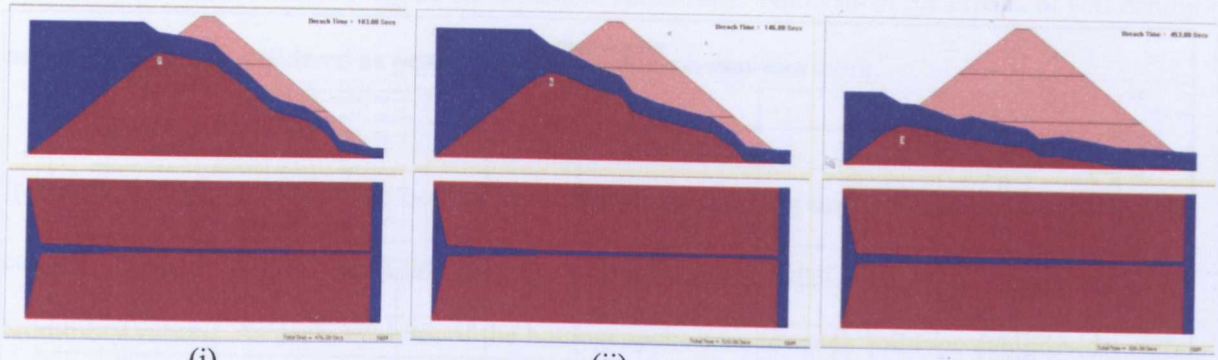

(i) (ii) (iii)

Type 1, 3-layer embankment: All layers 1.3m, K_d=100, 50, 10 from top to base

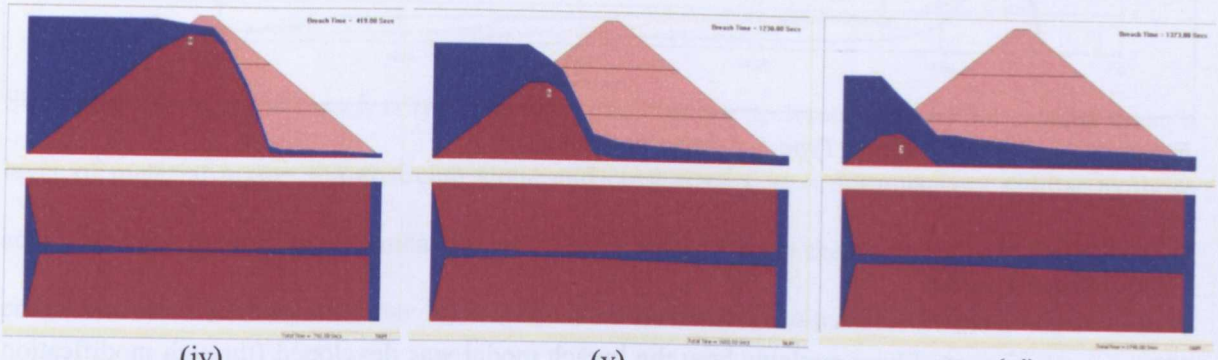

(iv) (v) (vi)

Type 1, 3-layer embankment: All layers 1.3m, K_d=10, 50, 100 from top to base

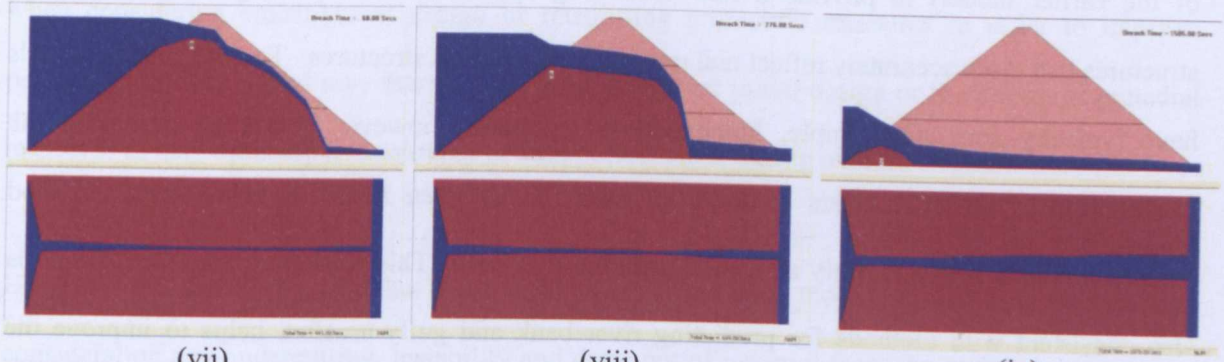

(vii) (viii) (ix)

Type 1, 3-layer embankment: All layers 1.3m, K_d=100, 10, 100 from top to base

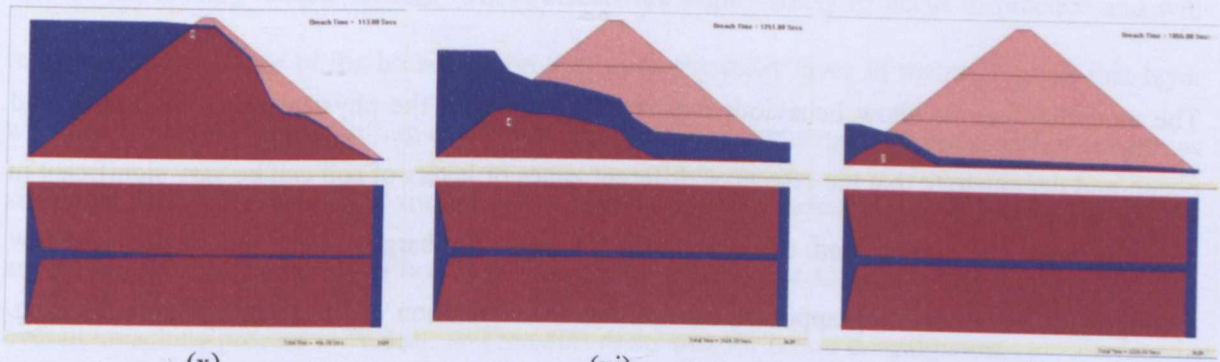

(x) (xi) (xii)

Type 1, 3-layer embankment: All layers 1.3m, K_d=10, 100, 10 from top to base

Figure 7-23 Model simulation of breach growth for homogeneous embankment

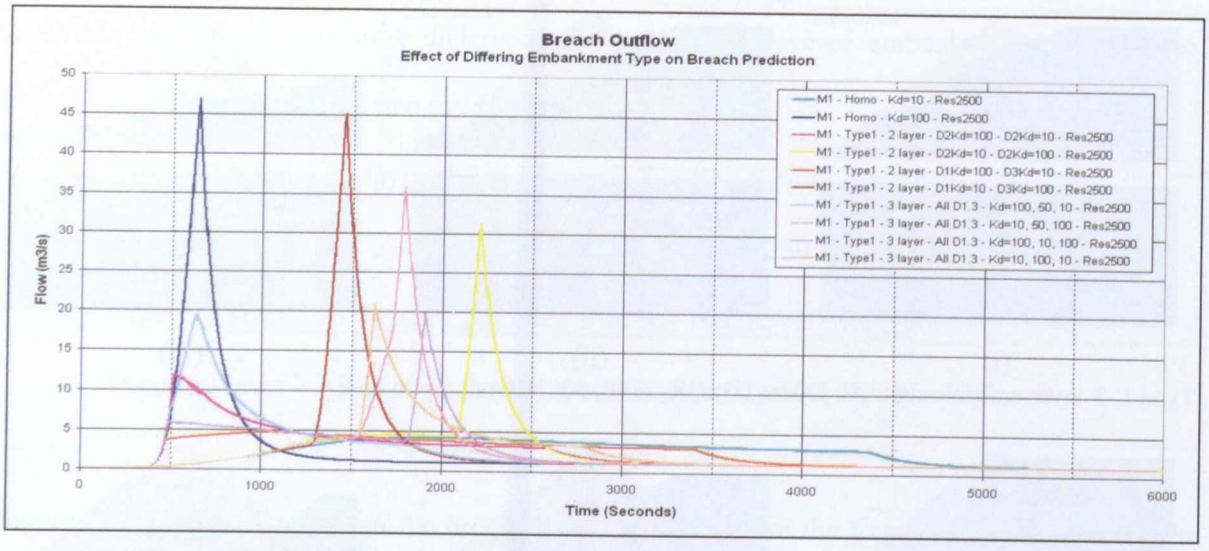

Figure 7-24 Breach outflow: Type 1, 3-layer embankment

7.4 Discussion

The research presented here explains how the breach model was developed (through modification of the earlier model) to provide a new modelling approach for simulating the breaching of structures that more accurately reflect real rather than simplified structures. To date, breach models have typically simulated simple, homogeneous structures, however it can be seen that the introduction of different layers or zones of material (as often found in many dams or flood embankments) can significantly affect the breaching process. This modelling approach, which is also consistent with methods for predicting river bank and gully erosion, helps to improve the flexibility and accuracy of breach prediction.

The modelling results show behaviour that is consistent with the physical processes that would occur, and demonstrate that the effects of different zones or layers of soil can be very significant in affecting both the timing and the magnitude of peak discharge within any breach outflow hydrograph. The modelling approach also allows for simulation of the effects of soil fissuring, since fissuring affects the soil erodibility for an outer layer of the embankment or dam. As such, this new approach for modelling breach provides improved functionality and allows the user to

simulate the effects of more realistic embankment conditions. Analysis of the effects of soil zoning must therefore be considered as part of any routine breach analysis work.

It can be seen that the effect (on outflow) of different layers tends to jump between conditions that can be predicted by considering just the homogeneous embankment case using the different zone erodibility values. As such, analysis of the homogeneous case for each soil type can provide useful boundary conditions within which the true event would sit.

Since flow through the breach is typically controlled by the upstream edge of the eroding crest, a layer of material across the upstream slope and crest results in conditions very similar to those achieved for a homogeneous embankment. Hence, according to these model predictions, a sand embankment covered by an outer layer (crest and upstream at minimum) of clay, would behave similarly to an embankment constructed completely from clay. Such a conclusion is interesting when considering embankment design or retrofitting protection measures in order to improve performance. The model may therefore be used to support initial design or the design of remedial measures to help optimise embankment or dam performance during overflow conditions.

However, it is also recognised that these findings are based upon modelling that does not take into consideration any undercutting, instability and draw out of material from the exposed downstream face of the eroding breach section. These effects are highly likely to occur in practice and will reduce the dependence of the breaching process upon the outer layer of material, since that layer will also fail through undercutting and block failure, rather than simply through surface erosion as simulated here. This process is similar to the process of breach widening described in Section 7.2 and to headcut migration described in Section 6.1. The degree to which this would affect the overall breaching process is unclear, and remains as an area for future investigation.

8. Evaluating Breach Model Performance

Breach model performance has been evaluated in two ways during this research; firstly, on a step by step basis as different ideas have been implemented and refined and secondly, through participation with the international Dam Safety Interest Group (DSIG) breach modelling project. This chapter provides details of model evaluation work undertaken by the writer as part of the DSIG project. This work assesses model performance using the original rather than new zoned breach modelling approach, but the science underpinning the modelling concepts is the same.

8.1 DSIG model performance evaluation

The DSIG breach modelling project (Section 2.5.1) provided a forum to present and discuss all aspects of breach modelling (i.e. physical processes, modelling approaches, case study data, etc.) with international colleagues drawn from both industry and academia around the world. The project goals of identifying and evaluating the most promising breach models meant that participants provided independent and objective feedback on modelling issues and performance. Over a period of 3 years and 3 international workshops, the DSIG project team investigated and reviewed the performance of three breach models (HR BREACH, SIMBA and FIREBIRD) as identified from an earlier international review of breach models (Kahawita, 2007). All team members were encouraged to use and apply the different breach models to selected test data.

A total of seven case studies were used for model performance evaluation. These case studies are detailed in Appendix 3 and breach modelling results presented and explained in the following sections. Conclusions regarding model performance were agreed by the DSIG team through a process of presentations and discussion by each person for each model and test case combination. This process allowed for consideration of important individual factors that affect results such as the individual modelling approaches and different parameters chosen and varied for each specific test case.

For each test case at least two sets of modelling results are given; the first represents an *initial best estimate* and the second a modelling *best fit*. The *initial best estimate* is the model prediction based upon given test case conditions only and without taking into considering the test case results. The modelling *best fit* is the result achieved when trying to manipulate the model to match observed test results. The difference between these two predictions often highlights how models do not address certain physical processes and how models can be manipulated by modellers to simulate certain processes. The *initial best estimate* is more likely to reflect the results that would be achieved in commercial use when no or very limited information on the failure conditions is available.

The assessment of model performance is made by qualitatively reviewing results on a test by test basis. Over the past decade there have been several attempts to objectively assess model performance (Mohamed, 2002, Morris and Hassan, 2005a) but in the writer's experience, the performance of models within various test cases is rarely routine and objective scoring systems typically do not take into account 'non standard' factors. For example, with the IMPACT Gravel test case, models cannot be expected to allow for the effects of ice within surface and body layers, or the delay in initiation caused by the use of stop logs within the initiation notch. These aspects can significantly affect the breaching process and need to be taken into consideration when assessing model performance.

The seven case studies that were selected by the DSIG project team reflect a range of breach cases, from controlled research tests through to uncontrolled dam failures. The type of embankment soil and condition varies from test to test and provides a range of different conditions to challenge the models. This helps to avoid the model performance assessment being skewed by testing against a limited or specific soil and embankment type. The seven test cases, as summarised in Table 2-12, comprised:

• ARS#1	2m high homogeneous earth embankment	USDA lab. data;
• ARS#2	2m high homogeneous earth embankment	USDA lab. data;
• IMPACT Clay	6m high homogeneous clay embankment	IMPACT field data;
• IMPACT Gravel	5m high homog. gravel embankment	IMPACT field data;
• IMPACT Composite	6m high composite embankment	IMPACT field data;
• Oros Dam (Brazil)	36m high zoned dam that failed	Case study data;
• Banqiao Dam (China)	25m high dam that failed	Case study data.

Details of each evaluation test case, including test geometry, soil properties and hydraulic load conditions, can be found in Appendix 3.

8.1.1 Evaluation Test No.1: ARS#1

Modelling results for the ARS#1 test case are shown in Figure 8-1. Additional results are shown in Figure 8-2, demonstrating the importance for breach models to incorporate accurate downstream boundary conditions.

Breach Flow Hydrograph (Figure 8-1 Upper)

The observed test case data is in black ('Observed') and the initial modelling estimate is the hydrograph to the left ('M6DR – Chen – TN71 – VarCd'), with the best fit estimate 'straddling' the observed data line to the right ('M7DR-Chen-t=5200-VarCd'). The initial estimate predicts a flood hydrograph that is similar in shape and magnitude to that observed, but which occurs too early in comparison to the observed test data. The best fit modelling result is achieved by manually delaying initiation of the breach (to run time = 5200s) within the model. This would appear to indicate that the breach initiation timing is not well predicted, either reflecting the poor prediction of grass cover erosion or critical shear stress for the soil.

One plausible explanation of the surges in breach discharge shown on the observed flood hydrograph is block failure into the breach. Breach flow has been calculated from changes in the

upstream pond level and the relatively small area of the pond makes this susceptible to highlighting the effects of step changes in breach flow area. It is important to recognise that the shape of the flood hydrograph is a function of both the breach formation process and the stage volume relationship for the upstream reservoir.

Reservoir Levels (Figure 8-1 Middle)

Behaviour of the predicted reservoir levels is consistent with the flow hydrographs, in as much as the best fit prediction simulates the test data well, whilst the initial modelling estimate shows a reservoir level that drops too early within the test. It can be noted, however, that the rate at which the reservoir level drops is comparable to that of the observed test data.

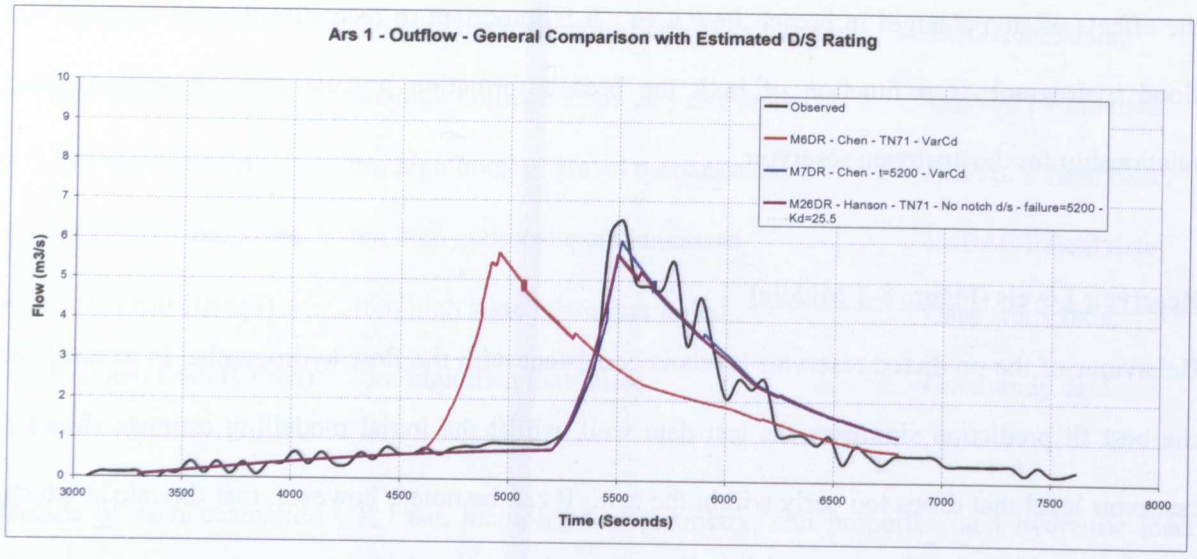

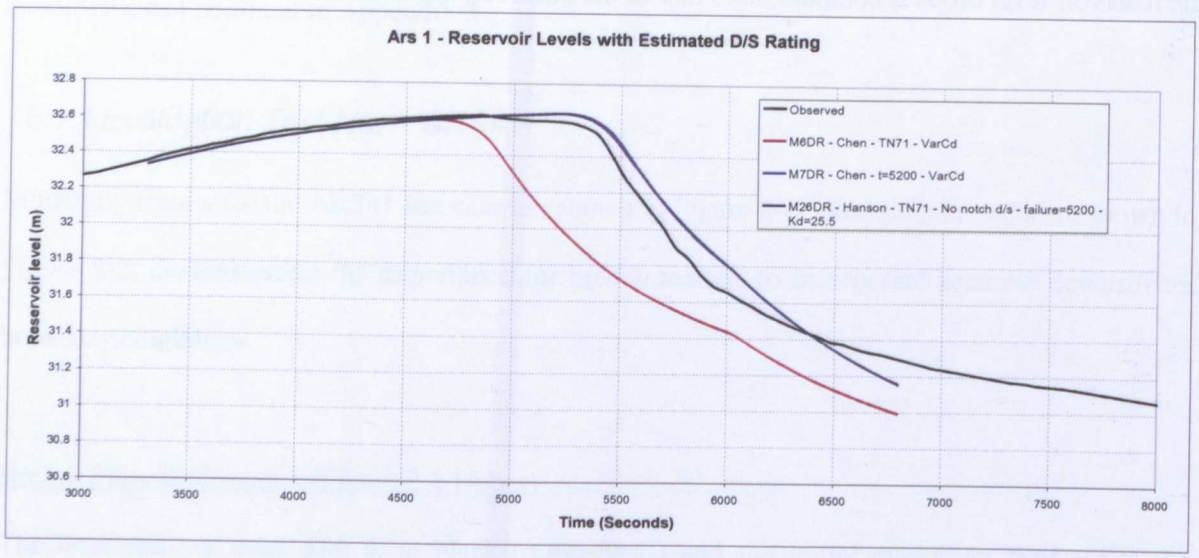

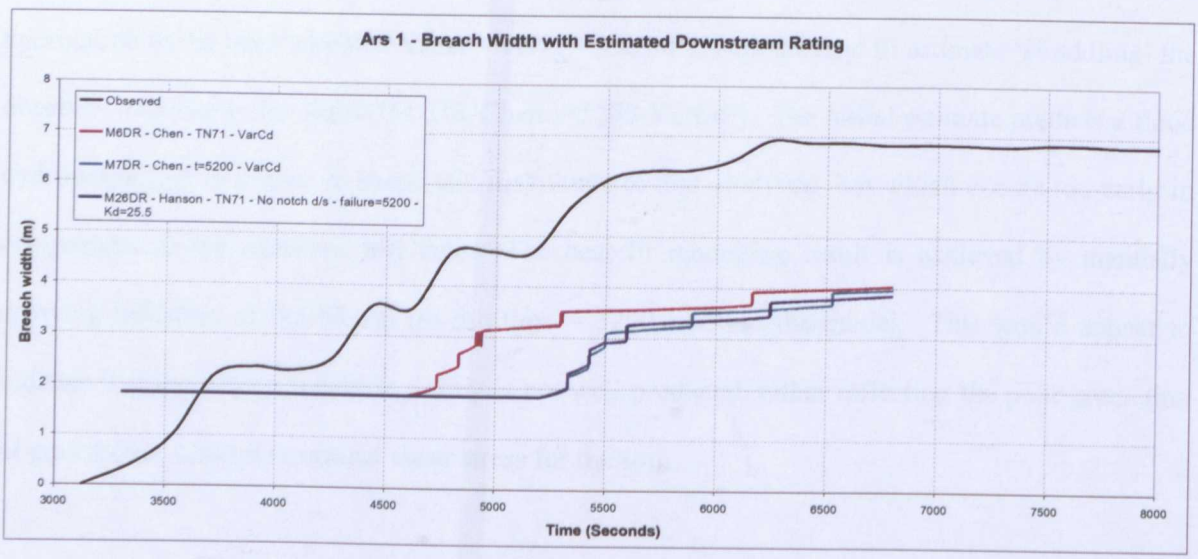

Figure 8-1 HR BREACH modelling results for DSIG test ARS#1 (Upper: breach flow; Middle: reservoir level; Lower: breach width)

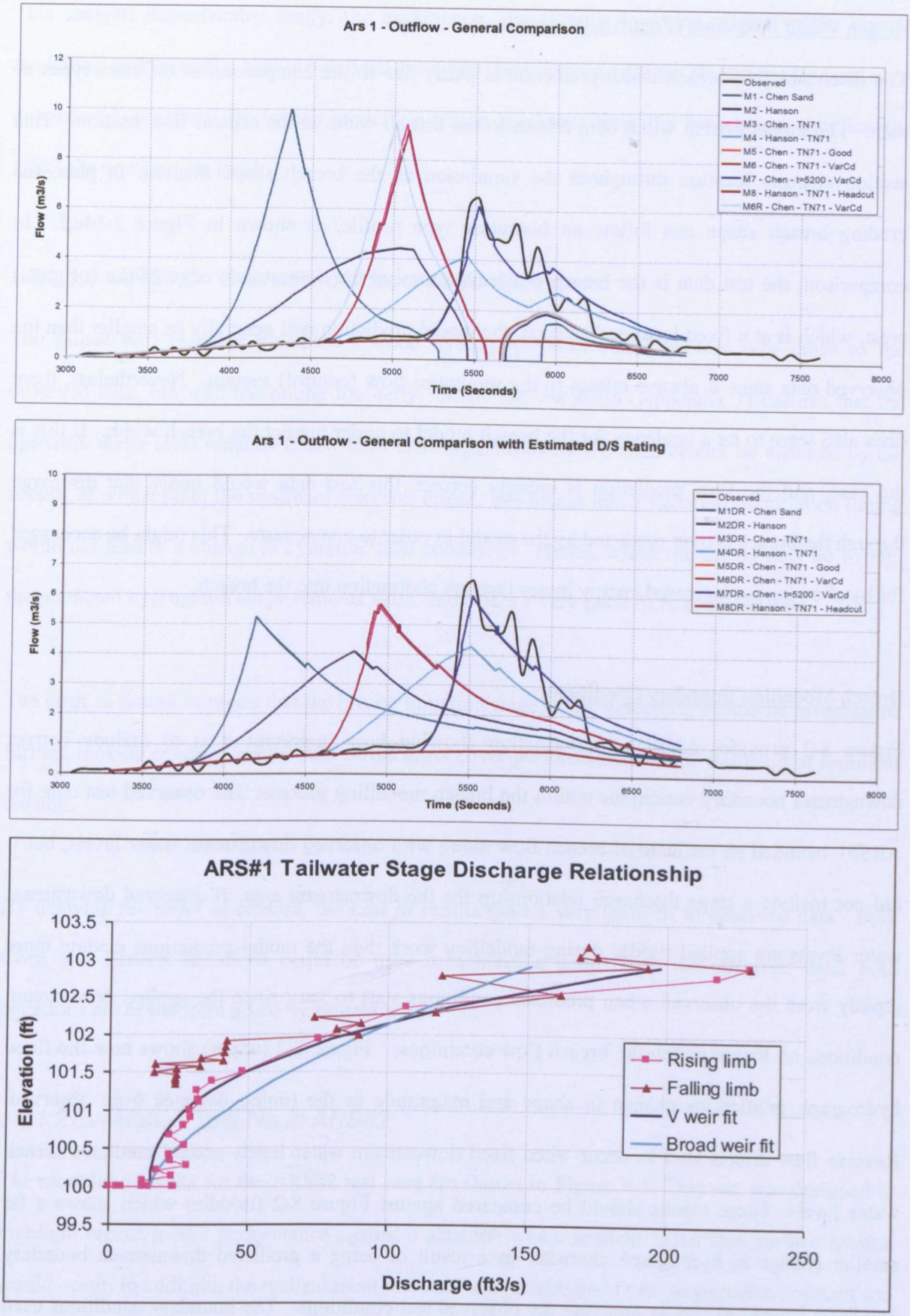

Figure 8-2 Analysis of boundary conditions for DSIG test ARS#1 (Upper: breach flow with fixed d/s boundary; Middle: breach outflow with predicted d/s boundary; Lower: Predicted d/s boundary relationship)

Breach Width Prediction (Figure 8-1 Lower)

The discrepancy in breach width prediction is partly due to the comparison of different types of data. The model breach width data relates to the breach width at the critical flow section. This section changes location throughout the simulation as the breach shape evolves. In plan, the eroding breach shape can follow an hourglass type profile, as shown in Figure 2-14e,f. In comparison, the test data is the breach width measured at the downstream edge of the (original) crest, which is at a fixed location. As such, the model prediction will generally be smaller than the observed data since it always relates to the minimum flow (control) section. Nevertheless, there does also seem to be a tendency for the breach model to under predict the breach width. If this is the case, and the flow prediction is broadly correct, this test data would imply that discharge through the breach is over predicted by the model in order to compensate. This might be accounted for by allowing for increased energy losses through contraction into the breach.

Breach Modelling Boundary Conditions

Figure 8-2 provides additional information showing how important it is to include correct downstream boundary conditions within the breach modelling process. The observed test data for ARS#1 included an estimate of breach flow along with observed downstream water levels, but it did not include a stage discharge relationship for the downstream area. If observed downstream water levels are applied rigidly during modelling work then the model predictions deviate more rapidly from the observed when predicted conditions start to vary since the applied downstream conditions no longer match the breach flow conditions. Figure 8-2 (upper) shows how the flood hydrograph predictions change in shape and magnitude as the timing deviates from observed. Reverse flow effects start to occur when fixed downstream water levels exceed predicted breach water levels. These results should be compared against Figure 8-2 (middle) which shows a far smaller change in hydrograph character as a result of using a predicted downstream boundary condition instead of rigidly applying the observed test conditions. The boundary conditions used were calculated by matching a predicted stage discharge curve to the observed downstream test data (Figure 8-2 (lower)). The best fit was achieved using a V shaped weir formula.

This analysis demonstrates firstly, the importance of including drowning effects within breach modelling and secondly, that pre-defined head-time boundary conditions should not be used as a downstream boundary for breach modelling where discharge from the breach can significantly affect the downstream level.

8.1.1.1 ARS#1 – Overview of model performance

The *initial best estimate* predicted a flood hydrograph with characteristics very close to the observed data, but with the timing too early. Since the test setup (Appendix 3) ensures that the upstream water level remains steady until discharge through the breach cannot be matched by the supply, at which point the upstream reservoir drains, this means that a variation in initiation timing would not lead to a change in hydraulic load conditions. Hence, whilst the timing may be wrong, the predicted hydrograph shape remains valid, and offers a very good fit to observed data.

The error in timing suggests that the breach initiation stage of the modelling should be investigated further, looking at either one or both of the grass cover performance and the initiation of sediment erosion.

By delaying the onset of erosion, the *best fit* results gave a very good fit to observed data. Both Chen and Hanson equations could be used to achieve a good fit to the observed data; both equations are of the form given by Equation 6.2.

8.1.2 Evaluation Test No.2: ARS#2

The modelling results for the ARS#2 test case are shown in Figure 8-3. This test was designed to highlight breach model performance against a situation where headcut rather than surface erosion would occur. In addition, the embankment material was constructed from very erosion resistant soil (measured K_d = 0.02ft/h / lb/ft^2), and the embankment did not breach during the test. Hence this is also a test to see whether models can predict that breach failure will not occur.

Breach Flow Hydrograph (Figure 8-3 Upper)

Results show a very good match between test and model prediction data. However, this reflects the fact that breach does not occur (which, in itself is a positive result from the model) and the model is showing that the overtopping outflow simply balances the steady inflow (to the reservoir upstream of the test embankment). Hence, the performance of the model in predicting that failure does not occur is important, whilst the flow hydrograph itself is less important. Since breach does not occur for either run, both simulations predict the same outflow hydrograph.

Reservoir Levels (Figure 8-3 Middle)

Analysis of the reservoir water level results reveals more than the outflow hydrograph results. This plot shows that the initial estimate, made using the Hanson erosion equation in surface erosion mode (Run M4), deviates from the observed data (and the best fit data). The best fit data was achieved by using the Hanson erosion equation, but in headcut rather than surface erosion mode (Run M5). When simulating headcut without embankment failure, the embankment crest elevation does not change. Hence, the predicted breach outflow matches the reservoir inflow and the reservoir level remains steady. When simulating surface erosion without embankment failure, some erosion of the embankment crest does occur, albeit not sufficient to initiate breach formation, hence there is a small but steady reduction in the reservoir level as the crest, and hence flow control point, erodes.

The transition or balance between headcutting and surface erosion processes during breach growth has not yet been clearly defined. At the extremes (i.e. highly erodible sand or a very resistant clay) it can be seen that one or other process clearly dominates, whilst in the area between, as erodibility of the soil changes, both processes may occur. The significance of these processes for the accuracy of breach prediction suggests that an integrated approach that uses and transitions between both processes within the breach model as a function of soil erodibility and load conditions would be a sensible approach for building a breach prediction model that could be applied to a range of soil types and conditions.

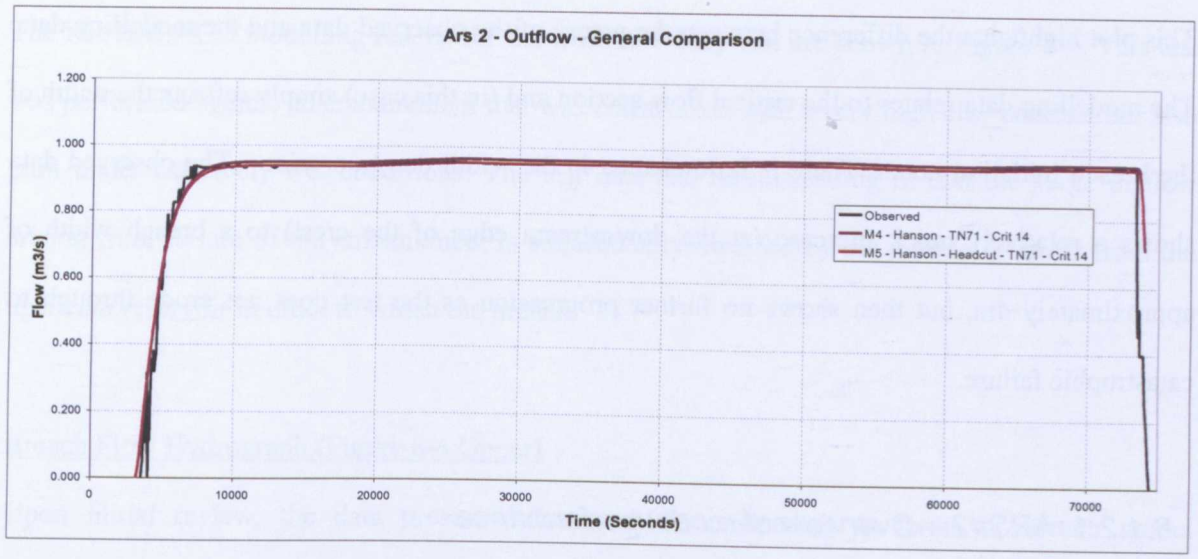

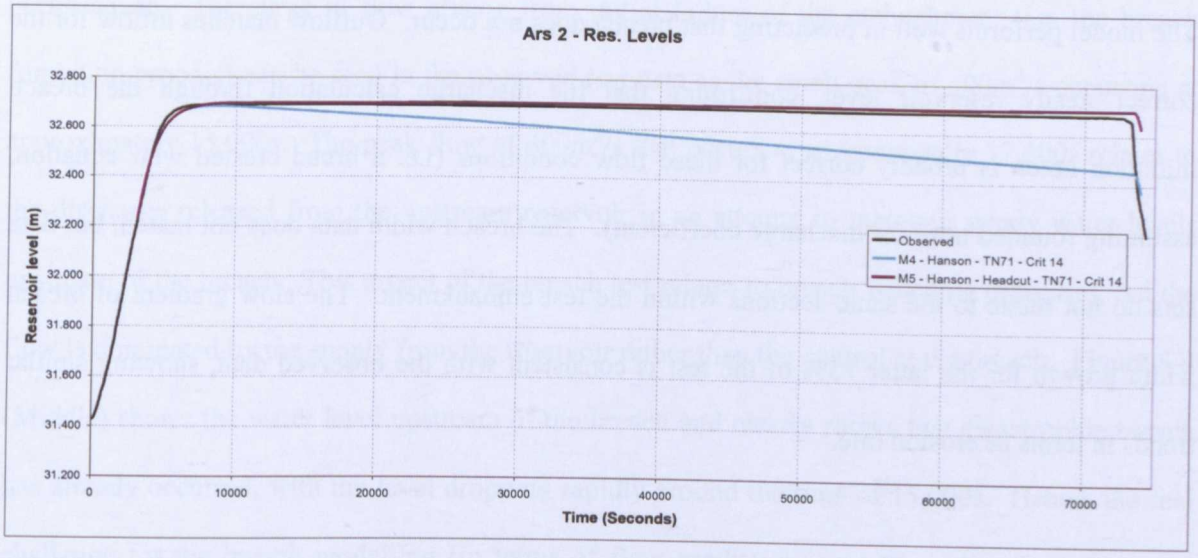

Figure 8-3 HR BREACH modelling results for DSIG test ARS#2 (Upper: breach flow; Middle: reservoir level; Lower: breach width)

Breach Width Prediction (Figure 8-3 Lower)

This plot highlights the difference between the nature of the observed data and the modelling data. The modelling data relates to the critical flow section and (in this case) simply reflects the width of the breach initiation notch. There is little change in the width due to erosion. The observed data shows a relatively quick increase (at the downstream edge of the crest) to a breach width of approximately 4m, but then shows no further progression as the test does not erode through to catastrophic failure.

8.1.2.1 ARS#2 – Overview of model performance

The model performs well in predicting that breach does not occur. Outflow matches inflow for the correct steady reservoir level, confirming that the discharge calculation through the breach initiation notch is broadly correct for these flow conditions (i.e. a broad crested weir equation, assuming rounded nose for discharge coefficient). The breach width data does not match, but data sets do not relate to the same sections within the test embankment. The slow gradient of breach width growth for the latter 75% of the test is consistent with the observed data, showing similar trends in terms of erosion rate.

Apart from demonstrating that the model can predict a non-failure case, this test really highlights the differences that will arise from the use of a headcut versus a surface erosion model. When applying the model to simulate surface erosion, a slow, but steady rate of erosion of the crest can be seen, which in turn leads to a steady drop in the reservoir water level as the crest flow control point drops. The headcut model assumes no crest erosion can occur, hence the discharge remains constant, as does the reservoir level. For this soil type and load conditions, the latter is a more appropriate modelling approach. This highlights the need for a model which can incorporate both headcut and surface erosion processes such that different processes can be used for different soil type and state conditions.

8.1.3 Evaluation Test No.3: IMPACT Clay (IMPACT Test1-02)

The HR BREACH modelling results for the IMPACT Clay test are shown in Figure 8-4. This test was performed against an embankment that was constructed with a very high clay content, but also built under extremely wet conditions. The test data can be misleading in that the surge in flow arising from failure of the embankment is subsequently dwarfed by the release of water from the upstream reservoir in order to widen the breach.

Breach Flow Hydrograph (Figure 8-4 Upper)

Upon initial review, the data presented here can be misleading in terms of breach model performance. The surge in flow arising from initial failure of the embankment (i.e. the breach formation process) can be seen in the observed test data as the small peak of $100m^3/s$ occurring at approximately 15,000s. The peak flow of $400m^3/s$ that occurs at approximately 17,500s relates to the discharge released from the upstream reservoir in an attempt to maintain steady water levels upstream of the breach. This aspect of the breach test relates to breach widening processes, but the flow is dominated by the supply from the reservoir rather than the control at the breach. Figure 8-4 (Middle) shows the water level upstream of the breach and clearly shows that catastrophic breach has already occurred, with the level dropping rapidly around the time of 15,000s. Hence, the real challenge for the breach modelling (in terms of flow prediction) was to predict the timing and magnitude of the surge arising from initial failure, rather than the through flow arising from the continued release of water from the upstream reservoir.

The *initial best estimate* (Run M2, Figure 8-4 upper) used the Hanson equation with a surface erosion breaching process. This missed the timing of the breach initiation stage, hence does not show a surge in flow at around 15,000s. The *best fit* model runs (Runs M7 and M19, Figure 8-4 upper) used very specific conditions in surface and headcut modes to try and recreate the timing, with some success. The best solution appears to be given by the headcut model, but only with specific soil erosion parameters applied.

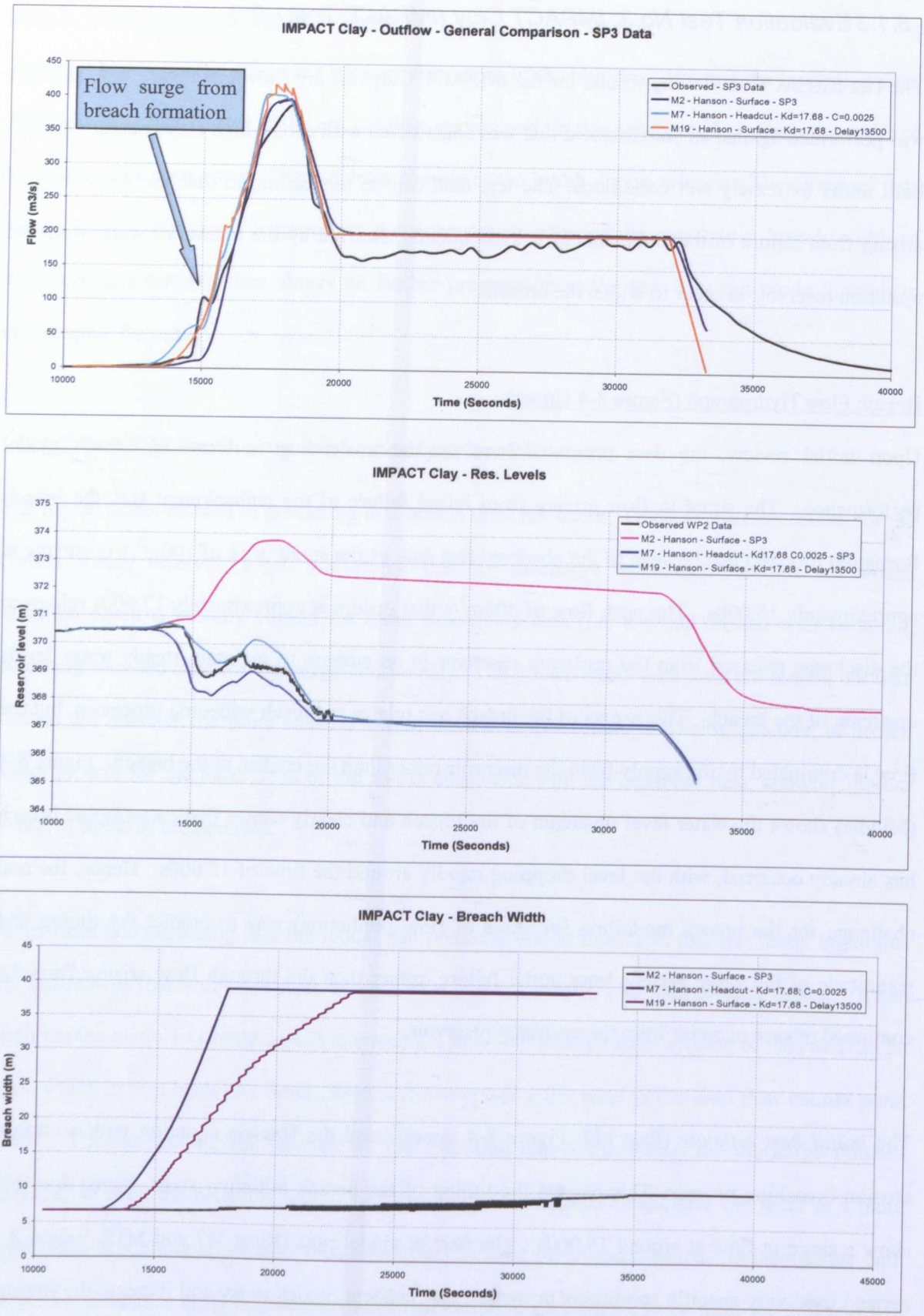

Figure 8-4 HR BREACH modelling results for the DSIG test IMPACT Clay (Upper: breach flow; Middle: reservoir level; Lower: breach width)

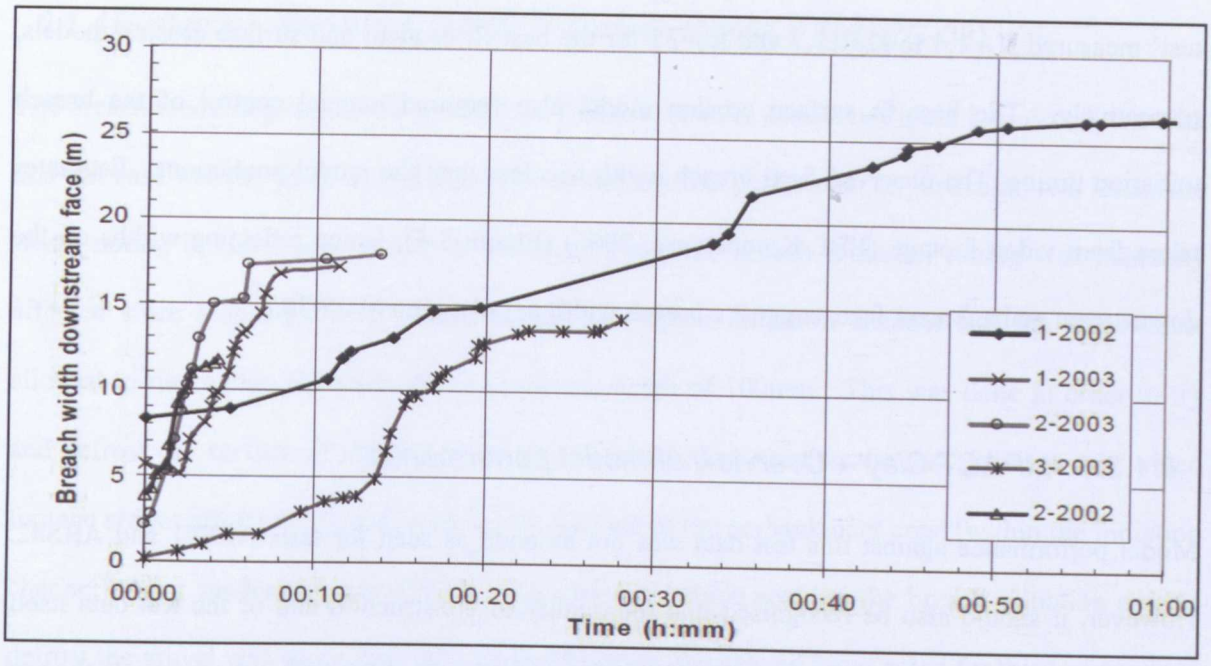

Figure 8-5 Initial estimates of breach width (at downstream embankment surface) taken from video footage of IMPACT project tests (EBL Kompetanse, 2006)

The test numbers listed in Figure 8-5 above relate to the five IMPACT project field tests, as detailed in Table A3-1. 1-2002 refers to the IMPACT clay test (Evaluation Test No. 3) and 2-2002 to the IMPACT gravel test (Evaluation Test No. 4).

Reservoir Levels (Figure 8-4 Middle)

Analysis of the water level immediately upstream of the breach shows how the model performed more clearly than the plots of breach discharge. The *initial best estimate* (Run M2) does not predict breach formation until upstream water levels have risen considerably. The subsequent *best fit* model runs (Runs M7 and M19) come closer to the observed data, reproducing similar characteristics. The headcut process appears to recreate the level behaviour best, but shows an error with the timing. This suggests that there are inconsistencies within the model between predicted initiation and breach widening rates for this particular case.

Breach Width Prediction (Figure 8-4 Lower)

This plot highlights the significant difference between the *initial best estimate* and subsequent *best fit* estimates for breach width. It should be noted that soil erodibility was modified from the 'jet

test' measured K_d=1.4 to K_d=17.7 and K_d=35 for the best fit headcut and surface erosion models, respectively. The best fit surface erosion model also required manual control of the breach initiation timing. The observed final breach width was less than the model predictions. Estimates taken from video footage (EBL Kompetanse, 2006) (Figure 8-5), hence reflecting widths on the downstream embankment face, suggest a breach width in the region of 25-30m.

8.1.3.1 IMPACT Clay – Overview of model performance

Model performance against this test data was not as good as seen for tests ARS#1 and ARS#2. However, it should also be recognised that the quality of construction and of the test data itself (Hassan and Morris, 2008) was lower than that provided for the ARS tests. A review of the test data quality emphasises the problems that occurred during construction (extremely wet weather conditions) that resulted in changes to the way in which material was compacted. Hence, it is unclear how the clay erodibility may have varied through the embankment construction. It is notable that in trying to achieve the *best fit* results, all modelling scenarios required the clay erodibility parameter to be significantly increased. In addition, cracks and fissures were visible in the structure before testing began and a piping failure along the left rock abutment nearly occurred during testing in preference to overtopping breach. This combination of factors means that there is a significant degree of uncertainty within the test data itself, and this should be recognised when comparing model performance.

The modelling results for this test case suggest that the best modelling approach was by using headcut simulation. Indeed, clear headcut processes could be seen during the field test. As detailed above, the use of significantly higher soil erodibility values was also needed within the model simulations to reproduce observed conditions probably reflecting the poor and variable construction quality of the embankment. Upon initial investigation the accuracy of breach width prediction appears relatively poor, although the spread of results between *initial best estimate* and *best fit*, including headcut simulation, does 'band' the observed results.

8.1.4 Evaluation Test No.4: IMPACT Gravel (IMPACT Test 2C-02)

The breach modelling results for the IMPACT Gravel test are shown in Figure 8-6. A concern with this test case was the freezing conditions when the test was performed. In particular, two issues are worth noting in relation to breach prediction: firstly, the breach initiation timing was manually affected since stop logs were placed across the breach initiation channel and the water level allowed to rise within the initiation channel to a depth of 100mm. This was done in order to try and defrost the surface of the embankment material before starting the test. Prior to this, video footage shows efforts to try and break up the surface of the embankment crest (within the initiation channel) using spades (Morris, 2009). The extent to which soaking the breach initiation area to defrost the gravel was successful, is unclear. However, the second issue noted for this test suggests that these efforts were not too successful since, when the breach test gets underway, the dam can be seen to erode predominantly by headcut erosion. This is not expected for erosion of a non cohesive gravel dam. A large, single step headcut was clearly visible right up until the point of embankment failure through to the upstream face of the reservoir (Figure 2-16). Similarly, the headcut channel sides were vertical. The 'slot' that developed through this embankment during breach initiation was more precise, with clean cut vertical sides to the breach, than that which developed during breach initiation of the IMPACT Clay embankment. Hence, it is difficult to gauge how effective the breach models can be for this test without greater clarification of the real test conditions (i.e. the real gravel state). If frozen to significant depths, then the performance of the gravel under breach conditions cannot be directly reproduced by the models without significantly reducing the assumed soil erodibility, to account for the ice. As with the IMPACT Clay test data, there is also uncertainty around the true values of measured flow data (Hassan and Morris, 2008). For this test case, the most likely solution could not be resolved, hence two potential outflow hydrographs are presented for comparison against modelling data and detailed discussion of the comparison of results is not possible.

Breach Flow Hydrograph (Figure 8-6 Upper)

This shows two breach model run results (*initial best estimate* (Run M5) and *best fit* (Run M10)) compared against two potential sets of observations (Hassan and Morris, 2008). Both the *initial best estimate* and the *best fit* simulations predict a breach flood hydrograph of approximately the right magnitude. However, even where the timing of stop log release is known, the *initial best estimate* model prediction of breach is far too quick in comparison to the observed data. Manual control of the initiation timing and erodibility parameters is required in order to produce results close to those that were observed. It is also noticeable that the predicted hydrograph shapes do not match those observed. Observed data suggests a very abrupt, catastrophic failure leading to a very rapid rate of rise in flood flow. This is more consistent with the failure of a rigid (frozen?) structure than the progressive erosion of a non cohesive gravel embankment. This is also consistent with observations from the video footage. Figure 8-7 shows results from a wider range of breach modelling runs, all of which struggle to reproduce the observed hydrograph shape.

Reservoir Levels (Figure 8-6 Middle)

The predicted variation in reservoir level is consistent with the observed flows discussed above, both in terms of timing and of hydrograph shape (i.e. the rate at which breach formation occurred).

Breach Width Prediction (Figure 8-6 Lower)

The observed breach width for this test was in the region of 12m (see also Figure 8-5) hence the prediction of approximately 9m is close. This is particularly so, given that the observed data (Figure 8-5) relates to observations on the downstream face, rather than at the critical flow section, and is hence likely to be greater than predictions from the critical flow section. However, the rate of predicted widening is slower than observed. Again, the relevance of this prediction is likely to be overshadowed by the uncertainty relating to the state of the gravel material during testing.

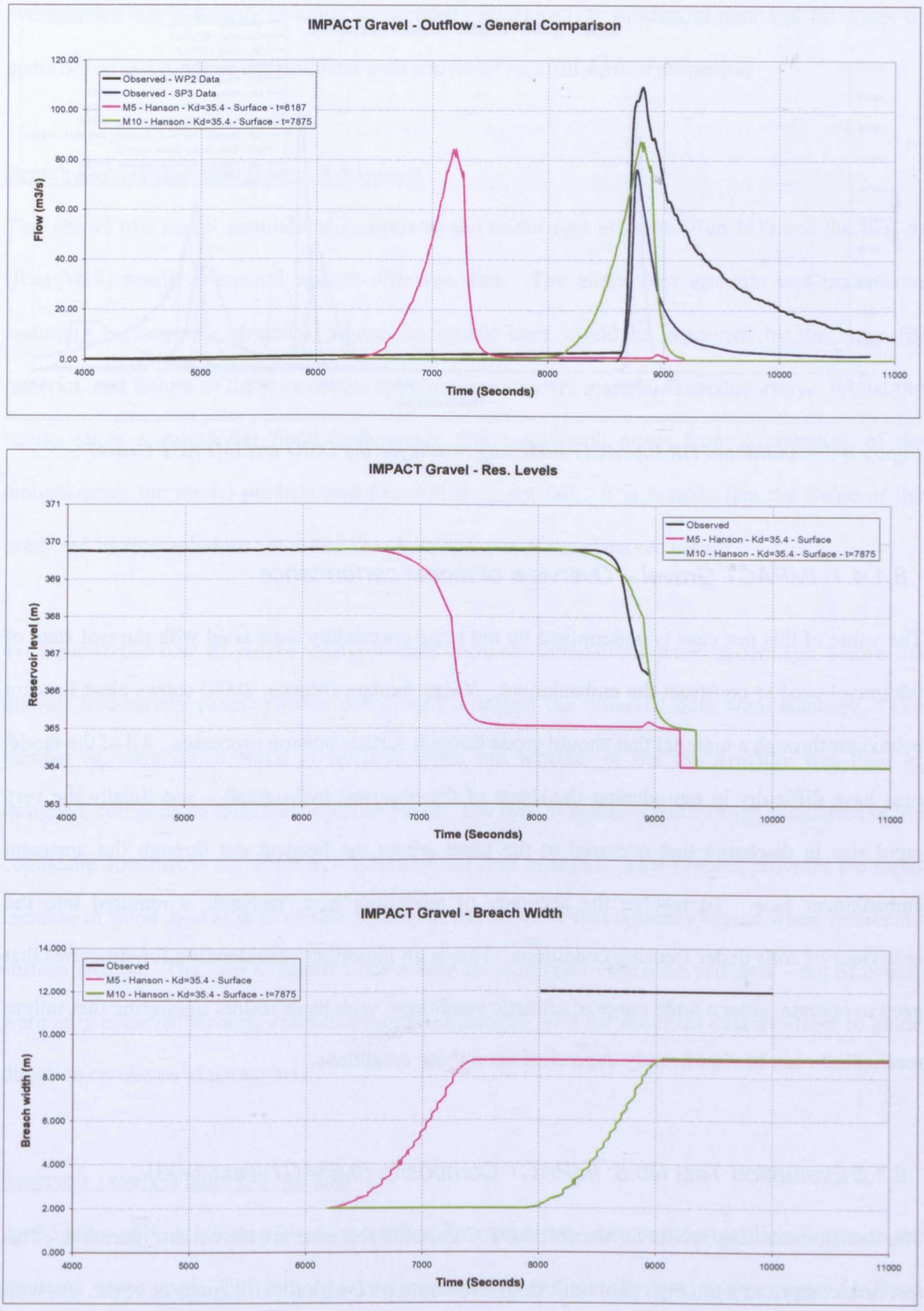

Figure 8-6 HR BREACH modelling results for the DSIG test IMPACT Gravel (Upper: breach flow; Middle: reservoir level; Lower: breach width)

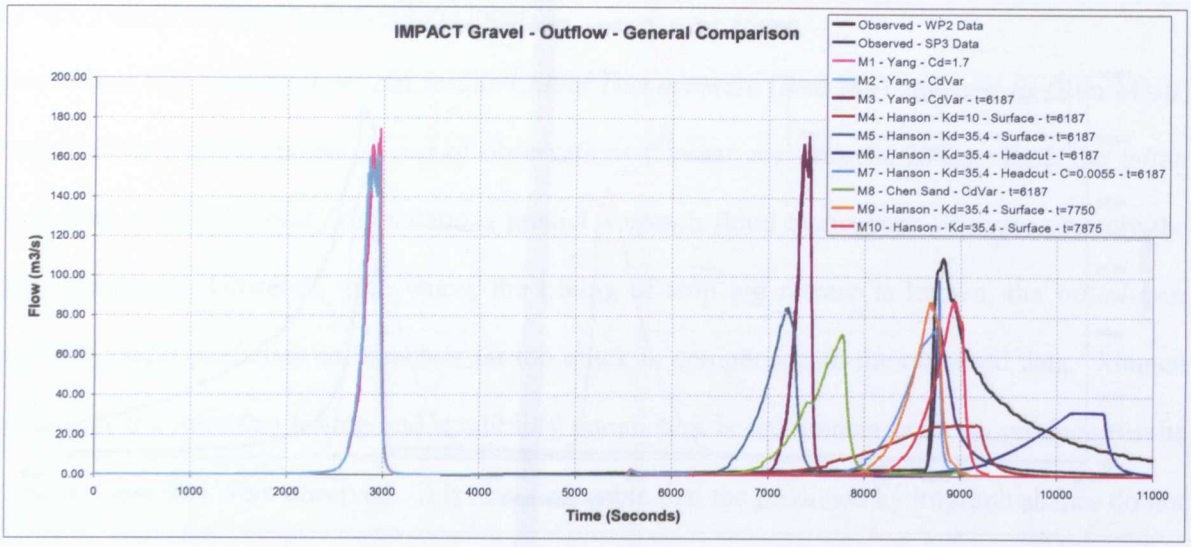

Figure 8-7 Additional HR BREACH modelling results for the DSIG test IMPACT Gravel

8.1.4.1 IMPACT Gravel – Overview of model performance

The value of this test case is undermined by the large uncertainty associated with the real state of the gravel used to construct the embankment. Video footage (Morris, 2009) shows clear headcut behaviour through a material that should erode through surface erosion processes. All of the model runs have difficulty in reproducing the shape of the observed hydrograph – specifically the very rapid rise in discharge that occurred at the point where the headcut cut through the upstream embankment face. To resolve the accuracy of modelling here, research is required into the behaviour of soils under freezing conditions. This is an important consideration for structures that need to operate under a wide range of climatic conditions, with these results suggesting that failure mechanisms can be significantly dependent upon those conditions.

8.1.5 Evaluation Test No.5: IMPACT Composite (IMPACT Test 1-03)

The breach modelling results for the IMPACT Composite test case are shown in Figure 8-8. This test case comprised a 6m high dam built from a moraine core with rockfill zones or cover. As with other IMPACT field data, there are some uncertainties surrounding the final test data (Hassan and Morris, 2008). Particularly relevant to this case is the quality of construction relating to the depth of rock fill. Video footage suggests that this may have been quite limited in places, hence the

embankment could behave as either a composite structure (i.e. substantial core and fill zones of material) or as a moraine embankment with a layer of rock fill surface protection.

Breach Flow Hydrograph (Figure 8-8 Upper)

This shows two model simulations comprising the *initial best estimate* (Run M1) and the *best fit* (Run M19) results compared against observed data. The *initial best estimate* was undertaken assuming a composite structure, where the central core would be supported by the outer fill material, and failure of the core occurs structurally as the fill material is eroded away. Whilst the results show a substantial flood hydrograph, this hydrograph arises from overtopping of the embankment; the model predicts that the core does not fail. It is notable that the shape of the predicted hydrograph does not match the characteristics of the observed data.

To achieve the *best fit* results nearly twenty different simulations were undertaken before the distinct hydrograph characteristics that closely matched the observed data were achieved. The number of variables in terms of material types and whether or not the structure was built as designed, complicated this modelling challenge. The best fit results arose through simulation of the composite structure – i.e. structural failure of the core material. This process provides the rapid increase in flood discharge as compared to a slower increase that typically occurs when simulating surface erosion. The *best fit* results offer a very close match to the observed data – but of course were only achieved through extensive model adjustment with the observed data available to guide direction on choice of parameters.

Reservoir Levels (Figure 8-8 Middle)

At the point of breach formation, the predicted flow conditions are consistent with variations in the upstream water level. The initial best estimate data shows that the level rises in order for flood flow to pass over the crest of the embankment, without breach occurring. The best fit data shows similarities to the observed data, but with a slight shift in timing.

However, the initial water levels (prior to breach or overtopping) do show a discrepancy. Both initial best estimate and best fit simulations predict lower than observed water levels for the given discharge. This may relate to confusion regarding the actual width and invert level of the test embankment initiation notch. Since earlier tests (e.g. ARS2) appeared to validate the notch flow simulation by the model, this is considered to be the most likely cause for the differences.

Breach Width Prediction (Figure 8-8 Lower)

The data relating to the initial best estimate shows a very large breach width of approximately 39m compared to the observed value of approximately 12m. However, these results were for conditions where the model predicted that the central core of the composite structure did not fail and hence the model eroded width data relates only to erosion of the supporting (outer) material rather than for a catastrophic breach. Results for the best fit simulation show much better agreement with the observed data. It should also be noted that the observed data (in detail in Figure 8-5) relates to the erosion width observed on the downstream face of the embankment, whilst the modelled data relates to the critical flow control section. Modelled data will therefore show a smaller value than the downstream face observations because of the typical hour glass plan form shape of a breach.

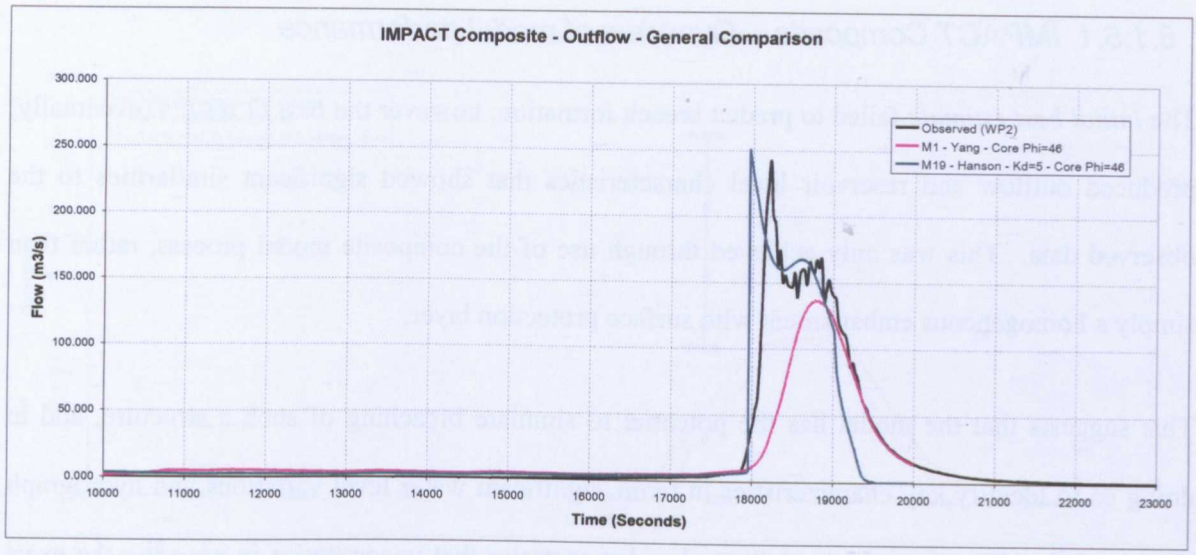

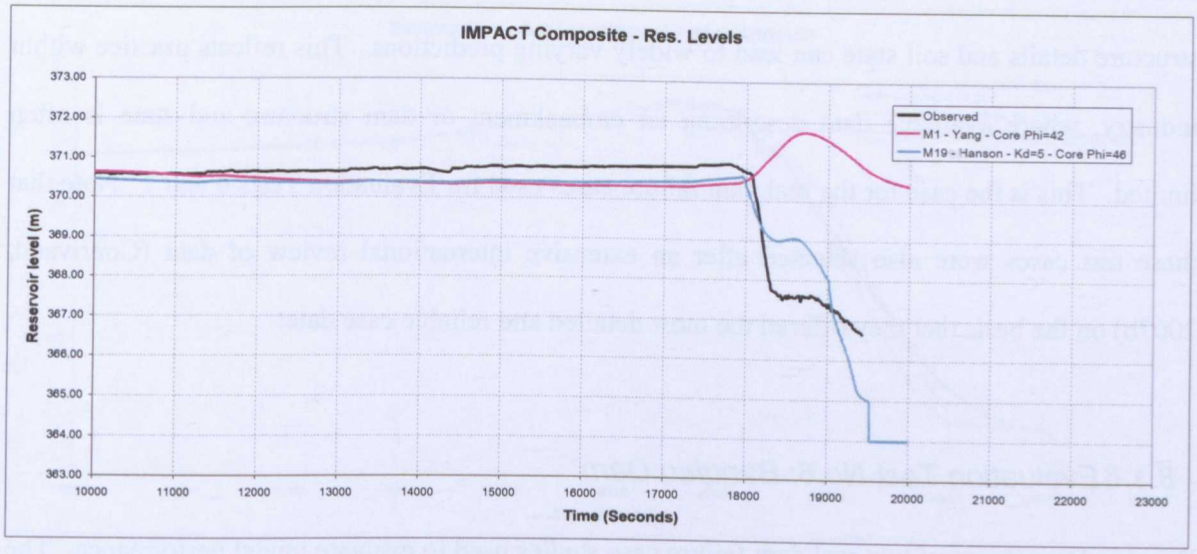

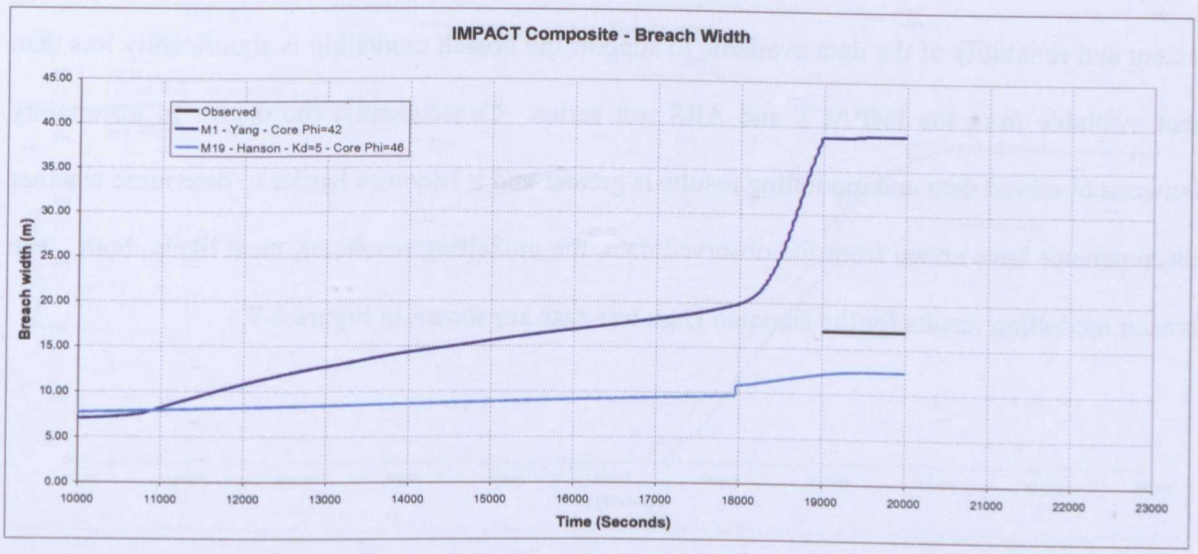

Figure 8-8 HR BREACH modelling results for the DSIG test IMPACT Composite (Upper: breach flow; Middle: reservoir level; Lower: breach width)

8.1.5.1 IMPACT Composite – Overview of model performance

The *initial best estimate* failed to predict breach formation, however the *best fit* results (eventually) produced outflow and reservoir level characteristics that showed significant similarities to the observed data. This was only achieved through use of the composite model process, rather than simply a homogeneous embankment with surface protection layer.

This suggests that the model has the potential to simulate breaching of such a structure, and in doing so to identify key characteristics in terms significant water level variations and hydrograph characteristics. However, the modelling also demonstrates that uncertainties in knowing the exact structure details and soil state can lead to widely varying predictions. This reflects practice within industry, where available data describing an embankment or dam structure and state is often limited. This is the case for the real dam failure cases used for Evaluation Tests 6 and 7. Note that these test cases were also selected after an extensive international review of data (Courivaud, 2007b) on the basis that they offered the most detailed and reliable case data!

8.1.6 Evaluation Test No.6: Banqiao Dam

Banqiao Dam is one of two real dam failure case studies used to evaluate model performance. The extent and reliability of the data available to support the breach modelling is significantly less than that available from the IMPACT and ARS test series. Consequently, the degree of uncertainty between observed data and modelling results is greater and it becomes harder to determine whether discrepancies have arisen from the observed data, the modelling results or, most likely, both. The breach modelling results for the Banqiao Dam test case are shown in Figure 8-9.

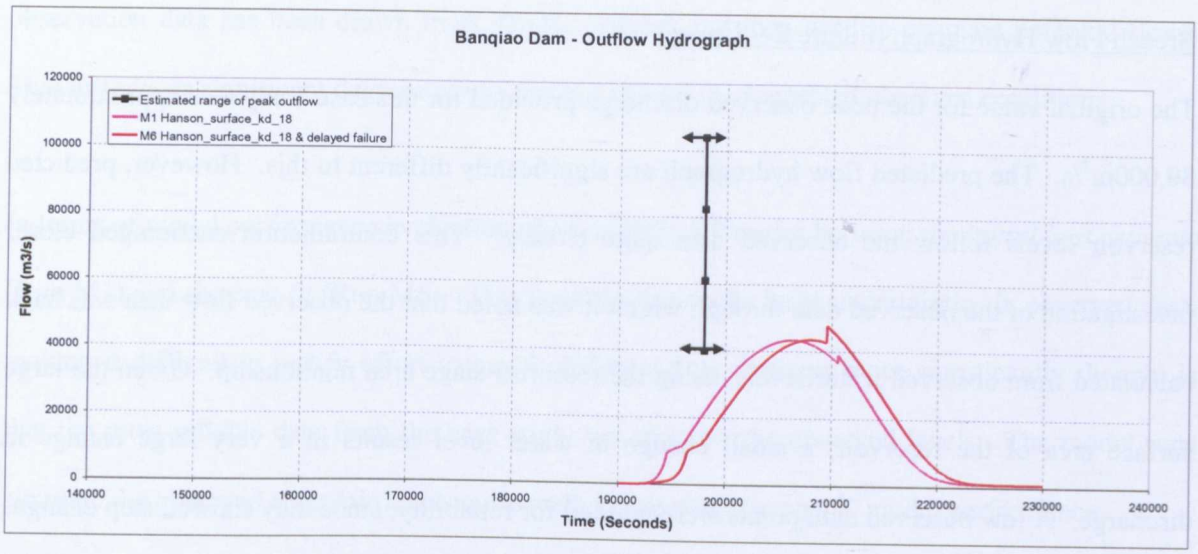

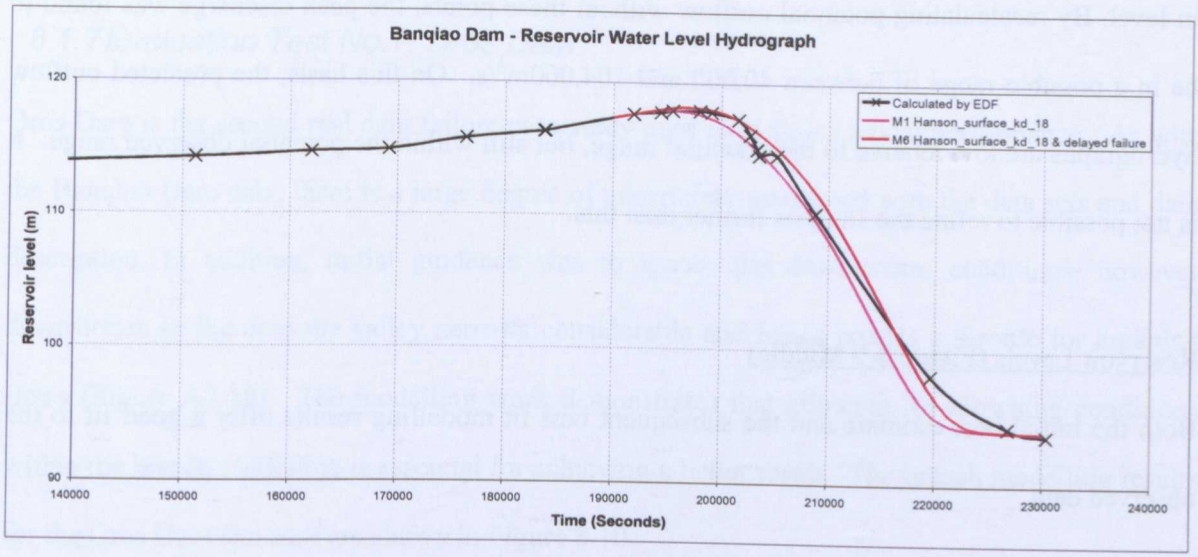

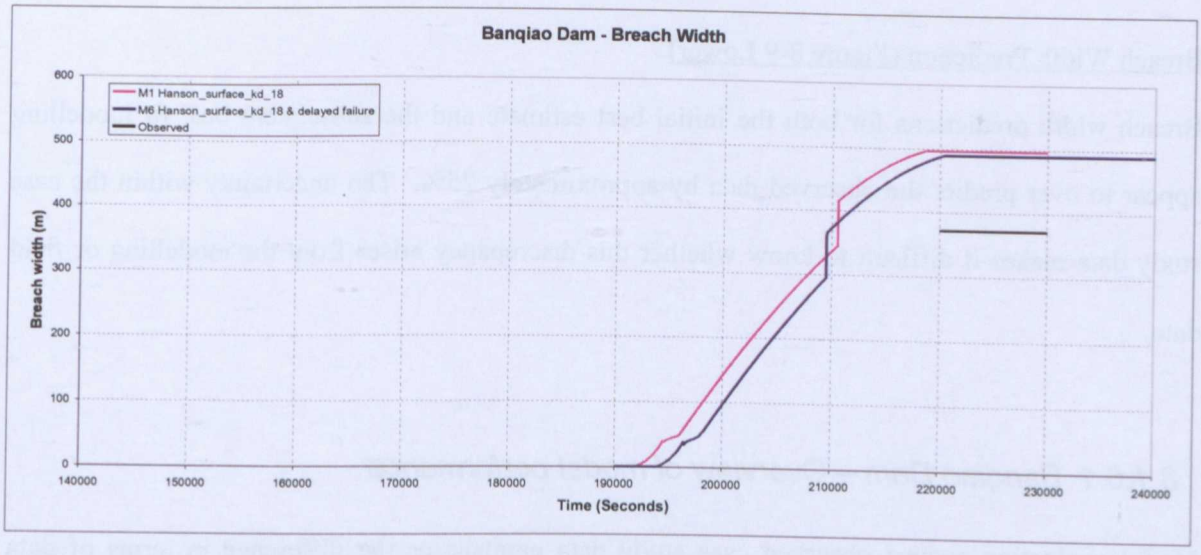

Figure 8-9 HR BREACH modelling results for the DSIG test Banqiao Dam (Upper: breach flow; Middle: reservoir level; Lower: breach width)

Breach Flow Hydrograph (Figure 8-9 Upper)

The original value for the peak observed discharge provided for this case study was approximately 80,000m^3/s. The predicted flow hydrograph are significantly different to this. However, predicted reservoir levels follow the observed data quite closely. This contradiction encouraged closer investigation of the observed data through which it was noted that the observed flow data was back calculated from observed water levels, using the reservoir stage area relationship. Given the large surface area of the reservoir, a small change in water level results in a very large change in discharge. A few observed data points were queried for reliability, since they showed step changes in level. By recalculating potential outflow without these points, the peak discharge was found to be in a possible range of between 40,000 and 104,000m^3/s. On this basis, the predicted outflow hydrographs are low relative to the potential range, but still within the potential observed range. It is not possible to refine the analysis further than this.

Reservoir Levels (Figure 8-9 Middle)

Both the initial best estimate and the subsequent best fit modelling results offer a good fit to the observed data.

Breach Width Prediction (Figure 8-9 Lower)

Breach width predictions for both the initial best estimate and the subsequent best fit modelling appear to over predict the observed data by approximately 25%. The uncertainty within the case study data makes it difficult to know whether this discrepancy arises from the modelling or field data.

8.1.6.1 Banqiao Dam – Overview of model performance

Model evaluation against observed case study data emphasises the difference in terms of data accuracy and reliability between laboratory and case study data. Large uncertainty exists regarding the nature of the dam construction – in particular the soil state and hence erodibility. Equally,

observation data has been drawn from various sources and then used to estimate potential flows. This introduces significant degrees of uncertainty around the suggested observed conditions.

In terms of model performance evaluation, there is little difference between the *initial best estimate* (Run M1) and the *best fit* (Run M6). This is partly due to the large uncertainties in observed data, making it difficult to justify effort to match different data. Perhaps more significantly though, is that the most reliable data from the case study was that for the observed levels. The model runs simulate the observed reservoir levels quite well, suggesting reasonable model performance.

8.1.7 Evaluation Test No.7: Oros Dam

Oros Dam is the second real dam failure case study used to evaluate model performance. As with the Banqiao Dam data, there is a large degree of uncertainty associated with the data sets and dam description. In addition, initial guidance was to ignore the downstream conditions, however downstream of the dam the valley narrows considerable and hence creates a throttle for escaping flows (Figure A3-18). The modelling work demonstrates that allowing for drowning conditions within the breach modelling is essential for achieving a better result. The breach modelling results for the Oros Dam test case are shown in Figure 8-10.

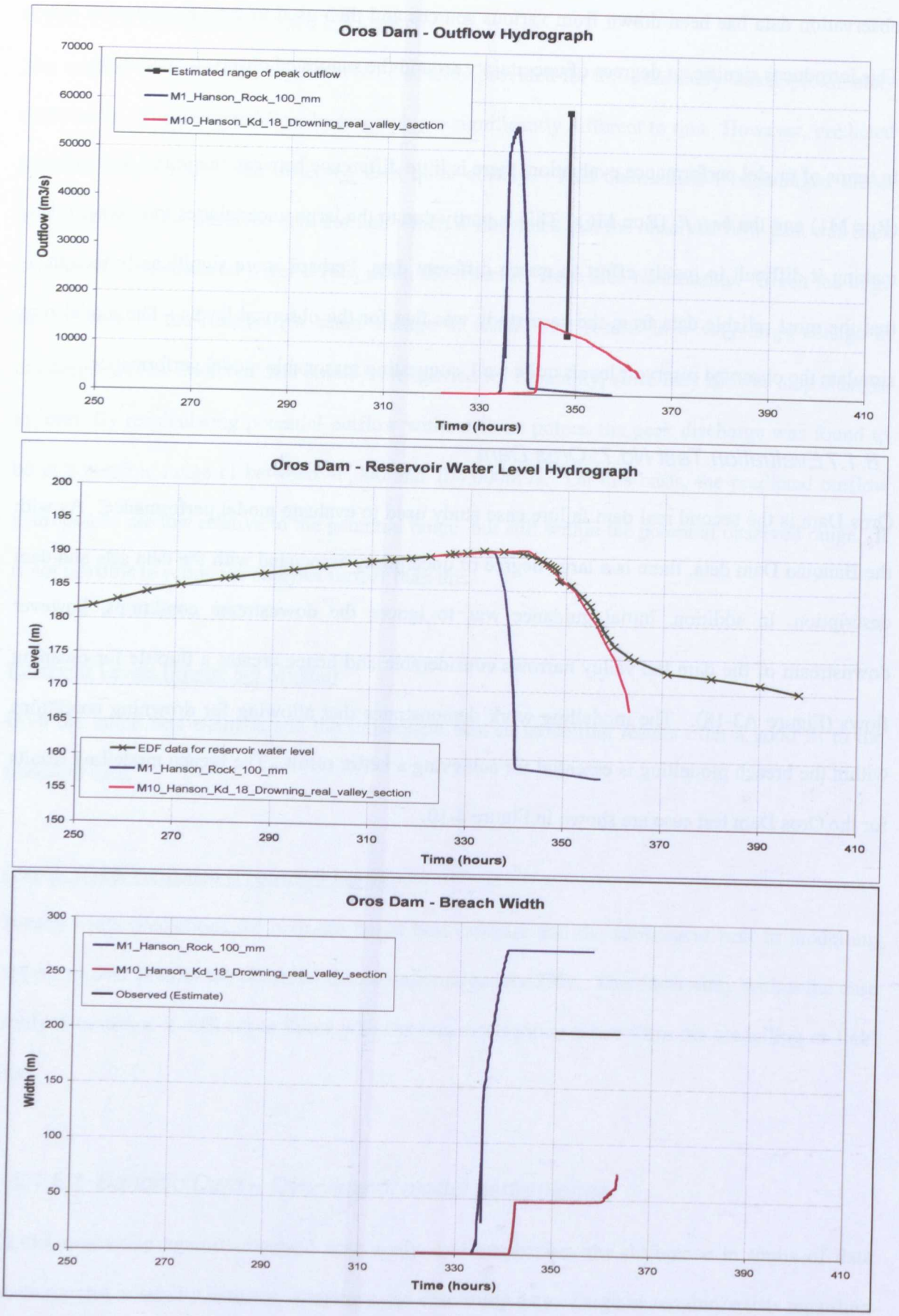

Figure 8-10 HR BREACH modelling results for the DSIG test Oros Dam (Upper: breach flow; Middle: reservoir level; Lower: breach width)

Breach Flow Hydrograph (Figure 8-10 Upper) and Reservoir Levels (Figure 8-10 Middle)

Figure 8-10 (Upper and Middle) shows the *initial best estimate* (Run M1) and the *best fit* (Run M10) results against observed data for both discharge and reservoir level. (Analysis of this case study data requires both outflow and reservoir level to be considered simultaneously). The observed discharge is represented by a range for the potential peak of the flood discharge. Initial guidance suggested that the observed peak discharge was approximately 58,000m^3/s however subsequent analysis of the data showed that there was considerable uncertainty with this prediction since, as with the Banqiao Dam data, the discharge was back calculated from observed reservoir levels, with which there was considerable uncertainty. Hence, the potential range for the peak discharge was estimated to be between approximately 12,000 and 58,000m^3/s.

The initial best estimate gives a peak outflow of approximately 55,000m^3/s, which seems reasonable in comparison to the upper observed value of 58,000m^3/s. However, consideration of the estimated reservoir water level shows a significant deviation from the observed data. This discrepancy was removed very effectively by including the effects of the downstream channel constriction to the breach model (i.e. by predicting the depth of flood flow through the downstream valley constriction and in turn the effect of high downstream water levels on the rate of breach formation). Simulating breach growth and allowing for drowning effects on breach growth resulted in a significantly smaller flood hydrograph, but one which was still within the range of uncertainty for the observed data. Perhaps more significantly, the prediction of reservoir water level gave a much closer fit to the observed data.

Breach Width Prediction (Figure 8-10 Lower)

An indicative value of 200m is given for the observed breach width. The *initial best estimate* exceeds this value at around 275m, whilst the *best fit* data significantly underestimates the width at approximately 75m.

8.1.7.1 Oros Dam – Overview of model performance

As with the Banqiao Dam data, there was considerable uncertainty within the case study data. However, both *initial* and *best fit* estimates gave scenarios that fitted within the range of uncertainty. Of greatest significance is the effect of including drowning within the model simulation. This transformed the *initial best estimate* to a result which gave a very good match to observed reservoir levels, whilst predicting an outflow hydrograph that remained within the range of potential observed data.

8.2 Overall assessment of model performance

During this programme of research the breach model has been refined, extended and improved in a range of areas. Application of the model to the seven evaluation test cases provided via the DSIG breach modelling project has provided an opportunity to assess model performance for a range of different structure types, scales and test conditions. Performance evaluation has been through expert review of the modelling data, with the DSIG project team reviewing each set of modelling assumptions and results on a case by case basis. Past experience has shown that many breach modelling cases have very specific conditions that are hard for an automated performance assessment process to accommodate, hence the expert review process. However, to make this process easier, a range of performance indicators have been used, such as peak discharge, timing, hydrograph characteristics etc. Each of these parameters is important, but their significance varies according to the particular end user application for the breach prediction results (e.g. outflow timing for emergency evacuation compared to breach width for emergency repair or flood hydrograph shape for flood risk assessments). Although final reporting from the DSIG project was incomplete at the time of writing (Morris et al., 2012 - In Press), key conclusions have been included below.

Overall model performance against the seven test cases is considered to be good. In terms of international review through the DSIG project, the model was selected as one of the three most

promising breach models (internationally) for closer evaluation and overall conclusions were that this model (HR BREACH model) and the USDA SIMBA model performed best, and offered the best opportunity for future industry use. These two models were selected rather than one, since the SIMBA model predicts headcut erosion, whilst the HR BREACH model predominantly predicts surface erosion processes. There are situations where each breaching process might dominate, or even flip between the two processes as more or less erodible material is exposed within the embankment during breach formation. It has become clear from the research and testing, that a model which can predict both headcut and surface erosion processes as a function of the soil erodibility (and hence likely over arching physical breach process) would be the best future solution.

The HR BREACH model also simulates breach through composite structures and the fifth evaluation test case showed this to be a useful feature compared to assuming a homogeneous structure, as for example with the SIMBA model. Development of the more complex approach to breach modelling through zoned embankments within the HR BREACH model was undertaken after the DSIG project completed, hence was not included in this particular evaluation. However, the results shown in Section 7 suggest that the new modelling approach could provide even better performance results for this test case.

The DSIG test cases clearly demonstrated how both uncertainty in modelling processes and uncertainty in test / case study data needs to be considered as part of the performance evaluation. The DSIG tests comprised data from laboratory tests, field tests and dam failure case studies. The uncertainty in data quality increased significantly from the laboratory tests, through field data to case study data.

The model prediction of peak discharge and flood hydrograph shape seemed most reliable. Prediction of reservoir water level closely followed. However, prediction of breach initiation timing was, at times, wrong and the accuracy of prediction of breach width varied significantly.

This suggests that the focus for refining the model should remain on improving the accuracy of modelling initiation processes – particularly since errors in initiation timing can magnify the differences in breach prediction results, since hydraulic load conditions rarely remain static (except for laboratory testing.). In addition, research should be focussed upon the lateral widening prediction; the scatter of results here perhaps suggest that the ratio of lateral widening rate in relation to bed erosion rate, varies according to the soil erodibility and / or type. The current modelling process, as with the earlier model of Mohamed (2002), assumes a fixed ratio between bed erosion rate and lateral widening rate for all breach simulations. The rate may also vary as the nature of flow through the breach changes. In particular, in relation to the formation of elongated vortices along the toe of each breach face. Analysis of these aspects would require extensive, large scale breach testing with various soils and close control of the upstream hydraulic conditions.

Two of the test cases provided clear demonstrations of the need to include breach drowning within the modelling process. Where downstream levels are sufficiently high to affect flow conditions through the breach, this can significantly affect breach formation and widening processes.

Finally, the test cases also confirmed the need for detailed consideration of the structure and load conditions by the modeller such that key features are included within the model. The accuracy of breach modelling results is highly dependent upon these case specific details. For the case study data, this meant identifying the material zones and structure shape that would control the overall breaching process; for the IMPACT test cases, it meant looking at ways in which the composite structure might behave and how the state of materials used may have been affected by the construction process.

8.3 Discussion

This chapter details the research undertaken to evaluate model performance against internationally recognised data and standards. This was primarily achieved through collaboration with the CEATI DSIG project, but also through wider use of the IMPACT project data.

The modelling assessment has shown that the breach model performs well across a wide range of test cases, covering different types and scale of structure. Some aspects of breach prediction appeared more accurate than others (for example, peak outflow versus time to breach initiation). However, the complex links between different processes make it difficult to pinpoint the exact cause and contribution of each source of error. The accuracy of results is dependent upon careful model setup, including judgement on key factors likely to affect any site specific case. Of particular note, were the different breaching processes of headcut and surface erosion that occur as a function of the soil erodibility. Future models need to include the option of selecting either process, or ideally, to automatically switch between processes as a direct function of the soil description. This conclusion was also identified in the closing stages of the DSIG project.

The complexity of breach initiation and formation processes, and hence also the breach models, is also reflected in the way in which breach model performance can be evaluated. The DSIG project approach was to review the performance of each model for each test case via open discussion between experts. This allowed for consideration of model features and limitations, test specific issues and modeller approach. With the potential for a very large number of permutations in terms of these three factors (affecting modelling results) the conclusions drawn by the project team were in the form of concluding comments rather than a specific performance score – the latter being very difficult to achieve in an objective, consistent manner. The conclusion for performance of the HR BREACH model (pre zoned version) was that it offered a "good basis" for the prediction of breach.

The HR BREACH model simulates a large number of physical processes using relatively simple models (i.e. 1D flow model; 2D side slope stability; 1D erosion etc.). Future developments of the model might refine and improve the accuracy of those calculations through the use of 2D or even 3D models; however a balance should always be maintained in terms of modelling accuracy and resolution between these hydraulic, soil and structural calculations. Sight should also not be lost of the accuracy to which we can determine the details of the embankment structure and the embankment soil state. The ability to reliably and routinely collect such data is a natural requirement to counterbalance or support the use of more detailed breach models.

9. Conclusions and Recommendations

The following sections summarise the main research outcomes arising from addressing the research goals summarised in Section 3.4, and the research questions, RQ1-RQ6, in Section 1.2. Three key outcomes were:

1. Advances in understanding breach processes through the investigation of physical processes, in particular using the IMPACT project data, and assessment as to how well existing models, such as the HR BREACH model, simulate these processes;
2. Better representation of complex flow processes for modelling breach initiation and growth;
3. Better representation of breach erosion processes through the use of non equilibrium erosion models as the basis for simulating breach initiation and growth.

In undertaking this research it became clear that the various flow, erosion and structure processes were tightly interlinked and care was needed to ensure that the overall modelling approach was built from a series of modelling processes that were consistent in terms of scientific assumptions and simplifications, and which were also appropriate for the degree of uncertainty within the available data.

9.1 Advances in understanding breach processes

Breach initiation and growth: large scale physical processes [RQ3]

Within the overall framework for modelling breach growth it has been shown that a number of larger scale processes can dictate how the breach will develop and hence significantly affect the nature of the outflow hydrograph timing and shape:

a. Two large scale physical erosion processes can occur – head cut erosion and surface erosion. Their occurrence depends upon the type and state of the soil being eroded. This thesis demonstrates how each process can result in significantly different outflows, but also that the two processes can occur within the same structure as soil conditions (rather than type) vary.

Case study examples of both are provided. This confirms the need for future breach models to incorporate both head cut and surface erosion processes if they are to be applicable to a wide range of typical structure types and state;

b. A 'competition'occurs between the rate at which the reservoir (upstream water level) can draw down and the rate at which erosion can occur within the breach. Depending upon the rate at which the soil erodes, and the surface area of the reservoir, either a rapid, high peaked flood hydrograph can occur or a much slower, prolonged, lower peak hydrograph can occur. This has significant implications for flood risk management. The dependence upon soil erodibility and magnitude of difference that this can make also emphasises the large uncertainty in results obtained from using simplified 'peak discharge' equations for predicting breach outflow. Such equations fail to take into account the nature of the materials in both earth dams and flood embankments, and hence cannot be used with confidence to determine the difference between rapid, peak outflow failure and slow, progressive draw down of the reservoir;

c. Growth of the breach through the embankment or dam typically occurs through erosion undercutting the sides of the breach resulting in block failure into the breach. This results in a breach section profile with vertical or undercut sides and not trapezoidal as many researchers suggest. A trapezoidal profile can arise after a breach event, once water levels have receded and the exposed soil face dries.

Understanding why breach model development has not progressed faster [RQ2]

The literature review shows that there have been a large number of research efforts looking at different aspects of breach prediction over the past few decades. However, many of these projects failed to recognise the overall framework that breach prediction sits within, in terms of large scale breaching process behaviour related to different soil types and state combined with hydraulic loading. Understanding this wider context is essential for the development of a breach modelling approach that will be applicable to a wide range of dams and flood embankments. An overall framework has been presented describing how physical processes vary according to hydraulic load and soil conditions. The shortcomings of not recognising and working within this overall

framework is that a model developed in this way will only be valid for the specific hydraulic and soil conditions used during testing and model development, rather than being generically applicable.

9.2 Better representation of complex flow processes

Breach initiation and growth: hydraulic processes [RQ3]

The research has advanced knowledge and practice in a number of areas:

a. The use of variable weir discharge coefficients in order to refine and improve the 1D flow calculation in response to a continually changing (eroding) breach crest profile;

b. Analysis and definition of a phase of flow during breach formation called *converging flow* which occurs during breach formation just after catastrophic failure of the upstream face, but before significant breach widening;

c. Demonstration of the importance of including drowned flow calculations within the overall breach model. Case study applications demonstrate significant model improvements with drowning processes integrated. The research also provided clarification on the correct use of the Villemonte Equation for drowned breach flow calculation (Section 5.3.1).

The importance of including valley shape [RQ1]

The research demonstrated the importance of including valley shape within the breach model for simulations where breach size in relation to the valley profile was large. Breach models typically assume a flat bed to the breach, which introduces errors into the flow prediction when the breach shape grows wider than the limiting valley profile.

9.3 Better representation of breach erosion processes

Breach erosion processes [RQ3]

Through detailed analysis of laboratory, field and case study data the physical processes associated with soil erosion and the overall breach growth process have been defined. These include:

a. Reasons for the use of dynamic erosion equations rather than equilibrium sediment transport equations (and so questioning the validity of a very high proportion of previous breach models and modelling approaches (see Section 6.4)). Also, postulation that whilst this would apply to breach processes within dams or embankments this might not apply over significantly longer length breaches, such as would occur for breaching through large landslide dams;
b. Identification of the combined processes of sediment erosion, mass erosion and soil wasting at different stages during breach development;
c. Definition of the shape of breach during the formation processes, rather than after the event. The breach side walls are typically vertical or undercut, rather than trapezoidal as many existing models suggest. This affects the breach flow calculation and is consistent with the block failure process of breach growth that is typically seen.

Refinement and testing of the breach model [RQ4]

The breach model was modified and tested as research proceeded into the various hydraulic, soil and structural processes. The scope and performance of the model evolved as positive research findings were implemented and subsequently built upon (Appendix 2). Key model developments included:

a. modification of modelling parameter tolerances;
b. testing and refinement of section erosion process, including the relationship between bed and lateral breach erosion rate;
c. implementation of dynamic sediment erosion calculation instead of equilibrium sediment transport equations;
d. introduction of headcut erosion processes;
e. refinement of the critical flow section location process;
f. introduction of a variable weir flow coefficient, adjusting in response to the evolving breach shape;
g. refinement of breach drowning functions.

New breach modelling approach [RQ6]

A new breach modelling approach was developed to allow for the simulation of breach through structures comprising zones of different soil, or different soil erodibility. The modelling approach used a modified version of the existing model (hence built upon the earlier thesis research findings) but allowed much greater flexibility in defining how the structure was built from layers or zones of material. Rules regarding erosion processes through multiple zones were identified and model performance tested. The results demonstrated how variations in construction, soil state, soil layers etc. could significantly affect breach performance and hence assessment of flood risk. The new modelling approach also allows the simulation of the potential effects of a fissured surface layer within the embankment, demonstrating how this can significantly affect overall embankment performance. The implications of this new modelling approach for design and remedial measures to ensure best performance from flood embankments during overflowing conditions were emphasised.

Evaluation of breach model performance [RQ5]

Breach model performance was evaluated via participation with the CEATI dam safety interest group breach modelling project. This project defined 7 test cases for model evaluation and provided a forum for exchange and review with international experts in this field of modelling. Performance of the breach model prior to development of the new zoned approach was tested in this way; data from the project was used to separately evaluate performance of the zoned model version.

Evaluation showed that the modelling approaches adopted provide a "good" basis for prediction of breach, although some aspects of breach prediction appeared more accurate than others (for example, peak outflow versus time to breach initiation). The process of expert discussion of the modelling approach and performance of each breach model for each test case highlighted the sensitivity of breach prediction to specific case conditions (hydraulic loading, structure type and condition etc.) combined with the modeller approach (and hence experience). This sensitivity makes generalised or automated model performance evaluation for breach difficult and liable to

error; evaluation should therefore be undertaken (as within the DSIG project) on a detailed, case by case and model by model basis.

The significance of including soil wasting within breach model simulation [RQ1]

Analysis of macro instability did not prove a strong dependence of the breach model upon the inclusion of soil wasting processes. This research raises the issue as to whether inclusion of block failure within the modelling process offers significant advantages or not. Earlier research (Mohamed, 2002) suggested a strong link between block failure and model performance. However, research here failed to demonstrate the dependence of breach modelling results upon the analysis of macro instability (block failure); for the extremes of soil erodibility, dependence is shown to be minimal (see Section 6.3.4). However, it is also hypothesised that there may be conditions between the two extremes that demonstrate greater dependency, and this may have led to the conclusions by Mohamed. Further research on this issue is required.

9.4 Research implications for breach modelling practice

The research has identified a range of points that should be taken into consideration for breach modelling practice. The following four questions should be considered before undertaking any breach analysis:

1. Why is the breach analysis needed? What is the objective of the study?
2. What degree of uncertainty is acceptable in the analysis?
3. Which breach modelling approach is most suitable?
4. What specific modelling processes should be included?

Based upon these four questions, the following points, identified during this research, should be taken into consideration:

a. **Uncertainty**: Breach modelling contains significant uncertainties, but the uncertainty can be reduced by applying more complex models combined with a sensitivity analysis. Large uncertainties exist within simple breach prediction methods, such as using peak discharge equations;

b. **Physical processes**: Breach may occur through headcut erosion, surface erosion, or a combination of these processes. The erosion process can significantly affect the breach formation process and outflow hydrograph. It is important to understand which physical processes a breach model simulates and hence model suitability for a particular application;

c. **Erodibility**: Soil erodibility plays a significant role in determining the breach physical process. Also, breach formation should be simulated using a soil erosion model rather than a sediment transport model. The soil erodibility will therefore need to be measured or estimated for a breach analysis;

d. **Outflow hydrograph**: Consideration of the soil erodibility in conjunction with the reservoir stage area relationship allows an assessment of the likely shape of the breach flood hydrograph (i.e. rapid with a high peak or prolonged with a lower peak);

e. **Modelling zoned structures**: Earth embankments or embankment dams are often built or extended using zones of different material type and state leading to zones of differing soil erodibility. These zones can significantly alter the way in which a breach develops and hence the flood hydrograph (see Section 7.3). A zoned approach to breach modelling should therefore be adopted under these conditions;

f. **Grass surface cover**: Guidance on the performance of grass cover layers during overflow is limited; many modellers use the guidance provided in CIRIA Report 116 (Hewlett et al., 1987). The design curves within this report were found to contain factors of safety. When applied within a breach model this results in the prediction of failure too quickly. It is recommended that the earlier CIRIA Technical Note 71 (Whitehead et al., 1976) performance curves are used instead, which appear not to contain a factor of safety;

g. **Breach shape**: The breach shape, during breach formation, was found to have vertical or undercut sides, rather than sloping sides as suggested by many modellers. Sloping sides typically form after the breach event as water levels fall and the soil dries;

h. **Drowning**: Drowning (i.e. when the downstream water level exceeds the breach invert) has a significant effect on the breach formation process. This process is interactive, hence for correct

breach simulation the model needs to include up and downstream flow simulation, or to be integrated within a flow model.

9.5 Recommendations for future research

During the research programme a number of issues were identified that require additional research which could not be undertaken as part of this work. Hence, the items detailed below are areas recommended for future research. These were identified as issues affecting the:

1. Underpinning process science;
2. Existing model refinement;
3. Longer term model development.

9.5.1 Underpinning process science

Soil erodibility

Soil erodibility is the most important factor affecting the rate of breach initiation and growth; however a comprehensive description of the factors and parameters affecting it remains elusive. Equally, the selection of simple methods or measures for reliably measuring or predicting erodibility in-situ are not available. Laboratory and field equipment for erodibility testing is available, but the different methods (e.g. Hole Erosion Test or Jet Erosion Test) offer different estimates of erodibility for the same samples. A greater understanding of soil erodibility and its dependencies is required so that consistency between methods of measurement may be agreed and simplified methods for estimation developed. In particular, consistent methods for the quantification of the effects of soil density and water content and soil structure, including effects of soil and water chemistry, need to be developed.

Performance of grass cover

The performance of grass cover on an embankment can significantly affect the timing of breach initiation and in turn the rate of breach development. Research here identified errors that would

occur in the direct use of existing grass performance curves because of the probable inclusion of factors of safety within the performance curves. The research also identified that these performance curves were based upon a very limited amount of data, and that the range for applicability ignored performance estimation between zero and one hour of water overflow. This is an important time zone for the performance of flood embankments since flood levels can rise rapidly with breach formation occurring within this period. Research into the reliability of existing guidance is required, and if appropriate, refinement of the performance curves using additional data. Recent initiatives such as the wave overtopping simulator (van der Meer et al., 2009) offer a very good approach for in-situ testing to assess the performance of different types of grass cover (and underlying soil type).

Extreme climate conditions

Analysis of the IMPACT project gravel test case demonstrated breach formation behaviour that was significantly affected by the freezing test conditions. It appears that frozen gravel caused the embankment to breach through a very strong headcut process, rather than by surface erosion. This significantly affects the predicted formation process and hence outflow hydrograph. It is suggested that the performance of flood embankments and dams under extreme climatic conditions (such as extreme hot and cold, extreme dry and wet) should be investigated to determine likely impacts on performance. This will be highly relevant where embankments are already constructed in extreme climatic areas and where significant climate change effects are anticipated.

9.5.2 Further model refinement

Valley shape

The effect of valley shape (or fixed bed profile) on breach development should be incorporated into the model. Initial efforts to implement this were stopped within this research programme when it became clear that this would require considerable development work within the confines of the existing modelling approach. In particular, the approach of identifying the critical flow section works on the assumption that there is only one critical flow transition across the breach;

implementing non standard breach sections complicates the process of identifying where the flow control section(s) would sit.

Drowning effects

The current model version uses the Villemonte Equation to estimate the effect on flow through the breach. The suitability of this and other equations might be considered in relation to different eroding embankment profiles, in a similar way in which the variable weir discharge coefficient was introduced. During analysis it was also noted that, within the model, downstream embankment sections that are drowned by the tail water level continue to erode. A reduction in erosion rate for these sections should be introduced in parallel with the breach flow reduction.

Integrating headcut and surface erosion modelling

The breach model already includes both headcut and surface erosion models, however the use of these models relies upon expert judgement to select which is appropriate for different soil conditions. A truly integrated approach would allow simulation of both processes within the same breach analysis run, and potentially automated selection of the process based upon defined soil type and state (erodibility). The new zoned modelling approach could be adapted to allow surface erosion of some layers integrated with headcut erosion of other layers.

The significance of soil wasting in prediction accuracy

Earlier research by Mohamed (Mohamed, 2002) suggested a strong link between simulation of block failure during the breach growth process and model performance. Research here did not validate that suggestion, but also only looked at extreme scenarios in terms of the product of $A_s K_d$ (i.e. where either reservoir volume or soil resistance to erosion dominated). Research is needed to understand how modelling block failure affects overall model performance across a wider range of scenarios in comparison to assuming an averaged rate of lateral erosion.

Varying lateral erosion rate as a function of soil erodibility

The existing model assumes a lateral erosion rate as a fixed ratio to the vertical bed erosion rate. However, it was recognised that the ratio between the vertical and lateral erosion could vary according to the soil erodibility, hence further model testing should be undertaken (using the existing test case data) to see whether a correlation can be found. A variable ratio as a function of soil erodibility could offer an approach to improve modelling accuracy across a wide range of structure types.

Introducing complex (real) structures

The new zoned modelling approach offers significantly more flexibility in defining a structure which comprises different materials or material states. However, it does not allow for the inclusion of hard structures such as wave walls, crest caps, toe piling etc. Such composite structures are particularly common for flood defence embankments. The ability to include these structures and simulate their integrated failure as part of the breaching process would be a significant (but complex) step forward.

9.5.3 Longer term model development

Moving to 2D/3D simulation and integrating geotechnical stability and breach analysis models

The existing breach model uses simplified methods for predicting the flow, erosion and slope stability. More complex models already exist for each of these processes. These have not been used to date in order to retain a model that is relatively fast and easy to apply. However, refinement of the simplified modelling approach has probably now achieved most gains in terms of performance without making the step change in modelling complexity. This is now considered the appropriate next step.

In parallel with breach modelling, analysis of embankment performance is also undertaken through detailed slope stability modelling (typically finite element analysis). There is a clear difference between these two approaches; breach modelling assumes failure is initiated and simulates erosion,

breach growth and flood flow whilst slope stability analysis simulates the loads and deformations within an embankment up to the point where failure of the soil is deemed to have occurred. However, the models do not then simulate the breaching process.

The next step is therefore to develop an integrated slope stability analysis and breach analysis model that combines flow, erosion and slope stability analysis to provide a single model which can predict embankment stability through to failure and breach. Care will be needed to ensure that the various components of the model undertake similar complexities of analysis and that no one area offers a greater source of uncertainty that the others. An important consideration will be whether to analyse conditions in 2D or 3D. Use of a 2D flow model may be appropriate for some stages of flow during the breaching processes (such as initiation and widening) but not for others (such as formation) where the conditions will be very dynamic and turbulent 3D flow. Consideration of the balance between the modelling approach and the resolution and uncertainty within the data needed for the modelling work will also be required.

Probabilistic approaches for soil uncertainty

Natural variability in soil type and state can significantly affect soil erodibility. Equally, variability in the quality of construction can also introduce significant uncertainty within the soil. Methods for determining and incorporating uncertainty within the soil structure need to be developed so that the sensitivity of breach modelling predictions to this variability can be assessed.

Wave induced breach

Initial work on wave induced breach was undertaken as part of the EU FLOODsite project. This work lead to the creation of research models that combined different erosion processes to try and predict how wave overtopping or wave impact would initiate and lead to breach formation. Since many flood embankments and dams are exposed to wave action, this aspect of breach modelling should be refined and improved to provide a reliable means for assessing the threat posed by wave action.

References

Ackers, P., White, W. R., Perkins, J. A. & Harrison, A. J. M. (1978). *Weirs and flumes for flow measurement.* (1 Edn). Bath, UK: John Wiley and Sons.

Allsop, N. W. H. A., Kortenhaus, A. & Morris, M. W. (2007). *Failure mechanisms for flood defence structures.* FLOODsite Report T04-06-01. UK: See www.floodsite.net.

ASTM (2003). *Annual Book of ASTM Standards, Section 4: Construction.* ASTM International (American Society for Testing and Materials).

ASTM (2011). A*STM D2487: Standard practice for classification of soils for engineering purposes (Unified Soil Classification System).* ASTM International (American Society for Testing and Materials).

ASTM International (2013). *About ASTM.* URL: http://www.astm.org. [8th January 2013].

Barnes, G. E. (2000). *Soil mechanics: Principles and practice.* (2nd Edn). Great Britain: Palgrave Macmillan.

BBC. (2010). *Hungary's toxic spill.* URL: http://www.bbc.co.uk/news/world-europe-11475136: [6/10/10].

Bechteler, W. & Broich, K. (1991). Effects in dambreak modelling. *In:* Congress of the International Association of Hydraulic Research (IAHR), 1991. Madrid, Spain.

Benahmed, N. & Philippe, P. (2012). *Comprehensive report on Action 3.1.1: Internal erosion.* FloodProBE Report WP03-01-12-05. The Netherlands: European FloodProBE Project (See www.floodprobe.eu).

Bennett, S. J. & Alonso, C. V. (2004). Modeling headcut development and migration in upland concentrated flows. *In:* 3rd international symposium on gully erosion, 28th April - 1st May, 2004. The University of Mississippi, Oxford, Mississippi, USA.

Bettess, R. & Bain, V. (2006). Boscastle and North Cornwall Floods, August 2004: Implications for dam engineers. *In:* British Dam Society 14th Biennial Conference, 2006: Improvements in reservoir construction, operation and maintenance, 2006. Durham, UK. Thomas Telford Ltd.

Bossut & Viallet (1764). Recherches sur la construction la plus advantageuse des digues. *L'Académie Royale de Sciences, Inscriptions et Belle-Lettres de Toulouse.*

Measurement of liquid flow in open channels; Part 4: Weirs and flumes; Part 4I V shaped broad crested weirs, (1986). BS 3680-4I ISO8333:1985 UK. BSI.

Measurement of liquid flow in open channels. Part 4 Weirs and flumes; Part 4f Round nosed horizontal broad-crested weirs, (1990). BS3680-4f; ISO 4374:1990 UK. Institution, B.S.

Hydrometry - Open channel flow measurement using rectangular broad crested weirs, (2008a). BS ISO 3846:2008 UK. Institution, B.S.

Hydrometry - Open channel flow measurement using triangular profile weirs, (2008b). BS ISO 4360:2008 UK. BSI.

Hydrometry - Open channel flow measurement using thin plate weirs, (2008c). BS ISO 1438:2088 UK. BSI.

British Waterways (2005). *Improving the understanding of the risk from canal breaches: Phase 1 - The technical framework, planned programme and initial findings.* UK:

British Waterways. (2009). *British Waterways*. URL: http://www.britishwaterways.co.uk/home: [31 July, 2009].

British Waterways (2010). *Improving the understanding of the risk from canal breaches: Phases 2 & 3 - Formulating a high level approach.* UK:

Broich, K. (1998). Mathematical Modelling Of Dam-Break Erosion Caused By Overtopping. *In:* CADAM - Concerted Action on Dambreak Modelling: 2nd project workshop (Munich), 8-9th October, 1998. Munich, Germany.

Brown, R. J. & Rogers, D. C. (1981). *BRDAM users manual.* USA: US Department of the Interior, Denver, Colorado, USA.

Buchholzer, Y. (2007). *TFE Report: Wave overtopping and breaching models.* Lyon, France: École Centrale de Lyon.

Burns, B. (2006). *Internal erosion of earth embankments.* D Phil, University of Birmingham.

Cambridge, M. (2008). The application of the Mines and Quarries (Tips) and the Reservoirs Acts. *In:* British Dam Society 15th Biennial Conference: Ensuring reservoir safety into the future, 10-13th September, 2008, 2008. University of Warwick. Thomas Telford Ltd.

Castro-Orgaz, O., Giraldez, J. V. & Ayuso, J. L. (2008). Transcritical flow due to channel contraction. *Journal of Hydraulic Engineering,* **Vol.134** (4), pp 492-496.

Chadwick, A. & Morfett, J. (1993). *Hydraulics in civil and environmental engineering.* (Second Edn). London, UK: E & FN Spon.

Chang, H. H. (1998). Riprap stability on steep slopes. *International journal of sediment research,* **Vol.13** (No.2), pp 40-49.

Chen, Y. H. & Anderson, B. A. (1986). *Development of a methodology for estimating embankment damage due to flood overtopping.* FHWA/RD-86/126.

Chow, V. T. (1959). *Open channel hydraulics.* (International edition; 22nd printing 1986 Edn). Singapore: McGraw Hill.

Coleman, S. E. & Andrews, D. (1998). *Embankment Failure Due to Overtopping Flow.* Final Project Report, Foundation for Research, Science and Technology. New Zealand: Foundation for Research, Science and Technology.

Coleman, S. E., Andrews, D. & G, W. M. (2002). Overtopping breaching of non cohesive embankment dams. *Journal of Hydraulic Engineering, ASCE,* **128** (9), pp 10.

Collins, A. R. (1972). Dam busting. *New Civil Engineer. May 1972.*

Courant, R., Friedrichs, K. & Lewy, H. (1928). Uber die partiellen differenzengleichungen der mathematischen physik. *Mathematische Annalen,* **Vol.100** (No.1), pp 32-74.

Courivaud, J.-R. (2007a). Validation test case for dam breach models. Test 1: Banqiao Dam. *In:* Dam Safety Interest Group Breach Modelling Project Workshop: Davis, 2007a. Davis, California, USA.

Courivaud, J.-R. (2007b). *Analysis of the dam breaching database.* CEATI Report No. T032700-0207B. Canada: Dam Safety Interest Group (DSIG).
Courivaud, J.-R. (2007c). Validation test case for dam breach models. Test 2: Oros Dam. *In:* Dam Safety Interest Group Breach Modelling Project Workshop: Davis, 2007c. Davis, California, USA.

Crabbe, A. D. (1974). Some hydraulic features of the square edged broad-crested weir. *Water services,* pp. 354-358.

Cristofano, E. A. (1965). *Method of computing erosion rate for failure of earthfill dams.* Bureau of Reclamation, Denver, Colorado, USA.

D'Eliso, C. (2007). *Breaching of sea dikes initiated by wave overtopping - a tiered and modular modelling approach.* PhD.

Damgaard, J. S. & Mitchener, H. (1997). River bank recession: Experiments on non-cohesive and cohesive banks. *In:* 3rd International conference on river flood hydraulics, 5-7th November, 1997. Stellenbosch, South Africa.

de Vroeg, J. H., Kruse, G. A. M. & van Gent, M. R. A. (2002). *Processes relating to breaching of dikes.* DC030202/H3803. The Netherlands: Delft Cluster.

Defra (2009). *Reservoir safety research and development strategy.* Report 5042263-006-DG-071-005. London, UK: Department for Environment Food and Rural Affairs (Defra).

Defra (2010). *Adapting to climate change: A new approach.* London, UK: Department for Environment Food and Rural Affairs (Defra).

DHI Software (2004). *MIKE 11: A modelling system for rivers and channels (Reference Manual).*

DoE (1986). *Modes of dam failure and flood damage following dam failure.* Report PECD 7/7/184. London, UK: Binnie & Partners (for Department of Environment (DoE)).

DoE (1991). *Dam Break Flood Simulation Program: DAMBRK UK.* London, UK: Department of the Environment (DoE).

Dun, R. W. A. (2007). An improved understanding of canal hydraulics and flood risk from breach failures. *Water and Environment Journal (CIWEM),* **21** (1), pp 10.

Dyer, M. & Gardener (1996). *Geotechnical performance of flood defence embankments.* R&D Technical Report W35. UK: Environment Agency.

Dyer, M. (2004). Performance of flood embankments in England and Wales. *Proceedings of the Institution of Civil Engineers: Water Management Journal,* **Vol.157** (WM4), pp 177-186.

Dyer, M., Utily, S. & Zielinski, M. (2007). *The influence of dessication fine fissuring on the stability of flood embankments.* Research Report UR11. UK:

Dyer, M., Utily, S. & Zielinski, M. (2009). Field survey of desiccation fissuring on flood embankments. *Water Management Journal,* **Vol.162** (WM3), pp 221-232.

EBL Kompetanse (2006). *Stability and breaching of embankment dams - Report on sub-project 3 (SP3): Breaching of embankment dams.* Norway: EBL Kompetanse.

Environment Agency (2003). *Reducing the risk of embankment failure under extreme conditions: Framework for action.* R&D Technical Report FD2411/TR1. UK:

Environment Agency (2007). *Management of flood embankments.* R&D Technical Report FD2411/TR1. UK: Environment Agency.

Environment Agency (2009a). *Reservoir inundation mapping - Trial Study.* UK: Environment Agency.

Environment Agency (2009b). *Scoping study for a guide to risk assessment for reservoirs.* SC070087/SR. UK:

Environment Agency (2011). *Lessons from historical dam incidents.* Report SC080046/R1. UK: Environment Agency.

Environmental Audit Commission (2010). *Adapting to Climate Change.* HC113. House of Commons.

Escarameia, M. (1998). *River and channel revetments: A design manual.* London, UK: Thomas Telford Ltd.

FERC (2006). *Taum Sauk Upper Dam Breach.* Report No. P-2277. USA: FERC.

Fleming, G., Frost, L., Huntington, S. W., Knight, D., Law, F. & Rickard, C. (2001). *Learning to live with rivers.* 0 7277 3104 1. London, UK: Institution of Civil Engineers.

Flikweert, J. & Simm, J. D. (2008). Improving performance targets for flood defence assets. *Journal of Flood Risk Management,* (No.1), pp 201-212.

Flikweert, J. & Underwood, S. (2008). *Technical analysis of defence failures: Summer floods 2007.* Report 9T0505/R00001/303226/PBor. UK: Royal Haskoning.

Flood and Water Management Act 2010, (2010). London, UK. HMSO.

Foster, M., Fell, R. & Spannagle, M. (2000a). A method for assessing the relative likelihood of failure of embankment dams by piping. *Canadian Geotechnical Journal,* **Vol.37** (No.5), pp 1025-1062.

Foster, M., Fell, R. & Spannagle, M. (2000b). The statistics of embankment dam failures and accidents. *Canadian Geotechnical Journal,* **Vol.37** (No.5), pp 1000-1024.

Fread, D. L. (1984). *DAMBRK: The NWS flood forecasting model.* USA: National Weather Service, Silver Spring, Maryland. See http://www.nws.noaa.gov,.

Fread, D. L. (1988a). *The NWS DAMBRK Model: theoretical and background / user documentation.* National Weather Service.

Fread, D. L. (1988b). *BREACH: An erosion model for earthen dam failures (Model description and user manual).* Silver Spring, Maryland, USA: National Weather Service. See http://www.nws.noaa.gov.

French, R. H. (1986). *Open channel hydraulics.* (First Edn). London, UK: McGraw-Hill.

Frith, C. W., Purcell, A. M. & Powell, A. S. (1996). *Earth embankment fissuring manual.* R&D Technical Report W41. UK: Binnie, Black & Veatch Ltd.

Froehlich, D. C. (1995a). Embankment dam breach parameters revisited. *In:* Water Resources Engineering Conference, 14-18 August, 1995a. San Antonio, Texas, USA. ASCE.

Froehlich, D. C. (1995b). Peak outflow from breached embankment dam. *Journal of Water Resources,* **Vol. 121** (No. 1), pp 90-97.

Froehlich, D. C. (2002). IMPACT Project field tests 1 & 2: 'Blind' simulation by Dave Froehlich. *In:* 2nd IMPACT Project workshop Mo-I-rana), 12-13th September, 2002. Mo-I-Rana, Norway. See www.impact-project.net.

Froehlich, D. C. (2004). Two dimensional model for embankment dam breach formation and flood wave generation. *In:* Association of State Dam Safety Officials (ASDSO) Dam Safety 2004 Conference, 26-30th September, 2004. Phoenix, Arizona, US.

Froehlich, D. C. & Tufail, M. (2004). Evaluation and use of embankment dam breach parameters and their uncertainties. *In:* Association of State Dam Safety Officials (ASDSO) Dam Safety 2004 Conference, 26-30th September, 2004. Phoenix, Arizona, USA.

Froehlich, D. C. (2008). Embankment dam breach parameters and their uncertainties. *Journal of Hydraulic Engineering, ASCE,* **Vol. 134** (No. 12), pp 1708-1721.

Fujita, Y. & Tamura, T. (1987). Enlargement of Breaches in Flood Levees on Alluvial plains. *Natural Disaster Science,* **Vol. 9** (No. 1), pp 37-60.

Giuseppeti, G. & Molinaro, P. (1989). A mathematical model of the erosion of an embankment dam by overtopping. *In:* International symposium on the analytical evaluation of dam related safety problems, 5th July, 1989. Copenhagen, Denmark.

Goff, C. A. & Hope, I. M. (2008). Investigation of potential reservoirs. *In:* The British Dam Society 15th Biennial Conference: Ensuring reservoir safety into the future, 10-13th September, 2008. Warwick, UK. Thomas Telford.

Goff, C. A. & Warren, A. L. (2008). The safety of small british reservoirs. *In:* The British Dam Society 15th Biennial Conference: Ensuring reservoir safety into the future, 10-13th September, 2008. Warwick, UK. Thomas Telford.

Gordon, L. M., Bennett, S. J., Wells, R. R. & Alonso, C. V. (2007). Effect of soil stratification on the development and migration of headcuts in upland concentrated flows. *Water Resources Research,* **43** (W07412), pp 13.

Gouldby, B. P. & Samuels, P. G. (2009). *Language of risk: project definitions.* FLOODsite Report T32-04-01. UK: See www.floodsite.net.

Graham, W. J. (2008a). The Teton dam failure - An effective warning and evacuation. *In:* Associate of State Dam Safety Officials 25th Anniversary Conference, 7-11th September, 2008a. Indian Wells, California, USA.

Graham, W. J. (2008b). The Teton Dam failure: Factors affecting the warning and evacuation success. *In:* Dam Safety Management 2008, 22-24th October, 2008b. Nanjing, China.

Hamilton-King, L. J., Hope, I. M. & Warren, A. L. (2008). Post-incident reporting: learning from experience to promote reservoir safety. *In:* The British Dam Society 15th Biennial Conference: Ensuring reservoir safety into the future, 10-13th September, 2008. Warwick, UK. Thomas Telford.

Hanson, G. J., Irwin, B., Temple, D. M., Graham, W., Pearre, C., Fiegle, E. & Hampton, T. (2001a). Dam failure analysis research and development topics. *In:* Issues, resolutions and research needs related to embankment dam failure analysis, 26-28th June, 2001a. Oklahoma City, Oklahoma. USDA.

Hanson, G. J., Robinson, K. M. & Cook, K. R. (2001b). Prediction of headcut migration using a deterministic approach. *Transactions of the American Society of Agricultural Engineers,* **Vol. 44** (No. 3), pp 525-531.

Hanson, G. J. & Simon, A. (2001). Erodibility of cohesive streambeds in the loess area of the Midwestern USA. *Hydrological Processes,* **Vol.20** pp 23-38.

Hanson, G. J. & Cook, K. R. (2004). Apparatus, test procedures and analytical methods to measure soil erodibility in situ. *Applied engineering in agriculture,* **Vol. 20** (No. 4), pp 455-462.

Hanson, G. J., Cook, K. R. & Hunt, S. L. (2005a). Physical modelling of overtopping erosion and breach formation of cohesive embankments. *Transactions of the American Society of Agricultural Engineers,* **Vol. 48** (No. 5), pp 1783-1794.

Hanson, G. J., Morris, M. W., Vaskinn, K. A., Temple, D. M., Hunt, S. L. & Hassan, M. A. A. M. (2005b). Research activities on the erosion mechanics of overtopped embankment dams. *ASDSO Journal of Dam Safety,* **Vol. 3** (No. 1), pp 4-16.

Hanson, G. J., Temple, D. M., Morris, M. W. & Hassan, M. A. A. M. (2005c). Simplified breach analysis model for homogeneous embankments: Part II, Parameter inputs and variable scale model comparisons. *In:* 25th United States Society on Dams (USSD) Annual Conference, 6-10 June, 2005c. Salt Lake City, Utah, USA.

Hanson, G. J. & Hunt, S. L. (2006). Determining the erodibility of compacted soils for embankment dams. *In:* 26th United States Society on Dams (USSD) Annual Meeting and Conference, 30th April - 3rd May, 2006. San Antonio, Texas, USA.

Hanson, G. J. (2nd April 2007). *RE: Material parameters for earthen embankment erosion.* Personal email to Mark Morris.

Hanson, G. J. & Hunt, S. L. (2007). Lessons learned using laboratory jet testing method to measure soil erodibility of compacted soils. *Journal of applied engineering in agriculture (ASABE),* **Vol. 23** (No. 3), pp 305-312.

Hanson, G. J., Tejral, R. D., Hunt, S. L. & Temple, D. M. (2010). Internal erosion and impact of erosion resistance. *In:* 30th United States Society on Dams (USSD) Annual Conference, 12-16th April, 2010. Sacramento, California, US.

Harris, G. W. & Wagner, D. A. (1967). *Outflow from Breached Earth Dams.* BSc., University of Utah, USA.

Hassan, M. A. A. M., Morris, M. W., Hanson, G. J. & Lakhal, K. (2004). Breach formation: Laboratory and numerical modelling of breach formation. *In:* Association of State Dam Safety Officials Dam Safety Conference, 2004, September, 2004. Phoenix, Arizona, USA.

Hassan, M. A. A. M. & Morris, M. W. (2008). *IMPACT Project field tests data analysis.* FLOODsite Report T04-08-04. UK: See www.impact-project.net.

Havnø, K., Van Kalken, T. & Olesen, K. (1989). A modelling package for dam break simulation. . *In:* International Symposium on analytical evaluation of dam related safety problems, 5th July, 1989. Copenhagen, Denmark.

Henderson, F. M. (1966). *Open channel flow.* (1st Edn). USA: The MacMillan Company.

Hewlett, H. W. M., Boorman, L. A., Bramley, M. E. & Whitehead, E. (1985). *Reinforcement of steep grassed waterways.* CIRIA Technical Note 120. London, UK: CIRIA.

Hewlett, H. W. M., Boorman, L. A. & Bramley, M. E. (1987). *Design of reinforced grass waterways.* CIRIA Report 116. London, UK: CIRIA.

Hinks, J. L. & Mason, P. J. (2007). *Ulley Dam: Post-incident review.* UK: Report prepared by Halcrow Group Ltd. for the Environment Agency, November 2007.

Hjulstrom, F. (1935). Studies on morphological activity of rivers as illustrated by the River Fyris. *Bulletin of the Geological Institute of Uppsala,* **Vol.25** pp 221-527.

HR Wallingford (1989). *Tees weir feasibility study - Phase 2 (Flood routing study).* EX1918. Wallingford, UK: HR Wallingford.

HR Wallingford (2009). *Reservoir inundation modelling pilot study: failure mode sensitivity.* EX5929. Wallingford, UK: HR Wallingford Ltd.

Hughes, A. J. (1981). *The erosion resistance of compacted clay fill in relation to embankment overtopping.* PhD PhD, University of Newcastle Upon Tyne.

Hunt, S. L., Hanson, G. J., Cook, K. R. & Kadavy, K. C. (2005). Breach widening observations from earthen embankment tests. *American Society of Agricultural Engineers,* **48** (3), pp 1115-1120.

Illes, P. A. (1977). *The predictive method of obtaining the discharge hydrograph resulting from a dam failure.* PhD PhD, University of Sheffield.

International Commission on Large Dams (ICOLD) (1998). *Dambreak flood analysis - review and recommendations.* ICOLD Bulletin 111. Paris, France:

Kahawita, R. (2007). *Dam breach modelling - a literature review of numerical models.* CEATI Report No. T032700-0207C. Canada: CEA Technologies (CEATI).

Kerisel, J. (1985). The history of geotechnical engineering up until 1700. *In:* XI International Conference on Soil Mechanics and Foundation Engineering, 12-16th August, 1985. San Francisco, US. Balkema.

King, H. W. (1954). *Handbook of hydraulics.* (4th Edn). USA: McGraw Hill Book Company Inc.

Klijn, F., de Bruijn, K., Olfert, A., Penning-Rowsell, E., Simm, J. D. & Wallis, M. J. (2009). *Flood risk assessment and flood risk management: An introduction and guidance based on experiences and findings of FLOODsite (an EU funded Integrated Project).* FLOODsite Report T29-09-01. UK: See www.floodsite.net.

Kraus, N. J. (2003). Analytical model of incipient breaching of coastal barriers. *Coastal Engineering Journal, JSCE,* **Vol. 45** (No. 4), pp 511-531.

Kruse, G. A. M. (1996). *Erosiebestendigheid klei-onderlaag en geulen onder blokken glooiing (Erosion resistance of clay lining and slope gullies).* Grondmechanica Delft Report CO-367430/13. Grondmechanica Delft.

Krzhizhanovskaya, V. V., Melnikova, N. & Gouldby, B. P. (2010). The UrbanFlood multiscale modelling cascade and virtual dike for simulation of dike stability under dynamic hydraulic loading. *In:* Joint UrbanFlood and SSG4Env Workshop on Monitoring and Flood Safety, 11-12th November, 2010. Amsterdam, Netherlands.

Lou, W. C. (1981). *Mathematical modelling of earth dam breaches.* PhD., Colarado State University, USA.

Loukola, E. & Huokuna, M. (1998). A Numerical Erosion Model for Embankment Dams Failure and Its Use for Risk Assessment. *In:* CADAM - Concerted Action on Dambreak Modelling. 2nd project workshop (Munich), 8-9th October, 1998. Munich, Germany.

Macchione, F. & Rino, A. (1999). Prediction capabilities of a simplified dam breach model. *In:* CADAM - Concerted Action on Dambreak Modelling: 3rd Project Workshop (Milan), 6-7th May, 1999.

MacDonald, T. C. & Landgridge-Monopolis, J. (1984). Breaching characteristics of dam failures. *Journal of Hydraulic Engineering,* **vol. 110** (no. 5), pp 567-586.

Malisa, J., Mtalo, F. W. & Lia, L. (2010). How fill material affects the overtopping process for earthfill dams. *HRW (Hydro Review Worldwide). December 2010.* p 8.

Marche, C. & Fuamba, M. (2002). Observation and prediction of a breach in a submerged dyke. *Canadian Journal of Civil Engineering,* **Vol. 29** (No. 6), pp 875-884.

Marsland, A. & Cooling, L. F. (1958). *Tests on full scale clay bank to study the effects of seepage and the effects of overtopping.* Internal Report No. C562. London, UK: Building Research Station.

McGahey, C., Mens, M., Sayers, P. B., Luther, J., Petroschka, M., Schanze, J. & Gouldby, B. P. (2009). *Methodology for a DSS to support long term flood risk management planning (D18.2).* FLOODsite Report T18-09-02. UK: See www.floodsite.net.

Mériaux, P. & Royet, P. (2007). *Surveillance, maintenance and diagnosis of flood protection dikes. A practical handbook for owners and operators.* (Éditions Quae 2007 Edn). France: Cemagref.

Mines and Quarries (Tips) Act 1969, (1969). London, UK. HMSO.

Mines and Quarries (Tips) Regulations 1971, (1971). London, UK. HMSO.

Mingsen, Q., Shuibo, P., Lianxiang, W., Dong, Z., Minmin, Y., Jun, S., Loukola, E., Reiter, P., Pyyny, J., Rytkonen, T. & Alanko, M. (1993). *Chinese-Finnish cooperative research work on dam break hydrodynamics. Part II: Report of hydraulic model test on fixed dam break opening.* Report 951-47-8610-6. Helsinki: National Board of Waters and the Environment.

Mohamed, M. A. A. (1998). *Informatic tools for the hazard assessment of dam failure.* MSc., IHE, Delft.

Mohamed, M. A. A., Samuels, P. G., Morris, M. W. & Ghataora, G. S. (1999). A new methodology to model the breaching of non-cohesive homogeneous embankments. *In:* CADAM - Concerted Action on Dambreak Modelling: 4th project workshop (Zaragoza), 18-19th November, 1999. Zaragoza, Spain.

Mohamed, M. A. A., Samuels, P. G. & Morris, M. W. (2001). Uncertainties in Dam Failure Modelling with the US NWS BREACH Model. *In:* First International Conference on River Basin Management, 2001. Cardiff, UK. WIT Press.

Mohamed, M. A. A. (2002). *Embankment breach formation and modelling methods.* PhD., The Open University, England.

Mohamed, M. A. A., Samuels, P. G., Morris, M. W. & Ghataora, G. S. (2002). Improving the accuracy of prediction of breach formation through embankment dams and flood embankments. *In:* International conference on fluvial hydraulics (Riverflow 2002), 3-6th September, 2002. Louvain-la-Neuve, Belgium.

Montes, J. S. (1998). *Hydraulics of open channel flow.* Reston, VA, USA: ASCE.

Morris, M. W. (2000). CADAM: A European Concerted Action Project on Dambreak Modelling. *In:* British Dam Society 11th Bienniel Conference: Dams 2000, 14-17th June, 2000. Bath, UK. Thomas Telford Ltd.

Morris, M. W. (2002). The IMPACT Project - Continuing European Research on Dambreak Processes and Failure of Flood Embankments. *In:* British Dam Society 12th Biennial Conference, 2002: Reservoirs in a Changing World, 4-8th September, 2002. Dublin, Eire. Thomas Telford Ltd.

Morris, M. W., Hassan, M. A. A. M., Zech, Y., Soares Frazao, S., Alcrudo, F. & Boukalova, Z. (2004). CADAM: IMPACT: FLOODsite. *In:* Association of State Dam Safety Officials (ASDSO): Annual Dam Safety Conference, 26-30th September, 2004. Phoenix, Arizona, USA.

Morris, M. W. (2005). *IMPACT Project: Final technical report.* UK: See www.impact-project.net.

Morris, M. W. & Hassan, M. A. A. M. (2005a). *IMPACT: Breach formation technical report (WP2).* UK: See www.impact-project.net.

Morris, M. W. & Hassan, M. A. A. M. (2005b). *IMPACT: Combined risk and uncertainty technical report (WP5).* UK: See www.impact-project.net.

Morris, M. W., Hassan, M. A. A. M. & Vaskinn, K. A. (2005). *Conclusions and recommendations from the IMPACT Project WP2: Breach formation.* UK: See www.impact-project.net.

Morris, M. W., Hanson, G. J. & Vaskinn, K. A. (2006). Recent advances in predicting breach formation through embankment dams. *In:* 22nd International Congress on Large Dams (ICOLD), 18-23rd June, 2006. Barcelona, Spain.

Morris, M. W., Hassan, M. A. A. M. & Vaskinn, K. A. (2007). Breach formation: field tests and laboratory experiments. *Journal of Hydraulic Research,* **Vol. 45** (Extra (2007)).

Morris, M. W., Hanson, G. J. & Hassan, M. A. A. M. (2008). Improving the accuracy of breach modelling: why are we not progressing faster? *Journal of Flood Risk Management,* **Vol. 1** (No. 4), pp pp. 150-161.

Morris, M. W. & Hughes, A. J. (2008). Dambreak and emergency planning. *In:* British Dam Society 15th Biennial Conference, 10-13th September, 2008. Warwick, UK. London: Thomas Telford Ltd.

Morris, M. W. (2009). *Breach Initiation and Growth: Physical Processes.* FLOODsite Report T06-08-11. UK: See www.floodsite.net.

Morris, M. W., Kortenhaus, A. & Visser, P. J. (2009a). *Modelling breach initiation and growth.* FLOODsite Report T06-08-02. UK: See www.floodsite.net.

Morris, M. W., Kortenhaus, A. & Visser, P. J. (2009b). *Modelling breach initiation and growth: Executive summary.* FLOODsite Report T06-08-01. UK: See www.floodsite.net.

Morris, M. W., Kortenhaus, A., Visser, P. J. & Hassan, M. A. A. M. (2009c). *Breaching processes: A state of the art review.* FLOODsite Report T06-06-03. UK: See www.floodsite.net.

Morris, M. W., Boorman, L. A. & Simm, J. D. (2010). Just how important is grass cover? *In:* British Dam Society 16th Biennial Conference, 23-26th June 2010, 2010. University of Strathclyde, Scotland.

Morris, M. W., Bowles, D. S., Brown, A. J., Gardiner, K., Hughes, A. J., Sayers, P. B. & Wallis, M. J. (2011a). *A guide to risk assessment for reservoirs in the UK: Task 1 - A framework.* Science Report - SC090001/R. UK: Environment Agency.

Morris, M. W., Hassan, M. A. A. M. & Escarameia, M. (2011b). *The performance of vegetation on flood embankments.* FloodProBE Report WP03-01-10-06. UK: See www.floodsite.net.

Morris, M. W., Hassan, M. A. A. M. & Escarameia, M. (2012). *The performance of vegetation on flood embankments.* FloodProBE Report WP03-01-10-06. The Netherlands: See www.floodprobe.eu.

Morris, M. W., Hassan, M. A. A. M., Wahl, T. L., Tejral, R. D., Hanson, G. J. & Temple, D. M. (2012 - In Press). Evaluation and development of physically based embankment breach models. *In:* FLOODrisk 2012, 20-22nd November, 2012 - In Press. Rotterdam, The Netherlands.

Mostafa, T. M. S. (2003). *Experimental modelling of local scour in cohesive soils.* PhD PhD, University of South Carolina.

Mostafa, T. M. S., Imran, J., Chaudhry, M. H. & Kahn, I. B. (2008). Erosion resistance of cohesive soils. *Journal of Hydraulic Research,* **Vol. 46** (No. 6), pp 777-787.

Muhunthan, B. & Pillai, S. (2008). Teton dam, USA: uncovering the crucial aspect of its failure. *Civil Engineering,* **Vol.161** (Special issue 2), pp 35-40.

National Resources Conservation Service (NRCS) (1997). Earth spillway erosion model. *National Engineering Handbook, Part 628 Dams.* USA.

Nogueira, V. (1984). *A Mathematical Model of Progressive Earth Dam Failure.* PhD., Colarado State University.

Orendorff, B. & Nistor, I. (2010). Embankment dam breach modelling: A state of the art review and research needs assessment. *In:* Candian Dam Association 2010 Annual Conference, 2-7th October, 2010. Niagra Falls, Ontario, Canada.

Paquier, A. (1998). 1D and 2D models for simulating dam-break waves and natural floods. *In:* CADAM - Concerted Action on Dambreak Modelling - Wallingford Meeting, 2-3rd March, 1998. Wallingford, UK.

Paquier, A., Nogues, P. & Herledan, R. (1998). Model of Piping in order to Compute Dam-break Wave. *In:* CADAM - Concerted action on dambreak modelling (Munich Meeting), 8-9th October, 1998. Munich, Germany.

Paquier, A. (2002). Rupro, breach model used by Cemagref during IMPACT project. *In:* IMPACT Project - 1st Project Workshop (Wallingford Meeting), 16-17th May, 2002. Wallingford, UK.

Partheniades, E. (1965). Erosion and deposition of cohesive soils. *Journal of the Hydraulics Division ASCE,* **Vol.91** (No. HY1), pp 105-139.

Peviani, M. A. (1999). Simulation of earth-dams breaking processes by means of a morphological numerical model. *In:* CADAM - Concerted Action on Dambreak Modelling: 4th Project Workshop (Zaragoza), 18-19th November, 1999. Zaragoza, Spain.

Pickert, G., Jirka, G. H., Bieberstein, A. & Brauns, J. (2004). Soil / water interaction during the breaching process of overtopped embankments. *In:* River Flow 2004, 23-25th June, 2004. Naples, Italy. Taylor & Francis.

Pitt, M. (2008). *Learning lessons from the 2007 floods.* London, UK: The National Archives [see http://webarchive.nationalarchives.gov.uk/20100807034701/http://archive.cabinetoffice.gov.uk/pittreview/thepittreview/final_report.html].

Ponce, V. M. & Tsivoglou, A. J. (1981). Modelling gradual dam breaches. *Journal of Hydraulics,* **Vol. 107** (No. 7), pp 829-838.

Pugh, C. A. (1985). *Hydraulic model studies of fuse plug embankments.* Report REC-ERC-85-7. USA: United States Bureau of Reclamation (USBR), Denver, Colarado.

Ralston, D. C. (1987). Mechanics of embankment erosion during overflow. *In:* National conference on hydraulic engineering, 3-7th August, 1987. Reston, Virginia, USA. ASCE Hydraulics Division.

Regazzoni, P. L., Hanson, G. J., Wahl, T. L., Marot, D., Courivaud, J. & Fry, J. (2008a). The influence of some engineering parameters on the erosion of soils. *In:* Fourth International Conference on Scour and Erosion (ICSE-4), 5-7th November, 2008a. Tokyo, Japan.

Regazzoni, P. L., Marot, D., Courivaud, J., Hanson, G. J. & Wahl, T. L. (2008b). Soils erodibility: A comparison between the jet erosion test and the hole erosion test. *In:* Inaugural International Conference of the Engineering Mechanics Institute, 18-21st May, 2008b. Minneapolis, Minnesota, USA.

Regazzoni, P. L., Wahl, T. L., Hanson, G. J., Courivaud, J. & Marot, D. (2008c). Caracterisation de la sensibilite a l'erosion des sols: confrontation de deux erodimetres. *Journées Nationales de Géotechnique de l'Ingenieur.*

Regazzoni, P. L. (2009). *Confrontation et analyse d'érodimetres et caractérisation de la sensibilité a l'érosion d'interface.* PhD, Université de Nantes.

Reservoirs (Safety Provisions) Act 1930, (1930). London, UK. HMSO.

Riha, J. & Danacek, J. (2000). Mathematical modelling of earth dam breach due to overtopping. *Journal of Hydrology and Hydromechanics (Slovakia),* **Vol. 48** pp 165-179.

Ritchey, J. C. (Year). Embankment dam failure analysis: State assessment criteria, issues and experience - Northeastern United States. *In:* Dam failure analysis research and development topics, 26-28th June, 2001. Oklahoma City, Oklahoma, USA. USDA, pp. 7.

Robinson, K. M. & Hanson, G. J. (1994). Influence of a sand layer on headcut advance. *In:* Hydraulic Engineering, 1-5th August, 1994. Buffalo, USA.

Rozov, A. L. (2003). Modeling of washout of dams. *Journal of Hydraulics Research,* **Vol. 41** (No. 6), pp 13.

Samuels, P. G. & Morris, M. W. (2010). Idealised model for flow towards a dam breach. *In:* First Congress of European Division IAHR, 4-6th May, 2010, 2010. Edinburgh, Scotland.

Samuels, P. G., Morris, M. W., Sayers, P. B., Creutin, J.-D., Kortenhaus, A., Klijn, F., van Os, A., Mosselman, E. & Schanze, J. (2010). A framework for integrated flood risk management. *In:* 1st European IAHR Congress, 4-6th May, 2010. Edinburgh.

Saxena, K. R. & Sharma, V. M. (2006). *Dams: Incidents and Accidents.* UK: Taylor & Francis.

Sayers, P. B., Hall, J. W. & Meadowcroft, I. C. (2002). Towards risk based flood hazard management in the UK. *Proceedings of the Institution of Civil Engineers Civil Engineering Journal,* **Special Edition, Vol. 150.** pp 36-42.

Sayers, P. B. & Meadowcroft, I. C. (2005). RASP - A heirachy of risk-based methods and their application. *In:* 40th Defra flood and coastal management conference, 5-7th July, 2005. York, UK.: Defra.

Schmocker, L. & Hager, W. H. (2009). Modelling dike breaching due to overtopping. *Journal of Hydraulic Research,* **Vol. 47** (No. 5), pp 585-597.

Shuibo, P., Mingsen, Q., Lianxiang, W., Guoyi, X., Yongqiang, S., Longda, X., Cuiyu, M., Loukola, E., Pyyny, J., Reiter, P., Rytkonen, T. & Alanko, M. (1993). *Chinnese-Finnish cooperative research work on dam break hydrodynamics. Part I: Investigation report on dam safety research in China.* Helsinki, Finland: National Board of Waters and the Environment.

Simm, J. D. (2006). Research perspectives on flooding and flood risk management in United States and Europe. *In:* International workshop on flooding and flood risk management in United States and Europe, 7-9th November, 2006. Budapest, Hungary. HR Wallingford.

Simon, A., Thomas, R., Curini, A. & Bankhead, N. (2008). *Bank Stability and Toe Erosion Model.* PowerPoint Presentation. USDA-ARS National Sedimentation Laboratory Oxford, Mississippi, USA. [See http://www.ars.usda.gov/Research/docs.htm?docid=5044&page=1]. May, 2008.

Singer, J. (1964). Square edged broad-crested weir as a flow measurement device. *Water and water engineering,* **Vol. 28** (No. 820), pp 229-235.

Singh, V. P. & Quiroga, C. A. (1987). A Dam-Breach Erosion Model: 1. Formulation. *Water Resources Management,* **Vol. 1** pp 177-197.

Singh, V. P. & Scarlatos, P. D. (1989). *Breach Erosion of Earth-Fill Dams and Flood Routing (BEED) Model.* Miscellaneous Paper El-79-6, Military Hydrology Report 14. Environmental Laboratory, US Army Corps of Engineers.

Singh, V. P. (1996). *Dam breach modeling technology.* (1st Edition Edn). The Netherlands: Springer.

Smart, G. M. (1984). Sediment transport formula for steep channels. *Journal of Hydraulic Engineering,* **Vol. 110** (No. 3), pp 267-276.

Smith, N. (1972). *A history of dams.* UK: Citadel Press.

Spagni, D., Pender, G. & Cluckie, I. (2009). *Flood Risk Management Research Consortium (FRMRC) 2: Project Implementation Plan.* UK: See www.floodrisk.org.uk.

Stanczak, G., Oumeraci, H. & Kortenhaus, K. (2007). *Breaching of sea dikes initiated from the seaside.* Report 952. Braunschweig, Germany: Leichtweiß-Institut für Wasserbau der Technischen Universität Braunschweig.

Sundborg, A. (1956). The River Klaralven, a study in fluvial processes. *Geogfrafiska Annaler,* **Vol.38** pp 125-316.

Temple, D. M. & Hanson, G. J. (1994). Headcut development in vegetated earth spillways. *Applied engineering in agriculture,* **Vol. 10** (Issue 5), pp 677-682.

Temple, D. M., Hanson, G. J., Neilsen, M. L. & Cook, K. R. (2005). Simplified breach analysis model for homogeneous embankments: Part 1, Background and model components. *In:* 25th Annual United States Society on Dams (USSD) Conference, 6-10th June, 2005. Salt Lake City, Utah, USA.

Temple, D. M., Hanson, G. J. & Neilsen, M. L. (2006). Windam-Analysis of Overtopped Earth Embankment Dams *In:* American Society of Agricultural and Biological Engineers (ASABE) Annual International Meeting, 9-12th July, 2006. Portland, Oregon, USA.

The Reservoirs Act, (1975). London, UK. HMSO.

Theriot, P. O. (2008). *Comparison between a laboratory test and a 3D numerical simulation.* Dam Safety Interest Group Breach Modelling Project, Portland Workshop (Portland, Oregon, USA). 2-3rd May, 2008.

Tingsanchali, T. & Hoai, H. C. (1993). Numerical modelling of dam surface erosion due to flow overtopping. *Advances in Hydroscience and Engineering,* **Vol. 1** pp 883-890.

Tingsanchali, T. & Chinnarasri, C. (2001). Numerical modelling of dam failure due to flow overtopping. *Hydrological Sciences Journal,* **Vol. 46** (No. 1), pp 113-130.

Tucker, R. C. & Spencer, T. M. (2010). Selection of breach parameters for the Herbert Hoover Dike (Very large storage low head reservoir). *In:* 30th United States Society on Dams (USSD) Annual Conference, 12-16th April, 2010. Sacramento, California, USA.

United States Army Corps of Engineers (USACE) (2007). *Performance evaluation of the New Orleans and Southeast Louisiana hurricane protection system. The performance - Levees and floodwalls.* Final Report, Volume 5. USA: Interagency Performance Evaluation Taskforce (IPET).

van Damme, M. (2010). *Embankment Breach Modelling (PhD Transfer Report).* UK: University of Oxford.

van der Meer, J. W. (2006). *Development of alternative overtopping resistant sea defences.* FLOODsite Report T04-07-05; ComCoast WP3 Final Report. UK: See www.floodsite.net.

van der Meer, J. W., Schrijver, R., Hardeman, B., van Hoven, A., Verheij, H. & Steendam, G. J. (2009). Guidance on erosion resistance of inner slopes of dikes from three years of testing with the wave overtopping simulator. *In:* Coasts, Marine Structures and Breakwaters Conference, 16-18th September, 2009. Edinburgh, UK. ICE.

Vaskinn, K. A., Lovell, A., Hoeg, K., Morris, M. W., Hanson, G. J. & Hassan, M. A. A. M. (2004a). IMPACT: Physical modelling of breach formation: Large scale field tests. *In:* Association of State Dam Safety Officials (ASDSO): Dam Safety Conference 2004, 26-30th September, 2004a. Phoenix, Arizona, US.

Vaskinn, K. A., Lovoll, A. & Hoeg, K. (2004b). *WP2.1 Breach formation: Large scale embankment failure.* UK: See www.impact-project.net.

Vaskinn, K. A., Lovell, A. & Hoeg, K. (2005). *IMPACT Project WP2.1 Breach formation: Large scale embankment failure.* UK: See www.impact-project.net.

Verheij, H. (2002). Time dependent breach development in cohesive material. *In:* IMPACT Project Wallingford Workshop, 2-3rd March, 2002. Wallingford, UK. IMPACT Project - www.impact-project.net

Villemonte, J. R. (1947). Submerged weir discharge studies. *Engineering news record,* pp 866-869.

Visser, K., Hanson, G. J., Temple, D. M., Lobrecht, M., Neilsen, M. L., Funderburk, T. & Moody, H. (2010). WinDAM B earthen embankment overtopping analysis software. *In:* Joint Federal Interagency Sedimentation and Hydrologic Modeling Conference, 27th June - 1st July, 2010. Las Vegas, Nevada, USA.

Visser, P. J. (1998a). *Breach growth in sand dikes.* PhD PhD, Delft University of Technology.

Visser, P. J. (1998b). *Breach Growth in Sand-Dikes (Communication on Hydraulic and Geotechnical Engineering).* TU Delft, Report No. 98-1. Delft, The Netherlands: TU Delft.

Wahl, T. L. (1997). Predicting embankment dam breach parameters - a needs assessment. *In:* 27th International Association for Hydro-Environment Research (IAHR) Congress, 10-15th August, 1997. San Francisco, USA.

Wahl, T. L. (1998). *Prediction of embankment dam breach parameters: A literature review and needs assessment.* DSO-98-004. USA: US Bureau of Reclamation, Water Resources Research Laboratory.

Wahl, T. L. (2004). Uncertainty of prediction of embankment dam breach parameters. *Journal of Hydraulic Engineering,* **Vol. 130** (No. 5), pp 389-397.

Wahl, T. L. (2007). *Laboratory investigation of embankment dam erosion and breach processes.* Report No. T032700-0207A. Canada: CEA Technologies (CEATI).

Wahl, T. L. (2008a). *Determining erosion indicies of cohesive soils with the hole erosion test and jet erosion test.* Report DSO-08-05. USA: United States Bureau of Reclamation (USBR), Technical Service Centre, Denver, Colorado.

Wahl, T. L. (15th November 2008b). *RE: Uncertainty within Froehlich peak discharge equation estimations.* Email to Morris, M. W.

Wahl, T. L., Hanson, G. J., Courivaud, J.-R., Morris, M. W., Kahawita, R., McClenathan, J. T. & Gee, D. M. (2008). Development of next generation embankment dam breach models. *In:* United States Society on Dams (USSD) Annual Meeting and Conference, April 28th - May 2nd, 2008. Portland, Oregon. USA.

Wahl, T. L. (2009). Evaluation of new models for simulating embankment dam breach. *In:* Association of State Dam Safety Officials (ASDSO) Dam Safety 2009, 27th Sept - 1st Oct, 2009. Hollywood (Florida), USA.

Wahl, T. L., Hanson, G. J. & Regazzoni, P. L. (2009). Quantifying erodibility of embankment materials for the modeling of dam breach processes. *In:* Association of State Dam Safety Officials (ASDSO) Dam Safety 2009 September 27th - 1st October, 2009. Hollywood (Florida), USA.

Walder, J. S. & O'Connor, J. E. (1997). Methods for predicting peak discharge caused by failure of natural or constructed earthen dams. *Water Resources Research,* **Vol. 33** (No. 10), pp 2337-2348.

Wan, C. F. & Fell, R. (2004). Investigation of rate of erosion of soils in embankment dams. *Journal of geotechnical and geoenvironmental engineering, ASCE,* **Vol.130** (4), pp 373-380.

Wang, P. & Kahawita, R. (2002). Modelling the hydraulics and erosion process in breach formation to overtopping. *In:* Symposium of Sedimentation and Sediment Transport, 2-6th September, 2002. Monte Verita, Switzerland.

Wang, P., Kahawita, R., Mokhtari, A., Phat, T. M. & Quach, T. T. (Year). Modelling breach formation in embankments due to overtopping. *In:* 22nd International Congress on Large Dams (ICOLD), 18-23rd June, 2006. Barcelona, Spain. pp. -.

Wang, Z. & Bowles, D. S. (2006a). Overtopping breaches for a long dam estimated using a three-dimensional model. *In:* 26th United States Society on Dams (USSD) Annual Conference, 1-5th May, 2006a. San Antonio, Texas, USA.

Wang, Z. & Bowles, D. S. (2006b). Three dimensional non cohesive earthen dam breach model. Part 1: Theory and methodology. *Advances in Water Resources,* **Vol. 29** pp 1528-1545.

Wang, Z. & Bowles, D. S. (2006c). Dam breach simulations with multiple breach locations under wind and wave actions. *Advances in Water Resources,* **Vol. 29** pp 1222-1237.

Wang, Z. & Bowles, D. S. (2006d). Three-dimensional non-cohesive earthen dam breach model. Part 2: Validation and application. *Advances in Water Resources,* **Vol. 29** pp 1490-1503.

Watson, A. J. & Basher, L. R. (2006). *Stream bank erosion: a review of processes of bank failure, measurement and assessment techniques, and modelling approaches.* Report 2005-2006/01. New Zealand: Landcare Research, Nelson. [See www.landcareresearch.co.nz].

Webber, N. B. (1971). *Fluid Mechanics for Civil Engineers.* (1st Edn). London, UK: Chapman and Hall.

Weisstein, E. W. (2011). *Greens Theorem.* URL: http://mathworld.wolfram.com/GreensTheorem.html [March 2011].

Wetmore, J. N. & Fread, D. L. (1984). *The NWS simplified dam-break flood forecasting model for desktop and hand-held microcomputer.* USA: Federal Emergency Management Agency (FEMA).

White, C. M. & Gayed, Y. K. (1943). Hydraulic models of breached earthen banks. *The Civil Engineer in War (The Institution of Civil Engineers),* pp 181-200.

Whitehead, E., Schiele, M. & Bull, W. (1976). *A guide to the use of grass in hydraulic engineering practice.* Technical Note 71. London, UK:

Wikipedia Contributors. (2011a). *History of the British Canal System.* URL: http://en.wikipedia.org/wiki/History_of_the_British_canal_system: [23rd August 2011].

Wikipedia Contributors. (2011b). *Banqiao Dam.* URL: http://en.wikipedia.org/wiki/Banqiao_Dam: [29th August 2011].

Wikipedia Contributors. (2011c). *Principal Component Analysis.* URL: http://en.wikipedia.org/wiki/Principal_component_analysis [8th December 2011].

Wilby, R. L., Beven, K. J. & Reynard, N. S. (2008). Climate change and fluvial flood risk in the UK: more of the same? *Hydrological Processes,* **Vol.22** pp 2511-2523.

Wurbs, R. A. (1987). Dam-breach flood wave models. *Journal of Hydraulic Engineering,* **Vol. 113** (No. 1), pp 29-46.

Yang, C. T. (1979). Unit stream power equation for total load. *Journal of hydrology,* **Vol.40** pp 123-138.

Yang, C. T. (1996a). *Sediment transport: Theory and practice.* USA: McGraw-Hill.

Yang, C. T. & Simoes, F. (2000). *User manual for GSTARS (Generalized Stream Tube model for Alluvial River Simulation, Version 2.1).* USA: United States Bureau of Reclamation (USBR), Technical Service Centre, Denver, Colorado.

Yang, J. (1996b). *Breach of embankment dams and evaluation of material uncertainty by Monte Carlo simulation.* Internal Report No.US96:20. Alvkarleby, Sweden: Vattenfall Utveckling AB.

Young, M. J. (2005). *Wave overtopping and grass cover layer failure on the inner slope of dikes.* MSc. MSc., UNESCO-IHE Institute for Water Education.

Zhu, Y. H. (2006). *Breach growth in clay dikes.* PhD, Delft University of Technology.

Zielinski, M. & Sentenac, P. (2010). Dessication cracking detection in flood defences and its detection using miniature resistivity array. *In:* 6th International Conference on Environmental Geotechnics, 8-12th November, 2010. New Delhi, India.

Appendix 1

The HR BREACH model (Mohamed, 2002)

Appendix 1 contains a description of the HR BREACH model (Mohamed, 2002) and how it simulates breach initiation and growth processes.

The existing HR BREACH model was developed by Mohamed in conjunction with research at HR Wallingford (Mohamed, 2002, Mohamed et al., 2002). Mohamed supported earlier research findings that identified breach simulation and breach parameter estimation as the greatest source of uncertainty in dambreak flood forecasting (Morris, 2000, Singh, 1996, Wurbs, 1987) and that tools available to predict breach were not very accurate (Mohamed et al., 2001). Having reviewed existing models, the approach taken was to develop a new model rather than modify an existing model. This allowed the simulation of key physical processes to be integrated within the model.

The model integrates hydraulics, soil mechanics and structural failure processes to a broadly consistent degree of complexity. The model undertakes analysis on a section by section basis through the model (Figure A1-1) and, unlike other models such as BRES (Visser, 1998a, Zhu, 2006) or SIMBA (Hanson et al., 2005c, Temple et al., 2005), does not predefine the breaching process in terms of stages and geometry. The 'penalty' for this more detailed approach to analysis is that the model takes some minutes to run rather than seconds.

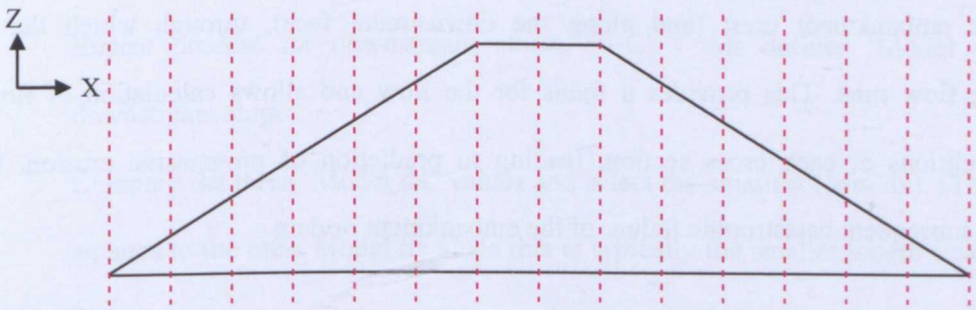

Figure A1-1 Modelling embankment breach by division of embankment into sections

Figure A1-2 provides a flow chart showing the order in which the hydraulic, soil and structural processes are analysed. Each of these stages are considered in more detail below.

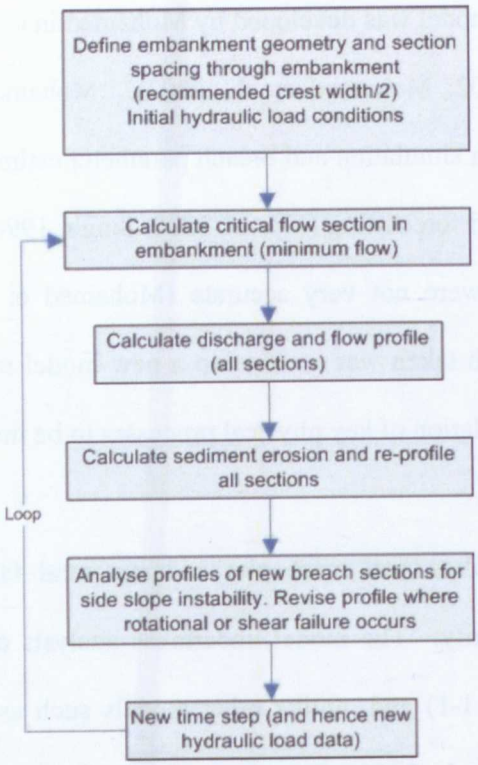

Figure A1-2 HR BREACH model processes

Geometry and Section Spacing

The breach model works by initially requiring the user to define a notch (breach initiation notch) through the embankment crest (and along the downstream face), through which the initial overtopping flow runs. This provides a focus for the flow and allows calculation of flow and erosion conditions at each cross section, leading to prediction of progressive erosion, breach growth and subsequent catastrophic failure of the embankment or dam.

Hence, the embankment profile used for flow calculation (Figure A1-3) has a slightly different profile to the outer profile used to define the embankment shape in general (Figure A1-1). The flow profile is defined by points A, B`, C`, D` rather than A,B,C,D. Since the initiation notch is not present in the upstream face, and the notch depth is parallel to both the crest and the downstream face, the modified profile results in different offsets for points B → B` and C → C`, hence a small change in crest width.

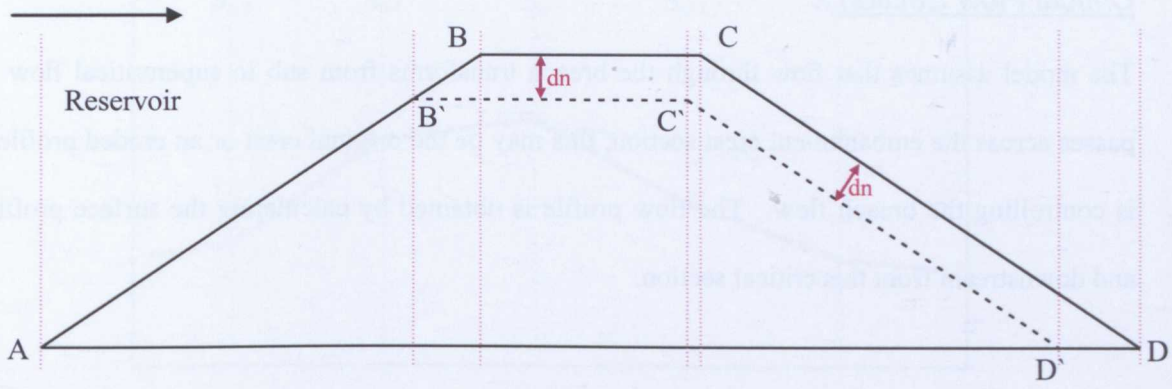

Figure A1-3 Embankment profile showing breach initiation notch

When running the model, the user is asked to define the section spacing (dx). User dx is typically defined as half the crest width, hence (B-C)/2. In order to identify specific section locations for modelling that also coincide with the key geometry points A, B`, C`, D` the following rules are applied:

1 User defines 'User dx';

2 Calculate the number of sections between A – B` (i.e. [(A-B`) / User dx]). Round up to the nearest whole number. This defines 'Model dx' for the upstream slope;

3 Repeat process for crest, B`-C` - this defines 'Model dx' for the crest;

4 Repeat process for downstream slope, D`-C` - this defines 'Model dx' for the downstream slope;

5 Compare the three 'Model dx' values and select the smallest (Min dx). (This normally equates to the crest Model dx since this is typically the smaller length subdivided into dx.);

6 Calculate specific section locations across the entire embankment working from:

   a. Upstream crest (B`)→ upstream toe (A);

   b. Downstream crest (C`) → upstream crest (B`);

   c. Downstream toe (D`) → downstream crest (C`);

   Where spacing does not allow an exact fit of sections using Min dx, last three spaces are divided into two sections (i.e. two sections with spacing > Min dx, rather than two sections of dx plus one undefined remainder).

Critical Flow Section

The model assumes that flow through the breach transforms from sub to supercritical flow as it passes across the embankment crest section; this may be the original crest or an eroded profile that is controlling the breach flow. The flow profile is obtained by calculating the surface profile up and downstream from this critical section.

There are five different methods provided within the HR BREACH model to locate the critical flow section. Correct identification of this section is important within the model because once identified, the flow profile is calculated upstream (sub critical) and downstream (super critical) from this section. The section flow conditions define shear stress and hence soil erosion at each section. The five approaches comprise:

1 Up and downstream slopes;

2 Up to downstream slope;

3 Upstream edge of downstream face;

4 Maximum energy;

5 Minimum flow.

Up and downstream slopes

This method considers how the eroding embankment slope changes between sections, with the goal of identifying the crest, either side from which the sections slope downwards. For each section, the critical slope is calculated using the Manning's equation. Slopes between this and adjacent sections are then calculated and compared to determine whether the flow might transition from a sub to super critical state at that particular section (Figure A1-4).

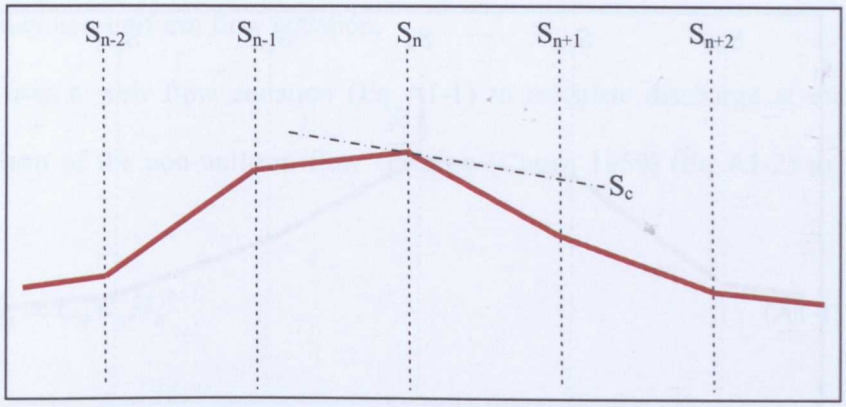

Figure A1-4 Critical section - up and downstream slope method

Up to downstream slope

This method calculates the average slope between upstream and downstream sections and then compares this slope to the critical slope for the section S_n. If the average slope exceeds the critical slope, then it is assumed that section S_n is the approximate location of the critical flow section.

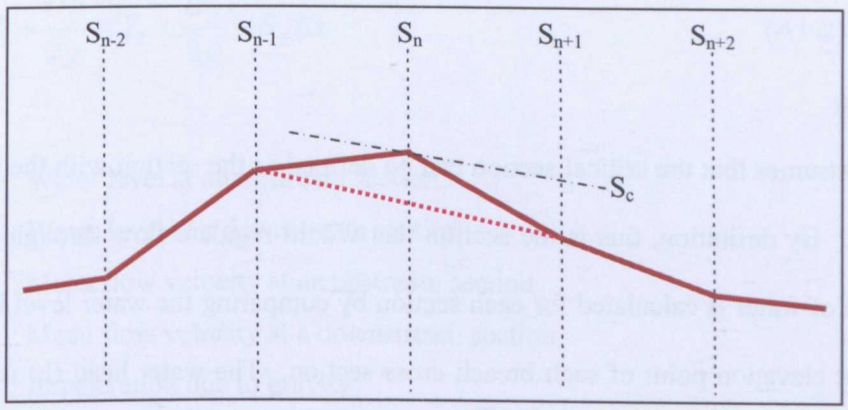

Figure A1-5 Critical section - up to downstream slope method

Upstream edge of downstream face

This simple approach looks at the downstream slope of each section and the section bed level in order to identify the upstream edge of the downstream face. This analysis starts from the downstream toe and works upstream until a suitable section is identified. Since this method will be 'trapped' into a false answer if a dip in section bed levels is found, this method should only be used if the other approaches fail.

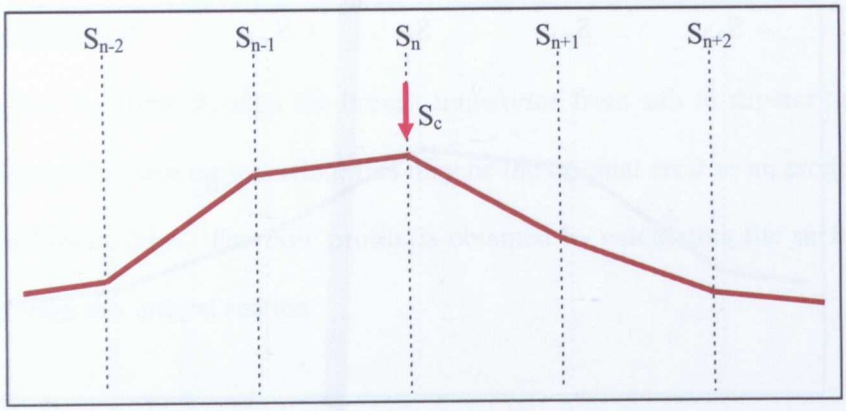

Figure A1-6 Critical section – upstream edge of downstream face method

Maximum energy

This method assumes that the critical section can be defined as the section with the maximum energy in the system. Therefore, the critical energy is calculated for all sections, based on the Bernoulli equation, and the section with the maximum energy is assumed to be the critical section.

Minimum flow

This method assumes that the critical section can be defined as the section with the minimum flow in the system. By definition, this is the section that would regulate flow through the breach. A potential head of water is calculated for each section by comparing the water level in the reservoir and the lowest elevation point of each breach cross section. The water head (h) is calculated for each section through the embankment and the weir formula is used to calculate the potential flow at each section using the section average width (h). The section that gives the minimum flow value is assumed to be the critical section. This method is the preferred approach for calculating the critical flow section within the breach model.

Discharge and Flow Profile

Breach models typically use one of the following approaches to calculate flow conditions through the breach (Table 2-5)

- 1D or 2D Saint Venant equations;
- The steady uniform flow equation;

- The steady non-uniform flow equation.

HR BREACH uses a weir flow equation (Eq A1-1) to calculate discharge at the critical flow section and a form of the non-uniform flow equation (Chow, 1959) (Eq A1-2) to map the flow profile:

$$Q_b = C_d B_b H_b^{3/2} \qquad \text{(A1-1)}$$

Where

Q_b	Flow through breach	m^3/s
C_d	Discharge coefficient	-
B_b	Section averaged breach width	m
H_b	Total head over the breach	m

$$Y_1 + \frac{U_1^2}{2g} = Y_2 + \frac{U_2^2}{2g} + S_f \Delta x \qquad \text{(A1-2)}$$

where: Y_1 : Water level at an upstream section

Y_2 : Water level at a downstream section

U_1 : Mean flow velocity at an upstream section

U_2 : Mean flow velocity at a downstream section

g : Acceleration due to gravity

Δx : Distance between the two sections

S_f : The friction slope that can be represented by the Manning's equation:

$$S_f = \frac{U_m^2 n^2}{R_m^{4/3}} \qquad \text{(A1-3)}$$

where: U_m : Average mean velocity = $(U_1+U_2)/2$

R_m : Average hydraulic radius = $(R_1+R_2)/2$

n : Manning's roughness coefficient

The equations are solved iteratively with the computations proceeding in the upstream direction for the sub-critical flow zone and in the downstream direction for the supercritical flow zone.

Sediment Erosion and Section Profile

The model predicts erosion of the breach section by calculating the shear stress distribution around the flow section and then calculating sediment removal based upon a user selected sediment transport or erosion equation. This process leads to undercutting of the breach sides, as observed in many of the IMPACT project field tests (Section 2.4). Figure A1-7 shows how the process is replicated within the model. At an initial time step the section and water level is defined by seven points. During each time step the model calculates a new breach section profile, and subsequently a new water level at the start of the next time step. Each loop potentially adds two more points to the definition of the breach geometry. This is not sustainable for a model which will run many hundreds or thousands of time steps, hence when a section is defined by 9 points this is reduced back to 7 points (Figure A1-8).

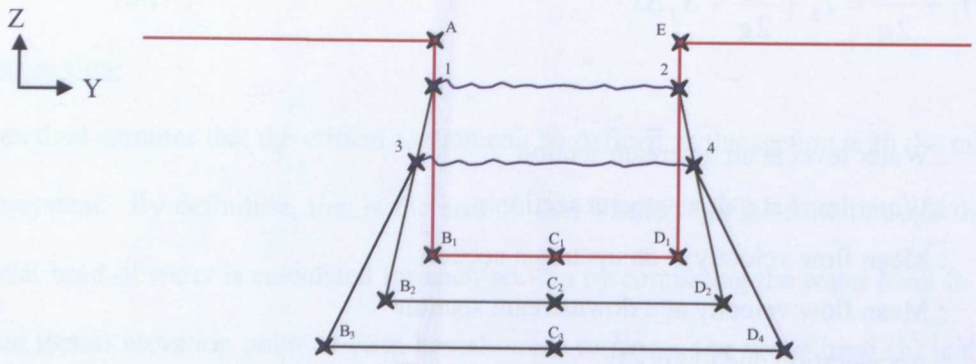

Figure A1-7 Existing modelling process for calculating growth of breach section

The initial breach section is shown by the profile A-B_1-C_1-D_1-E. The water level within this section is defined by the line 1-2. Note that point C_1 is specified as a low point in the section, and is established 1mm below the horizontal defined by B_1–D_1. This assists in maintaining the stability of model flow calculations with negligible effect on the breach profile. Hence, the initiation notch is defined by 5 points, and the water level by an additional 2 points, giving 7 points in total at time step t_0. Having established an initial breach section profile, a new profile may be calculated for the given flow conditions. This is shown by the profile of 7 points A-1-B_2-C_2-D_2-2-E. Subsequently, at t_1, a new water level may be established (line 3-4). The breach profile is now determined by 9 points, and the calculation process predicts a new eroded profile defined by the line A-1-3-B_3-C_3-

D_3-4-2-E. At this point, the section is redefined (using Green's theorem(Weisstein, 2011)) so as to maintain the same area of the soil wedge but to only use 7 points, as for example profile A-1-B_2-C_2-D_2-2-E. The transformation between a 9 point and a 7 point definition is shown in Figure A1-8. Notation is consistent with Figure A1-7. The wedge of soil defined by A-1-3-B_1 is replaced by the wedge defined by A-N-B_1 which maintains the same wedge area. Analysis has shown the effect on subsequent hydraulic calculations to be negligible (Buchholzer, 2007).

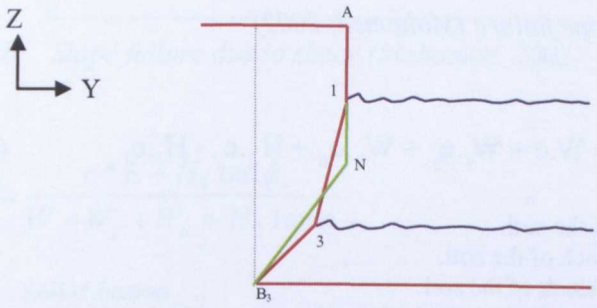

Figure A1-8 Process for maintaining breach section description between 7 and 9 points.

Whilst the erosion rate is calculated section by section through the embankment, large variations in erosion rate between adjacent sections are avoided by applying an averaged value at each section rather than the individual section specific value. Hence, the erosion rate at any given (internal) section is taken as the average value of that section plus the section up and downstream.

Breach Stability

A number of stability calculations are performed within the breach model. For breach development through a homogeneous embankment, breach side slope stability is assessed according to potential rotational and shear failure modes.

Rotational, or bending, failure occurs when the balance of forces on an overhanging block result in a force that exceeds the tensile strength of the soil.

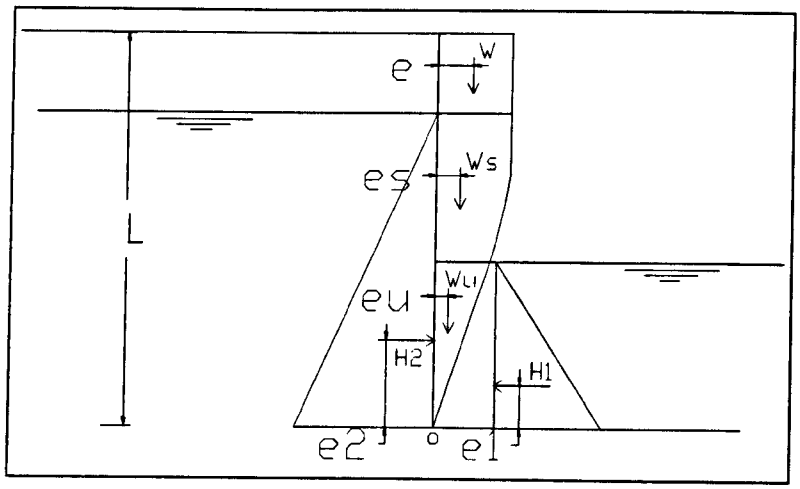

Figure A1-9 Rotational or bending slope failure (Mohamed, 2002)

$$\text{Moment about Point o } (M_o) = W.e + W_s.e_s + W_u.e_u + H_2.e_2 - H_1.e_1 \qquad \text{(A1-4)}$$

where:
- W : Weight of dry block of the soil.
- Ws : Weight of saturated block of the soil.
- Wu : Weight of submerged block of the soil.
- H_1 : Hydrostatic pressure force in the breach channel
- H_2 : Hydrostatic pressure force inside the embankment.
- E, e_s,e_u : Weight forces eccentricities.
- E_1, e_2 : Hydrostatic pressure forces eccentricities.
- L : Length of the failure plane.

Based on the above analysis, the maximum actual tensile stress ($\sigma_{t(actual)}$) on the plane of failure can be computed as follows:

$$\sigma_{t(actual)} = (H_2 - H_1)/L + 6M_0/L^2 \qquad \text{(A1-5)}$$

Assuming that the allowable soil tensile strength ($\sigma t_{(soil)}$) is known, then failure occurs when $\sigma t_{(actual)}$ exceeds $\sigma t_{(soil)}$.The modeller can then select whether the failed block of soil remains within the breach for subsequent erosion or is removed instantly.

A similar approach may be adopted for the analysis of block failure due to shear (Figure A1-10), including the following assumptions:

- Suction is neglected in the zone above the water level inside the embankment and this zone is considered dry.
- Changes in water level inside the embankment during the embankment failure are slow to respond and can be neglected.

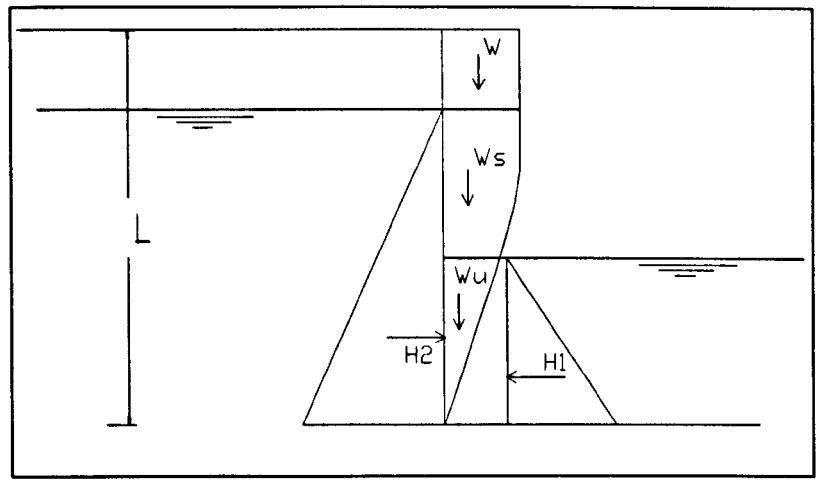

Figure A1-10 Slope failure due to shear (Mohamed, 2002)

$$FOS = \frac{c^* L + H_1 \tan\phi}{W + W_s + W_u + H_2 \tan\phi} \qquad \text{(A1-6)}$$

where: c : Soil cohesion.
ϕ : Soil angle of friction.
W : Weight of dry block of the soil.
W_s : Weight of saturated block of the soil.
W_u : Weight of submerged block of the soil.
H_1 : Hydrostatic water pressure in the breach channel.
H_2 : Hydrostatic water pressure in the embankment.
L : Length of the failure plane.

Further structural failure modes are considered for composite embankment structures (i.e. embankments with a core of relatively thin, but stronger, less erodible material). In these cases it is assumed that the core controls the rate of overall breach failure by withstanding erosion relative to the weaker, more erodible supporting material. Hence the model simulates erosion of the supporting material and structural failure of the core material. This process is clearly demonstrated by the scouring time contours from large scale testing on the Yahekou Dam, China (Shuibo et al., 1993) and can also be seen in dam failure case studies by Ritchey (Ritchey, 2001).

Failure mechanisms that are analysed include sliding of the clay core wall, overturning of the clay core wall and bending failure of the core wall (Hughes, 1981). Details of the force balance equations are provided by Mohamed (Mohamed, 2002).

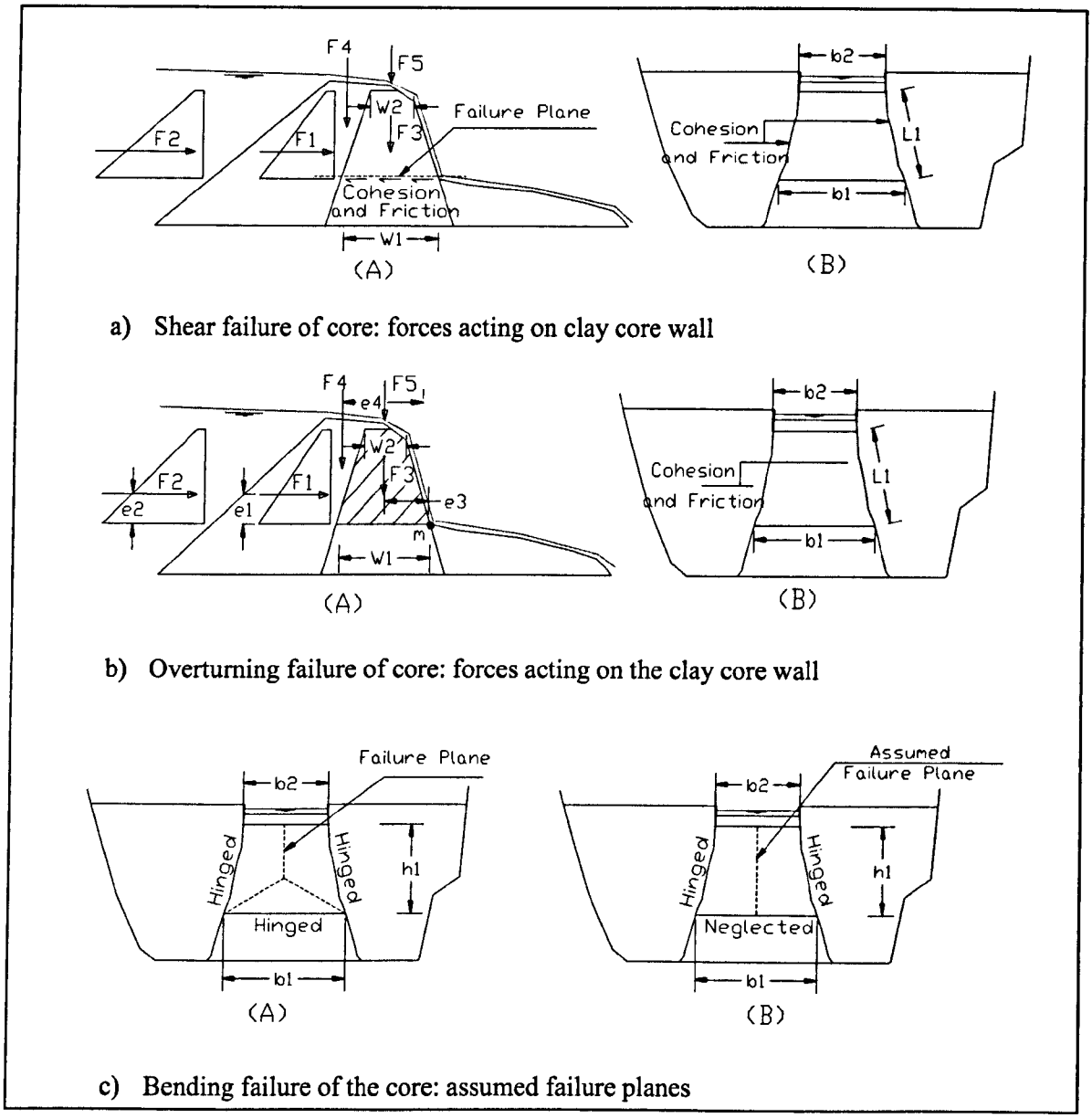

Figure A1-11 Structural failure mechanisms used for composite dam breach (Mohamed, 2002)

Surface Protection Layers

In addition to analysis of breach growth processes, the HR BREACH model also includes analysis of the role of surface protection layers comprising either grass or rock cover. The model allows calculation of the flow profile but prevents any breach erosion until flow conditions exceed the design stability of the grass or rock cover. At this point the cover layer is assumed to fail and breach initiation and growth processes continue unrestricted. The performance of grass cover is simulated using the CIRIA grass performance curves (Hewlett et al., 1985); the performance of

rock cover is simulated using the semi empirical formula developed by Chang (Chang, 1998) for the design of riprap on steep slopes.

Appendix 2

Summary of breach model development versions

Appendix 2 contains a tabular summary of the different HR BREACH model versions that have been developed during the PhD research programme. [Note that all model coding has been undertaken by Mohamed Hassan].

Model Version Ref.	Model Development
3.32	Initial research version
3.33	***Combined changes from V 3.33 to V 3.53_14_5:***
3.53_14_3 3.53_14_4 3.53_14_5 3.53_14_5_DSIG#2 3.53_14_5_DSIG#2+quickwins	1- Headcut failure. a. The model can simulate headcutting at the crest, the toe or both b. The headcut stress can be calculated using four different methods 2- Piping failure improvements. a. Pipe can grow asymmetrically in four directions b. Collapse of the pipe can now be handled instantaneously or distributed and eroded c. Failure of the downstream blocks can be modelled or not. 3- Variable Cd a. The model can either use fixed or variable methods to calculate the weir coeff. 4- UI improvements. a. Clipboard copy \ paste. b. Direct input of data into the grid control c. Input dialogs are more user friendly – added buttons to view \ save \ import data d. Added dimensions to the data view e. Added the a settings menu to change the run view display f. Added different units for data (i.e. seconds\ hours) g. Help file and examples can be accessed from the help menu. 5- Error handling. a. Most of the input data errors are either picked up during input or before running the model. b. The model crash peacefully with and error message to help the developer to identify what went wrong. 6- Help file update. a. Help file was updated to reflect most of the model updates 7- Other changes a. Erosion does not occur if the section has not sediment transported. Even if the section downstream has. b. Protection calcs are not calculated if the flow is less than the minimum flow. c. Kd, tc and C can now be changed explicitly through the user interface. d. Added the Meyer-Peter-Muller equation to the sed. Equations e. Critical section can now be located using one of four different methods. f. Improved the way the output files are created or read through the interface. g. Added a splash screen h. Added License information

Model Version Ref.	Model Development
	i. Old results file will not be overwritten unless the user approves that. j. The views no more flicker during the model run. 8- Bug fixes. a. A bug in the composite class to compute the breach invert. This was caused by correcting the calculation of the breach depth when a protection layer exists. (CcompDam::SetUpSecs()). b. Allow vertical erosion even if it has reached the core level. (if (/*(CrestSecst[iupdc]->Sec[CrestSecst[iupdc]->GetLowestPt()].y < CrestSecst[iupdc]->CoreLevel) ||*/ (!CrestSecst[iupdc]->ErodeZ))) c. Downstream level is not calculated if the flow is less than the minimum flow. d. Tension strength value is now set to the value entered by the user not a fixed value. e. Removal of the section after a core failure is now handled correctly. f. Downstream water level was not calculated correctly if it is below the foundation level. V3.53_14_5 released to DSIG in April 2007
3.53_headCutv_14_6_after_DSIG_workshop	1- Added a check for the DS section data. Low point should not be at the edges.
3.53_headCutv_14_7	1- Added an option to input data in metric or imperial units. Output is still only metric. 2- Added the ability to remove multiple rows 3- Added a warning if the DS time series is less than simulation time. 4- Kd and C now defaults to zero rather than unity. 5- Fixed a bug for Visser equation where the parameter 'deltas' was not calculated if critical shear stress is more than zero. This causes the model to crash.
3.53_headCutv_14_8	1- Model can now start from a non-zero time. Initial condition should be the same for water and breach size in order to obtain same results with and without a non-zero time.
3.53_headCutv_14_9	1- Added an option for inclusion of the initial notch with surface protection.
3.53_headCutv_14_10	1- Added an option to input reservoir stage volume curve.
3.53_headCutv_14_11	1- Model can output results in metric or imperial if input is imperial. 2- Modified the routines that calculate the US and DS angles for triangular weir calcs.
3.53_headCutv_14_11_1	To test the effect of changing the breach width calcs (mwm).
3.53_14_12	ver3.53_headCutv_14_12
3.53_14_12_Disableslope	

Model Version Ref.	Model Development
3.53_14_12xxx25AugLatestxxx	1- Model now does two iterations each time step to find a solution as follows: a. Calculate water depth and velocity for each section b. Calculate sediment transport flow for each section c. Update section based on (b) and the sediment continuity equation d. Calculate water depth and velocity for sections updated in (c) e. Calculate sediment transport flow for sections updated in (c) f. Update original sections (used in (a) above) based on (e) and the sediment continuity equation g. Final sections are average of sections updated in (c) and (f). h. Check slope stability.
3.53_14_12xxxCSMWSplit	as opposed to the old method which was: a. Calculate water depth and velocity for each section b. Calculate sediment transport flow for each section c. Update section based on (b) and the sediment continuity equation d. Check slope stability. 2- Added a file to check dt for slope failures 3- Added an 4 options for updating the breach sections
3.53_headCutv_14_13	1- Fixed a bug in the open file code. It causes an error "Unexpected File Format" 2- Fixed a bug in the input Wizard. It shows the Downstream BC title twice for head time boundaries 3- Fixed a bug in the flow output file. Breach depth was written as breach invert when modelling head cut.
3.53_headCutv_14_14	1- Area and length tolerances can now be set to zero.
3.53_headCutv_14_15	1- Breach width is now calculated at the critical section location rather than the minimum width.
3.53_14_16_Setup	ver3.53_headCutv_14_16 (through many subversions)
3.53_14_16_2_5	1- Erosion below the tolerance is now accumulated rather than being ignored.
3.53_14_16_2_6	2- Added a new routine to find the location of the critical section based on minimum flow
3.53_14_16_2_6_1	3- Added an option to fail the embankment at a set time.
3.53_14_16_2_6_4NewSeds(bugged)	4- Added a new routine to update the section area based on analytical solution rather than iterative solution.
3.53_14_16_2_6_5NewSeds	5- Fixed a bug in the Headcut module 6- Fixed a bug in the piping module 7- Sediment calcs are now split into bed and sides.
3.53_14_16_2_6_6NewSeds_NoCritSectControl	8- We tried within this version an implicit solution but it didn't work. 9- We also tried within this version the concept of adaptation length but it did not prove useful.
3.53_14_16_2_6_7_NewSedFactors	We ended up using the one variation of ver3.53_headCutv_14_16 which is then converted to Ver. 4.0 that was sent to DSIG in
3.53_14_16_2_6_7_2_Da	

Model Version Ref.	Model Development
mpedCritSect	December 2007.
3.53_14_16_2_6_7_3_Debug	
3.53_14_16_2_6_8_AdaptationLengths	Instigation of adaptation lengths to investigate transition between solid and mobile bed
3.53_14_16_2_6_9_AdaptationLengthExpo	
	ver3.53_headCutv_14_17 (through many subversions)
3.53_headCutv_14_17	1- Added the ability to have Interpolated sections with small dx or staggered.
3.53_14_5	Released to DSIG in April 2007
4.0	Released to DSIG in December 2007
	Fixed the following:
4.01	1- A bug in Update Sec in CanySec class where predicted level was above the top of the dam.
4.02SE_TN71	Inclusion of TN71 grass curves instead of CIRIA 116
	Developed to add tn71 grass resistance and also fixing the following bug:
4.02	1- NoOfSkipStepsForCrSec variable was set to 1 in older versions of the input files instead of 0. This was corrected and now it is set to 0.
	2- DsTwl was not initialised correctly. Now this is corrected.
4.021	Developed to fix the water depth and slope bugs on the downstream face and adjust the breach width to damp the critical section changes.
4.022	Min C_d value = 1.7 if variable C_d is selected
4.023	Approach Flow at an angle.
4.024	Approach Flow radial or at an angle. (Not completed – Still having problems with radial flow)
4.025	Approach flow only at an angle. Sections are updated from the upstream crest limit based on the critical section width wherever it is.
4.0251	Bug Fix in the composite module.

Model Version Ref.	Model Development
4.1	Version released to DSIG
4.11	Same as 4.1 but default values for Breach depth and width and Damping time steps are corrected to 1.6, 0.75 and 0 respectively.
4.12	To match Wallingford Software IWRS release v9
4.13 – 4.15	To fix piping bugs.
4.16	To fix two bugs in the downstream boundary section: 1- Lowest point was picked up wrongly if there are local Minimum point in the section (dips) 2- Downstream control (drowning) was assumed incorrectly in some special cases (Tracey runs)
4.17	To set default of angle of Approach to 30 correct C units and a typo in the interface Update display warnings for bed and side erosion factor, Width to depth ratio and Angle of approach Fix a bug in the headcut erosion when toe and crest are used with maximum of overall and conventional shear stress.
4.18 v121009 no notch	Modification to allow 'glass walls' concept for breach initiation notch (instead of physical cut into embankment profile).
4.19 v231009	Introduced HRW drowning function
4.19	Drowning and head cut bug fix
4.19.5 v310111	Piping code error fix. The breach model piping process is not investigated in detail within this research, but an error in the coding was identified through a parallel research project. The correction is as follows and relates to (Mohamed, 2002). Thesis page 203 quotes the piping head loss equation (No.48) as follows: $h_L = (0.05 + \frac{fL}{D})$ This equation is missing a term and should read as follows: $h_L = (1 + 0.05 + \frac{fL}{D})$
4.19.6	Fixed a minor bug at the downstream calcs of the Headcut. This does not affect the results as it is not related to the control section
4.19.7	Fixed a bug in the piping module. Erosion was still calculated using the old update profile function rather than the updateZ and updateW profile functions.

Model Version Ref.	Model Development
	Replaced the code of CHomoPiping::ReDivideSec function by CHomodam::DivideSec() function code. Improved SetupSec function in homodam to avoid doubling dx at the upstream edge of the crest.
4.19.8	Fixed a bug in the instantaneous failure in the piping module. This version is now part of the SVN repository of HRW.

New Branch of development (4.20 to 4.23) to test drowning settings. Conclusion was to use original settings as in Version 4.19:

4.20	Changed drowning function to Ackers (mwm emails 15\16-2-2010)
4.21	Changed modular limit from 0 to 0.75
4.21 vxx0210	Option of H as well as h for drowning function
4.22	Changed drowning function to modified Bute equation (mwm email 17-2-10). Added a user defined modular limit.
4.23	Added the above drowning options to the user interface.

New Branch of development (version 5 and above) to include zones and layers in the model:

5.00 to 5.06	Coding trials to reach a stable model and acceptable user interface
5.07 to 5.10	New modelling approach testing
5.07	New modelling approach – introducing zoned erodibility
5.09	Macro instability
5.11.1	Macro instability bug fix
5.11.2	Variable erodibility bug fix
5.11_3	Added user interface capability to have a valley shape and to find maximum Rectangle within the valley section
5.11.4	Added capability to save Valley section data – Updated the input wizard – Updated create new document module
5.11.5	Added the intersect sections with Valley shape function to define breach boundaries along the dam.
5.11.6	Implement functions to deal with irregular section shapes
5.11.7	Initial method for including valley shape within breach section
5.12	Second iteration for including valley shape within breach section. Problem when certain valley shapes (e.g. triangular) constrict the breach at the downstream end of the dam creating a control section

Appendix 3

Test case data used for breach model performance evaluation

This appendix contains a description of the 7 sets of test data used to evaluate breach model performance. These data sets were used by the Dam Safety Interest Group breach modelling project and were identified after a review of internationally available data sets (Courivaud, 2007b, Wahl, 2007).

Two sources of data were used for analysis of breaching processes and performance evaluation of the breach model:

1. The EU IMPACT Project field test data (up to five tests);
2. Seven individual test cases collated for use by the Dam Safety Interest Group Breach Modelling project (including some of the IMPACT project field test data).

The EU IMPACT Project field test data

The IMPACT Project was a European FP5 funded project that took place between 2001 and 2004 and which was coordinated by the writer (Contract EVG1-CT2001-00037. See www.impact-project.net). The focus of the project was to improve understanding and tools for the simulation of extreme flood processes. The six work packages addressed:

1. Project coordination;
2. Breach formation;
3. Flood propagation;
4. Sediment transport;
5. Process uncertainty / end user implications;
6. Geophysics and field data.

Research under WP2 comprised a series of large-scale field tests, smaller scale (1:10) laboratory tests and an extensive programme of numerical model testing and comparison. A series of five large-scale tests were undertaken as part of the IMPACT project. Additional tests were also undertaken as part of a parallel Norwegian funded national project. The five IMPACT project tests are summarised in Table A3-1 below.

Table A3-1 Summary of IMPACT project breach field tests

No	*Reference*	*Height*	*Description*	*Failure initiation*
1	Test1-02	6m	Homogeneous cohesive structure (clay)	Overtopping
2	Test2C-02	5m	Homogeneous non-cohesive structure (gravel)	Overtopping
3	Test1-03	6m	Composite structure (gravel with moraine core)	Overtopping
4	Test2-03	6m	Composite structure (gravel with moraine core)	Piping
5	Test3-03	4.5m	Homogeneous structure (moraine)	Piping

Details of these tests and analysis of the physical processes (Morris, 2009) is summarised in Section 2.4.1. Analysis of the test data quality was also undertaken, which includes a description of each test case (Hassan and Morris, 2008).

The Dam Safety Interest Group Breach Modelling project

The Dam Safety Interest Group (DSIG) Breach Modelling project was initiated in 2004 with a plan for three phases of work comprising (I) information gathering, (II) breach model evaluation, and (III) model refinement and integration. Details of this project are given in Section 2.5.1.

Finding reliable, detailed data for validation of breach models is a difficult task. Laboratory tests are often small scale and hence suffer from scale effects. Large scale tests are rare and real failures often have little detailed and reliable data associated with them. EDF undertook a review of potential data sets drawing on sources worldwide (Courivaud, 2007b) and concluded that the seven test cases listed in Table A3-2 offered the best quality data for a range of different conditions. These seven test cases are drawn from a variety of data sources comprising 2 tests from the US Department of Agriculture, Agricultural Research Service laboratory (USDA-ARS, Stillwater, Oklahoma), 3 tests from the European IMPACT project and 2 real dam failure case studies.

A brief description of each test is given in the following sections.

Table A3-2 Summary of DSIG test data used for model evaluation

Evaluation Test No.	*Name & Source*	*Description*	*Comment*
1	ARS#1	2m high, homogeneous embankment constructed from silty sand. Includes grass cover.	Controlled construction. Head cut failure occurs
2	ARS#2	2m high, homogeneous embankment constructed from clay-loam. Includes grass cover.	Controlled construction. Head cut starts, but failure does not occur within timeframe
3	IMPACT Clay (Field Test#1 / Test1-02)	5.9m high homogeneous embankment with ~25% clay content. No surface protection (grass etc.)	Very wet construction. Variable compaction. Head cut failure.
4	IMPACT Gravel (Field Test#2 / Test2C-02)	5.0m high homogeneous embankment constructed from gravel (D_{50} 4.75mm)	High degree of compaction. Freezing conditions. Head cut failure occurs
5	IMPACT Composite (Field Test#3 / Test1-03)	5.9m high composite embankment constructed from moraine core with rock fill cover layer	Mixture head cut and surface erosion failure
6	Oros Dam (Brazil)	35.5m high zoned dam with mass clay core, sand and rock fill shoulders	Real dam failure case study Uncertainty within data means test data are calculated / estimated
7	Banqiao Dam (China)	24.5m high zoned dam with clay core and earth shoulders. Failed during construction - condition at failure uncertain.	Real dam case study. Limited data (for example, core geometry unknown) hence test data are calculated / estimated

Evaluation Test No.1: ARS#1 – 2m high, silty sand, overtopping failure

Test ARS#1 comprises a 2m high, homogeneous embankment constructed from silty sand. The embankment includes grass cover, although the quality of this cover is unclear. Figure A3-1 - Figure A3-3 and Table A3-3 - Table A3-4 provide description data for the embankment geometry and soil conditions.

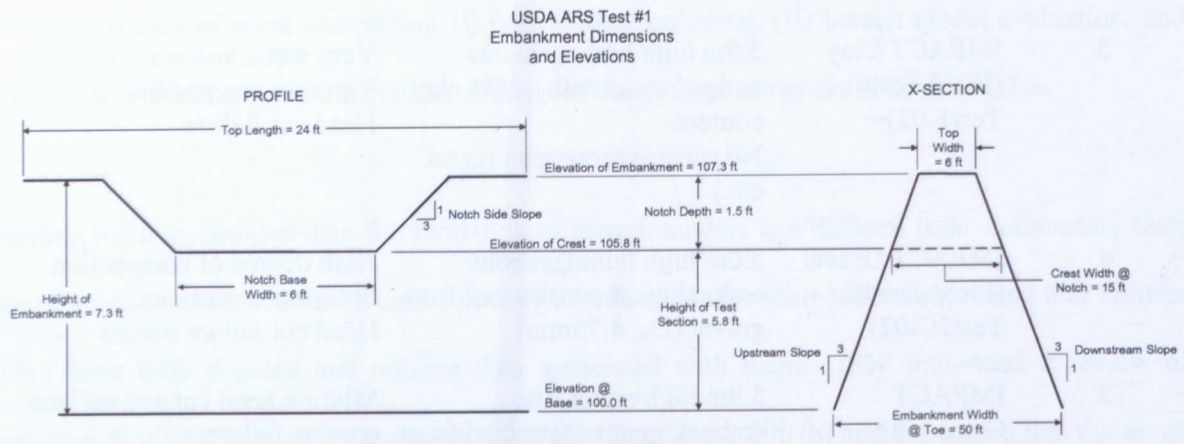

Figure A3-1 Geometry for ARS#1 test embankment

Figure A3-2 ARS#1 test embankment

Table A3-3 Embankment and test section dimensions

Embankment Dimensions		Test Section Dimensions	
Height of Embankment	7.3 ft	Height of Test Section	5.8 ft
Elevation of Embankment	107.3 ft	Notch Base width	6.0 ft
Top Length	24 ft	Notch Side Slopes	3/1 (H/V)
Top Width	6 ft	Notch Depth	1.5 ft
Upstream Slope	3/1 (H/V)	Crest Width @ Notch	15 ft
Downstream Slope	3/1 (H/V)	Elevation of Crest	105.8 ft
Elevation @ Base	100 ft		
Embankment Width @ Toe	50 ft		

Table A3-4 Embankment soil properties

Gradation		
% Clay < 0.002 mm	5	
% Silt > 0.002 mm	25	
% Sand > 0.105 mm	70	
Plasticity Index	Non-plastic	
USCS	SM	
Grain Density g/cm^3	2.67	
Unconfined Compressive Strength qu (lb/ft^2)	425	
Average Dry Density (lb/ft^3)	107.05	
Average Water Content @ construction %	8.9	
Average Total Density (lb/ft^3)	116.6	
Erodibility Coefficient kd (ft/h)/(lb/ft^2)	5.77	
Critical stress τ_c lb/ft^2	0	
Construction		
Compaction Effort	~4000 ft-lb/ft^3	
Loose Lift Thickness	0.5 ft	
Compacted lift thickness	0.4 ft	
Constructed 9/1998		
Sieve Analysis	mm	% Finer
0.002 mm	0.002	5
0.005 mm	0.005	7
# 200 (0.075 mm)	0.075	30
# 140 (0.106 mm)	0.106	39
# 60 (0.250 mm)	0.25	71
# 40 (0.425 mm)	0.425	93
# 20 (0.850 mm)	0.85	99
# 10 (2.00 mm)	2	100

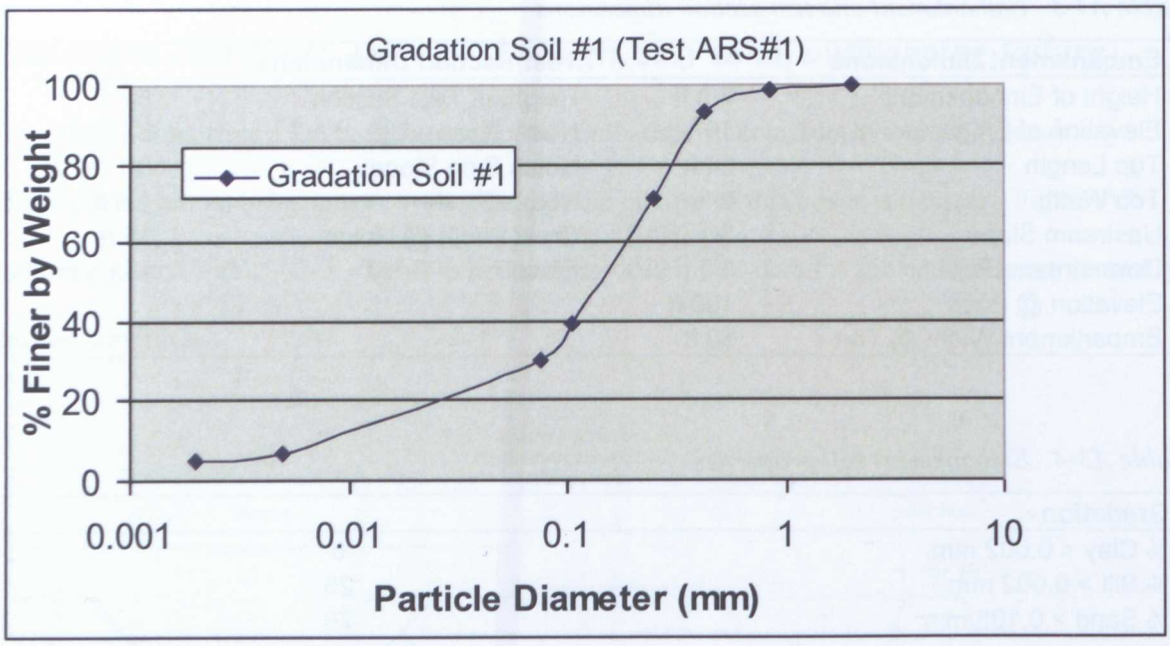

Figure A3-3 ARS#1 soil grading curve

Evaluation Test No.2: ARS#2 – 2m high, clay loam, overtopping failure

Test ARS#2 comprises a 2m high, homogeneous embankment constructed from clay-loam. The embankment includes grass cover, although the quality of this cover is unclear. Figure A3-4 - Figure A3-6 and Table A3-5 - Table A3-6 provide description data for the embankment geometry and soil conditions.

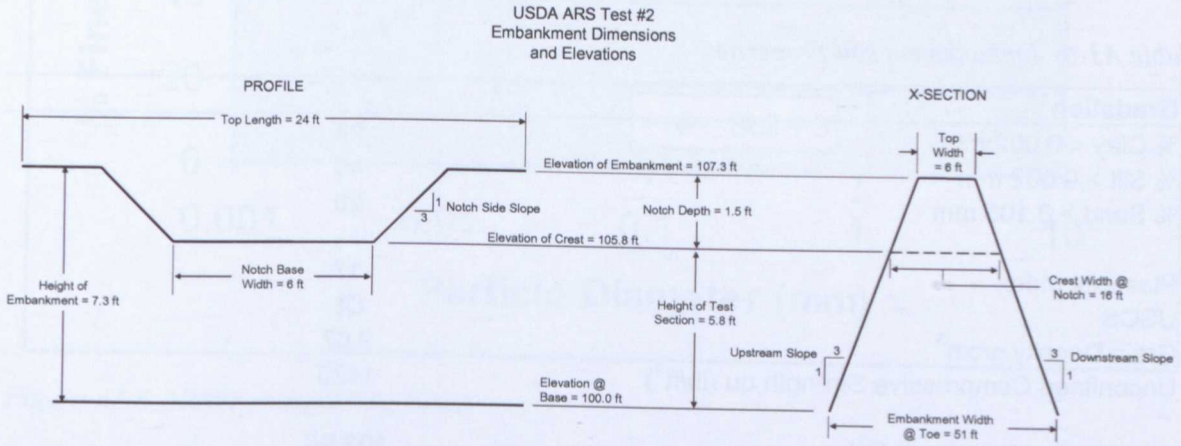

Figure A3-4 Geometry for ARS#2 test embankment

Figure A3-5 ARS#2 test embankment

Table A3-5 Embankment and test section dimensions

Embankment Dimensions		Test Section Dimensions	
Height of embankment	7.3 ft	Height of Test Section	5.8 ft
Elevation of embankment	107.3 ft	Notch Base width	6.0 ft
Top Length	24 ft	Notch Side Slopes	3/1 (H/V)
Top Width	6ft	Notch Depth	1.5 ft
Upstream Slope	3/1 (H/V)	Crest width @ Notch	16 ft
Downstream Slope	3/1 (H/V)	Elevation of Crest	105.8 ft
Elevation @ Base	100.0 ft		
Embankment Width @ Toe	51 ft		

Table A3-6 Embankment soil properties

Gradation		
% Clay < 0.002 mm	26	
% Silt > 0.002 mm	49	
% Sand > 0.105 mm	25	
Plasticity Index	17	
USCS	CL	
Grain Density g/cm^3	2.67	
Unconfined Compressive Strength qu (lb/ft^2)	1423	
Average Dry Density (lb/ft^3)	102.96	
Average Water Content @ construction %	16.4	
Average Total Density (lb/ft^3)	120	
Erodibility Coefficient kd (ft/h)/(lb/ft^2)	0.022	
Critical stress τ_c lb/ft^2	0.3	
Construction		
Compaction Effort	~4000 ft-lb/ft^3	
Loose Lift Thickness	0.5 ft	
Compacted lift thickness	0.4 ft	
Constructed 9/1998		
Sieve Analysis	mm	% Finer
0.002 mm	0.002	26
0.005 mm	0.005	32
# 200 (0.075 mm)	0.075	75
# 10 (2.00 mm)	2	100

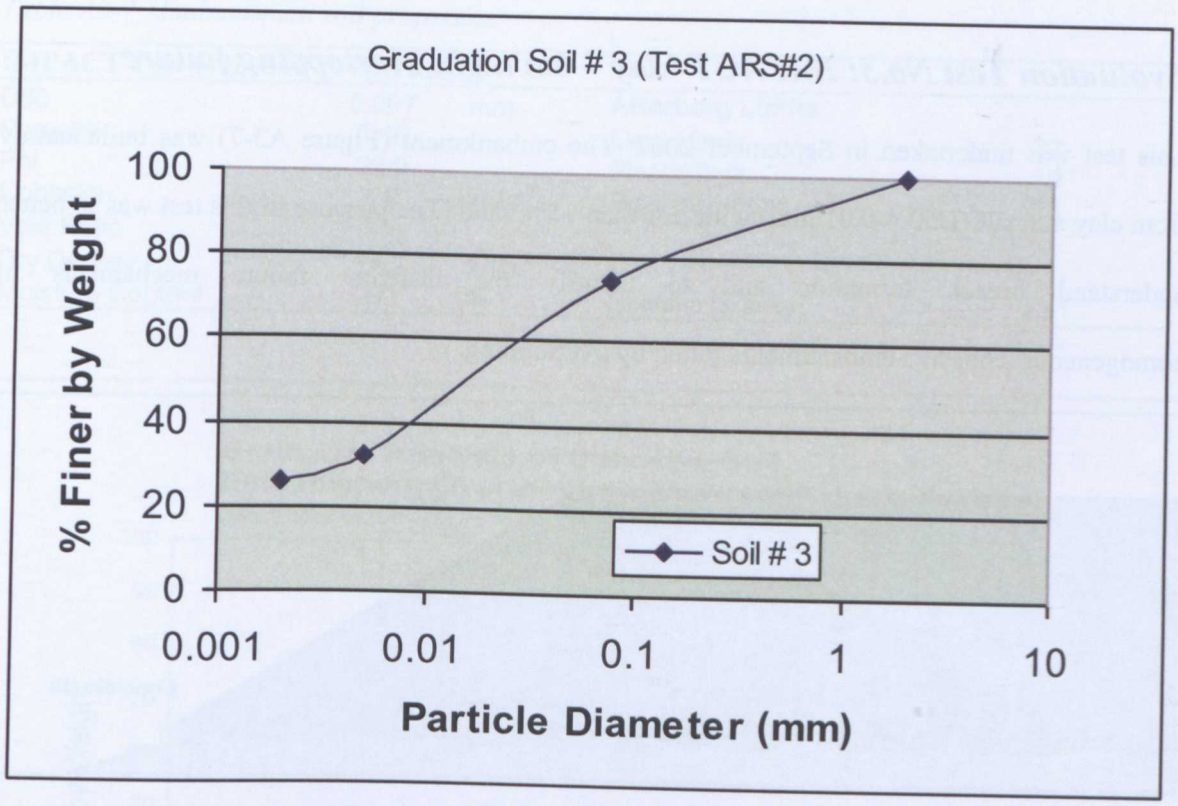

Figure A3-6 ARS#1 soil grading curve

Evaluation Test No.3: IMPACT Clay – 6m high, overtopping failure

This test was undertaken in September 2002. The embankment (Figure A3-7) was built mainly from clay and silt (D50 < 0.01 mm) with less than 15% sand. The purpose of this test was to better understand breach formation and to identify the different failure mechanisms in homogeneous cohesive embankments failed by overtopping.

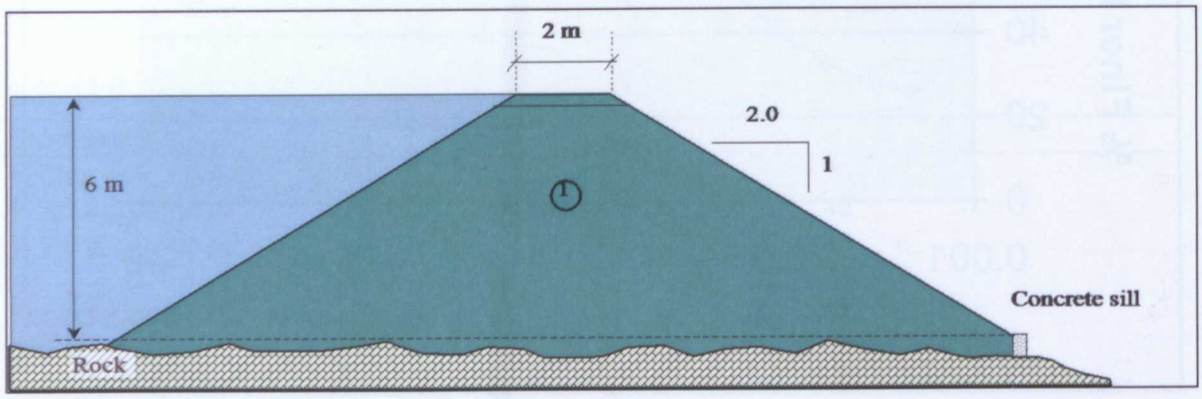

Figure A3-7 Design data for Test 1-02

The embankment constructed actually had a crest height of 5.9m, crest width of 2.0m, upstream slope of 1:2.4 and downstream slope of 1:2.25 (Hassan and Morris, 2008).

Figure A3-8 Early stages of breach testing for the 'IMPACT Clay' test

Table A3-7 Embankment soil properties

IMPACT Test 1-02 Soil Properties				
D50	0.007	mm	**Atterberg Limits**	
Porosity	0.46		Liquid limit	32
Phi	22.9		Plastic limit	19
Cohesion	4.9	kn/m^2	Plasticity Index	13
Void Ratio	---			
Dry Density	14.7	kn/m^3		
Moisture Content	30	%	Specific Gravity	2.81

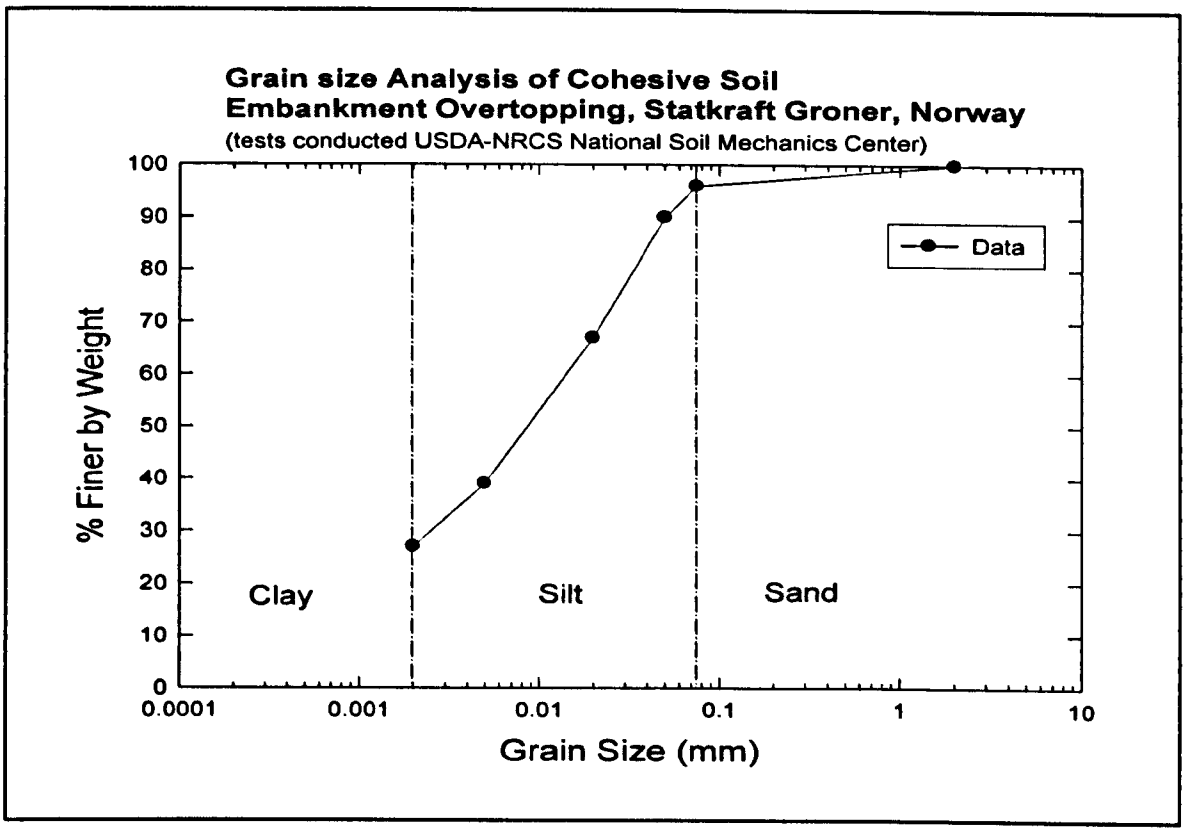

Figure A3-9 IMPACT Test 1-02: Embankment soil grading

More information on this IMPACT Project test case can be found on the IMPACT and FLOODsite websites (www.impact-project.net; www.floodsite.net) and in FLOODsite report T04-08-04 (Hassan and Morris, 2008).

Evaluation Test No.4: IMPACT Gravel – 5m high, overtopping failure

This test was undertaken in October 2002. The embankment (Figure A3-10) was built mainly from non-cohesive materials (D50 ≈ 5 mm) with less than 5 % fines. The purpose of this test was to better understand breach formation and to identify the different failure mechanisms in homogeneous non-cohesive embankments failed by overtopping and also to assess / inspect the effect of seepage on the breach formation processes. The embankment constructed actually had an upstream slope of 1:1.9 and downstream slope of 1:1.6 (Hassan and Morris, 2008).

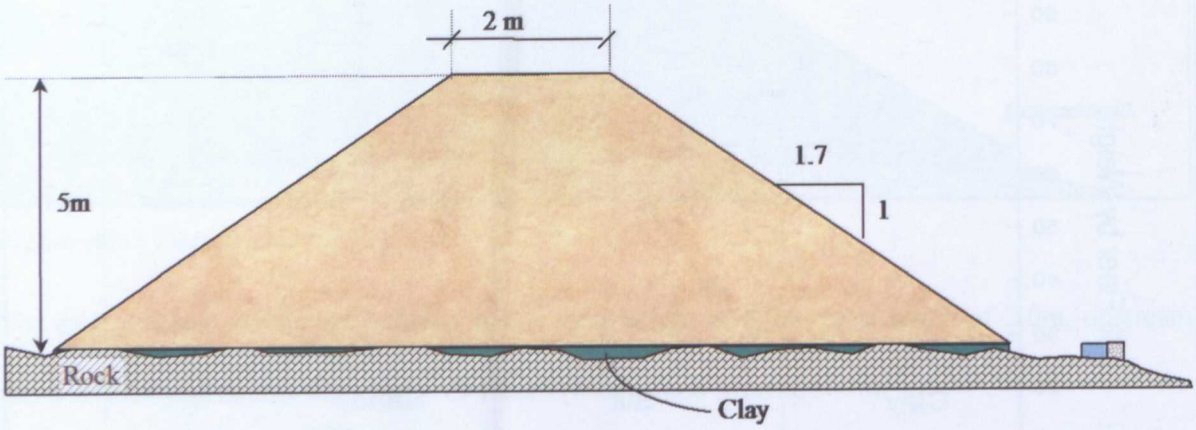

Figure A3-10 Design data for Test 2C-02

Figure A3-11 Early stages of breach testing for the 'IMPACT Gravel' test

As can be seen in Figure A3-11 above, testing was undertaken during freezing conditions and the degree to which ice affected the test is unclear. It is suspected that the surface layers of the embankment (at minimum) were frozen. Video footage shows prolonged efforts by the researchers to thaw the crest layer prior to test initiation.

Table A3-8 Embankment soil properties

IMPACT Test 2C-02 Soil Properties				
D50	4.75	mm	**Atterberg Limits**	
Porosity	0.22		Liquid limit	N/A
Phi	42		Plastic limit	N/A
Cohesion	0.9	kn/m^2	Plasticity Index	N/A
Void Ratio	---			
Dry Density	27.7	kn/m^3		
Moisture Content	7	%	Specific Gravity	2.75

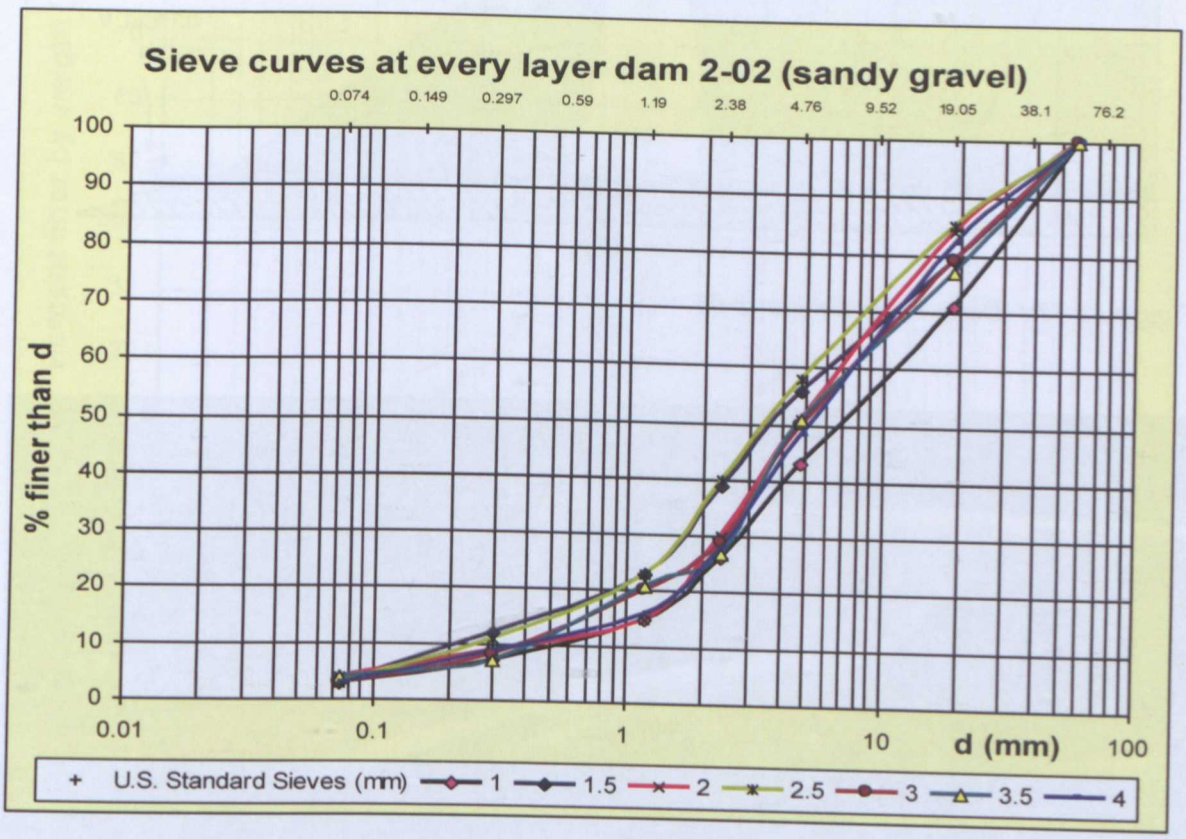

Figure A3-12 IMPACT Test 2C-02: Embankment soil grading

More information on this IMPACT Project test case can be found on the IMPACT and FLOODsite websites (www.impact-project.net; www.floodsite.net) and in FLOODsite report T04-08-04 (Hassan and Morris, 2008).

Evaluation Test No.5: IMPACT Composite – 6m high, overtopping failure

This test was undertaken in August 2003. The upstream and downstream shoulders were built from rock fill with a central moraine core. The purpose of this test was to better understand breach formation and to identify the different failure mechanisms in composite embankments failed by overtopping. The embankment was actually constructed to a height of 5.9m and had upstream and downstream slopes of 1:1.55 (Hassan and Morris, 2008). Dimensions of the core also varied from the original construction specification.

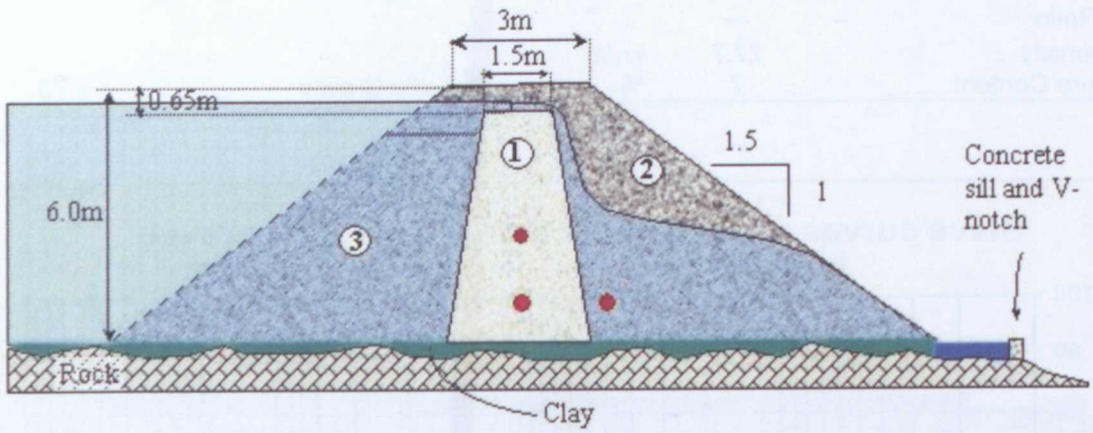

Figure A3-13 Design data for Test 1-03

Figure A3-14 Early stages of breach testing for the 'IMPACT Composite' test

Table A3-9 Embankment soil properties

IMPACT Test 2C-02 Soil Properties					
Moraine Core			**Rockfill Outer Layer**		
D50	7	mm	D50	85	mm
Porosity	0.24		Porosity	0.24	
Phi	45.6		Phi	42	
Cohesion	20	kn/m^2	Cohesion	0	kn/m^2
Void Ratio	---		Void Ratio	---	
Dry Density	20.9	kn/m^3	Dry Density	27.76	kn/m^3
Moisture Content	6	%	Moisture Content	2	%

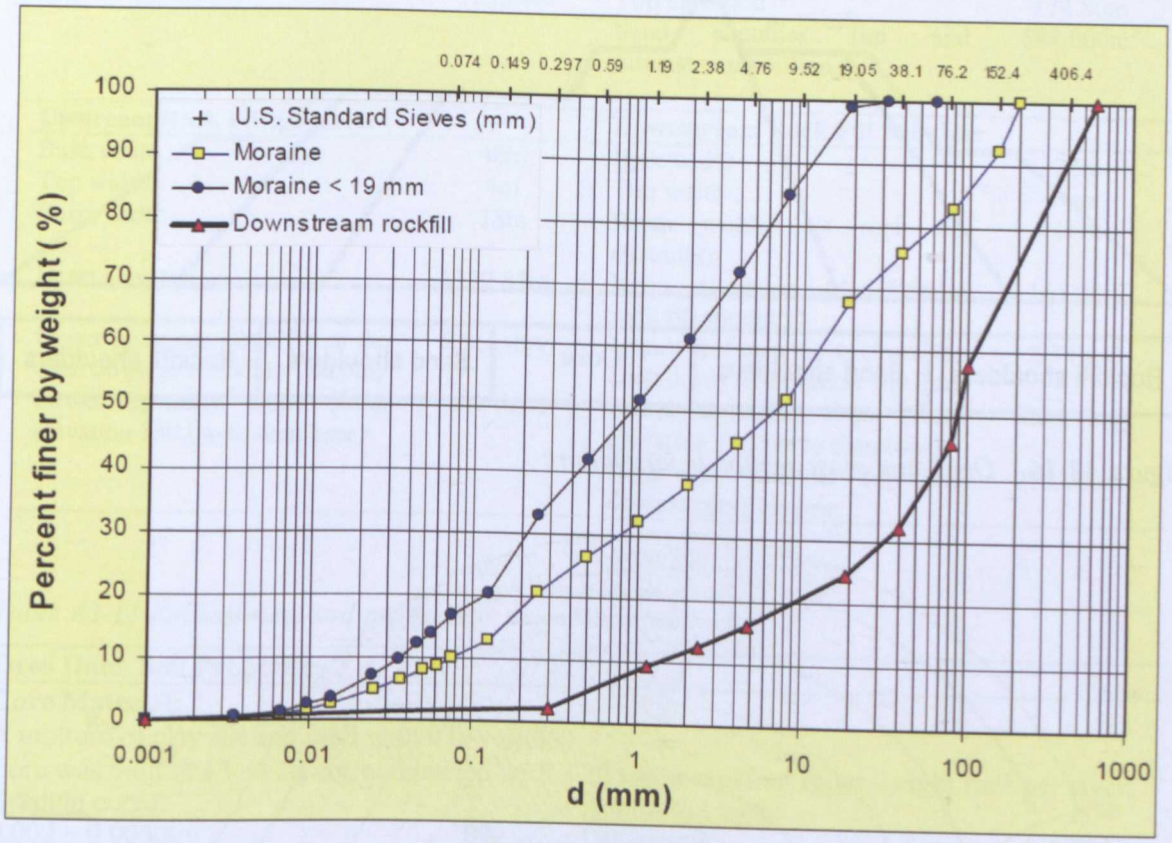

Figure A3-15 IMPACT Test 1-03: Embankment soil grading

More information on this IMPACT Project test case can be found on the IMPACT and FLOODsite websites (www.impact-project.net; www.floodsite.net) and in FLOODsite report T04-08-04 (Hassan and Morris, 2008).

Evaluation Test No.6: Oros Dam (Brazil) – 36m high, mass clay core with rock fill shoulders, overtopping failure

The Oros was constructed in Brazil in Ceara State, on the Jaguaribe river. It failed on March 26th 1960 during construction, as a result of flood flow overtopping the dam. 100,000 people were evacuated before the dam failed, and there were no fatalities. Before failure the dam stood 35.5m above ground level with a crest length of 510m built from 2Mm^3 of material.

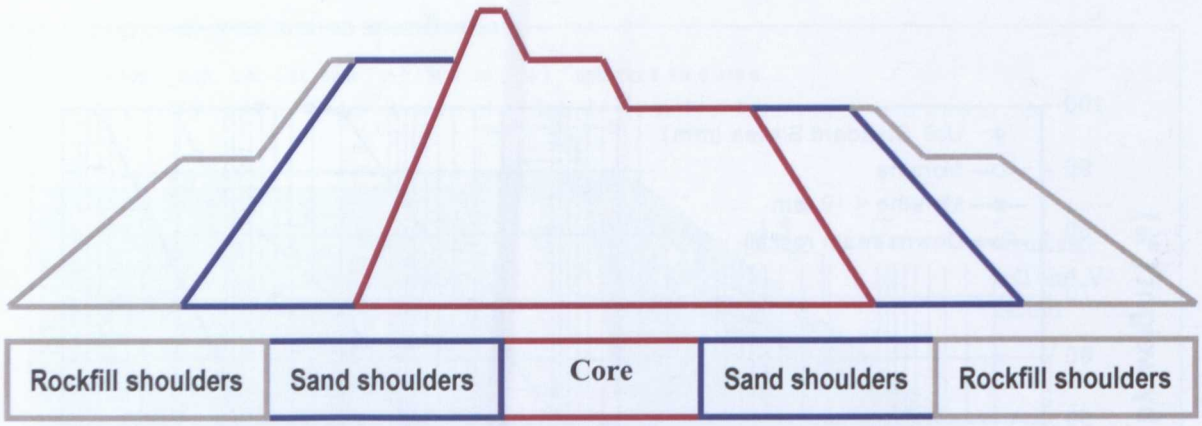

Figure A3-16 Oros dam cross section before failure

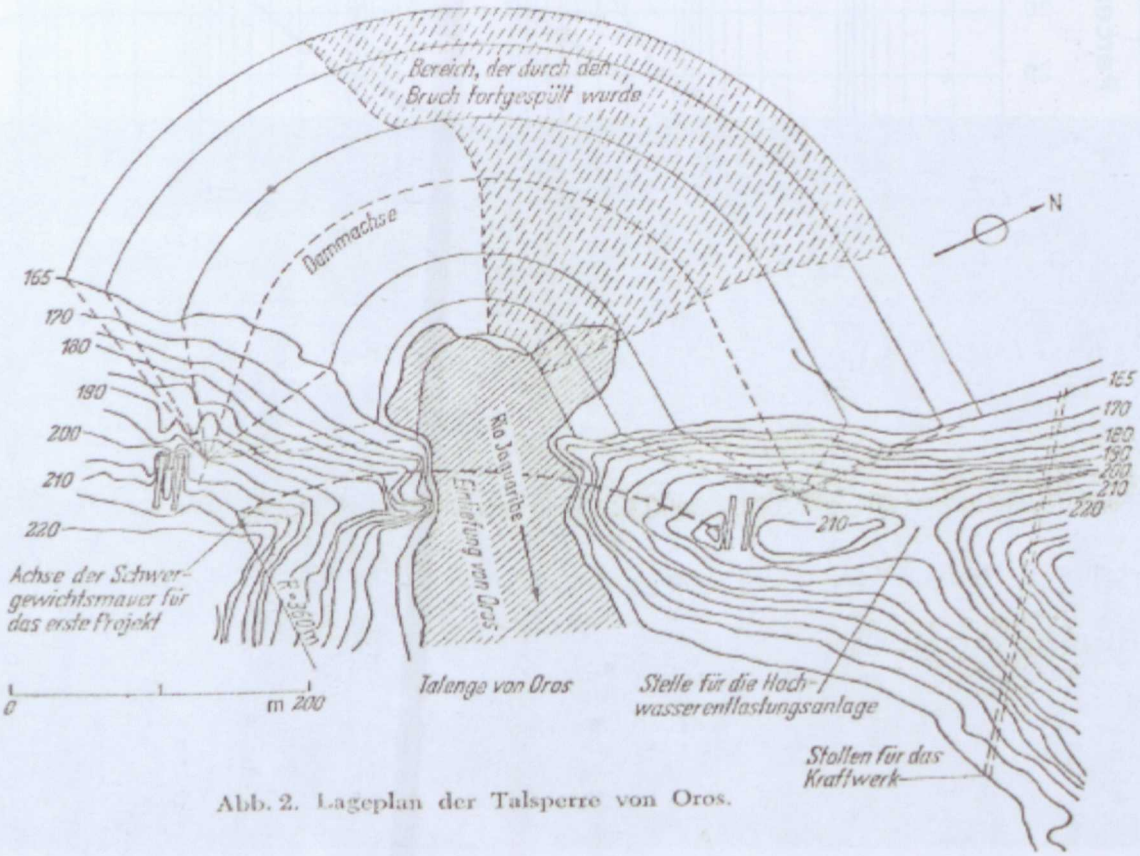

Figure A3-17 Plan view of the proposed Oros Dam

Table A3-10 Oros dam geometry

Core Geometry			
Base width	110m	Base elevation	155.00m
Crest width	5m	Crest elevation	190.50m
Upstream slope of core	1:1 (h:v)	Downstream slope of core	1:1 (h:v)
Width of upper berm of core	18m	Elevation of upper berm of core	183.40m
Width of lower berm of core	22m	Elevation of lower berm of core	174.80m
Core material volume	1.212Mm^3		

Upstream Sand Shoulder		**Downstream Sand Shoulder**	
Base width	60m	Base width	38m
Top width	26m	Top width	24m
Upstream slope	2:1 (h:v)	Downstream slope	1.75:1 (h:v)
Top elevation	183.80m	Top elevation	174.80m
		Sand shoulder (up and downstream) volume	588,000m^3

Upstream Rock Fill Shoulder		**Downstream Rock Fill Shoulder**	
Base width	40m	Base width	32m
Top width	4m	Top width	4m
Berm width	18m	Berm width (d/s rock fill shoulder)	16m
Berm elevation	170.85m	Berm elevation (downstream rock fill shoulder)	165.80m
Upper upstream slope (from the crest down to elevation 180.0m)	2.5:1 (h:v)	Upper upstream slope (from the crest down to elevation 180.0m)	2:1 (h:v)
Lower upstream slope (from elevation 180.0m to dam base)	3:1 (h:v)	Lower upstream slope (from elevation 180.0m to dam base)	2.5:1 (h:v)
		Rock fill shoulder (up and downstream) volume	215,000m^3

Table A3-11 Embankment soil properties

Oros Dam Soil Properties

Core Material:

A mixture of clay silt and sand with a few rocks.

Core was built in 15cm layers, compacted with a 20 ton sheepsfoot roller – eight runs per layer.

Grading curve:		Atterberg Limits:	
0.002 – 0.005mm	9%	Liquid limit	27%
0.005 – 0.05mm	19%	Plastic limit	17%
0.05 – 5mm	67%	Plasticity Index	10%
> 5mm	5%		
Specific density saturated soil	2110kg/m^3	Internal friction angle	27°
Moisture content	15.5%	Permeability	3.7x10-10m/s
Cohesion	420g/cm^2		

Sand Shoulder Material:

Material was a mixture of sand and coarse aggregates

Shoulder was built in 30cm layers, compacted with vibratory roller.

Specific density saturated soil 2120kg/m^3

Rock Fill Shoulder Material:

Rock fill was made from blocks ranging from 0.1 – 0.5m^3

Blocks were placed in 1m thick layers without any compaction.

Specific density saturated soil 2010kg/m^3

Figure A3-18 Oros dam during (left) and after (right) failure (Courivaud, 2007b)

More information on this test case can be found in the CEATI Dam Safety Interest Group Breach Modelling Project Report T032700-0207B (Courivaud, 2007b).

Evaluation Test No.7: Banqiao Dam (China) – 25m high, clay core with earth fill shoulders, overtopping failure during construction

The Banqiao Dam was constructed in Henan Province, Bivan County, China and impounded in 1956. The dam failed by overtopping on 8th August 1975. The Shimantan Dam also failed at the same time, along with two medium sized reservoirs and 58 small reservoirs. The combination of failures resulted in the deaths of approximately 26,000 people.

The embankment dam had a clay core constructed with 'arenaceous' shale. No information is available on the core geometry. The upstream and downstream shoulders comprised homogeneous earth sections. It can be assumed that dam material was poorly compacted (due to the date of construction within China). No information is available upon the dam foundations. The dam geometry is summarised in Table A3-12 below.

This test case represents the situation of a large reservoir with a dam constructed from highly erodible material, which, when failing will lead to rapid breach growth and hence the creation of a rapid, high peak value flood hydrograph.

Table A3-12 Banqiao dam geometry

Banqiao Dam Geometry			
Dam height above ground level	24.5m	Upstream slope	1:3 (v:h)
Ground elevation	91.84m	Downstream slope	1:2.5 (v:h)
Dam crest elevation	116.34m	Top width	6m
Wave wall top elevation	117.64m	Base width	141m
Dam crest length	2020m	Dam volume	6.632Mm^3
Dam base length	Unknown	Core geometry	Unknown

Figure A3-19 Failure of Banqiao Dam (Courivaud, 2007b)

Appendix 4

A new modelling approach for breach simulation through variable erodibility zones

The new breach modelling approach allows for an embankment or dam to be represented by a series of different zones of material, each with different erodibility properties. This appendix contains details of the testing of the various zone combinations and the assessment as to whether the modelling approach provides realistic and improved modelling results.

A series of model tests were undertaken to assess model performance for a range of conditions (Table 7-1). The purpose of these tests was to investigate how the model performed against different geometric arrangements of variable erodibility (and hence also soil type) zones. Five different generic geometric arrangements were tested, comprising homogeneous and then embankment arrangement Types 1, 2, 3 and 4 (see Figure 7-5 reproduced below). The following sections contain detailed plots showing modelling results for each of these tests compared against the 'base condition' produced from modelling the homogeneous embankment.

Table A4-1 Summary of erodibility model testing (Table 7-1)

No.	*Description*	*Run Reference*
1	Homogeneous embankment; Erodibility K_d=10	*M1-Homo-Kd10-Res2500*
2	Homogeneous embankment; Erodibility K_d=10	*M1-Homo-Kd100-Res2500*
3	Two horizontal layers; Upper layer 2m thick with K_d=100; Lower layer 2m thick with K_d=10	*M1-Type1-2layer-D2Kd100-D2Kd10-Res2500*
4	Two horizontal layers; Upper layer 2m thick with K_d=10; Lower layer 2m thick with K_d=100	*M1-Type1-2layer-D2Kd10-D2Kd100-Res2500*
5	Two horizontal layers; Upper layer 1m thick with K_d=100; Lower layer 3m thick with K_d=10	*M1-Type1-2layer-D1Kd100-D3Kd10-Res2500*
6	Two horizontal layers; Upper layer 1m thick with K_d=10; Lower layer 3m thick with K_d=100	*M1-Type1-2layer-D1Kd10-D3Kd100-Res2500*
7	Raised embankment landward side; Extra layer 1m thick with Kd=100; base 3m thick with Kd=10	*M1-Type3-2layer-D1Kd100-D3Kd10-Res2500*
8	Raised embankment landward side; Extra layer 1m thick with Kd=10; base 3m thick with Kd=100	*M1-Type3-2layer-D1Kd10-D3Kd100-Res2500*
9	Raised embankment load side; Extra layer 1m thick with Kd=100; base 3m thick with Kd=10	*M1-Type4-2layer-D1Kd100-D3Kd10-Res2500*
10	Raised embankment load side; Extra layer 1m thick with Kd=10; base 3m thick with Kd=100	*M1-Type4-2layer-D1Kd10-D3Kd100-Res2500*
11	Centrally raised embankment; Extra layer 2m thick with Kd=100; base 2m thick with Kd=10	*M1-Type2-2layer-D2Kd100-D2Kd10-Res2500*
12	Centrally raised embankment; Extra layer 2m thick with Kd=10; base 2m thick with Kd=100	*M1-Type2-2layer-D2Kd100-D2Kd10-Res2500*
13	Three horizontal layers; All layers 1.3m thick with K_d=100, 50, 10 respectively.	*M1-Type1-3layer-D1.3Kd100-D1.3Kd50-D1.3Kd10-Res2500*
14	Three horizontal layers; All layers 1.3m thick with K_d=10, 50, 100 respectively.	*M1-Type1-3layer-D1.3Kd10-D1.3Kd50-D1.3Kd100-Res2500*
15	Three horizontal layers; All layers 1.3m thick with K_d=100, 10, 100 respectively.	*M1-Type1-3layer-D1.3Kd100-D1.3Kd10-D1.3Kd100-Res2500*
16	Three horizontal layers; All layers 1.3m thick with K_d=10, 100, 10 respectively.	*M1-Type1-3layer-D1.3Kd10-D1.3Kd100-D1.3Kd10-Res2500*

Note: All tests were performed using the same modelling scenario, as described in Section 6.3. A reservoir surface area of 2500m^2 was used in conjunction with erodibility (K_d) values of 10 and 100 respectively. This provided examples where the breach behaviour was controlled by soil erodibility and lake size (See Section 6.3).

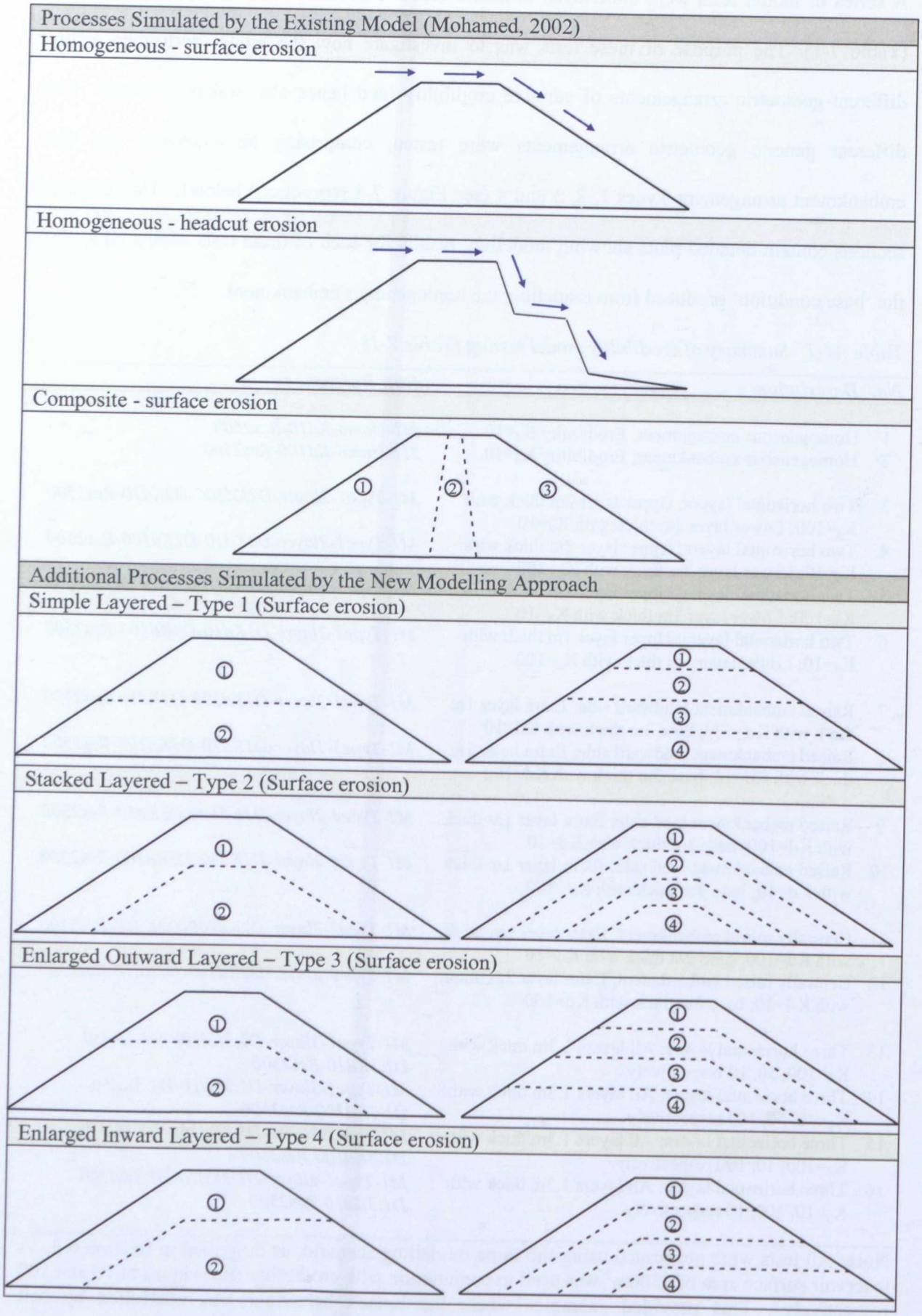

Figure A4-1 Generic options for simulating different zoned geometries (Figure 7-5)

Comparison of all modelling data

Figure A4-2- Figure A4-6 shows results for breach outflow, reservoir level, breach width, breach depth and depth on breach for all of the model simulations. Subsequent sections of this appendix provide an analysis of results for each type of embankment in comparison to the 'base conditions' produced by simulation of breach through the homogeneous embankment for two different magnitudes of erodibility (K_d=100 and K_d=10).

Note that all of the results presented are for conditions predicted at the critical flow section. This is the section at which the model predicts transition from sub to super critical flow conditions. As erosion occurs at different sections through the embankment, the critical control section can, and does change. Under some conditions, two sections with significantly different depth / width ratios can offer very similar conveyance and the location for critical flow control can oscillate between these sections. This appears as oscillations in the data – as seen in Figure A4-4, Figure A4-5 and Figure A4-6 below. This is not model instability (for example, Figure A4-2 and Figure A4-3 show no inconsistencies) and does reflect how the critical control section within a breach typically jumps around as erosion changes the shape of the embankment surface. In practice, this occurs in 3D rather than in 2D as simulated here.

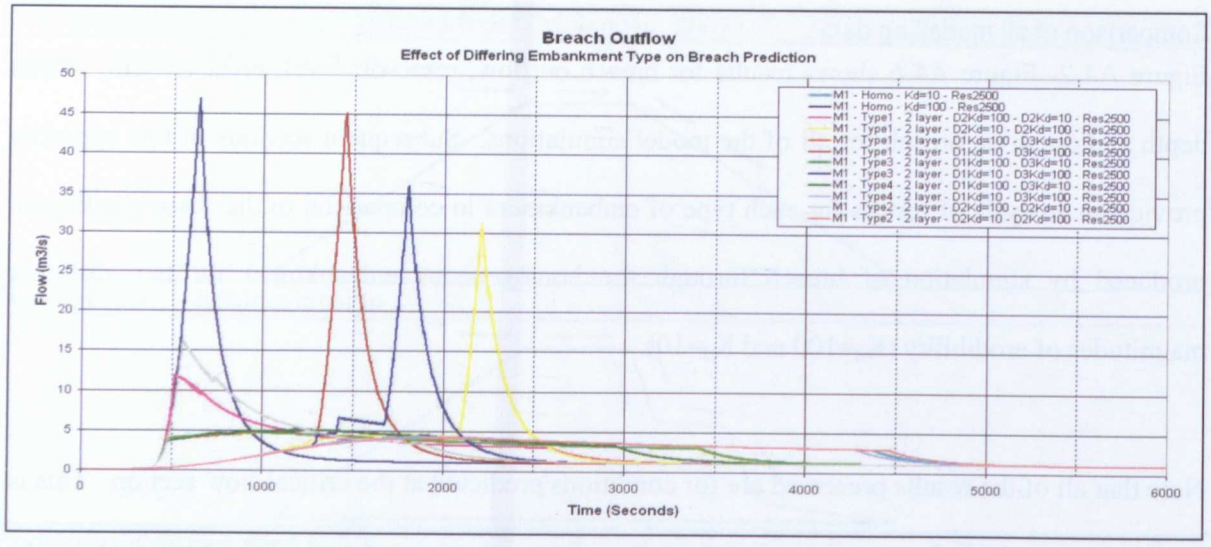

Figure A4-2 Breach outflow: Comparison of all erodibility zone runs

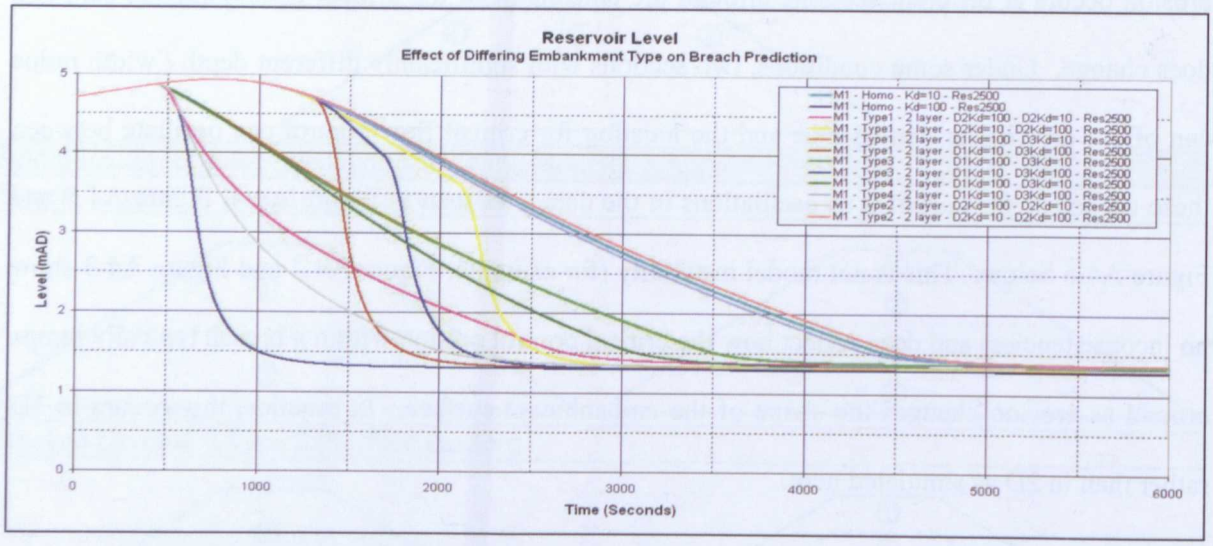

Figure A4-3 Reservoir level: Comparison of all erodibility zone runs

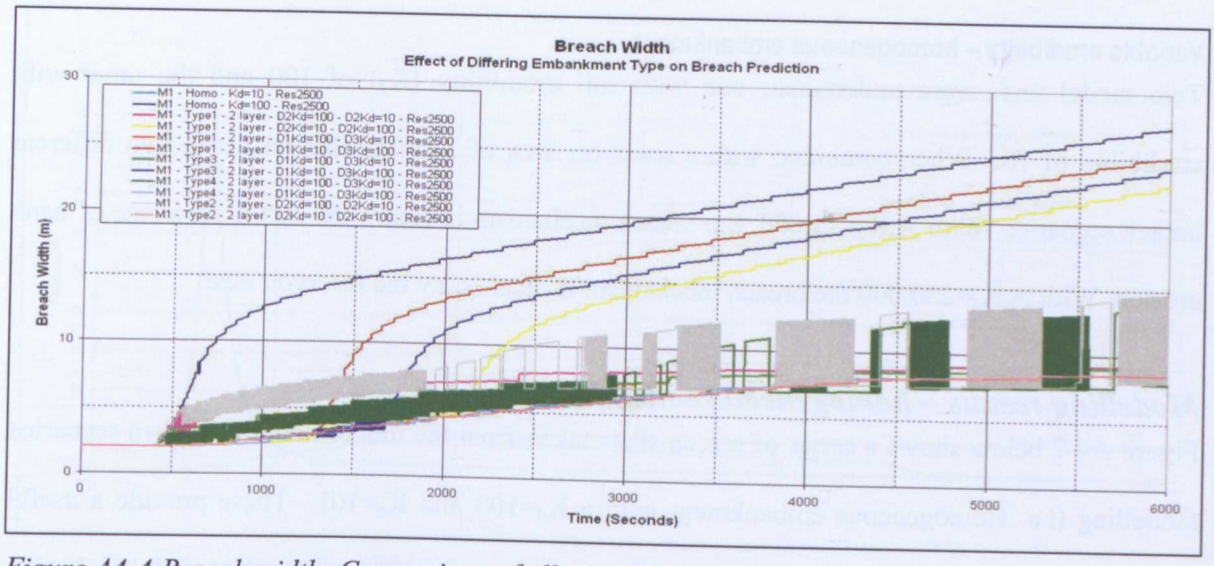

Figure A4-4 Breach width: Comparison of all erodibility zone runs

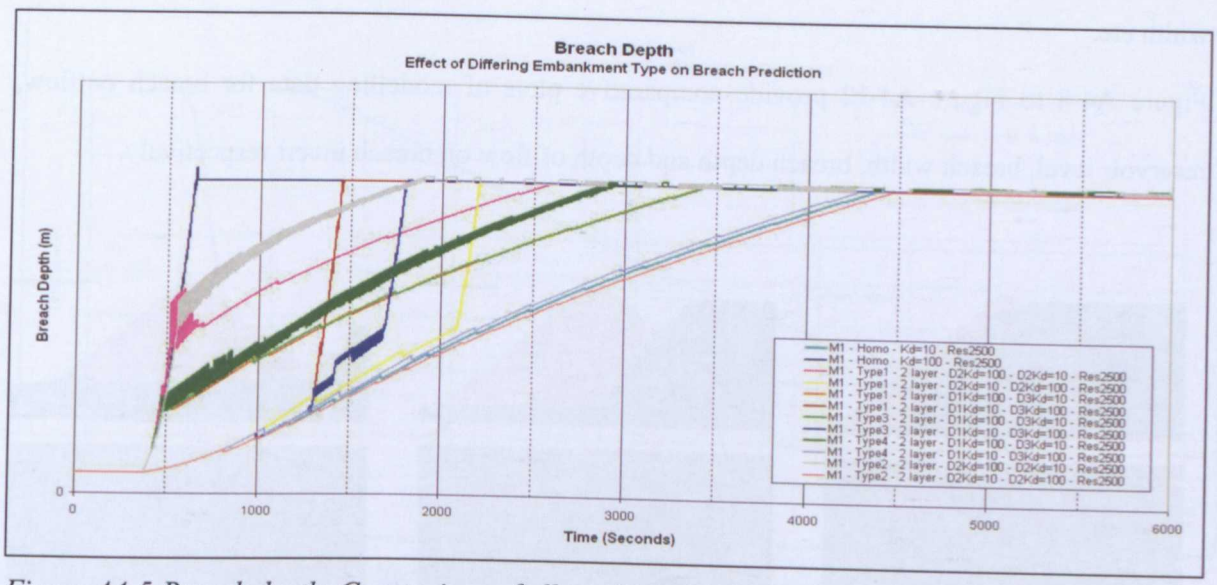

Figure A4-5 Breach depth: Comparison of all erodibility zone runs

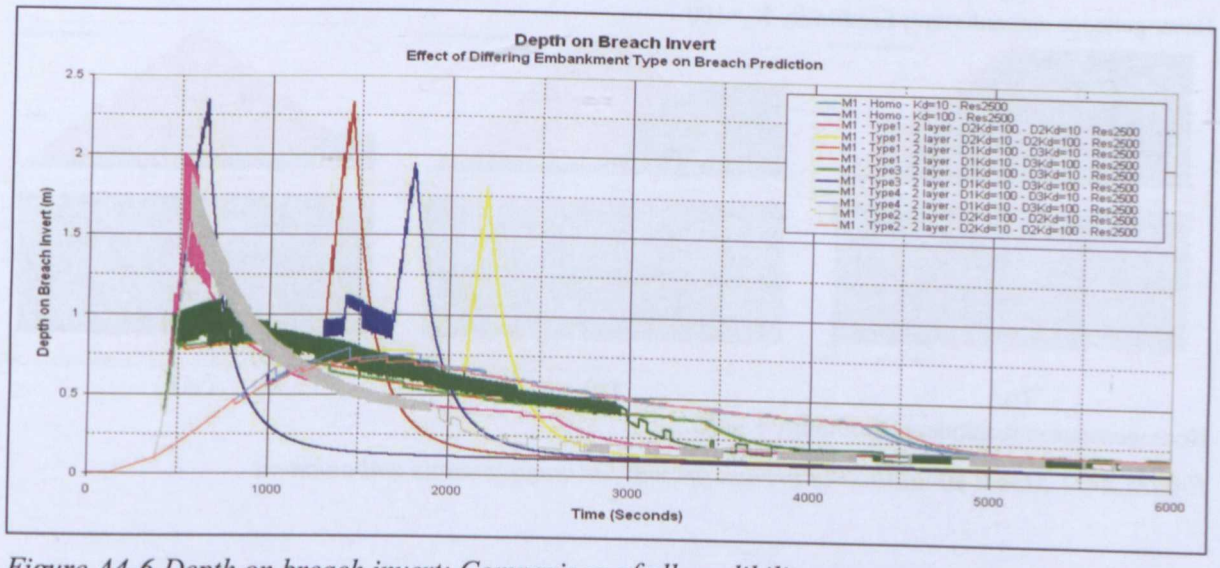

Figure A4-6 Depth on breach invert: Comparison of all erodibility zone runs

Variable erodibility – homogeneous embankment

Two model tests were undertaken; one with soil erodibility (K_d) of 100 and the other with erodibility of 10. When combined with a reservoir area of 2,500m^2 this results in two different breach scenarios. With A_sK_d=25,000, the breach mechanism is controlled by the slow rate of bank erosion. With A_sK_d=250,000 the breach mechanism is dictated by the reservoir size.

Modelling results – homogeneous embankment

Figure A4-7 below shows a series of screen shots taken from the model runs for the two scenarios modelling (i.e. Homogeneous embankment with a K_d=100 and K_d=10). These provide a useful indication of how the erosion processes are simulated in conjunction with reservoir level, breach width etc.

Figure A4-8 to Figure A4-12 provide comparative plots of modelling data for breach outflow, reservoir level, breach width, breach depth and depth of flow on breach invert respectively.

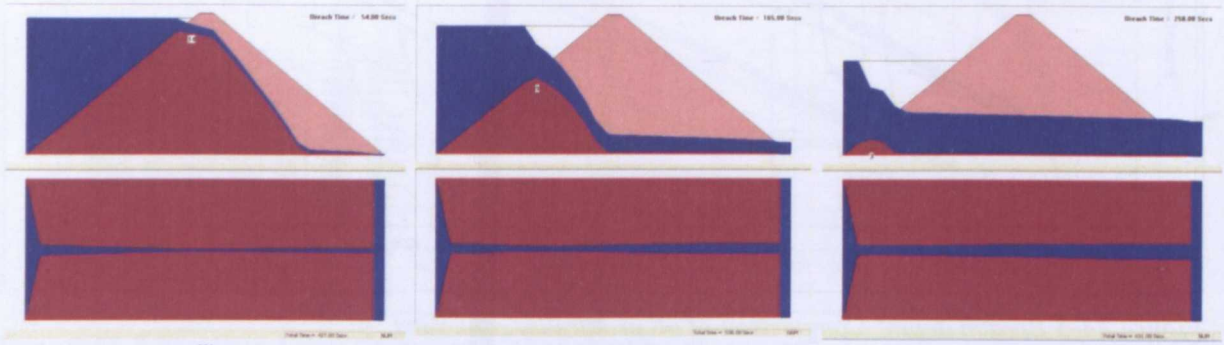

(i) (ii) (iii)

Homogeneous embankment; Erodibility K_d=100

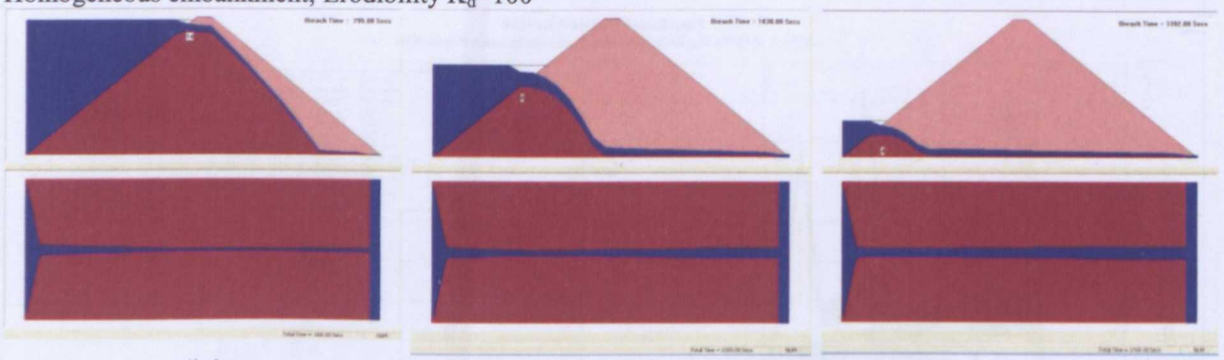

(iv) (v) (vi)

Homogeneous embankment; Erodibility K_d=10

Figure A4-7 Model simulation of breach growth for homogeneous embankment

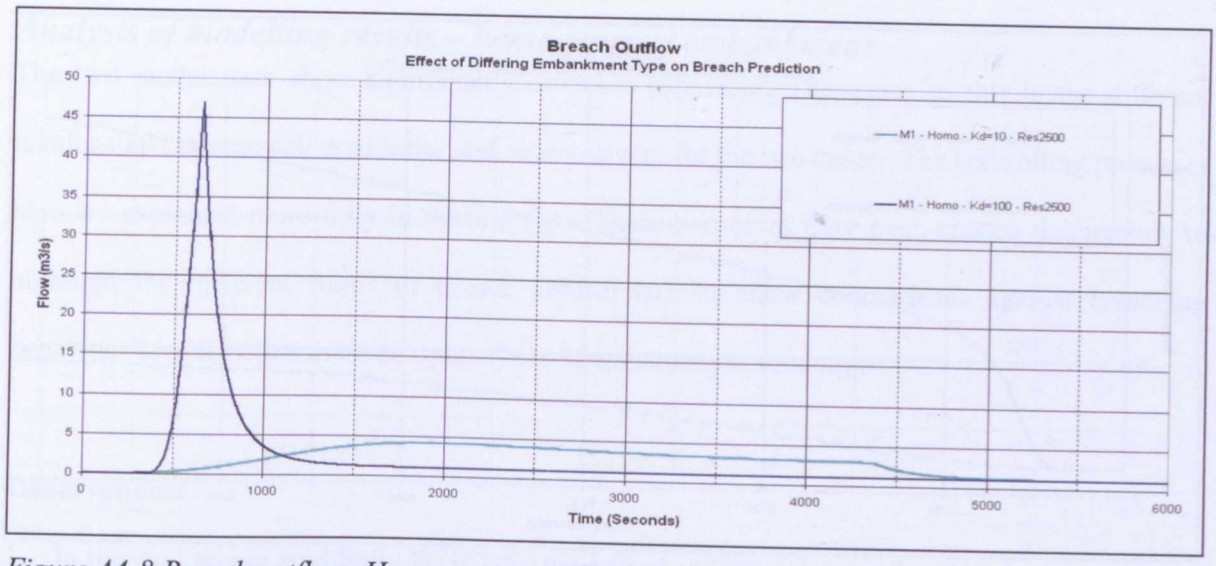

Figure A4-8 Breach outflow: Homogeneous embankment

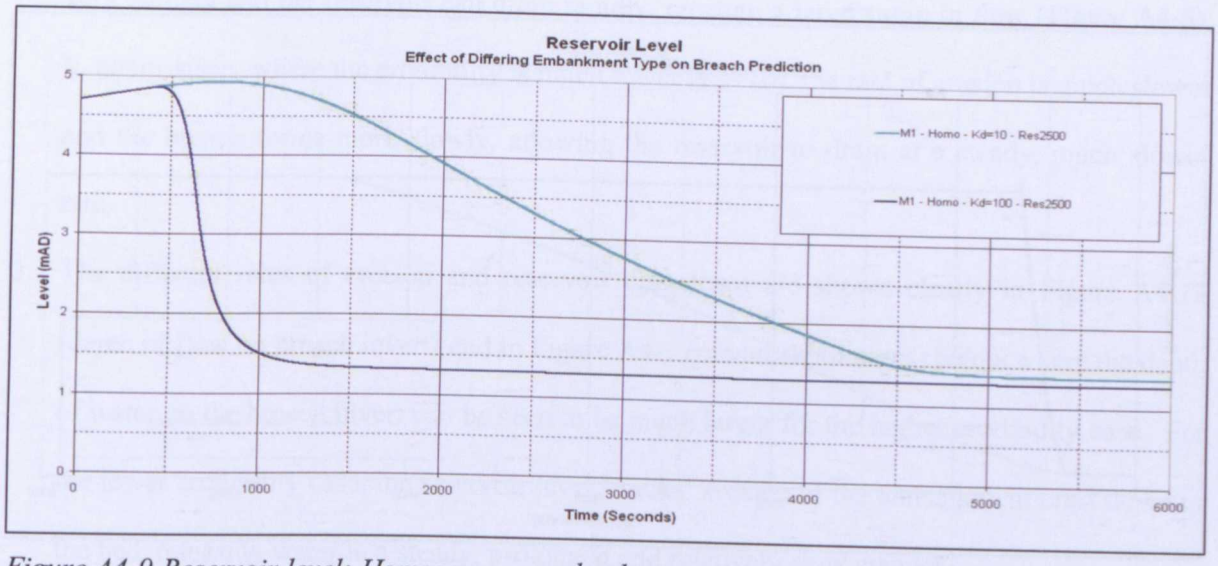

Figure A4-9 Reservoir level: Homogeneous embankment

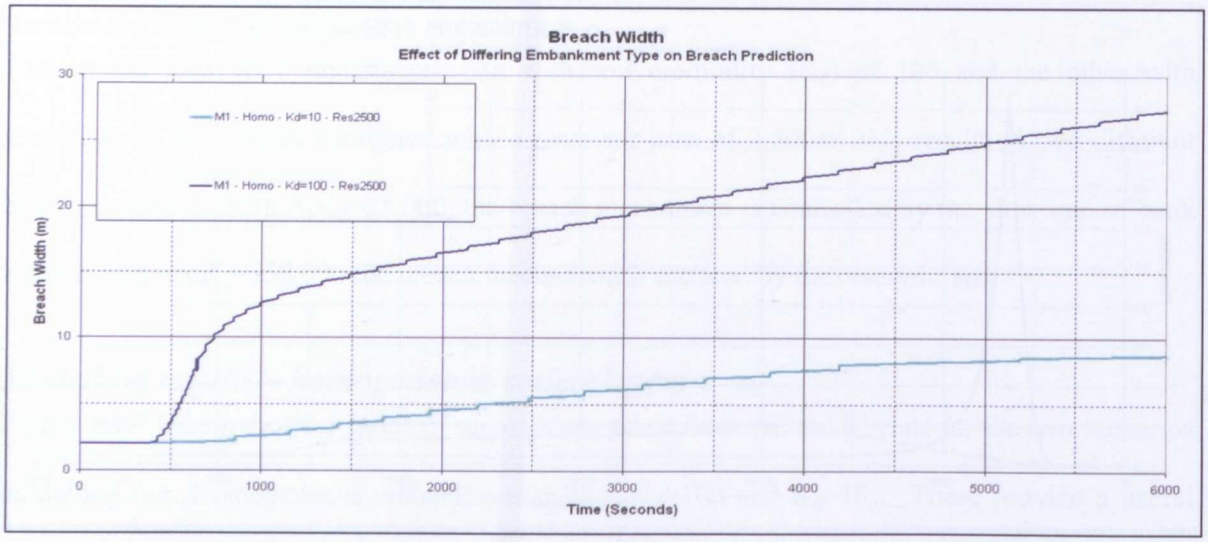

Figure A4-10 Breach width: Homogeneous embankment

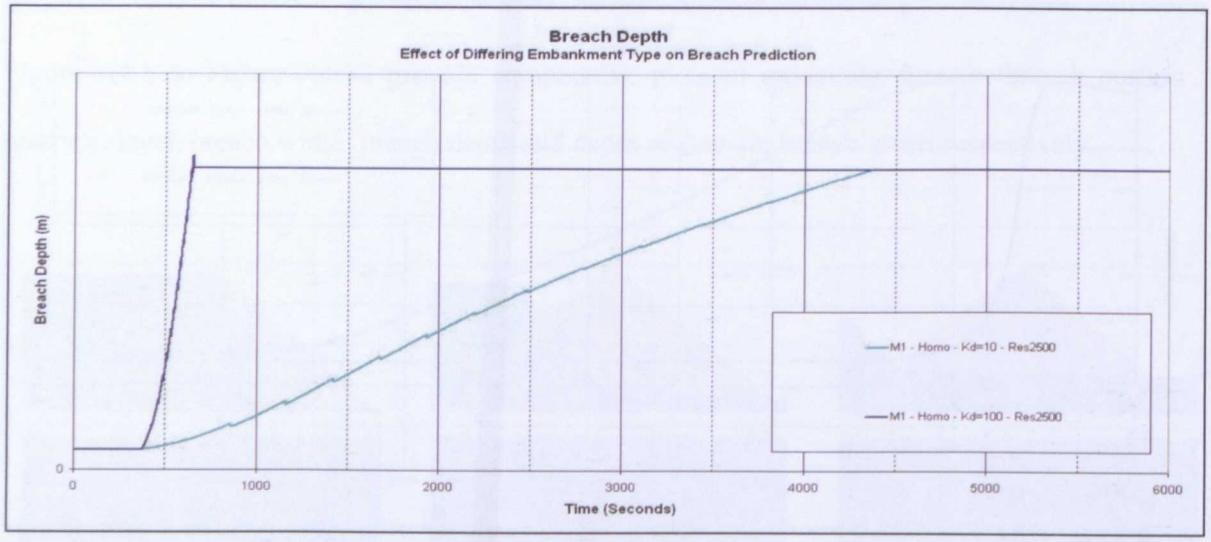

Figure A4-11 Breach depth: Homogeneous embankment

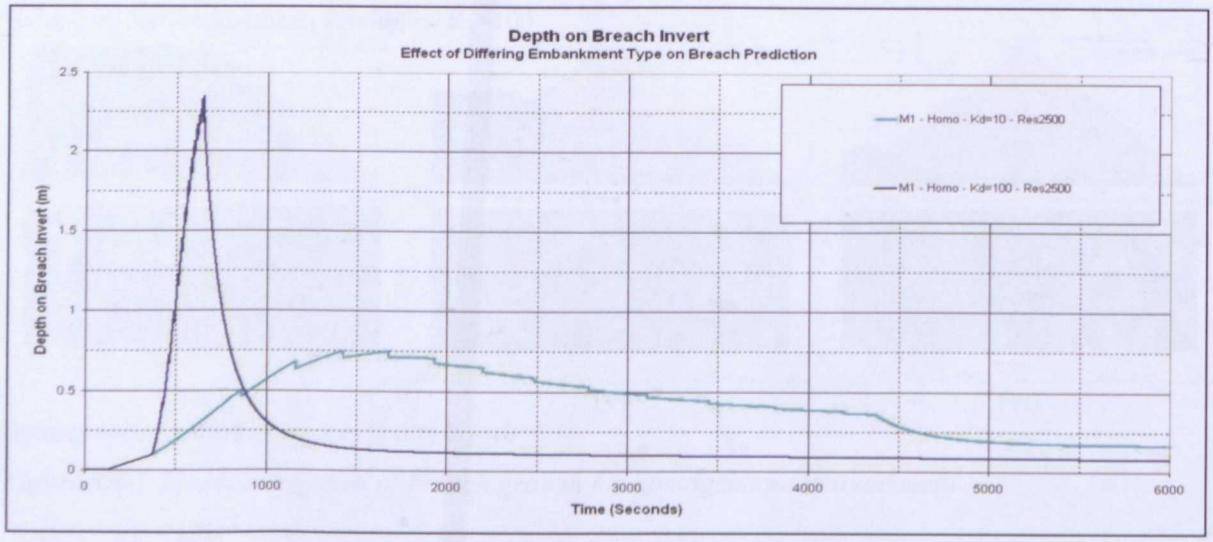

Figure A4-12 Depth on breach invert: Homogeneous embankment

Analysis of modelling results – homogeneous embankment

The two model tests show significantly different behaviour. The cause of this is the different relationship between soil erodibility and reservoir size for the two cases. The controlling processes here are explained more fully in Section 6.3. These two cases have been chosen deliberately to highlight the different forms of breach control and to allow comparisons against breaching behaviour seen for other more complex types of embankment structure.

Observations:

1. In the case where erodibility K_d is 100, the rate of soil erosion is so fast that the breach forms very quickly and the reservoir can drain rapidly, creating a large surge in flow (Figure A4-8). In comparison, where the erodibility is much lower (K_d=10), the rate of erosion is much slower and the breach forms more slowly, allowing the reservoir to drain at a steady, much slower rate.
2. The different rates of erosion and reservoir drawdown are shown clearly in Figure A4-12 (depth of flow on breach invert) and in Figure A4-7 (model simulations) below where the depth of water on the breach invert can be seen to be much larger for the higher erodibility case. For the lower erodibility case, the reservoir level 'tracks' erosion of the embankment crest down to the bed, releasing water in a steady, prolonged and relatively slow manner
3. Consistent with the flow and erosion observations, the reservoir level drops rapidly (Figure A4-9) for the high erodibility case and more slowly for the less erodible case.
4. The rate of breach width growth (Figure A4-10) shows two distinct zones for the high erodibility case. The first relates to the condition where flow through the breach is rapid, and is draining the reservoir. The second, slower rate corresponds to the later period where breach outflow matches inflow to the reservoir (a steady $1 m^3/s$).
5. The rates of breach depth growth are consistent with the observations above (Figure A4-11).

Variable erodibility modelling results – Type 1, 2-layer embankment

Four model tests were undertaken for a 'Type 1' layered embankment (Figure A4-13). All tests were for an embankment with two layers of different erodibility soil. Two combinations of layer thickness were considered, namely 2m+2m and 1m+3m. As with all of the modelling tests, two different soil erodibilities were considered comprising K_d=100 and K_d=10. Embankment geometry was as shown in Section 6.3 and the reservoir surface area was constant at A_s=2,500m^2.

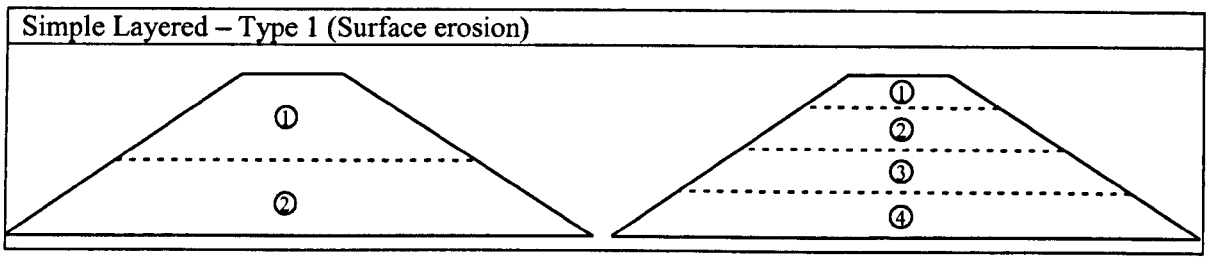

Figure A4-13 Generic geometry for Type 1 layered embankment

Modelling results – Type 1, 2-layer embankment

Figure A4-14 below shows a series of screen shots taken from the model runs for the four scenarios modelled (i.e. Type 1, 2-layer embankment with layer thicknesses of 2m+2m and 1m+3m and erodibility values of K_d=100 and K_d=10). These provide a useful indication of how the erosion processes are simulated in conjunction with reservoir level, breach width etc.

Figure A4-15 to Figure A4-19 provide comparative plots of modelling data for breach outflow, reservoir level, breach width, breach depth and depth of flow on breach invert respectively.

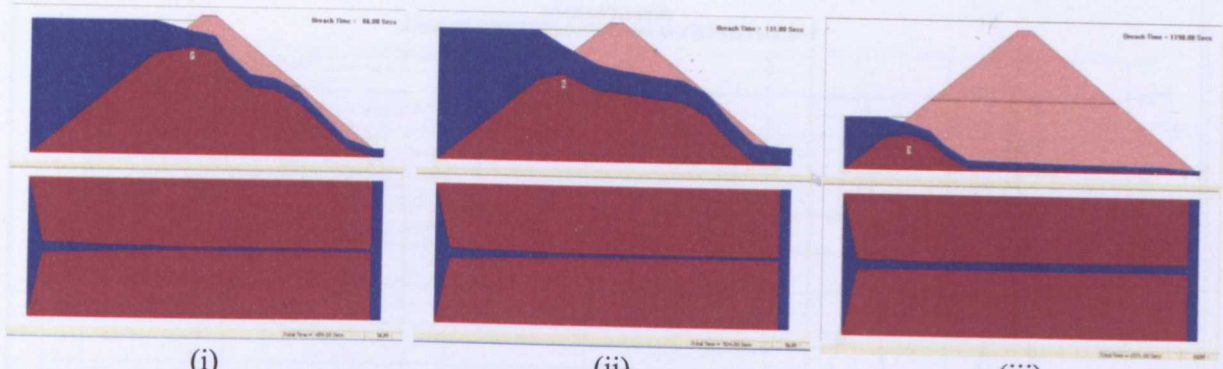

(i) (ii) (iii)

Type 1, 2 layer embankment: Layer 1= 2m, K_d=100; Layer 2 = 2m, K_d=10

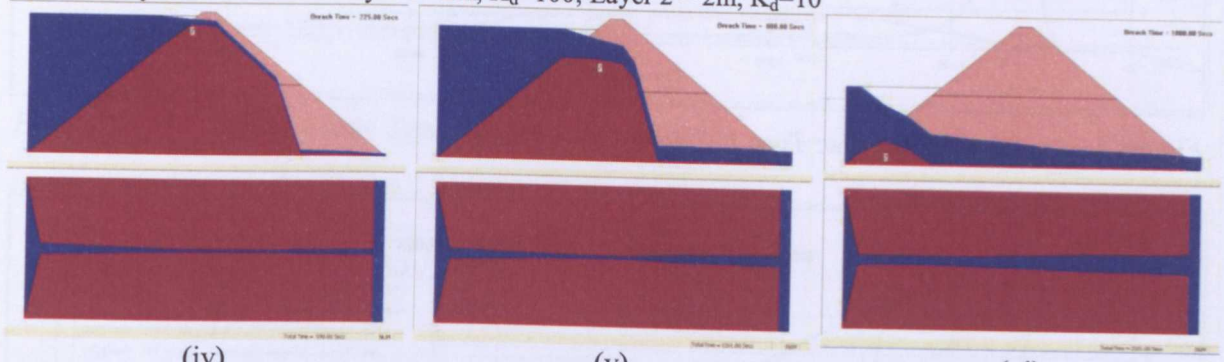

(iv) (v) (vi)

Type 1, 2 layer embankment: Layer 1= 2m, K_d=10; Layer 2 = 2m, K_d=100

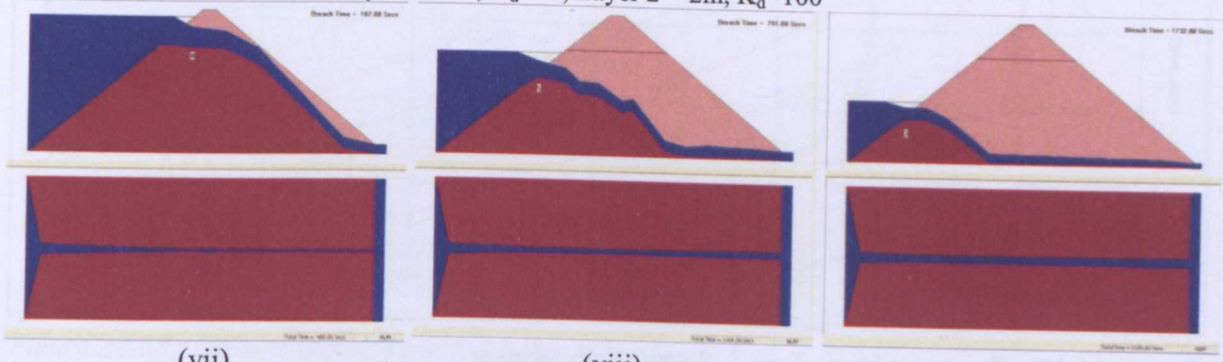

(vii) (viii) (ix)

Type 1, 2 layer embankment: Layer 1= 1m, K_d=100; Layer 2 = 3m, K_d=10

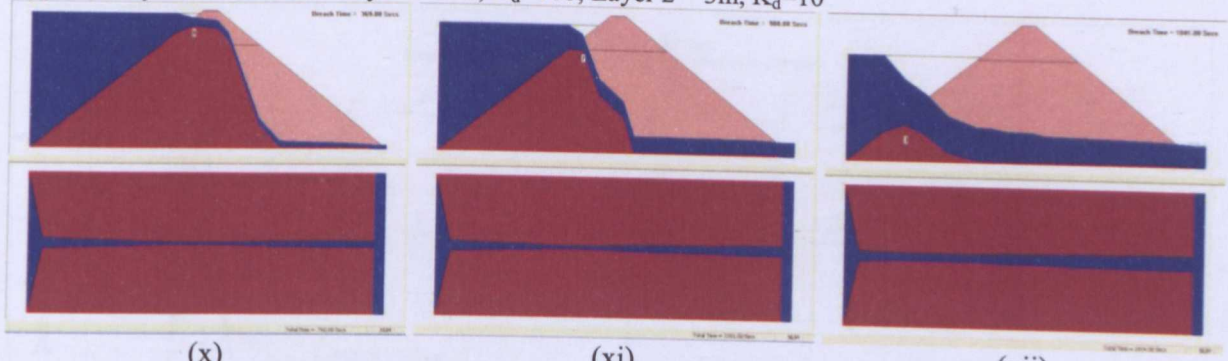

(x) (xi) (xii)

Type 1, 2 layer embankment: Layer 1= 1m, K_d=10; Layer 2 = 3m, K_d=100

Figure A4-14 Model simulation of breach growth for homogeneous embankment

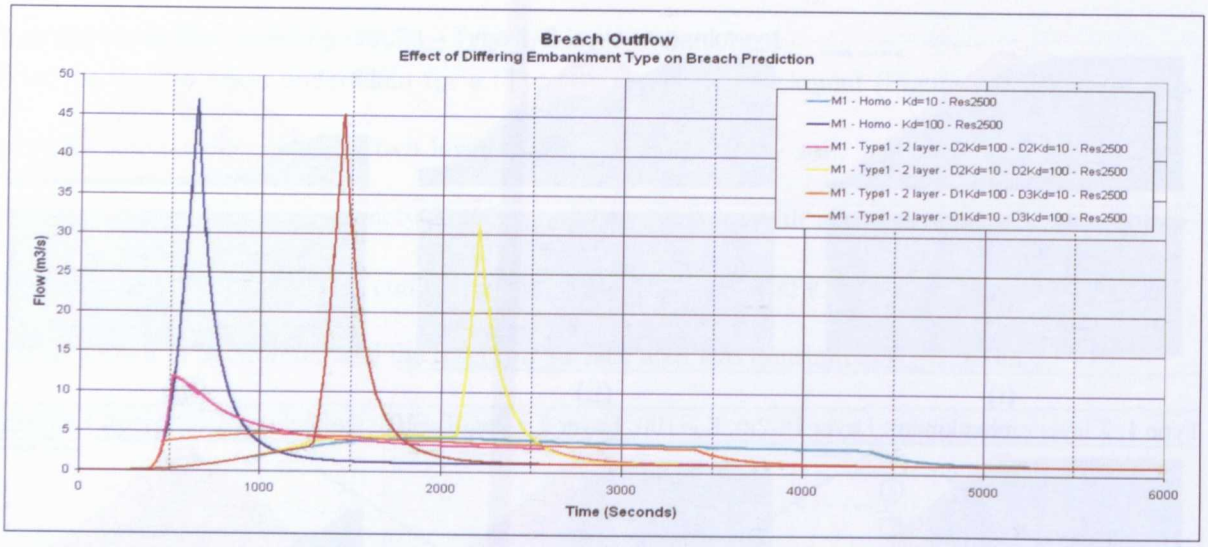

Figure A4-15 Breach outflow: Type 1, 2 layer embankment

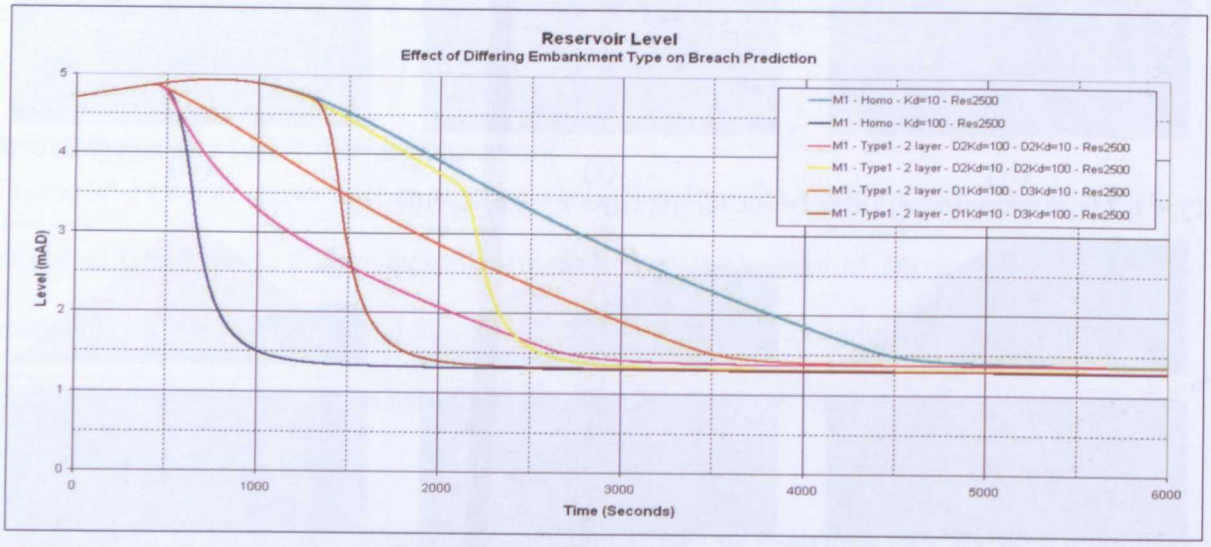

Figure A4-16 Reservoir level: Type 1, 2 layer embankment

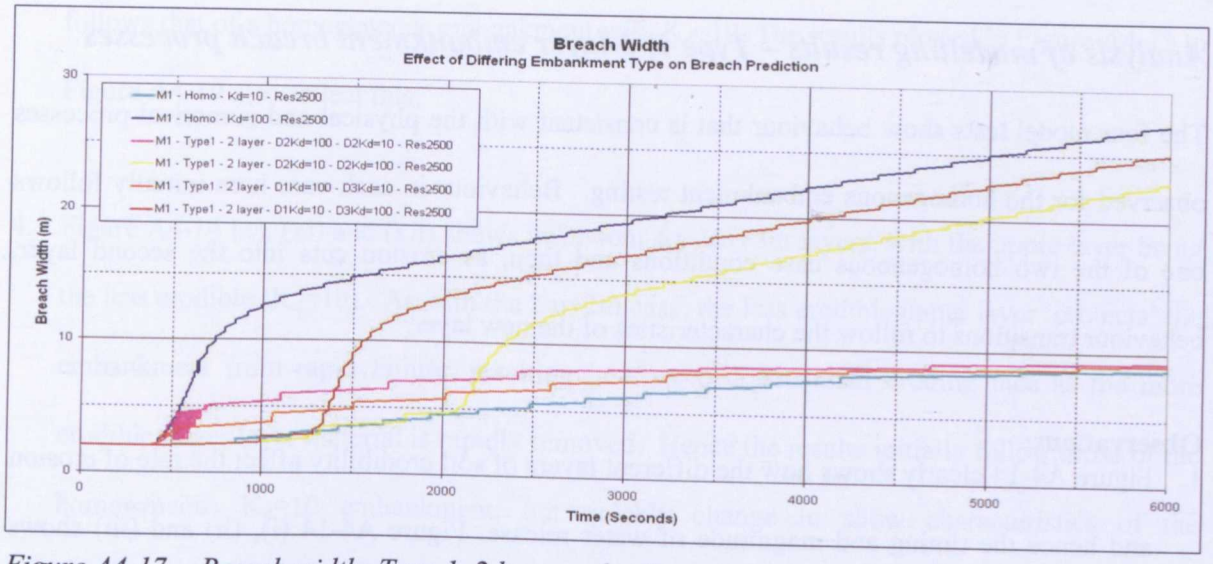

Figure A4-17 Breach width: Type 1, 2 layer embankment

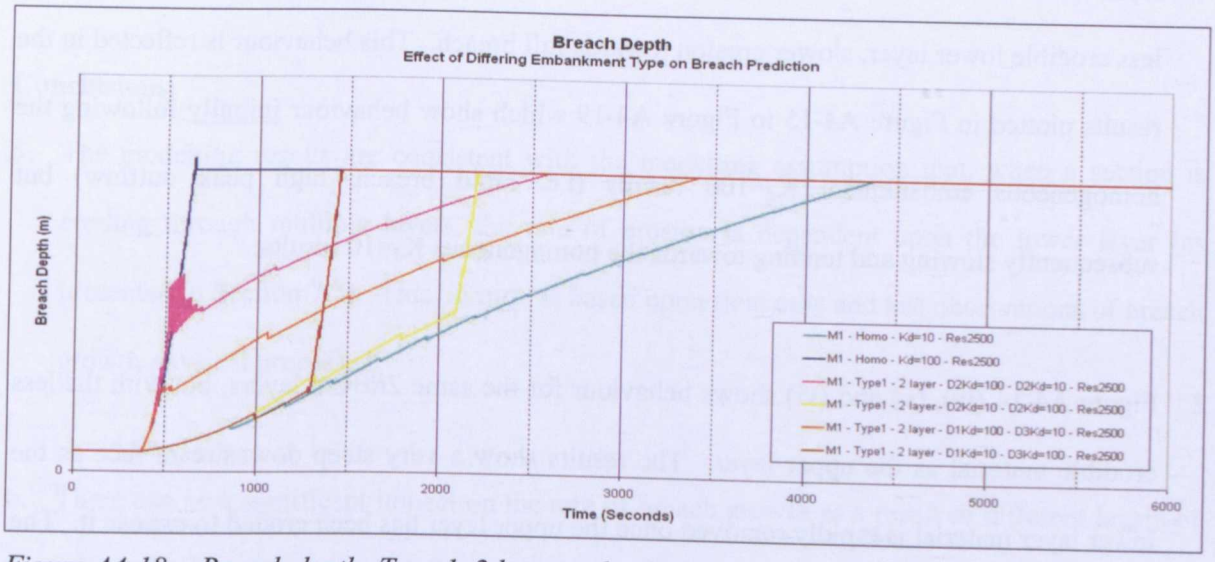

Figure A4-18 Breach depth: Type 1, 2 layer embankment

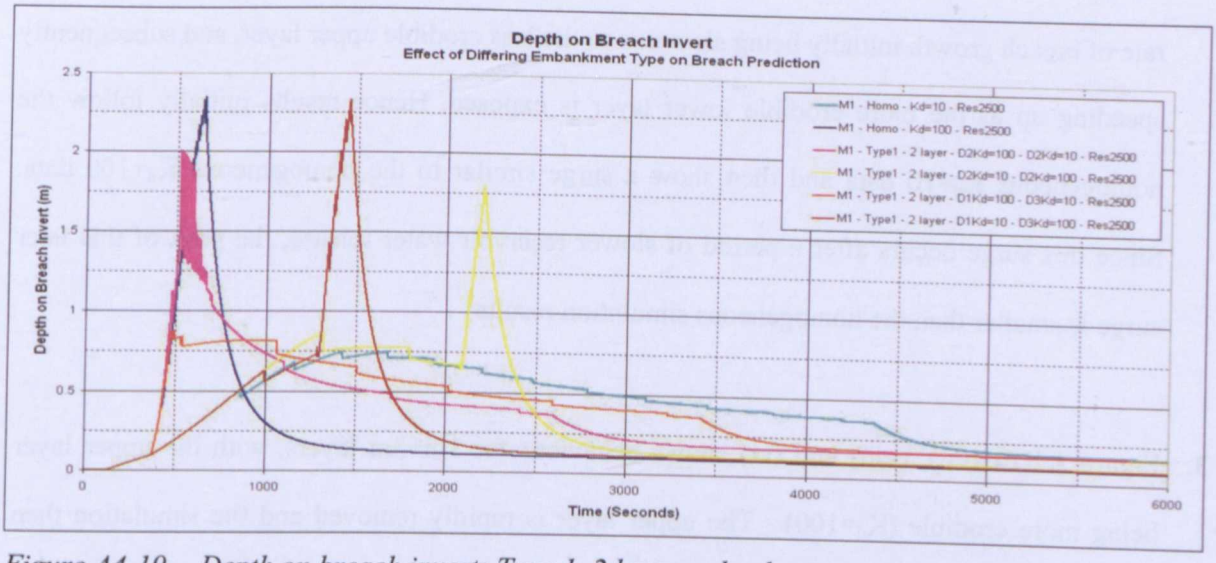

Figure A4-19 Depth on breach invert: Type 1, 2 layer embankment

Analysis of modelling results – Type 1, 2-layer embankment breach processes

The four model tests show behaviour that is consistent with the physical and numerical processes observed for the homogenous embankment testing. Behaviour in each case here initially follows one of the two homogeneous case conditions and then, as erosion cuts into the second layer, behaviour transitions to follow the characteristics of the new layer.

Observations:

1. Figure A4-14 clearly shows how the different layers of soil erodibility affect the rate of erosion and hence the timing and magnitude of water release. Figure A4-14 (i), (ii) and (iii) shows rapid removal of the more erodible top layer on the embankment and, once erosion reaches the less erodible lower layer, slower erosion towards full breach. This behaviour is reflected in the results plotted in Figure A4-15 to Figure A4-19 which show behaviour initially following the homogeneous embankment K_d=100 results (i.e. rapid breach, high peak outflow) but subsequently slowing and tending towards the homogeneous K_d=10 results;

2. Figure A4-14 (iv), (v) and (vi) shows behaviour for the same 2m+2m layers, but with the less erodible material as the upper layer. The results show a very steep downstream face as the lower layer material is rapidly removed once the upper layer has been eroded to expose it. The results plotted in Figure A4-15 to Figure A4-19 show consistent behaviour, with the overall rate of breach growth initially being slow due to the less erodible upper layer, and subsequently speeding up as the more erodible lower layer is exposed. Hence results initially follow the homogeneous K_d=10 data and then show a surge similar to the homogeneous K_d=100 data. Since this surge occurs after a period of slower reservoir water release, the peak of this later surge is smaller than the homogeneous simulation results;

3. Figure A4-14 (vii), (viii) and (ix) shows behaviour for 1m+3m layers, with the upper layer being more erodible (K_d=100). The upper layer is rapidly removed and the simulation then

follows that of a homogeneous embankment with K_d=10. The results plotted in Figure A4-15 to Figure A4-19 also reflect this;

4. Figure A4-14 (x), (xi) and (xii) shows behaviour for 1m+3m layers, with the upper layer being the less erodible (K_d=10). As with the 2m+2m case, the less erodible upper layer 'protects' the embankment from rapid failure, resulting in a steep downstream eroding face as the more erodible lower layer material is rapidly removed. Hence the results initially follow those of the homogeneous K_d=10 embankment, but quickly change to show characteristics of the homogeneous K_d=100 embankment once the 'protective' upper layer is lost.

Conclusions:

5. The modelling results are consistent with the modelling assumption that, when a section is eroding through multiple layers, the rate of erosion is dependent upon the lower layer (as presented in Section 7.2). This, in turn, is based upon field case and test observations of breach growth physical processes;

6. There can be a significant impact on the rate of breach growth as a result of different layers of soil erodibility within an embankment or dam.

Variable erodibility modelling results – Type 3 & 4, 2-layer embankment

Two model tests each were undertaken for Types 3 and 4 layered embankments (Figure A4-20). All tests were for an embankment with two layers of different erodibility soil. The layer thicknesses were 1m+3m in all cases with the soil erodibility comprising either K_d=100 or K_d=10. Embankment geometry was as shown in Section 6.3 and the reservoir surface area was constant at A_s=2,500m^2.

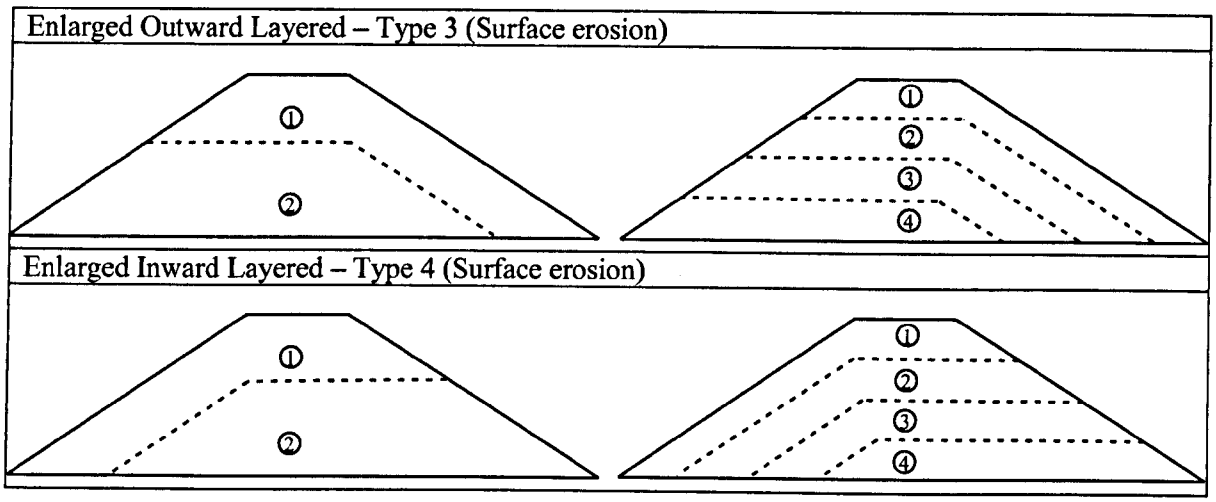

Figure A4-20 Generic geometry for Type 4layered embankment

Modelling results – Type 3 & 4, 2-layer embankment

Figure A4-21 below shows a series of screen shots taken from the model runs for the four scenarios modelled (i.e. 2 Type 3 runs and 2 Type 4 runs). Figure A4-22 to Figure A4-26 provide comparative plots of modelling data for breach outflow, reservoir level, breach width, breach depth and depth of flow on breach invert respectively.

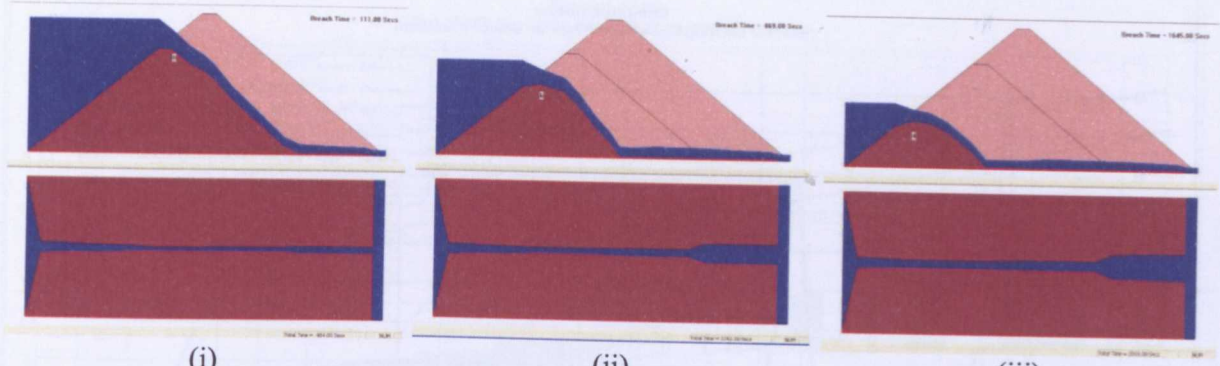

(i) (ii) (iii)

Type 3, 2 layer embankment: Layer 1= 1m, K_d=100; Layer 2 = 3m, K_d=10

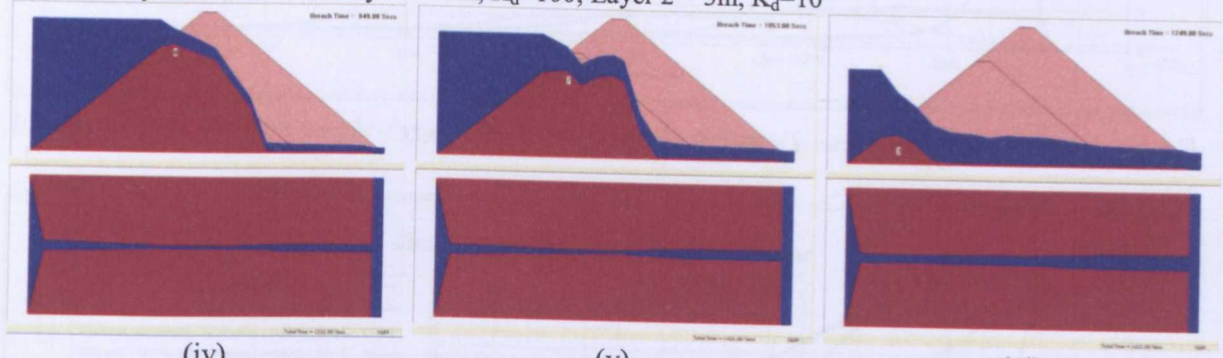

(iv) (v) (vi)

Type 3, 2 layer embankment: Layer 1= 2m, K_d=10; Layer 2 = 2m, K_d=100

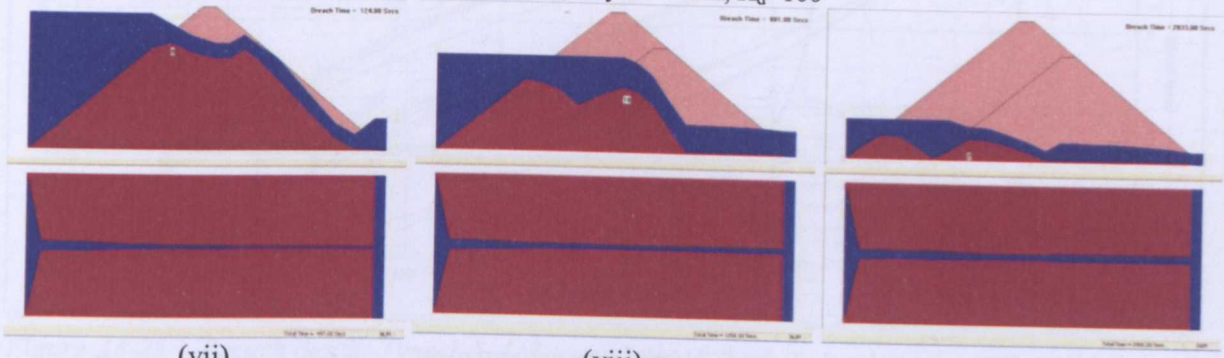

(vii) (viii) (ix)

Type 4, 2 layer embankment: Layer 1= 1m, K_d=100; Layer 2 = 3m, K_d=10

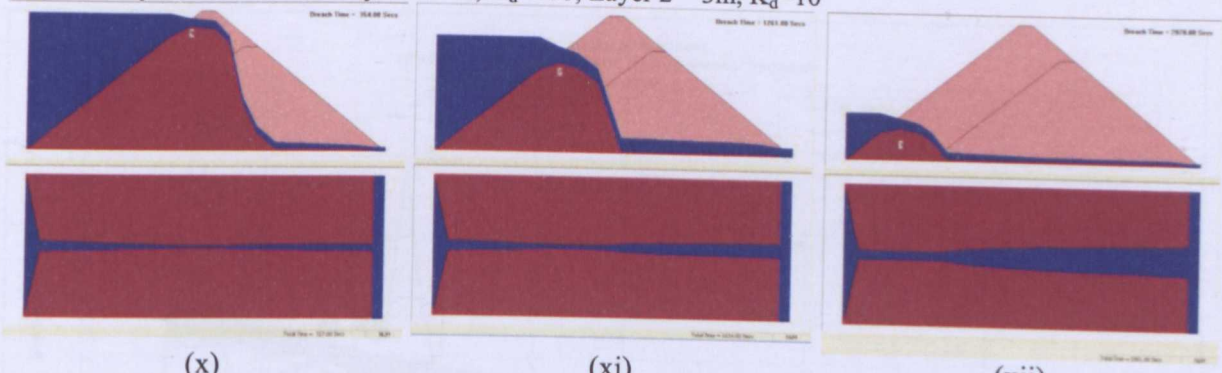

(x) (xi) (xii)

Type 4, 2 layer embankment: Layer 1= 1m, K_d=10; Layer 2 = 3m, K_d=100

Figure A4-21 Model simulation of breach growth for homogeneous embankment

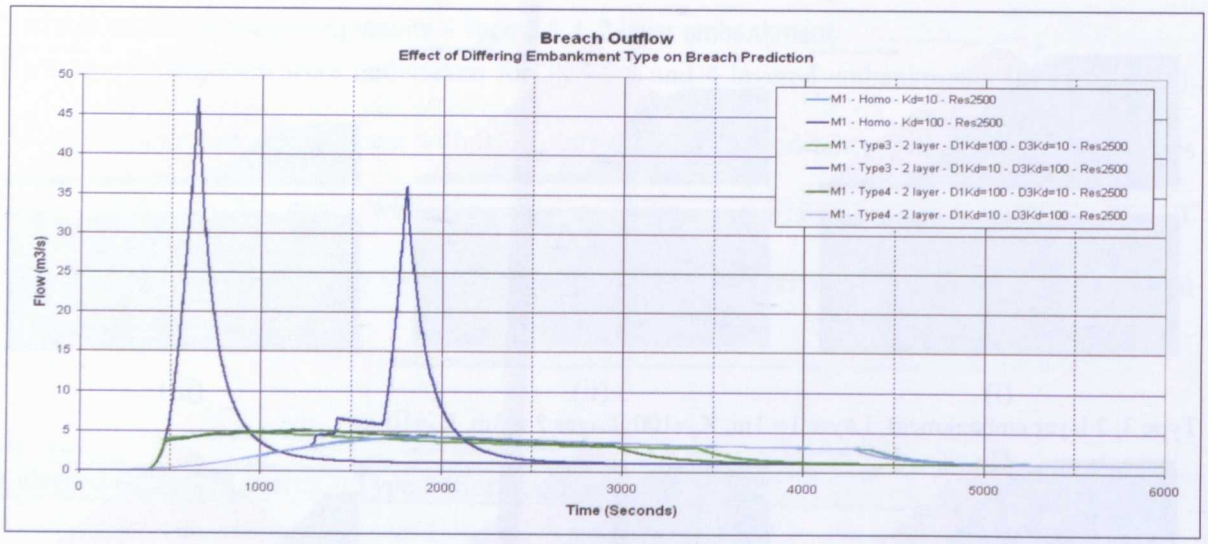

Figure A4-22 Breach outflow: Type 3 & 4, 2 layer embankments

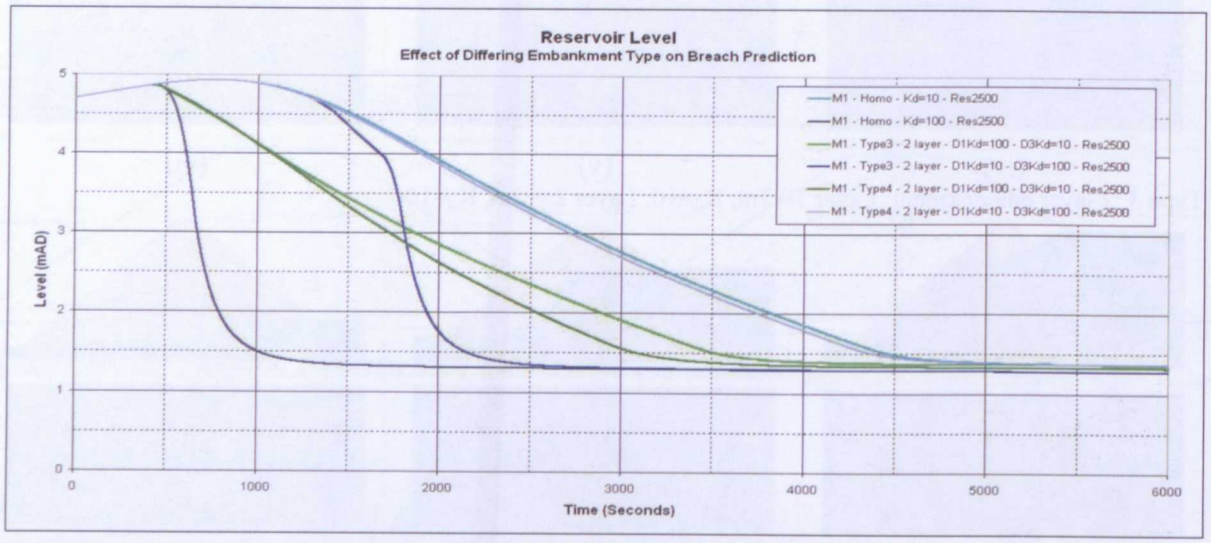

Figure A4-23 Reservoir level: Type 3 & 4, 2 layer embankment

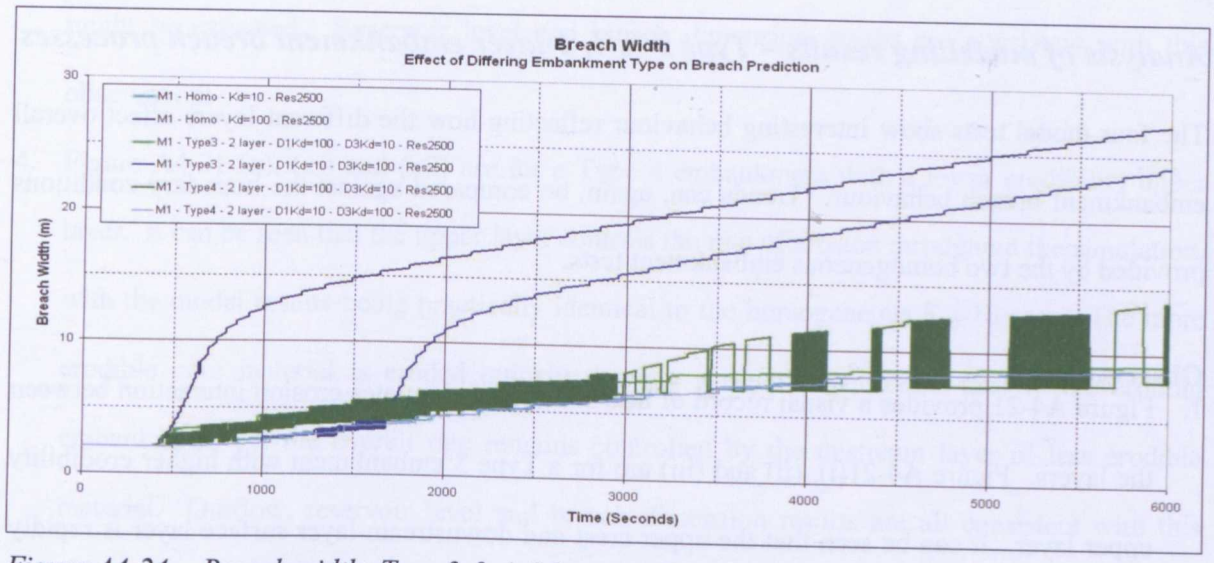

Figure A4-24 Breach width: Type 3 & 4, 2 layer embankment

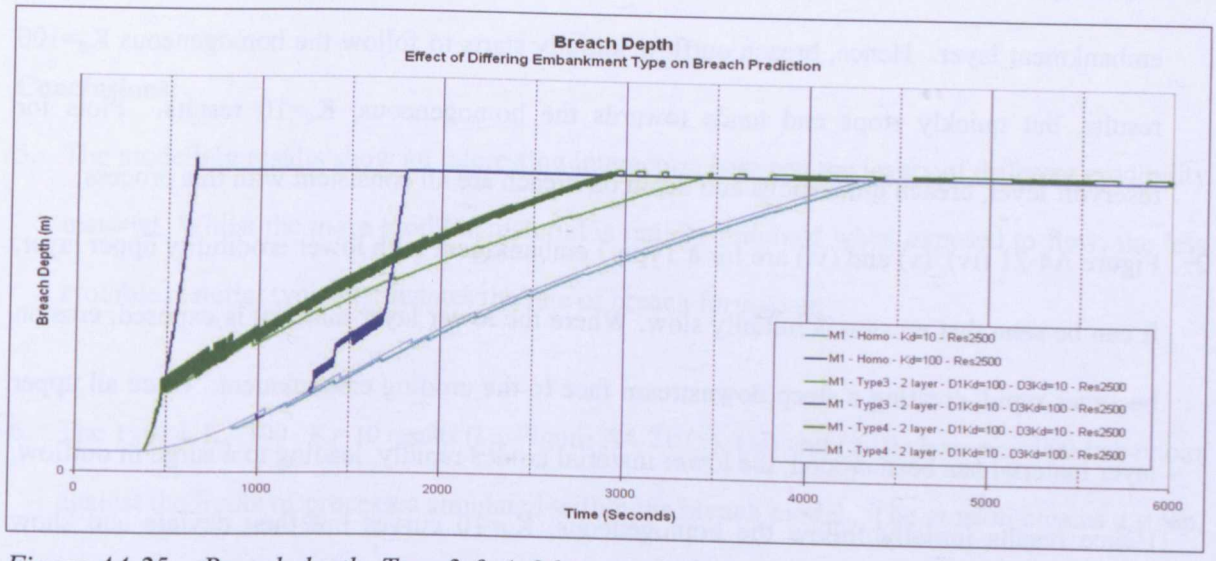

Figure A4-25 Breach depth: Type 3 & 4, 2 layer embankment

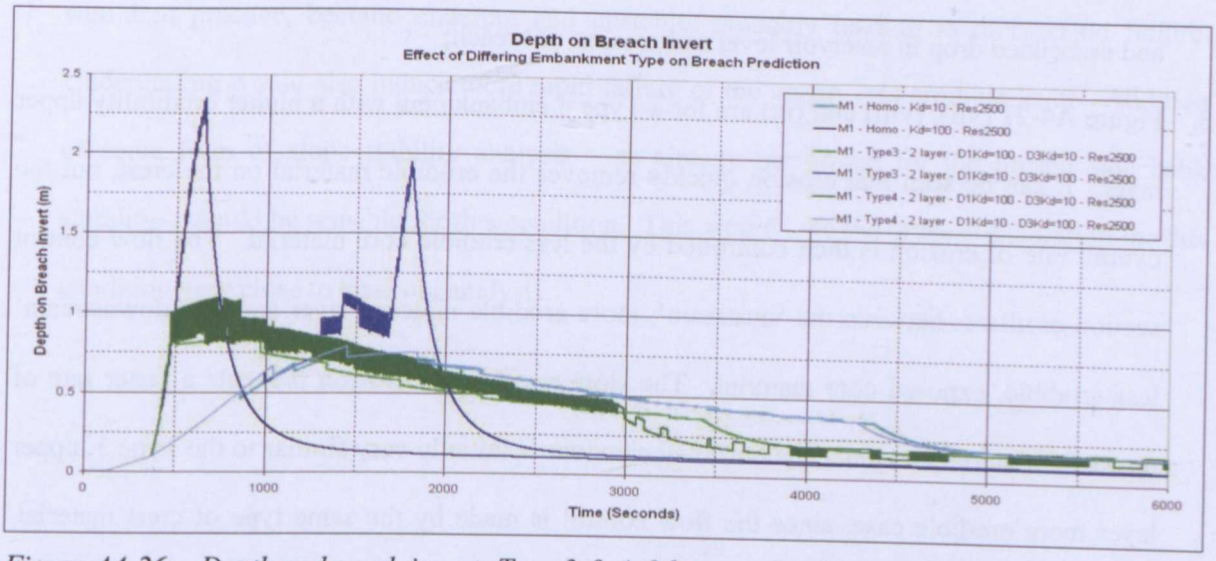

Figure A4-26 Depth on breach invert: Type 3 & 4, 2 layer embankment

Analysis of modelling results – Type 3 & 4, 2-layer embankment breach processes

The four model tests show interesting behaviour reflecting how the different layers affect overall embankment breach behaviour. Trends can, again, be compared against the boundary conditions provided by the two homogeneous embankment tests.

Observations:

1. Figure A4-21 provides a visual record of how the model simulates erosion interaction between the layers. Figure A4-21(i), (ii) and (iii) are for a Type 3 embankment with higher erodibility upper layer. It can be seen that the upper crest and downstream layer surface layer is rapidly removed, and then the overall rate of erosion is dictated by the less erodible 'core' embankment layer. Hence, breach outflow initially starts to follow the homogeneous K_d=100 results, but quickly stops and tends towards the homogeneous, K_d=10 results. Plots for reservoir level, breach dimensions and depth on breach are all consistent with this process;
2. Figure A4-21 (iv), (v) and (vi) are for a Type 3 embankment with lower erodibility upper layer. It can be seen that erosion is initially slow. Where the lower layer material is exposed, erosion becomes rapid, creating a steep downstream face to the eroding embankment. Once all upper layer material has been eroded, the lower material erodes rapidly, leading to a surge in outflow. Hence results initially follow the homogeneous, K_d=10 curves but then deviate and show homogeneous, K_d=100 type behaviour after 1500s resulting in a significant surge in outflow and associated drop in reservoir level and erosion of breach;
3. Figure A4-21 (vii), (viii) and (ix) are for a Type 4 embankment with a higher erodibility upper layer. It can be seen that erosion quickly removes the erodible material on the crest, but the overall rate of erosion is then controlled by the less erodible core material. The flow control section oscillates between the 'upstream', more erodible material layer and the 'downstream' less erodible, exposed core material. The slow rate of core erosion prevents a faster rate of upstream material erosion. The outflow behaviour is initially very similar to the Type 3, upper layer more erodible case, since the flow control is made by the same type of crest material. Following removal of this material, behaviour tends towards the homogeneous K_d=10 case, as

might be expected. Reservoir level and breach dimension results are consistent with this observation;

4. Figure A4-21 (x), (xi) and (xii) are for a Type 4 embankment with a lower erodibility upper layer. It can be seen that the upper layer controls the rate of erosion throughout the simulation, with the model results being practically identical to the homogeneous K_d=10 case. The more erodible core material is eroded quickly, leaving a steep downstream face to the eroding embankment, but the overall rate remains controlled by the upstream layer of less erodible material. Outflow, reservoir level and breach dimension results are all consistent with this behaviour.

Conclusions:

5. The modelling results show an interesting interaction between the layers of different erodibility material. Whilst the more erodible material is rapidly removed when exposed to flow, the less erodible material typically dictates the rate of breach formation;

6. The Type 4, K_d=100 / K_d=10 results (i.e. Figure A4-21 (x), (xi) and (xii)) show physical behaviour against the limits of processes simulated within the breach model. The erosion creates a steep, near vertical wall (headcut) on the downstream face. This is simulated by surface erosion, but would in practice, become undercut and unstable, probably leading to more rapid failure. Undercutting would also induce more rapid failure of the upper, less erodible layer. Addition of some form of slope stability analysis – as already performed for the breach side bank stability – would be sensible for this condition. This would take the process simulation for this condition very close to head cut analysis.

Variable erodibility modelling results – Type 2, 2-layer embankment

Two model tests each were undertaken for a Type 2, 2-layered embankment (Figure A4-27). The layer thicknesses were 2m+2m in each case with the soil erodibility comprising either K_d=100 or K_d=10. Embankment geometry was as shown in Section 6.3 and the reservoir surface area was constant at A_s=2,500m^2.

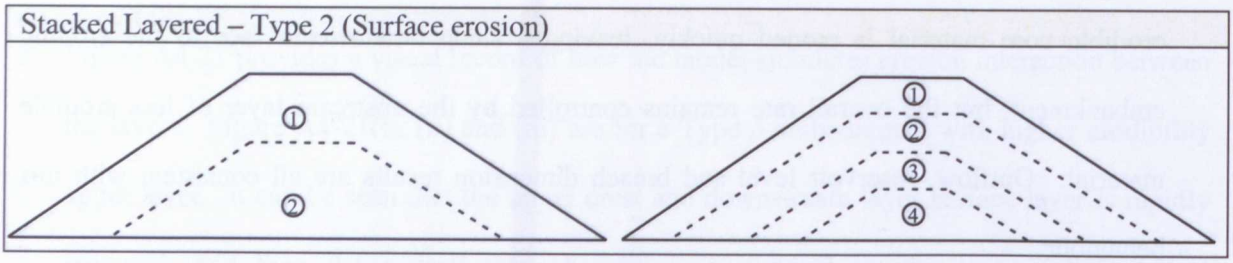

Figure A4-27 Generic geometry for Type 4layered embankment

Modelling results – Type 2, 2-layer embankment

Figure A4-28 below shows a series of screen shots taken from the model runs for the two scenarios modelled. Figure A4-29 to Figure A4-33 provide comparative plots of modelling data for breach outflow, reservoir level, breach width, breach depth and depth of flow on breach invert respectively.

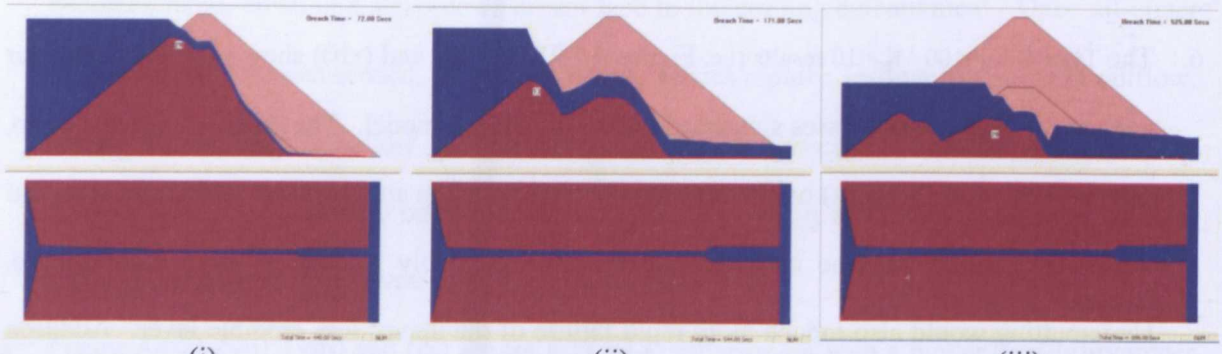

(i) (ii) (iii)

Type 2, 2 layer embankment: Layer 1= 2m, K_d=100; Layer 2 = 2m, K_d=10

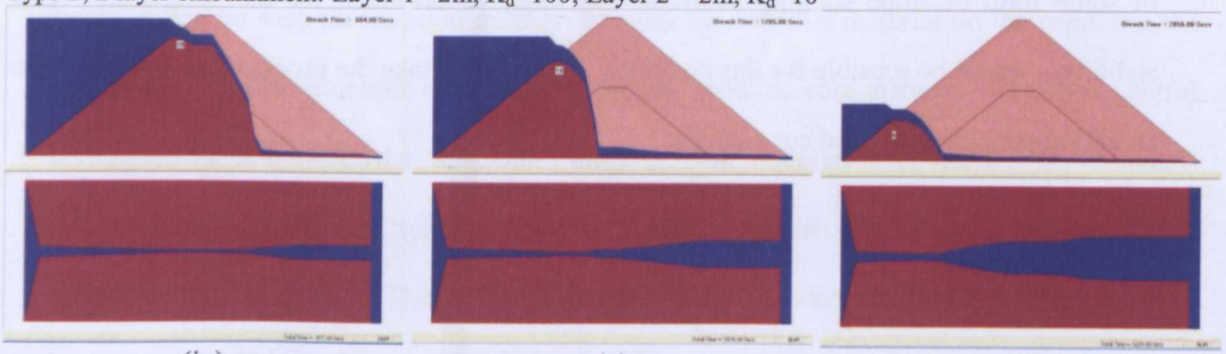

(iv) (v) (vi)

Type 2, 2 layer embankment: Layer 1= 2m, K_d=10; Layer 2 = 2m, K_d=100

Figure A4-28 Model simulation of breach growth for homogeneous embankment

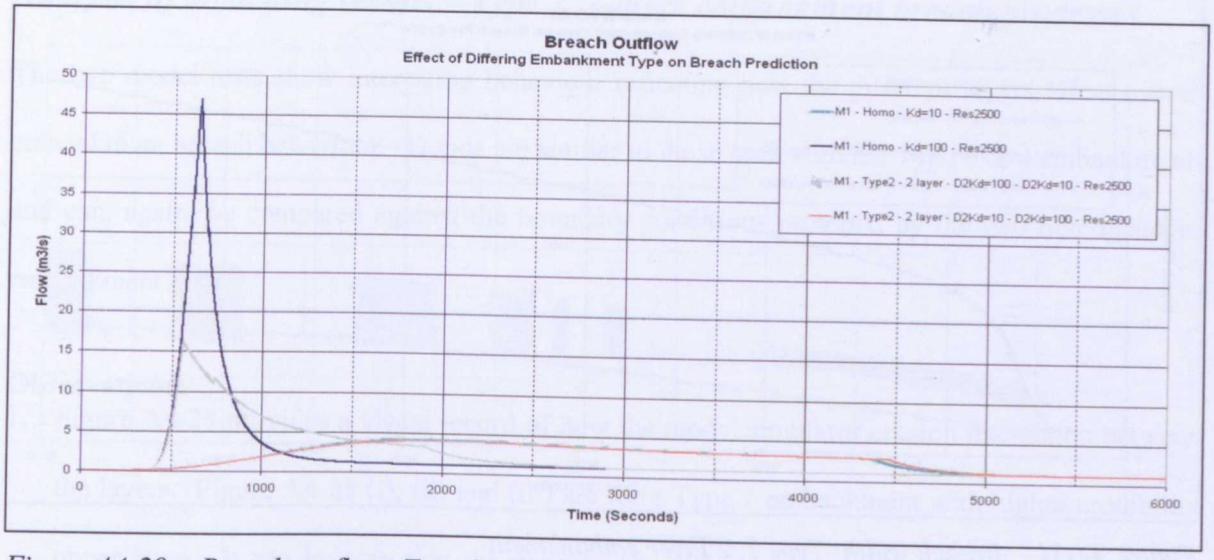

Figure A4-29 Breach outflow: Type 2, 2 layer embankment

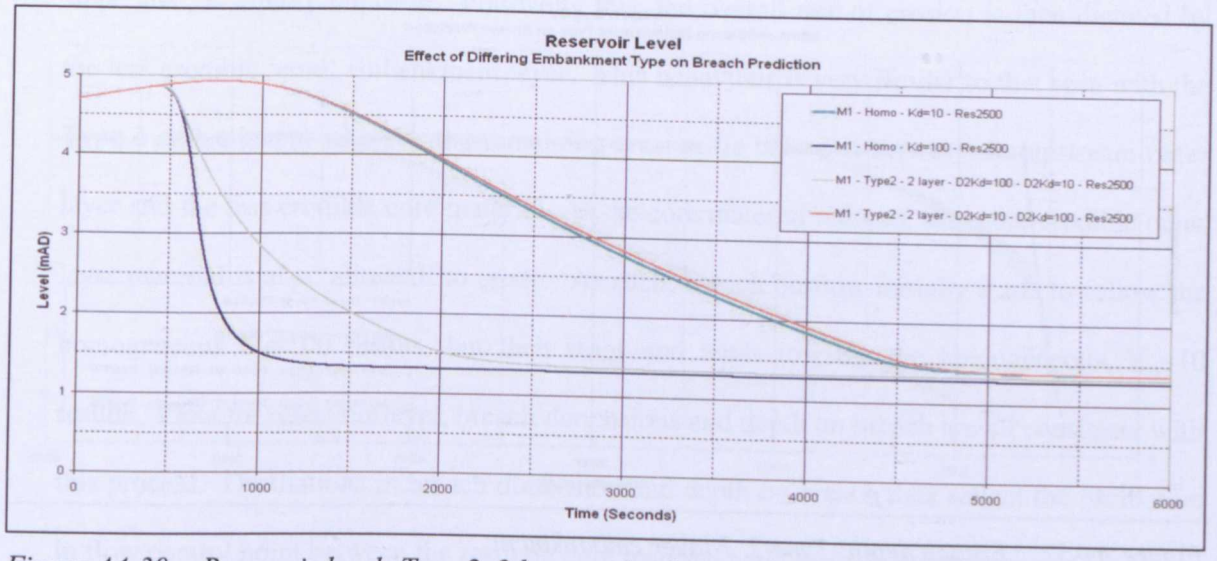

Figure A4-30 Reservoir level: Type 2, 2 layer embankment

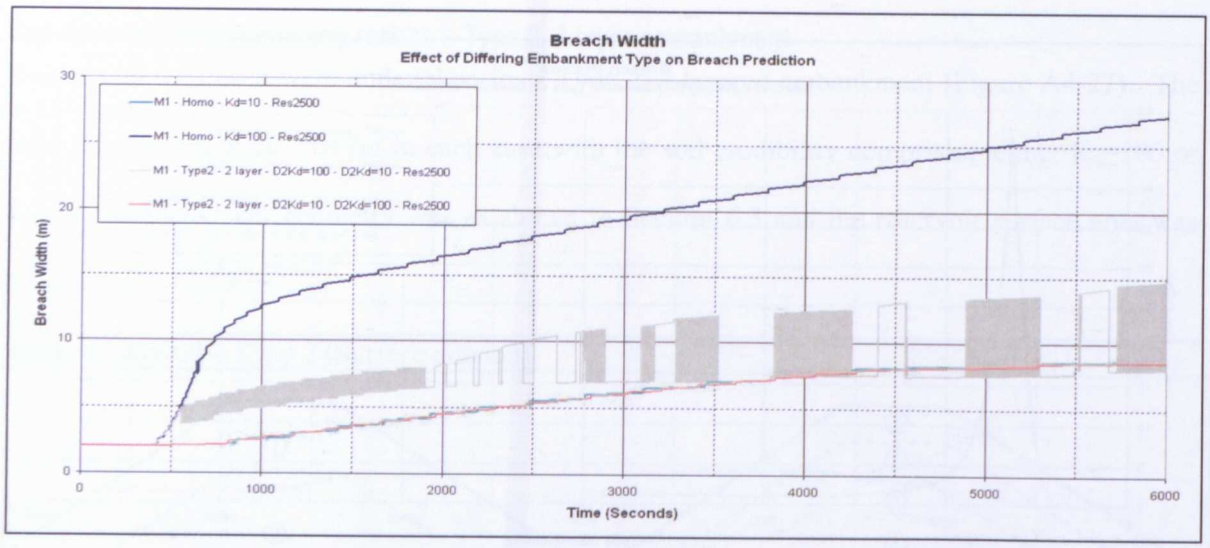

Figure A4-31 Breach width: Type 2, 2 layer embankment

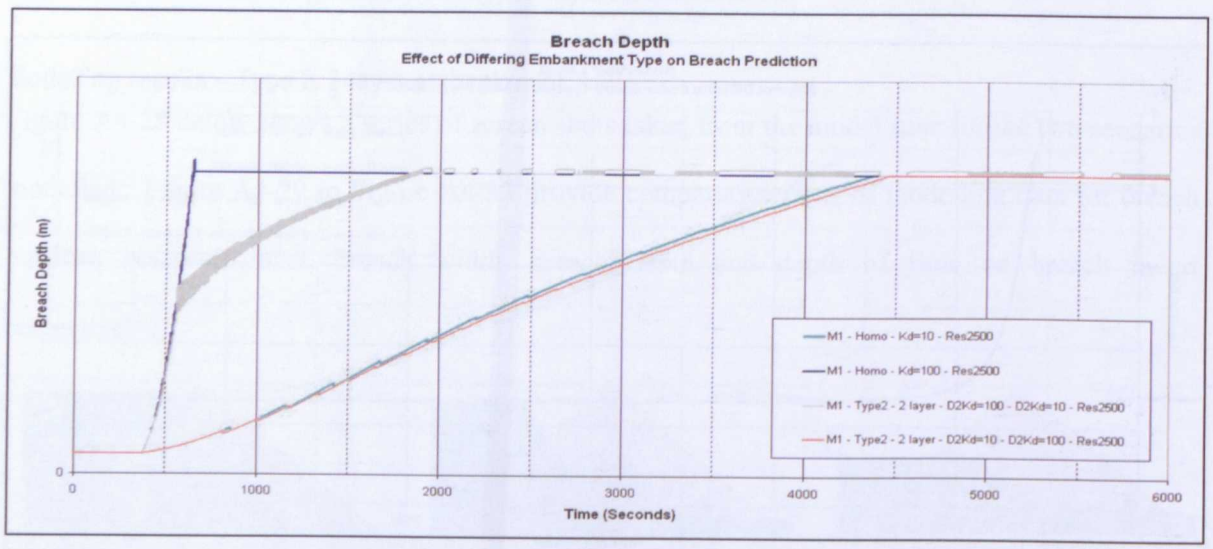

Figure A4-32 Breach depth: Type 2, 2 layer embankment

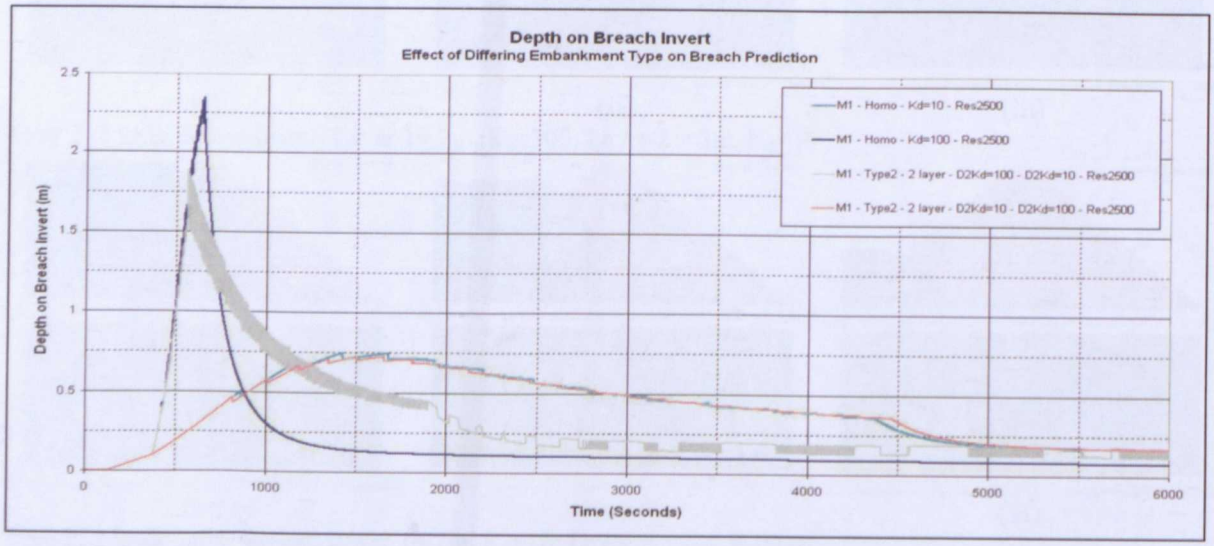

Figure A4-33 Depth on breach invert: Type 2, 2 layer embankment

Analysis of modelling results – Type 2, 2-layer embankment breach processes

The two model tests show interesting behaviour reflecting how the different layers affect overall embankment breach behaviour. Trends are similar to those seen with the Type 3 & 4 embankments and can, again, be compared against the boundary conditions provided by the two homogeneous embankment tests.

Observations:

1. Figure A4-28 provides a visual record of how the model simulates erosion interaction between the layers. Figure A4-28 (i), (ii) and (iii) are for a Type 2 embankment with higher erodibility upper layer. It can be seen that the upper layer, and in particular the crest and downstream slope area, is rapidly removed. Following this, the overall rate of erosion is then dictated by the less erodible 'core' embankment layer. This behaviour is very similar to that seen with the Type 4 embankment whereby the remaining erosion 'is balanced between the upstream outer layer and the less erodible core material. As the core material reduces, the more erodible outer layer material is also 'allowed' to erode. As such, breach outflow initially starts to follow the homogeneous K_d=100 results, but then stops and tends towards the homogeneous, K_d=10 results. Plots for reservoir level, breach dimensions and depth on breach are all consistent with this process. Oscillations in breach dimension and depth on breach data reflect the oscillation in flow control point between the resilient core material and upstream outer layer material;
2. Figure A4-28 (iv), (v) and (vi) are for a Type 2 embankment with a lower erodibility upper layer. It can be seen that the upper layer controls the rate of erosion throughout the simulation, with the model results being practically identical to the homogeneous K_d=10 case. The more erodible core material is eroded quickly, leaving a steep downstream face to the eroding embankment, but the overall rate remains controlled by the upstream layer of less erodible material. Outflow, reservoir level and breach dimension results are all consistent with this behaviour.

Conclusions:

3. Performance of the outer layer of soil in the crest and upstream face area has the greatest effect in delaying overall breach growth. (This assumption is valid where headcutting or erosion underneath the less erodible outer layer is not considered). This would suggest that when raising an embankment with less erodible material, the greatest impact will be had if the raised material covers at least the crest and upstream slopes.

Variable erodibility modelling results – Type 1, 3-layer embankment

A further four model tests were undertaken for a 'Type 1' layered embankment (Figure A4-34), but this time incorporating three rather than two soil layers. All tests were for an embankment with equal layer thickness of 1.3m and different combinations of soil erodibility. Two tests considered gradually varying erodibility through the bank (i.e. K_d=100, 50, 10 or K_d=10, 50, 100). The other two tests considered a layer of weaker or stronger soil 'sandwiched' between other material (i.e. K_d=100, 10, 100 or K_d=10, 100, 10). Embankment geometry was as shown in Section 6.3 and the reservoir surface area was constant at A_s=2,500m^2.

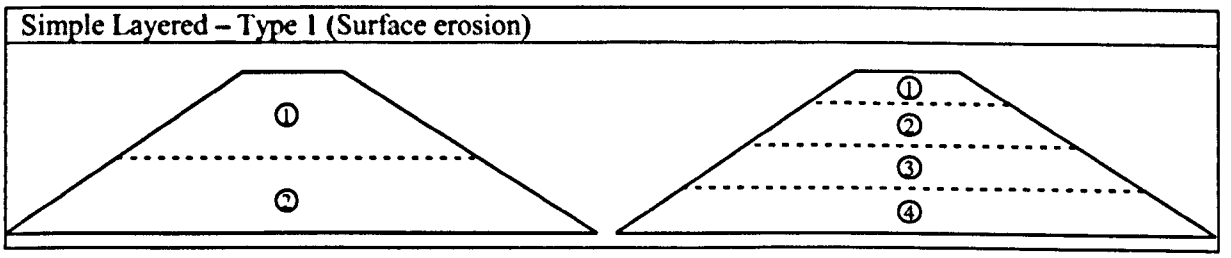

Figure A4-34 Generic geometry for Type 1 layered embankment

Modelling results – Type 1, 3-layer embankment

Figure A4-35 below shows a series of screen shots taken from the four model runs (i.e. Type 1, 3-layer embankment with equal layer thicknesses of 1.3m and erodibility values from the top to bottom layers respectively of K_d=100, 50, 10, K_d=10, 50, 100, K_d=100, 10, 100 and K_d=10, 100, 10). These provide a useful indication of how the erosion processes are simulated in conjunction with reservoir level, breach width etc.

Figure A4-36 to Figure A4-40 provide comparative plots of modelling data against homogeneous and Type 1, 2-layer results for breach outflow, reservoir level, breach width, breach depth and depth of flow on breach invert respectively.

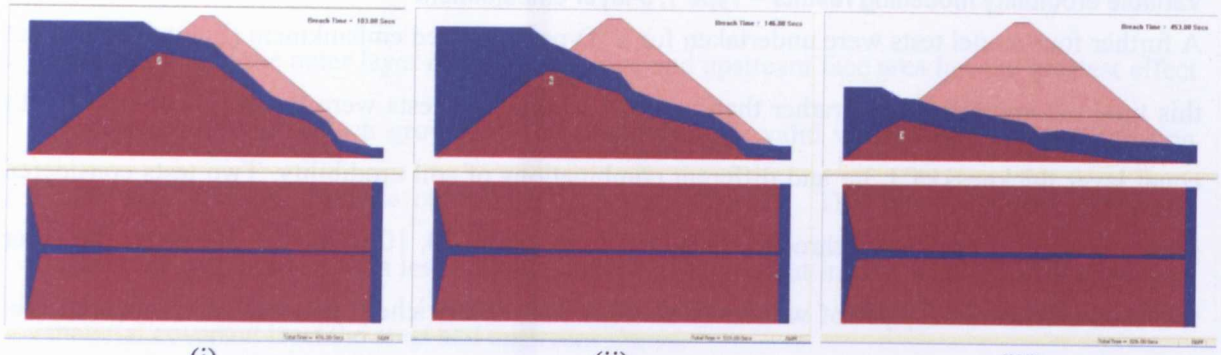

(i) (ii) (iii)

Type 1, 3-layer embankment: All layers 1.3m, K_d=100, 50, 10 from top to base

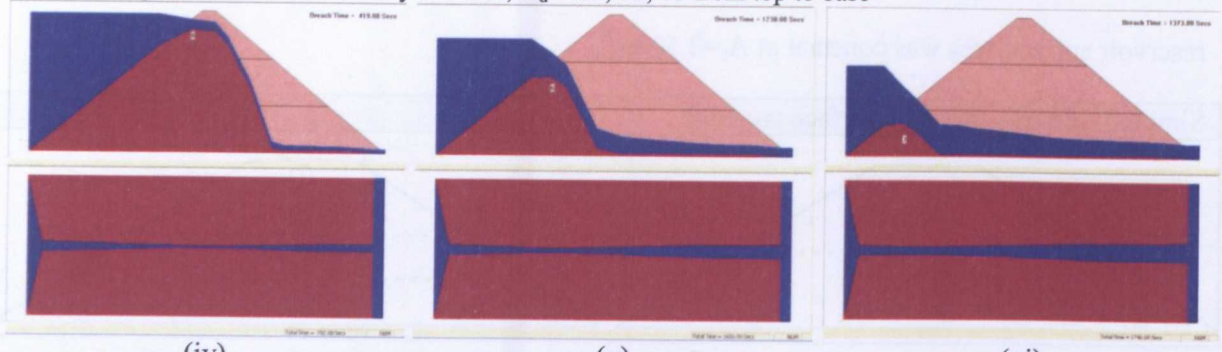

(iv) (v) (vi)

Type 1, 3-layer embankment: All layers 1.3m, K_d=10, 50, 100 from top to base

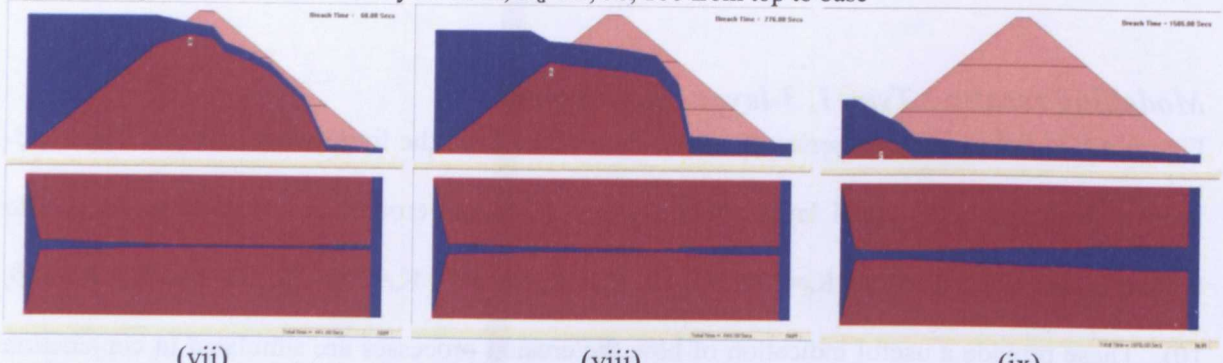

(vii) (viii) (ix)

Type 1, 3-layer embankment: All layers 1.3m, K_d=100, 10, 100 from top to base

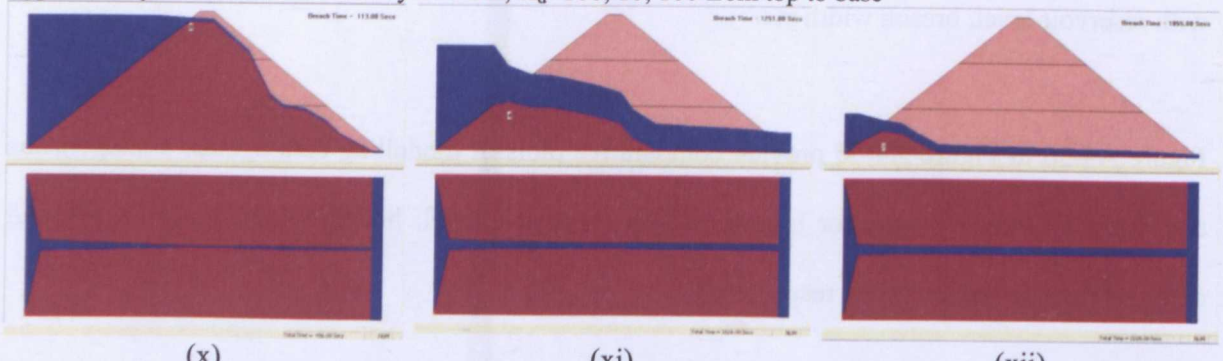

(x) (xi) (xii)

Type 1, 3-layer embankment: All layers 1.3m, K_d=10, 100, 10 from top to base

Figure A4-35 Model simulation of breach growth for homogeneous embankment

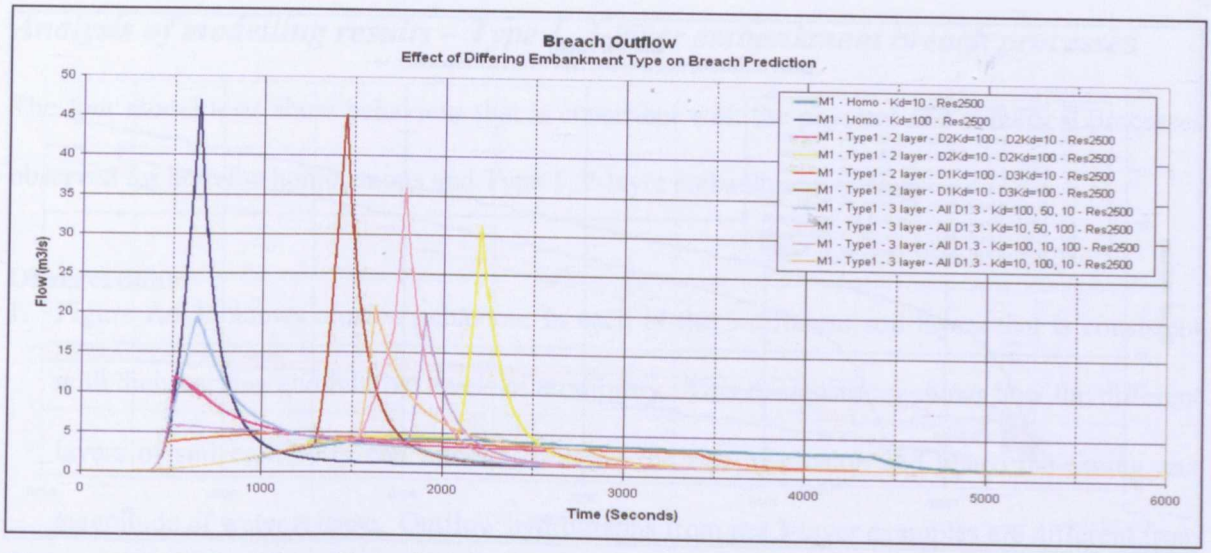

Figure A4-36 Breach outflow: Type 1, 3-layer embankment

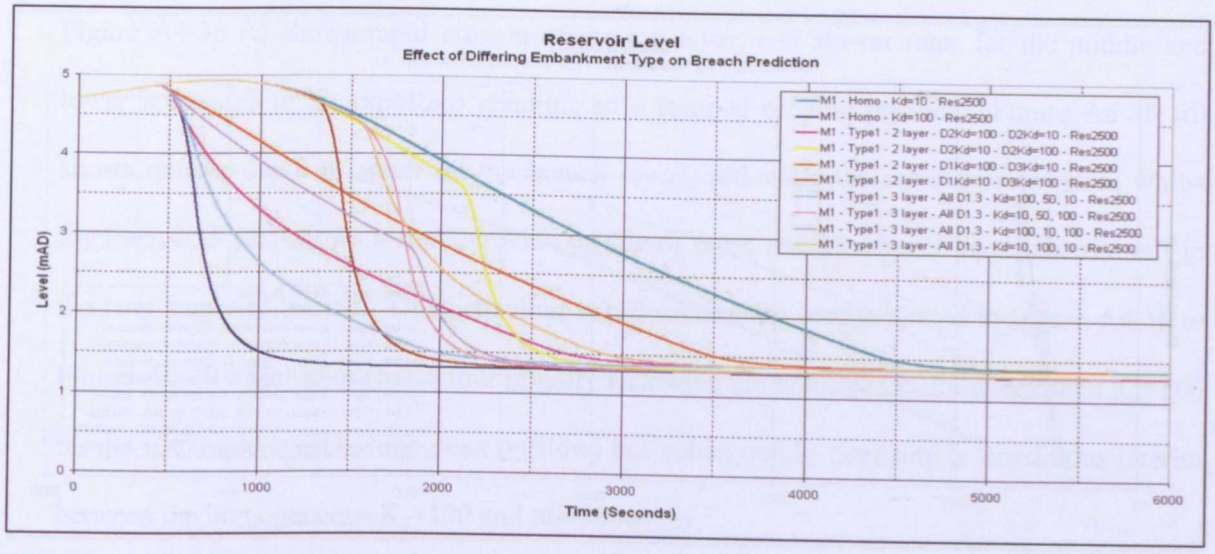

Figure A4-37 Reservoir level: Type 1,3-layer embankment

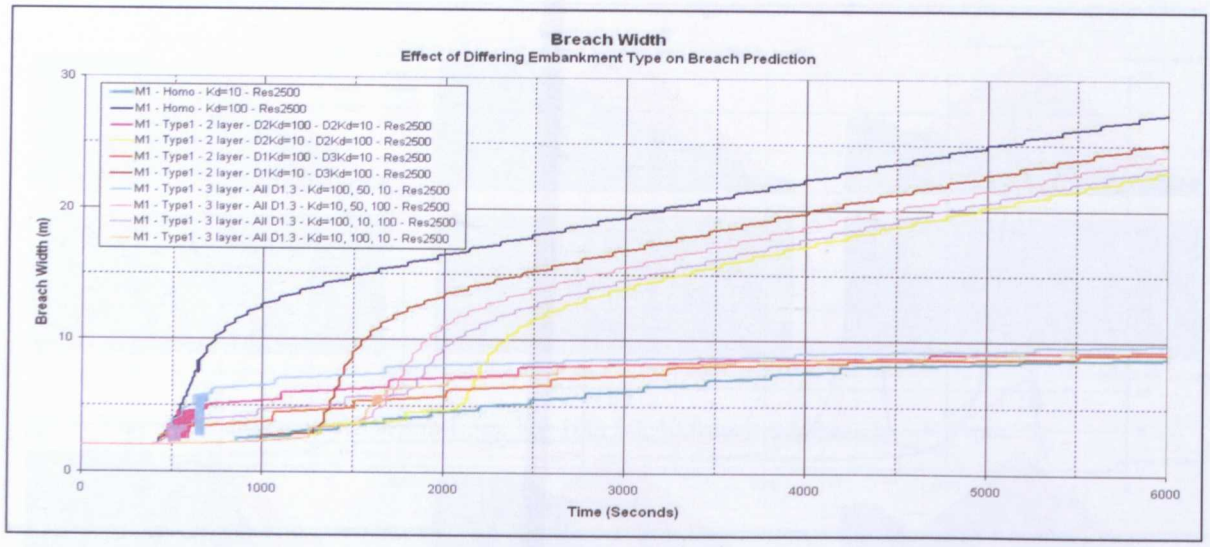

Figure A4-38 Breach width: Type 1, 3-layer embankment

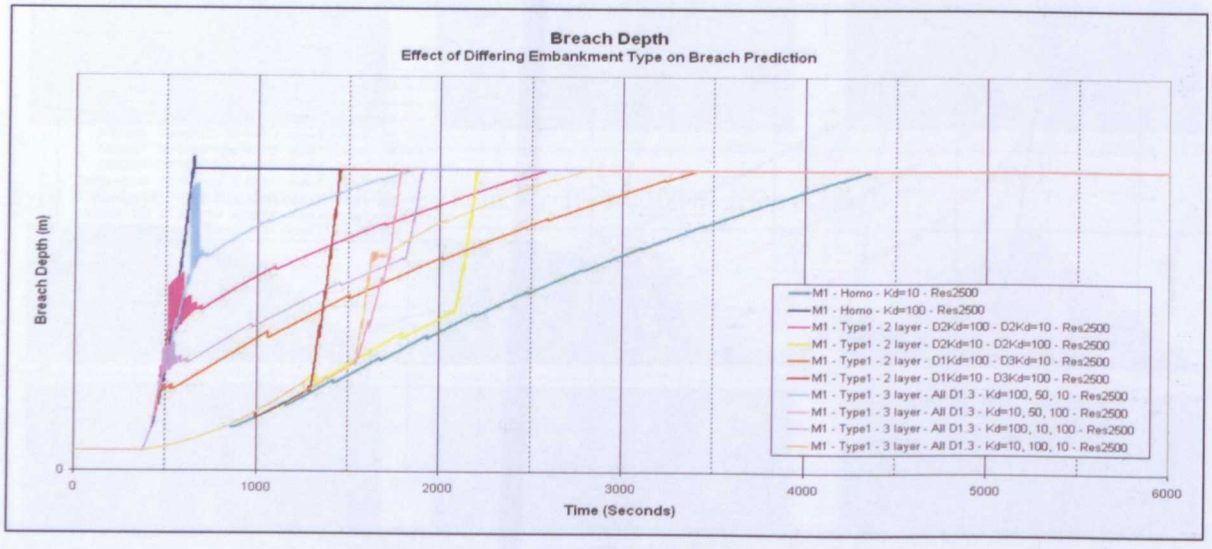

Figure A4-39 Breach depth: Type 1, 3-layer embankment

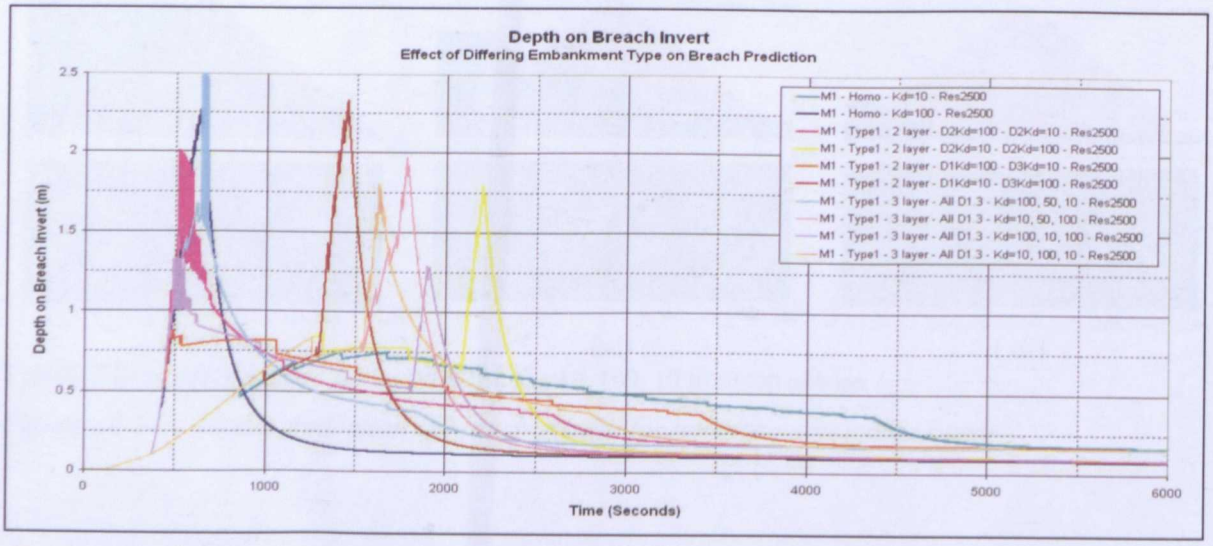

Figure A4-40 Depth on breach invert: Type 1, 3-layer embankment

Analysis of modelling results – Type 1, 3-layer embankment breach processes

The four model tests show behaviour that is consistent with the physical and numerical processes observed for both the homogenous and Type 1, 2-layer embankment testing.

Observations:

1. Figure A4-35 shows erosion behaviour in each of the 3 different soil layers that is consistent with their varying and relative levels of erodibility. This demonstrates shows how the different layers of soil erodibility can interact to affect the rate of erosion and hence the timing and magnitude of water release. Outflow hydrographs from the 3-layer examples are different from those seen previously, but all can be explained through consideration of the physical processes. Figure A4-35 (i) shows rapid erosion of the top layer, and slower rates for the middle and lower layers (as to be expected) resulting in a stepped eroding profile. Figure A4-35 (ii) shows quite a depth of water on the breach invert, reflecting the rapid crest erosion, whilst Figure A4-35 (iii) shows a shallow wide profile of more resistant lower layer material left in the later stages of breach. This behaviour is reflected in the results plotted in Figure A4-36 to Figure A4-40 which show behaviour initially following the homogeneous embankment K_d=100 results (i.e. rapid breach, high peak outflow) but subsequently deviating to conditions interim between the homogeneous K_d=100 and K_d=10 results;

2. Figure A4-35 (iv), (v) and (vi) shows behaviour for 3-layers with the erodibility reversed to K_d=10, 50, 100 respectively. The results (Figure A4-35 (iv)) show an initial steepening of the downstream face as the lower layer material is more rapidly removed than the middle and upper layers. Figure A4-35 (v) and (vi) show more rapid erosion of the middle and lower layers as the less erodible, 'protective' upper layer is removed. The speed of removal is reflected by the greater depth of water remaining on the breach invert. The results plotted in Figure A4-36 to Figure A4-40 show consistent behaviour, with the overall rate of breach growth initially being slow due to the less erodible upper layer, and subsequently speeding up as the more erodible lower layers are exposed;

3. Figure A4-35 (vii), (viii) and (ix) shows behaviour for 3 layers with similar erodibility in the outer two layers. In this case, the sandwiched layer was K_d=10, with the outer layers K_d=100. Figure A4-35 (vii) shows rapid erosion of the upper crest layer, and steepening of the downstream slope through the lower layer. Figure A4-35 (viii) and (ix) show slow erosion through the middle layer, with a wide flat surface eroded during this process, followed by rapid removal of the lower layer. The results plotted in Figure A4-36 to Figure A4-40 all reflect this series of processes;

4. Figure A4-35 (x), (xi) and (xii) shows behaviour for 3 layers with similar erodibility in the outer two layers - in this case, the sandwiched layer was K_d=100, and the outer layers K_d=10. Figure A4-35 (x) shows a stepped profile reflecting slow erosion of the crest layer, more rapid erosion of the middle layer and slower erosion of the lower layer. Figure A4-35 (xi) and (xii) show rapid erosion of the middle layer leaving a wide, flatter profile of the lower layer in the latter stages, consistent with physical processes expected for this combination of soil erodibilities. Results shown in Figure A4-36 to Figure A4-40 also all reflect this series of physical processes.

Conclusions:

5. The modelling results for 3-layer Type 1 tests are consistent with the physical processes likely to occur with multiple layers of differing erodibility. This suggests that the modelling assumption applied and tested for the different 2-layer geometries should be extendible to multiple layers of soil type.

Appendix 5

Selected publications

This Appendix contains references for selected papers and reports by the writer detailing research and findings that were published during this PhD. The papers have been accepted as part of international research programmes, journal or conference publication.

Paper numbers 6, 7 and 8 are included within the Appendix on CD ROM.

Report numbers 10 and 11 can be accessed online via the web links provided.

The publications comprise:

1) Recent Advances in Predicting Breach Formation through Embankment Dams
Morris, M.W., Hanson, G.J. and Vaskinn, K.A. (2006) 'Recent advances in predicting breach formation through embankment dams', *22nd International Congress on Large Dams (ICOLD),* Barcelona, Spain, June 2006, 2006.

2) Breach formation: Field tests and laboratory experiments
Morris, M.W., Hassan, M.A.A.M. and Vaskinn, K.A. (2007) 'Breach formation: field tests and laboratory experiments', *Journal of Hydraulic Research,* Vol. 45 (Extra (2007)).

3) HR BREACH: Developing a practical breach model to meet industry needs
Morris, M.W., Hassan, M.A.A.M., Buchholzer, Y. and Davies, T. (2008). HR BREACH: Developing a practical breach model to meet industry needs. US Society on Dams 28th Annual Meeting and Conference, April 28th -May 2nd Portland, Oregon.

4) Development of the HR BREACH model for predicting breach growth through flood embankments and embankment dams
Morris, M.W., Hassan, M.A.A.M., Samuels, P.G. and Ghataora, G.S. (2008). Development of the HR BREACH model for predicting breach growth through flood embankments and embankment dams. Riverflow2008 International conference on fluvial hydraulics, 3-5th September, 2008. Izmir, Turkey

5) Modelling breach initiation and growth
Morris, M.W., Hassan, M.A.A.M, Kortenhaus, A., Geisenhainer, P., Visser, P.J. and Zhu, Y. (2008). Modelling breach initiation and growth. FLOODrisk 2008 conference, 30th September – 2nd October, 2008. Oxford, UK

6) Improving the accuracy of breach modelling: Why are we not progressing faster?
Morris, M.W., Hanson, G.J. and Hassan, M.A.A.M. (2008) 'Improving the accuracy of breach modelling: why are we not progressing faster?' *Journal of Flood Risk Management,* Vol. 1 (No. 4), pp. pp. 150-161.

7) Breach formation: Identifying key physical processes to support improved breach numerical modelling
Morris, M.W., Hassan, M.A.A.M., Ghataora, G.S. and Samuels, P.G. (2009) 'Breach formation: Identifying key physical processes to support improved breach numerical modelling', 33rd IAHR Congress, Vancouver, British Colombia,

8) Idealised model for flow towards a dam breach
Samuels, P.G. and Morris, M.W. (2010) 'Idealised model for flow towards a dam breach', First European Division IAHR Congress, Edinburgh. 4-6th May, 2010.

9) Just how important is grass cover?
Morris, M.W., Boorman, L.A. and Simm, J.D. (2010) 'Just how important is grass cover?' British Dam Society 16th Biennial Conference, University of Strathclyde, Scotland. 23-26th June 2010.

10) Breach initiation and growth: Physical processes
The European FLOODsite Project (www.floodsite.net) FLOODsite Report T06-08-11 (2008).

This report can be downloaded directly from the following link:
http://www.floodsite.net/html/partner_area/search_results3b.asp?docID=445

11) Review of the IMPACT project breach field test data
The European FLOODsite Project (www.floodsite.net) FLOODsite Report T04-08-04 (2008). (Note: Not the lead writer for this report)

This report can be downloaded directly from the following link:
http://www.floodsite.net/html/partner_area/search_results3b.asp?docID=365